THE CHARACTERIZATION OF SOME METHACRYLATE AND ACRYLATE HOMOPOLYMERS, COPOLYMERS AND FIBERS VIA DIRECT PYROLYSIS MASS SPECTROSCOPY

A THESIS SUBMITTED TO
THE GRADUATE SCHOOL OF NATURAL AND APPLIED SCIENCES
OF
MIDDLE EAST TECHNICAL UNIVERSITY

BY

SURİYE ÖZLEM GÜNDOĞDU

IN PARTIAL FULFILLMENT OF THE REQUIREMENTS
FOR
THE DEGREE OF DOCTOR OF PHILOSOPHY
IN
POLYMER SCIENCE AND TECHNOLOGY

DECEMBER 2012

Approval of the thesis:

THE CHARACTERIZATION OF SOME METHACRYLATE AND ACRYLATE HOMOPOLYMERS, COPOLYMERS AND FIBERS VIA DIRECT PYROLYSIS MASS SPECTROSCOPY

submitted by **SURİYE ÖZLEM GÜNDOĞDU** in partial fulfillment of the requirements for the degree of **Doctor of Philosophy in Polymer Science and Technology Department** by,

Prof. Dr. Canan Özgen
Dean, Graduate School of **Natural and Applied Sciences** _____

Prof. Dr. Teoman Tinçer
Head of Department, **Polymer Science and Technology** _____

Prof. Dr. Jale Hacaloğlu
Supervisor, **Chemistry Dept., METU** _____

Examining Committee Members:

Prof. Dr. Nursel Dilsiz
Chemical Engineering Dept., Gazi University _____

Prof. Dr. Jale Hacaloğlu
Chemistry Dept., METU _____

Prof. Dr. Göknur Bayram
Chemical Engineering Dept., METU _____

Prof. Dr. Cevdet Kaynak
Metallurgical and Materials Engineering Dept., METU _____

Prof. Dr. Ahmet M. Önal
Chemistry Dept., METU _____

Date: 19.12.2012

I hereby declare that all information in this document has been obtained and presented in accordance with academic rules and ethical conduct. I also declare that, as required by these rules and conduct, I have fully cited and referenced all material and results that are not original to this work.

Name, Last Name : SURİYE ÖZLEM GÜNDOĞDU

Signature :

ABSTRACT

THE CHARACTERIZATION OF SOME METHACRYLATE AND ACRYLATE HOMOPOLYMERS, COPOLYMERS AND FIBERS VIA DIRECT PYROLYSIS MASS SPECTROSCOPY

Özlem Gündoğdu, Suriye

Ph.D., Department of Polymer Science and Technology

Supervisor: Prof. Dr. Jale Hacaloğlu

December 2012, 177 pages

Poly(methyl methacrylate) possesses many desirable properties and is used in various areas. However, the relatively low glass transition temperature limits its applications in textile and optical-electronic industries. Monomers containing isobornyl, benzyl and butyl groups as the side chain are chosen to copolymerize with MMA to increase Tg and to obtain fibers with PMMA.

In this work, thermal degradation characteristics, degradation products and mechanisms of methacrylate homopolymers, poly(methyl methacrylate), poly(butyl methacrylate), poly(isobornyl methacrylate) and poly(benzyl methacrylate), acrylate homopolymers, poly(n-butyl acrylate), poly(t-butyl acrylate), poly(isobornyl acrylate), two, three and four component copolymers of MMA and fibers are analyzed via direct pyrolysis mass spectrometry. The effects of substituents on the main and side chains, the components present in the copolymers and fiber formation on thermal stability, degradation characteristics and degradation mechanisms are investigated.

According to the results obtained, the depolymerization mechanism yielding mainly the monomer is the main thermal decomposition route for the methacrylate polymers, acrylate polymers degradation occurs by H-transfer reactions from the main chain to the carbonyl groups. However, when the alkoxy group involves γ-H, then, H-transfer

reactions from the alkoxy group to the CO group also takes place leading to a complex thermal degradation mechanism.

The thermal degradation mechanisms and the relative yields of products are affected by copolymerization due to the inter and intra-molecular interactions. As a consequence of transesterification reactions new fragments can be generated.

In general, the samples taken from different parts of the fibers do not show different thermal degradation behavior. However, upon fiber formation, enhancements in intermolecular interactions decreasing the thermal stability and changing the product distribution are detected.

Keywords: PMMA copolymers, fiber formation, thermal degradation, direct pyrolysis mass spectrometry.

ÖZ

BAZI METAKRİLAT VE AKRİLAT HOMOPOLİMERLERİNİN, KOPOLİMERLERİN VE FİBERLERİNİN DİREKT PİROLİZ KÜTLE SPEKTROMETRESİ İLE KARAKTERİZASYONU

Özlem Gündoğdu, Suriye
Doktora, Polimer Bilimi ve Teknolojisi Bölümü
Tez Yöneticisi: Prof. Dr. Jale Hacaloğlu

Aralık 2012, 177 sayfa

Poli(metil metakrilat) fiziksel ve kimyasal özellikleri nedeniyle oldukça geniş uygulama alanı olan bir polimer türü haline gelmiştir. Buna rağmen, oldukça düşük olan T_g'si bu polimerin tekstil ve optik-elektronik endüstrisinde kullanımını kısıtlamaktadır. Bu nedenle, PMMA, T_g'si arttırılmak amacıyla yan zincir olarak bütil, benzil ve izobornil grupları içeren monomerlerle kopolimerleştirilmekte ve fiberleştirilmektedirler.

Bu çalışmada, metakrilat homopolimerler, poli(metil metakrilat), poli(bütil metakrilat), poli(izobornil metakrilat), poli(benzil metakrilat) akrilat homopolimerler, poli(n-bütil akrilat), poli(t-bütil akrilat), poli(izobornil akrilat), ve bu monomerlerin ikili, üçlü ve dörtlü kopolimerlerinin, elyaflarının ısıl bozunum karakterleri, ürünleri ve mekanizmaları doğrudan piroliz kütle spektrometresi yöntemi kullanılarak analiz edilmiştir. Bu çalışmalar neticesinde, ana ve yan zincirlerdeki moleküllerin çeşitliliği, kopolimeri oluşturan her bir parçanın birbiri üzerindeki etkisi ve elyaf oluşumunun ısıl kararlılık, bozunum karakteristiği ve ısıl bozunum mekanizması üzerindeki etkisi incelenmiştir.

Elde edilen sonuçlara göre, metakrilat polimerleri için temel bozunum mekanizmasının monomer oluşumuna neden olan depolimerizasyon olduğu görülmüştür, akrilat polimerlerinin bozunumu ise ana zincirden karbonil gruba hidrojen transfer reaksiyonuyla başlamaktadır. Fakat alkoksi grup γ-H içeriyorsa bu gruptan karbonil gruba hidrojen transfer reaksiyonları da oluşabilmektedir ve bu tür durumlarda genellikle reaksiyon, karmaşık termal bozunum mekanizmalarıyla devam etmektedir.

Kopolimerleşme nedeniyle moleküller arası etkileşimin farklılaşmasının, maddelerin ısıl bozunum mekanizmalarını ve ürünlerinin bağıl verimliliğini etkilediği gösterilmiştir. Transesterifikasyon reaksiyonları sonucunda da yeni ürünler oluşmuştur.

Genel olarak, elyafların farklı bölgelerinden alınan örnekler farklı ısıl bozunum davranışları sergilemezler. Fakat elyaf oluşumun etkisiyle moleküller arası etkileşimin farklılaşması nedeniyle termal bozunum ürünlerinde ve bu ürünlerin ısıl kararlılıklarında bazı değişikliklerin olabildiği gösterilmiştir.

Anahtar Kelimeler: PMMA kopolimerleri, elyaf oluşumu, ısıl bozunum, doğrudan piroliz kütle spektrometresi.

To my lovely husband, Gençay……..

ACKNOWLEDGEMENTS

I would like to express my deepest gratitude to my thesis supervisor Prof. Dr. Jale Hacaloğlu for her guidance, patience, understanding, kind support, encouraging advices, criticism, and valuable discussions throughout my thesis. I thank Prof. Dr. Ahmet M. Önal, Prof. Dr. Göknur Bayram, Prof. Dr. Cevdet Kaynak and Prof. Dr. Nursel Dilsiz for their helpful comments and suggestions as committee members.

I would sincerely thank to Dr. Yusuf Nur for his guidance, patience and valuable friendship during my learning stage of using the concerning laboratory instruments and Dr. Evren Güler for her contribution in providing most of the polymers used in my experiments.

My special thanks go to my mother, father and my brother for their continuous support, patience and encouragement.

Last but not the least; I wish to express my sincere thanks to my husband Gençay Gündoğdu for his support, understanding and endless love.

TABLE OF CONTENTS

LIST OF TABLES

TABLES

LIST OF FIGURES

FIGURE

LIST OF SCHEMES

SCHEMES

LIST OF ABBREVIATIONS

HDPE	High Density Polyethylene
PMMA	Polymethyl Methacrylate
PVC	Polyvinyl Chloride
TG	Thermogravimetry
TGA	Thermo Gravimetric Analysis
DSC	Differential Scanning Calorimetry
TVA	Thermal Volatilization Analysis
FTIR	Fourier Transform Infrared Spectroscopy
MS	Mass Spectrometry
Py	Pyrolysis
GC	Gas Chromatography
TIC	Total Ion Chromatogram
DESI	Desorption Electrospray Ionization
MALDI-MS	Matrix Assisted Laser Desorption Mass Spectroscopy
APCI	Atmospheric Pressure Chemical Ionization
PBMA	Poly(butyl methacrylate)
PtBMA	Poly(tert-butyl methacrylate)
PHFBMA	Poly(hexafluoro butyl methacrylate)
PMA	Poly(methy acrylate)
LC–PB-MS	Liquid Chromatograpy- Particle Beam-Mass Spectrometry
p(MMA-co-BA)	Poly(methyl methacrylate-*co*-butyl acrylate)
PBA	Poly(butyl acrylate)
PBMA	Poly(butyl methacrylate)

PBzMA	Poly(benzyl methacrylate)
PVAc	Polyvinyl Acetate
PIBA	Poly(isobornyl acrylate)
PIBMA	Poly(isobornyl methacrylate)
ATRP	Atom Transfer Radical Polymerization
DMA	Dynamic Mechanical Analyses
SAXS	Small-Angle X-Ray Scattering

CHAPTER 1

INTRODUCTION

1.1 Polymers and Fibers

The chemistry and technology of man-made, fiber forming polymers dates back to 1885 when an artificial silk was patented by Chardonnet in France. Since then, these materials have progressed to become the focus of a major global industry with applications ranging from the everyday world of apparel to biomedical and advanced aerospace engineering concepts.

Fiber is a class of materials that are continuous filaments or are in discrete elongated pieces. They impart elasticity, flexibility, and tensile strength. They can be spun into filaments, string, or rope, used as a component of composite materials, or matted into sheets to make products such as paper. Fibers are often used in the manufacture of other materials. The strongest engineering materials are generally made as fibers, for example carbon fiber and ultra-high-molecular-weight polyethylene fiber [1].

In the manufacture of all man-made fibers the most crucial step is the production of polymers or polymer derivatives suitable for spinning into fibers**.** For fiber formation, the polymer should contain crystallinity as much possible as in the structure. Polyethylene, polypropylene, nylon, polyester, polyacrylonitrile and polyurethanes are the most common polymers that are used in fiber formation due to their regular structure which gives rise to the close packing of the chains so the polymers can be spun into fibers.

Fibers are polymers characterized by a high initial modulus in the range of 10^{10} to 10^{11} dynes.cm^{-2}. They have a low range of extensibility of the order 10 to 20 percent.

Parts of this extensibility is permanent, part of it shows delayed recovery, and part of the elasticity is instantaneous. Most of the mechanical properties of fibers are relatively independent of temperature over a fairly long range from above -50°C to about 150°C, depending on the particular fiber [2].

The polymers used for synthetic fibers are similar, and in many cases identical to those used as plastics, but for fibers, the processing operation must produce an essentially infinite length-to-diameter ratio. In all cases this is accomplished by forcing the plasticized polymer through a spinneret, a plate in which the multiplicity of holes has been formed to produce the individual fiber. The cross section of the spinneret holes obviously has a lot to do with the fiber cross section, which in turn greatly influence the properties of the fiber and this is obtained with a fiber spinning operation [3].

1.1.1 Fiber Spinning

Fiber spinning is used to manufacture synthetic fibers. During fiber spinning, a filament is continuously extruded through an orifice and stretched to diameters of 100 μm and smaller. The schematic diagram of fiber spinning process is shown in Figure 1.

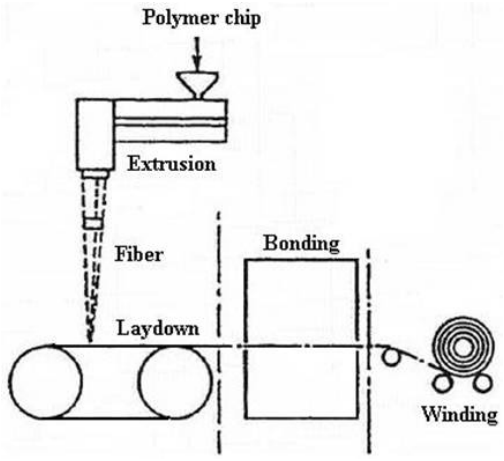

Figure 1. Schematic diagram of fiber spinning process.

In this process the molten polymer is first extruded through a filter to eliminate small contaminants. The melt is then extruded through a spinneret, or die composed of multiple orifices. The fibers are then drawn to their final diameter, solidified and wound onto a spool. The solidification takes place either in a water bath or by forced convection. The drawing and cooling processes determine the morphology and mechanical properties of the final fiber. For example, ultra high molecular weight (high density polyethylene) HDPE fibers with high degrees of orientation in the axial direction can have the stiffness of steel with today's fiber spinning technology [4].

There are basically four types of spinning operations which are wet spinning, dry spinning, melt spinning and gel spinning, differing mainly in the method of plasticizing and deplasticizing the polymer.

1.1.1.1 Wet Spinning

Of all the four processes, wet spinning is the oldest process. It is used for polymers that need to be dissolved in a solvent to be spun. The spinneret remains submerged in a chemical bath that leads the fiber to precipitate, and then solidify, as it emerges out of the spinneret holes (Figure 2). Acrylic, rayon, aramid, mod acrylic and spandex fibers all are manufactured through wet spinning.

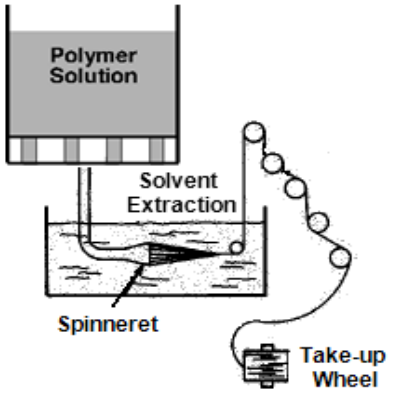

Figure 2. Schematic diagram of wet spinning process.

1.1.1.2 Dry Spinning

In dry spinning, a solution of the polymer is forced through the spinneret. As the fiber proceed downward to the drawing rolls, a counter-current stream of warm air evaporates the solvent. The schematic diagram of dry spinning process is shown in Figure 3. In this process the cross-section of the fiber is determined not only by the shape of the spinneret holes, but also by the complex nature of the diffusion-controlled solvent evaporation process, because there is considerable shrinkage as the solvent evaporates. The acrylic fibers, mainly polyacrylonitrile fiber, are produced by dry spinning.

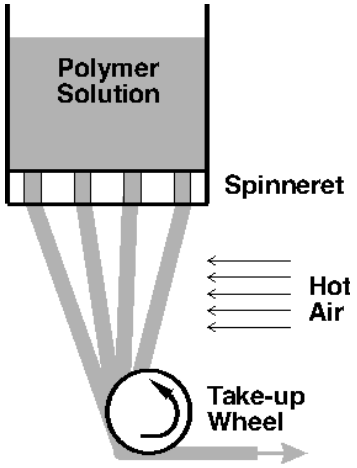

Figure 3. Schematic diagram of dry spinning process.

1.1.1.3 Melt Spinning

Melt spinning is basically an extrusion process. The polymer is plasticized by melting and pumped through a spinneret (Figure 4). The fibers are usually solidified by a cross current blast of air as they proceed to the drawing rolls. The drawing step stretches the fibers, orienting the molecules in the direction of stretch and inducing high degrees of crystallinity, a necessity of good fiber properties. Nylon fibers are commonly melt spun [3].

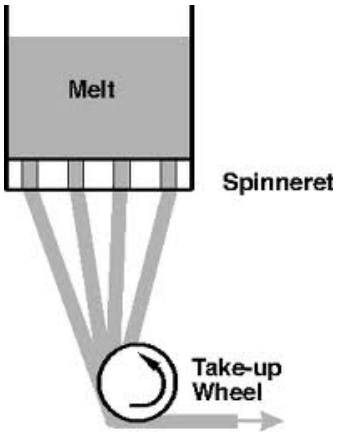

Figure 4. Schematic diagram of melt spinning process.

1.1.1.4 Gel spinning

Gel spinning is also known as dry-wet spinning because the filaments first pass through air and then are cooled further in a liquid bath. The polymer, here is partially liquid or in a "gel" state, which keeps the polymer chains somewhat bound together at various points in liquid crystal form. This bond further results into strong inter-chain forces in the fiber, increasing its tensile strength. The polymer chains within the fibers also have a large degree of orientation, which increases its strength. The filaments come out with an unusual high degree of orientation relative to each other. The high strength polyethylene fiber and aramid fibers are manufactured through this process [5].

1.1.2 Application Areas of Fibers

Several billion pounds of fibers are consumed every year, with a significant fraction of the amount constituting synthetic polymeric fibers. Traditional applications of polymeric fibers have been in textiles and furnishings. However, fiber applications have expanded dramatically with penetration of synthetic fibers into industries such as geotextiles, composites, insulation, filtration, aerospace components, biomedical products, and protective clothing. Thus, synthetic fibers usually need to satisfy a broad spectrum of performance criteria. For example, fibers employed in the textile

industry needs a high softening temperature, adequate tensile strength over fairly wide temperature range, solubility or meltability for spinning, high modulus, dyeability, chemical, biological and thermal stability, flame resistance, and good appearance. Enhancing the quality of fibers requires changes not only in the chemistry of the material to obtain desired properties, but also significant modifications in the spinning process. The search for higher performance materials has led researchers to either blend existing polymers or polymerize different monomers simultaneously. Blending and copolymerization approaches to obtain specific properties usually require relatively little investment in comparison to the development of new polymers or new processes. Hence, fibers from polymer blends and copolymers have assumed to have an important role in the synthetic fiber industry [6]. Thermal degradation properties of the materials are one of the performance characteristics for determination of application areas.

1.2 Thermal Degradation of Polymers

When the polymers are exposed to high temperature thermal degradation takes place. The degradation characteristics such as thermal stability, thermal degradation products and thermal degradation mechanism are mainly determined by the chemical structure of the corresponding polymer. In general, thermal degradation starts with vaporization of additives and is followed by thermal degradation of high molecular weight components.

Thermal degradation of polymers may follow a depolymerization mechanism producing mainly monomer and low molecular weight oligomers. If statistical or random cleavage of the polymer chain takes place, products that may have quite different structure than the monomer are generated. In the presence of thermally labile side chains, generally, two-step decomposition occurs; the first being the elimination of side chains and the second being the decomposition of the polymer backbone forming more stable condensed structures. A non-free radical process involving intermolecular exchange reactions yielding mainly cyclic oligomers may also be involved during thermal degradation [7].

1.2.1 Depolymerization

In depolymerization process, the end of polymer chain separates and generates a free radical with low activity under thermal effect. Then according to the chain reaction mechanism, the polymer loses monomers one by one. This process called as unzipping produces mainly monomer and low molecular weight oligomers. This process is common for poly(methyl methacrylate) (PMMA) and polystyrene decomposition [8].

1.2.2 Random chain scission

In the random chain scission process the backbone breaks down randomly at any position of the backbone. Therefore, the molecular weight decreases rapidly and monomer can not be obtained in this process. As the new free radicals generated has high activity and intermolecular chain transfer and disproportion termination reactions can readily occur. Thermal degradation of polyethylene is an example for polymers that decomposes by random chain scission [9].

1.2.3 Side group elimination

Elimination of side chains is generally a first step of a two-step thermal degradation process. Side groups held by bonds which are weaker than the bonds connecting the main chain are stripped off before the decomposition of the main chain during the heating process. For example, the first step of thermal degradation of polyvinyl chloride (PVC) is the elimination of the side groups to form hydrogen chloride. With the side groups removed, the polyene macromolecule remains. This then undergoes reactions to form aromatic molecules [10].

1.3 Thermal Degradation Techniques

The study of the thermal degradation of the polymers is important in understanding their usability, storage and recycling. Various kinds of thermal analysis techniques have been proposed to define suitable processing conditions and give useful service

guidelines for their wise application area. Some of the most common techniques used to study the thermal degradation characteristics of the polymers are thermogravimetry (TG), differential scanning calorimetry (DSC), thermal volatilization analysis (TVA) and pyrolysis techniques.

1.3.1 Thermogravimetric Analysis (TGA)

Thermogravimetry is the branch of thermal analysis which examines the mass change of a sample as a function of temperature in the scanning mode or as a function of time in the isothermal mode. TG is used to characterize the decomposition and thermal stability of materials under a variety of conditions and to examine the kinetics of the physicochemical processes occurring in the sample [8].

TGA has been utilized to determine some important kinetic parameters for polymeric materials degradation. These kinetic parameters are the reaction order, *n,* and the overall activation energy, *E.* These values can be of great importance in the elucidation of the mechanisms involved in polymer degradation since these degradation parameters manifest themselves in changes in the slope and shape of the TG curves [11].

Thermogravimetry curves are characteristic for a given polymer or compound because of the unique sequence of the physciochemical reaction that occurs over specific temperature ranges and heating rates and are function of the molecular structure. The principal applications of TGA in polymers are determination of the thermal stability of polymers, compositional analysis and identification of polymers from their decomposition pattern. Also, TGA curves are used to determine the kinetics of thermal decomposition of polymers and the kinetics of cure where weight loss accompanies the cure reaction (as in condensation polymerizations, such as cure of phenolic resins) [8].

In 1989 Compton and coworkers integrated TGA and FTIR (Fourier Transform Infrared Spectroscopy) (TGA/FTIR) and since then it has been in progression for use as a valuable instrument in observation of thermal behavior of synthetic polymer.

This technique has also been applied to distinguish homopolymers, copolymers, and blends and to determine compositions of copolymers [12].

Thermogravimetry can also be coupled with a mass spectrometry (TG-MS) which enables in addition to the weight loss information, identification of the evolved gases in sequential order during thermal degradation of a polymer in controlled atmospheric conditions. In addition, the technique is also used to differentiate trapped solvents, unreacted reagents, and trace impurities. As the products of degradation are flushed out with the purged gas the possibility of secondary reactions is reduced compared to sealed tube pyrolysis experiments. Also no sample contamination occurs and sample preparation is minimal [13].

Although TGA is a widely used method in polymer degradation there are some drawbacks of TGA analysis. TGA measurements only record the loss of volatile fragments of polymers, caused by decomposition. TGA cannot detect any chemical changes or degradation properties caused by cross-linking [8].

1.3.2 Thermal Volatilization Analysis (TVA)

Use of thermal volatilization analyses in observation of polymer degradation dates back to 1960's. McNeill was the one who proposed TVA as a comprehensive tool for the identification of pyrolysis products from commodity polymers [14]. In this method sample is heated in vacuum system (0.001 Pa) equipped with a liquid nitrogen tank (77°K) between the sample and the vacuum pump. Any volatiles produced will increase the pressure in the system until they reach the liquid nitrogen and condense out. As a theory, in TVA the variation in pressure of volatile products is recorded during a degradation in which the temperature of the polymer sample is increased at a steady rate. When this pressure (measured by Pirani gauge) is recorded as the sample temperature is increased in a linear manner, a TVA thermogram, showing one or more peaks, is obtained. The apparatus required for TVA is simple. It consists of a flat-bottomed glass tube containing the polymer sample as a fine powder or film which is inserted into the top of a small oven, the temperature of which is varied by means of a linear temperature programming unit. The glass tube is connected first to a trap surrounded with liquid nitrogen and then to a mercury diffusion pump and rotary oil pump.

Between the tube and the trap is attached a Pirani gauge head. The gage control unit provides an output for a 10-mV potentiometric strip chart recorder so that a continuous trace of pressure versus time (temperature) may be obtained. Polymer samples from 10 to 250 mg can conveniently be handled.

Guo et al. used spectroscopic methods together with TVA for the identification of polymer degradation products [15]. They used a vacuum-tight long-path gas IR cell, as an interface allowing for the application of FTIR for the on-line analysis of volatile products of polymer in TVA analysis. This relatively new analytical technique was named as TVA/FT-IR.

1.3.3 Differential Scanning Analysis (DSC)

In addition to the rate of decomposition, heat of reaction of decomposition process also gives information about the thermal degradation characteristics of polymers. DSC is one of the most widely used instruments in that respect in polymer thermal degradation analysis field. In all degradation processes heat must be supplied to the polymer to get it to a temperature at which a significant degradation takes place. However, once this temperature is obtained, further thermal decomposition process may either generate or consume additional heat. The magnitude of this energy generation or requirement can be measured with DSC. It is a technique in which the heat flow rate difference into a substance and a reference is measured as a function of temperature, while the sample is subjected to a controlled temperature program. DSC is an extremely useful instrument when only a limited amount of substance is available, since only milligrams of sample is required for analysis [16].

In DSC analysis both the sample and the reference are maintained at nearly the same temperature throughout the experiment. The basic principle underlying this technique is that, when the sample undergoes a physical transformation such as phase transitions, more (or less) heat will need to flow to it than the reference to maintain both at the same temperature. Whether more or less heat must flow to the sample depends on whether the process is exothermic or endothermic. For example, as a solid sample melts to a liquid it will require more heat flowing to the sample to increase its temperature at the same rate as the reference. Likewise, as the sample undergoes exothermic processes (such as crystallization) less heat is required to raise the sample temperature.

By observing the difference in heat flow between the sample and the reference, differential scanning calorimeter is able to measure the amount of heat absorbed or released during such transitions. For example, the cross-linking of polymer molecules that occurs in the curing process is exothermic; resulting in a positive peak in the DSC curve that usually appears soon after the glass transition.

DSC provides a rapid method for the determination of the thermal properties of polymeric materials, including thermal history studies, oxidation induction time testing and dynamic and isothermal kinetic studies, evaluation of sample purity and glass transition temperature. The result of a DSC experiment is a heating or cooling curve.

Drawback of DSC is that; the DSC experiments are carried out by placing the sample inside a sealed sample holder and this technique is seldom suitable for thermal decomposition processes. It is ideally suited for physical changes but not for chemical processes [17].

1.3.4 Pyrolysis (Py)

Basically, pyrolysis is the thermal degradation of a compound in an inert atmosphere or vacuum. When vibrational excitation, as a result of distribution of thermal energy over all modes of excitation, is greater than the energy of specific bonds, decomposition of the molecule takes place. Temperature and heating rate have significant importance on product distribution. At low temperatures, thermal degradation may be too slow to be useful. On the other hand, at very high temperatures extensive decomposition generating only very small and nonspecific products may be generated. Product distribution is also affected by the heating rate depending on the kinetics of thermal equilibrium among several vibrational modes. Thus, thermal decomposition of a compound always occurs in a reproducible way producing a fingerprint only at a specific temperature and at a specific heating rate [7].

The fragments often contain sufficient information to identify the chemistry of the original polymer. This is a relatively straightforward method to establish the chemical structure of an unknown polymer material [18].

Pyrolysis technique can be coupled with FT-IR, GC (Py-GC), GC/MS (Py-GC/MS) or MS (DP-MS). Among these various analytical pyrolysis techniques, pyrolysis gas chromatography mass spectrometry, Py-GC/MS and direct pyrolysis mass spectrometry, DP-MS, have several advantages such as sensitivity, reproducibility, minimal sample preparation and consumption and speed of analysis [8].

1.3.4.1 Pyrolysis GC/MS (Py-GC/MS)

Pyrolysis-gas chromatography-mass spectrometry (Py-GC/MS) is a widely used instrument for the separation and identification of volatile pyrolysis products of polymers. It can be both used for quantitative and qualitative analysis. The number of peaks seen in the total ion chromatogram (TIC) represents the number of compounds detected by GC-MS. The relative intensity of each peak corresponds to the relative concentration of each product.

The principle technique behind the Py-GC/MS is that; after the chosen pyrolysis time, the carrier gas sweeps volatiles in to the GC column where they are separated according to their boiling points and polarities. The separated components are then measured and characterized by the mass spectrometer.

Most existing pyrolysis units are designed for the degradation of solid or highly viscous materials such as polymers. However, the volatile oily samples were used to evaporate before degradation. This difficulty is overcome with the investigation of in-line pyrolysis units for the MS study of thermal stability of volatile liquid polymers.

To conclude, the advances in this technique such as design of pyrolysis units, the use of sufficiently small samples have provided reliable quantitative data that can be used to obtain information about the polymer degradation process and help deducing the initial polymer structure [17].However, there are also some drawbacks of Py-GC/MS method. As thermal degradation occurs in a close container secondary reactions can not be eliminated totally.

Also, as pyrolyzers are mounted external to the GC system, deposition of higher-boiling point pyrolyzates and condensation of thermal degradation products in the transfer line is likely causing discrimination of high mass components and sample losses. Thus, Py-GC/MS can be used only for identification of stable volatile thermal degradation products.

In addition, there is always the possibility of not detecting some of the thermal degradation products retained in the pyrolytical zone, injection system or capillary column as a consequence of molecular weight and high polarity. Polar pyrolyzates even if they enter the gas chromatography column may often display peak tailing characteristics, poor reproducibility, long elution times and in some cases no chromatographic peak [19].

1.3.4.2 Direct Pyrolysis-MS (DP-MS)

Pyrolysis techniques are widely applied to elucidate thermal stability, degradation products and decomposition mechanism of a compound. Further subsequent MS characterization of the pyrolyzates is a powerful method for determination of composition, microstructure, and additives of industrial polymers, especially in unknown samples [7].

Direct pyrolysis mass spectrometry, DP-MS, technique is the only technique in which secondary and condensation reactions are at least partly avoided and detection of high mass pyrolyzates and unstable thermal degradation products are possible. Thus, a better understanding of the thermal characteristics, polymerization, crosslinking and char formation processes can be achieved [19].

The DP-MS, in general, is a four step process: Thermal degradation of the sample followed by the ionization of thermal degradation products, fragmentation of ionized species involving excess energy and finally, detection of all ions generated by MS [20].

In direct insertion probe pyrolysis, thermal degradation occurs inside the mass spectrometer and pyrolyzates are rapidly transported from the heating zone to the source region and ionized, almost totally eliminating the possibility of secondary and condensation reactions. Furthermore, as the high vacuum inside the mass spectrometer favors vaporization, analysis of higher molecular mass pyrolyzates are

possible. The rapid detection system of the mass spectrometers also enables the detection of unstable thermal degradation products. Thus, a better understanding of the thermal characteristics, polymerization, crosslinking and char formation processes can be achieved. However, direct pyrolysis mass spectra of polymers are almost always very complicated due to concurrent degradation processes and dissociative ionization of the thermal degradation products inside the mass spectrometer. Thus, in DP-MS analysis not only the detection of a peak but also the variation of its intensity as a function of temperature, single ion evolution profiles or single ion pyrograms, are important. When analyzing the DP-MS spectra, all ions with identical evolution profiles should be grouped and analyzed separately. In each group ion with highest mass may be assumed to be generated during thermal degradation. On the other hand the low mass fragments having similar evolution profiles may be generated either during thermal degradation or during ionization in the mass spectrometer [7, 19, 20].

Since thermal degradation products further dissociate during ionization and yield very complicated pyrolysis mass spectra soft ionization techniques may seem to be more appropriate. However, for soft ionization techniques secondary reactions may take place. Then, investigation of thermal degradation mechanism may be even more difficult [19].

There are some developments eliminating the drawbacks of DP-MS instrument analysis which makes it more widely applicable for polymer degradation analysis. For the analysis of non-volatile pyrolytic residues by MS and MS/MS analyses Zhang et al. described the development of an on-probe pyrolyzer interfaced to a desorption electrospray ionization (DESI) source as a novel in situ and rapid pyrolysis technique [21]. In their study for the analysis of synthetic polymer, poly(ethylene glycol), the on-probe pyrolysis DESI-MS system yielded data and information equivalent to previous Matrix Assisted Laser Desorption Mass Spectroscopy (MALDI-MS) analysis, where the use of a matrix compound and cationizing agent were required. Advantages of this system can be summarized to be its simplicity and speed of analysis since the pyrolysis is performed in situ on the DESI source probe and hence, extraction steps and/or use of matrices are avoided.

Another development about DP-MS instrument is done by Witson and coworkers in which a simple modification of a commercial quadruple ion trap to permit in situ

pyrolysis of synthetic polymers inside an atmospheric pressure chemical ionization (APCI) ion source was developed [22]. Results obtained indicated that DP-APCI mass spectrometry technique provides a rapid and cost effective means for analysis of thermal stability and chemical composition of complex synthetic polymers that are too large or too complex for direct mass spectrometry analysis. Witson and coworkers claimed that; although, the traditional direct probe analysis combined with chemical ionization MS and MS/MS allows more precise temperature control and provides a steadier ion current profile and less background noise, thereby leading to more reproducible spectra. DP-APCI conducts pyrolysis at atmospheric pressure, which is more similar to a thermogravimetric analysis experiment and, hence, may provide more useful information on the thermal properties of materials.

To conclude, the difficulties in interpretation of quite complex pyrolysis mass spectra due to dissociation of thermal degradation products during ionization that limits the application of the technique seem to be resolved with the applications of soft ionization techniques such as APCI and DESI.

Pyrolysis mass spectrometry techniques have find wide applications in the field of polymer science which includes molecular weight distribution, the fingerprint pattern for polymer identification, the sequence of monomeric units, the branching, cross-linking, end groups and chain substitution and the copolymer structure and grafting functionalities or variations in polymeric systems, and identification of additives or impurities present [20].

1.4 Acrylate Polymers

Acrylate monomers used to form acrylate polymers are based on the structure of acrylic acid, which consists of a vinyl and a carboxylic acid group. The resultant alkyl acrylate is given the generic formula (CH_2=$CHCO_2R$), with R representing the alkyl group. In commercial production, polymerization of acrylate polymers is conducted under the action of free-radical initiators, with the acrylates dissolved in a hydrocarbon solvent or dispersed in water by soap like surfactants. The general formula of the polyacrylate is given in Figure 5.

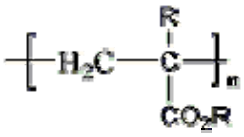

Figure 5. General formula of polyacrylate, R= alkyl group.

The dissolved or dispersed polymer can be further processed for use as a fiber modifier in textile manufacture, as a bonding agent in adhesives, or as a film-forming component in acrylic paints. The most common polyacrylates are polyethyl acrylate and polymethyl acrylate [23].

Understanding the degradation of acrylic polymers is of considerable interest because of their wide commercial applications. These polymers display several unique properties, such as weather and aging resistance, non-yellowing properties, low permeability to oxygen, good plasticizer resistance, photostability and resistance to hydrolysis. They are used as a primary binder in a wide variety of industrial coatings. Polyacrylates have many excellent properties, particularly exterior durability. They are excellent for adhesive applications, characterized by good compatibility with acrylic and methacrylic polymers as well as a wide range of other polymers. Forming plastic materials of notable clarity and flexibility under certain methods, they are employed primarily in paints and other surface coatings and in textiles [23-25].

Particularly in applications where extended exterior service lifetime is required, for example, in harsh Australian climate, in which surface coatings may reach temperatures of up to 95°C, high thermal stability formulation of surface coating is required. So, the roofing material made of thermally stable polyacrylates like poly(butyl methacrylate) PBMA, poly(tert-butyl methacrylate) PtBMA, and poly(hexafluoro butyl methacrylate) PHFBMA are readily applicable under these hard and replicated conditions [26].

1.4.1 Why acrylates are copolymerized?

The constantly advancing technologies demand new, high performance and more specialized materials with highly specialized functions. Such materials are no longer one component systems. The investigation on systems built with two or more components is in demand, especially for structure property correlations [27].

Copolymerization modulates both the intramolecular and intermolecular forces exercised between polymer segments. Therefore, some properties, such as the procedural decomposition temperatures (initial and final) with respect to thermal degradation and the glass-transition temperature, may vary within wide limits. So, copolymerization is an important and useful way to develop new materials [28].

Although certain homopolymers have properties almost ideally suited to an intended application they are deficient in some respect. A copolymer with only a small proportion of a second monomer often possesses the desirable properties of the parent homopolymer, while the minor component lends the qualities formerly lacking. As an example, synthetic fibers made from the homopolymer of acrylonitrile have excellent dimensional stability and resistance to weathering, chemicals, and microorganisms but poor affinity for dyes. Copolymerization of acrylonitrile with small amounts of other monomers yields the fiber orlon, with the desirable qualities of the homopolymer and the advantage of dyeability [23].

Acrylic/methacrylic polymers and their copolymers are widely used in many applications like paints, surface coatings, textiles, automobiles, fibers etc. because of their high chemical and thermal stability, optical clarity, adhesion and superior mechanical properties. Alkyl methacrylates have very high ability to react with alkyl acrylates to form copolymers. So, copolymers having a wide range of properties from rigid plastics to elastomeric materials can be prepared by combining alkyl methacrylates with alkyl acrylates [28-29].

For example, the experiment conducted by Vinu and coworkers to investigate the effect of copolymerization on physical properties of PMMA clearly shows that the copolymerization improves the properties of the resulting material [30]. Since PMMA is an optically clear, industrially and domestically important polymer it finds a multitude of applications from glass replacement, through paints and lubricating fluid

to fixing dentures and bones in medicine. The electrical, optical, thermal and transport properties of PMMA are tailor-made by copolymerizing it with another comonomer. This study also proved that, the copolymerization improves the impact strength, glass transition temperature (T_g) and thermal stability of the polymer.

1.4.2 Poly(methyl methacrylate) PMMA

Acrylate and methacrylate copolymers have excellent physical, chemical and mechanical properties. Also, copolymers based on acrylic or methacrylic acid esters and acrylic acid offer particular advantages, including excellent aging characteristics, resistance to elevated temperatures and plasticizers, and exceptional optical clarity. Therefore, in order to understand the degradation mechanism of these polymers some studies are conducted [24].The general formula for PMMA and poly(methyl acrylate) (PMA) is given in Figure 6.

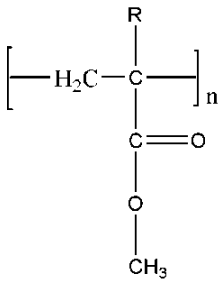

Figure 6. Poly(methyl acrylate) R=H, poly(methyl methacrylate) R=CH_3

N. Grassie et al. is the pioneer of the thermal degradation studies of acrylic polymers. They applied the technique of TVA in 1960's to methyl methacrylate homopolymers and copolymers having different molar ratios to investigate the copolymerization effect in terms of thermal degradation behavior of the polymer [31]. In this study it was demonstrated that the poly(methyl methacrylate) is stabilized upon copolymerization with methyl acrylate. The reason of inhibition of the depolymerization was explained by direct blockage of the chain by methyl acrylate units. In this work it was approved that the small amount of a comonomer may influence the stability of a polymer either favorably or adversely. When the

degradation process was examined in terms of the reaction and degradation products, the molecular weight of the copolymers was decreasing rapidly during degradation, showing that a random scission process was involved. The products of degradation consist of the monomers, carbon dioxide, chain fragments larger than monomer, and a permanent gas fraction which is principally hydrogen. Infrared and ultraviolet spectral measurements suggested that the residual polymer, which is colored, incorporates carbon-carbon unsaturation. Although the PMA homopolymer degradation products include methanol; the complete absence of methanol among the copolymer products was surprising for this study. However, in another study they showed that at least three adjacent units of MA are required in the polymer chain for methanol formation [32].

Grassie and coworkers also demonstrated that it is possible to use carbon dioxide production as a measure of chain scission and they investigate the relationship between chain scission and certain other features of the MMA and copolymer composition [33]. They showed that for a wide range of degradation temperatures and extents of reaction, the ratio of chain scissions to permanent gas production is constant for each copolymer but that the proportion of permanent gases increases with the MA content of the copolymer.

In another study, Manring proposed that the random scission degradation of PMMA is initiated by homolytic scission of a methoxycarbonyl side group followed by β scission rather than by main chain scission in the temperature range 350 to 400°C [34]. In addition, Holland and Hay concluded that the degradation of PMMA was initiated by a mixture of chain-end and random scission, followed by depropagation and first-order termination at low temperatures below 360°C, whereas initiation was a mixture of chain end and chain scission processes, followed by depropagation to the end of the polymer chain at temperatures above 385°C [35].

Lehrle and coworkers proposed that random scissions do not play a significant part in the mechanism for the thermal degradation of PMA and the depropagation, accompanied by intramolecular transfer, is the predominant degradation pathway [36-38]. It has also been determined by Bertini and coworkers that unlike poly(methyl methacrylate) which gives quantitative yields of monomer, the poly-n-alkyl methacrylates with longer alkyl chain produce also significant amounts of olefin and methacrylic acid [39].

In another study it was proposed that a side-group scission of a methoxycarbonyl group initiates PMMA-H degradation [40]. It was claimed that the side-group scission is favored due to a large 'cage" recombination effect which reduces the contribution of main-chain scission. It is anticipated that side-group scission will initiate polymer degradation whenever side-group bonds are of similar energy or weaker than main-chain bonds.

In recent years the thermal degradation of PMMA, PMA and their different composition copolymers was also studied by TGA [29]. In this study, the effect of alkyl group substituent on the thermal degradation behavior of the copolymers was investigated. It was shown that the pyrolysis of polymers mainly involves chain depolymerization along with the formation of alcohol and anhydride type of products. The normalized weight loss profiles showed that the temperature (Tm) at which maximum rate of degradation occurs, increases with alkyl acrylate content, indicating that the thermal stability of the copolymers poly(methyl methacrylate-co-alkyl acrylate)s increases with alkyl acrylate content.

The thermal stability and thermal degradation of copolymers based on selected alkyl methacrylates such as MMA, EMA and BMA was also analyzed by pyrolysis–gas chromatography at temperatures between 250 and 400°C [41]. In this study it was observed that the main thermal degradation products from alkyl methacrylate copolymers are monomers. Other pyrolysis by-products formed during thermal degradation were carbon dioxide, carbon monoxide, methane, ethane, methanol, ethanol, and propanol-1.

Czech et al. had also studied the thermal degradation of above discussed polymers at higher temperatures, between 300 and 800°C, again with by pyrolysis gas chromatography [42]. They showed that the main thermal degradation products were unsaturated monomeric alkyl methacrylates, carbon dioxide, carbon monoxide, methane, ethane, methanol, ethanol, and propanol. An increase in pyrolysis temperature leads to higher yields of products derived from the main and side chains at cracking temperatures, such as carbon dioxide, carbon monoxide, methane, ethane, or low molecular weight alcohols. During thermal degradation, poly(alkyl methacrylates) produce monomer methacrylates as the predominant breakdown product in all tested pyrolysis conditions. In this work it was shown that

the poly(alkyl methacrylates) undergo a thermal degradation process at high temperatures that includes main chain scission.

Degradation mechanism of PMMA was also studied by a liquid chromatography with a particle beam mass spectrometry (LC–PB-MS) by Murphya and coworkers[43].In this study, the effect of polymer composition, concentration, molecular mass and monomer unit sequence on HPLC retention and MS ion intensity were studied. According to this study, a monomer yield of 92–98 % has been reported regardless of the temperature, as long as there is sufficient energy to break an initial carbon–carbon bond. They showed that in contrast to the degradation of poly(alkyl methacrylate) polymers, poly(alkylacrylate) polymers containing α-hydrogen in the α position and do not form a stable radical upon β-scission, thus these polymers have a higher probability of inter and intramolecular chain transfer and degrade by a random depolymerization mechanism. Therefore a variety of products are produced in random depolymerization resulting in a lower monomer yield.

In general, it can be concluded that the principal degradation reactions which occur in polymethacrylates are depolymerization to monomer, and ester decomposition yielding methacrylic acid units in the polymer and liberating the corresponding olefin. The greater the number of hydrogen atoms in the ester group, the greater is the tendency towards ester decomposition. There is also a strong tendency to ester decomposition in polyacrylates incorporating large numbers of β-hydrogen atoms but the degradation processes which occur in primary esters are much more complex.

1.4.3 Poly(butyl acrylate) and Its Copolymer with Poly(methyl methacrylate) (PMMA)

Poly(methyl methacrylate-co-butyl acrylate), p(MMA-co-BA) copolymers are extensively used as adhesives and coatings. The general formula for poly(butyl acrylate) (PBA) and poly(butyl methacrylate) (PBMA) is given in Figure 7. By combining methyl methacrylate, which can be considered as hard sequences contributing stiffness, with butyl acrylate, as soft sequences the polymer with desired property is obtained.

Konaganti et al. studied the photocatalytic and thermal degradations of PMMA, PBA, and their copolymers of different compositions [44]. In this study thermal degradation of the copolymers was investigated by TGA in a nitrogen flow environment. The normalized weight loss profiles for the copolymers showed that the thermal stability of the copolymers was increased with the mole percentage of BA in the P(MMA-co-nBA) copolymer.

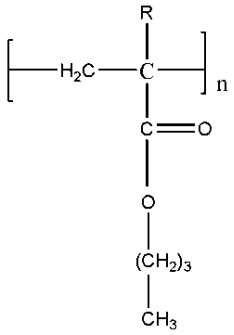

Figure 7. Poly(butyl acrylate) R=H, poly(butyl methacrylate) R=CH_3

Thermal stability of P(MMA-co-nBA) was also investigated by Leskovac and coworkers [45]. They studied the effect of crosslinking agents on the thermal stability of P(MMA-co-nBA) and P(S-co-nBA) polymers. Kinetic data indicated that the thermal degradation of the investigated copolymer systems is the first order reaction, and that the increase of activation energy may be an indication of thermal stability change in the copolymer systems. TGA curves for both copolymer series showed the existence of a one-step degradation mechanism above T_g in a relatively narrow temperature range from 350-410°C.min^{-1}. The results of this study also proved that butyl acrylate sequences increased the thermal stability of copolymers much more in the case of P(MMA-co-nBA) copolymers compared to those of the homopolymers, due to the stabilizing effect of BA units.

Mahalik et al. investigated the effect of the alkyl group's chain length on thermal degradation behavior of PMA, PBA and PEA homopolymers [25]. The thermal degradation was investigated at two different heating rates of 10 and 20°C.min^{-1} by TGA. As a result the kinetic parameters of the polymers degradation were calculated. In addition, thermal degradation of PBA and PMA was studied by pyrolysis and in solution.

On the basis of pyrolytic degradation studies, it was found that the degradability of the polymer decreases with an increase in the alkyl group chain length of poly(*n*-alkyl acrylate).

Another study investigating the thermal degradation behavior of poly(butyl acrylate) was done by Haken and coworkers [46]. They aimed to study the major pyrolysis products of PBA and its isomers. This study was investigated with a Curie Point Pyrolyser in conjunction with GC-MS. When the degradation products of poly(tertiary butyl acrylate) were considered, the formation of carbon dioxide, monomer and dimer was consistent with the mechanism for poly(n-butyl acrylate) degradation. In degradation products of poly(t-butyl acrylate) isobutylene formation was in agreement with the previous studies but the presence of carbon dioxide, monomer and dimer was first approved in this work.

Thermal degradation of some alkyl methacrylate's (methyl methacrylate, ethyl methacrylate, butyl methacrylate, and 2-ethylhexyl methacrylate) was also investigated by Czech et al. at temperatures between 300 and 800°C by another method which is pyrolysis gas chromatography [24]. In this work a simple degradation mechanism was suggested, providing a satisfactory explanation for the formation of the major breakdown products of alkyl methacrylates. Unsaturated monomeric alkyl methacrylates, carbon dioxide, carbon monoxide, methane, ethane, methanol, ethanol, and propanol were formed during thermal degradation of poly(alkyl methacrylates). These results quantified the various monomer yields, which depend on the number of carbon atoms in the alkyl side chain. The concentrations of monomers with short alkyl side chains (methyl and ethyl) were higher than for monomers with long side chains (butyl). Longer alkyl side chains in poly(alkyl methacrylates) corresponded to fewer monomers formed during pyrolysis. The mechanism of thermal degradation supported the absence of alkenes, the presence of alcohols, and monomeric alkyl acrylates. During cracking reactions, especially at higher temperatures, gaseous products and mixtures of low molecular weight alcohols were formed. An increase in pyrolysis temperature lead to higher yields of products derived from the main and side chains at cracking temperatures, such as carbon dioxide, carbon monoxide, methane, ethane, or low molecular weight alcohols. During thermal degradation, poly(alky methacrylates) produced mainly monomer as the predominant breakdown product in all tested pyrolysis conditions.

In another study the thermal-ageing of a series of commercial acrylic/methacrylic resins, homo and copolymers which are extensively used as stone protective, has been investigated under conditions of constant temperatures at 110, 135 and 150°C [47]. In this work, structural and molecular changes induced by the isothermal treatments in a forced-air circulation oven were followed by infrared and UV–VIS spectroscopy, and size exclusion chromatography (SEC), respectively. It was shown that the stability of the resins could be controlled by the reactivity of alkyl side groups, whose oxidative decomposition is favored in the case of long ester groups, like the isobutyl and butyl ones. At the same time, the polymers containing long ester groups undergo fast and extensive cross-linking, together with loss of short chain fragments. In the acrylic/methacrylic resins where all or the majority of the alkyl side groups are short, chain scissions prevail over cross-linking and no insoluble fractions were formed.

The degradation behavior of various high-molecular-weight acrylic polymers namely PMMA, PnBMA, PnBA and poly(lauryl methacrylate) (PLMA) was also investigated under extreme environmental conditions [48]. The degradation behavior of the polymeric materials on their surface was followed via attenuated total reflectance infrared Spectroscopy (ATR-IR), high resolution FTIR microscopy, and X-ray photoelectron spectroscopy. As a result of this study it was concluded that the general degradation mechanism of studied polymers involves the loss of the ester side groups to form methacrylic acid followed by cross-linking.

There are also some studies about the photooxidative stability of acrylic and methacrylic polymers in the literature. Chiantore et al. had investigated the photooxidative stability of poly(methyl acrylate), poly(ethyl acrylate), poly(ethyl methacrylate) and poly(butyl methacrylate) polymers under conditions of artificial solar light irradiation [49, 50]. Molecular and chemical changes induced by the light treatment were followed by size exclusion chromatography and fourier transform infrared spectroscopy. In this work, the acrylate units were found to be more reactive towards oxidation, in comparison with the methacrylate ones. With short alkyl side groups chain scissions prevailed over cross-linking reactions both in acrylate and methacrylate samples. This work showed that the degradation of poly(butyl methacrylate) proceeds in a completely different way, with extensive cross-linking and simultaneous fragmentation reactions.

The conditions required for alcohol production is an important step in polyacrylates degradation mechanism. Goikoetxea et al. investigated the mechanisms involved in the formation of n-butanol during the synthesis of butyl acrylate containing lattices [51]. The experimental results showed that neither the hydrolysis of butyl acrylate nor of the ester bond in the butyl acrylate segments of the polymer played a major role in the formation of n-butanol, which was mainly generated from the polymer backbone, by transfer reactions to polymer chain followed by cyclization. It was found that the hydrolysis of either butyl acrylate monomer or of the ester bond in the BA units in the copolymer was not responsible for the formation of any significant fraction of n-butanol. Mainly from the polymer backbone n-butanol was formed. The proposed mechanism was as follows: radicals abstracted hydrogen from the tertiary carbon of the n-BA unit. This radical could propagate or if there were at least two adjacent acrylate units, cyclize to form one molecule of n-butanol. The propagation is a second order process and it was favored in the presence of free monomer, whereas cyclization is a first order process, and it was important when the concentration of free monomer was low. According to this mechanism process variables that lead to low concentration of monomer in the system will yield higher n-butanol concentrations.

Another type of degradation for the polymers is photocatalytic degradation. In recent years the photocatalytic degradation of the homopolymers, poly(methyl methacrylate) (PMMA), poly(butyl methacrylate) (PBMA), and their copolymers P(MMA-co-BMA) was studied in o-dichlorobenzene in the presence of commercial TiO_2 (Degussa P-25) [52]. Gel permeation chromatography was used to determine the evolution of molecular weight distributions with reaction time. The experimental data indicated that the polymers PMMA and PBMA and their copolymers degrade by simultaneous random and chain end scission. A continuous distribution model was developed for the mechanism involved in degradation by both random and chain end scission and used to determine the degradation rate coefficients. In this work the degradation of PMMA, PBMA, and their copolymers was also investigated by thermogravimetric analysis. The copolymers exhibited better thermal stability than the homopolymers in contrast to that observed for photocatalytic degradation. The photodegradation of these copolymers was determined in the absence of catalyst and in the presence of two different catalysts. Simultaneous random and chain end scission was observed in all cases for all polymers.

A model based on continuous distribution kinetics was developed considering both random and chain end scission. The degradation rate coefficients were determined by fitting the model to experimental data. The photocatalytic degradation rate coefficient of the copolymers increased linearly with the increase in MMA composition for both random and chain end scission. However, the thermal stability of the copolymers depends on the degree of degradation with the copolymers being more stable than the homopolymer at higher conversions.

1.4.4 Poly(benzyl methacrylate) PBzMA and Its Copolymer with Poly(methyl methacrylate) PMMA

Polybenzyl methacrylate (PBzMA) is mostly used as curing agent in polymer science. For example, due to T_g value intermediate between those of polyvinyl acetate (PVAc) and PMMA, it has been selected as modifier of epoxy thermosets. In the system epoxy/PBzMA good interactions between ether groups of epoxy and phenyl groups of PBzMA would take place, affecting the initial miscibility and phase separation on curing [53]. The general formula for PBzMA is given in Figure 8.

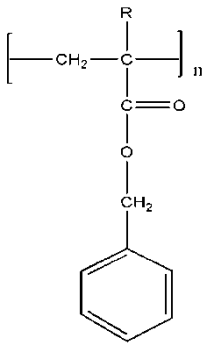

Figure 8. Poly(benzyl acrylate) R=H, poly(benzyl methacrylate) R=CH_3

Tsai and coworkers reported a top-down/bottom-up approach for nanoimprint, in which benzyl methacrylate was selected as the monomer for surface-initiated polymerization [54]. The reaction step involves the growth of polymer brushes from the surface of the patterned network via controlled-radical polymerization.

Consequently, various nanoscopic structures with different feature sizes and functional groups can be grown from the original molded template**.** Although most controlled-radical polymerization reactions on surfaces have been conducted at fairly raised temperatures, mostly between 90 and 120°C, grafting reaction of the patterned polymers to a certain thickness should be completed rapidly and under ambient temperature. That's why benzyl methacrylate is selected as the monomer for surface-initiated polymerization.

Copolymer of BzMA with MMA is also a valuable end product especially in pharmaceutical industry. Ishikawa and coworkers have obtained controlled-release tablet by oxygen plasma irradiation [55]. Since PBzMA has dual intramolecular functions, a plasma degradable main chain and a plasma-cross-linkable benzyl group in the side chain as an effect of plasma irradiation copolymer of MMA and BzMA was used as a single wall material. In this work it was shown that the dissolution profiles can be varied so as to cause release of drug at different rates, depending on the set of conditions chosen for tablet manufacture and for plasma operation which is mainly depended on the degradation of copolymer. Although PBzMA and its copolymer with PMMA are very valuable end products, there is no study evaluating the thermal degradation behavior of this polymers.

1.4.5 Poly(isobornyl acrylate) (PIBA) and Its Copolymer with Poly(methyl methacrylate) (PMMA)

Poly(isobornyl acrylate) has a number of interesting physical properties, such as a high glass transition temperature (T_g) (94°C) and hardness (19.6 kg/mm^2 at 20°C). While polyacrylates have, in general, a low T_g, the bulky side group of isobornyl acrylate is responsible for the high T_g, comparable with the one of poly(methyl methacrylate) (PMMA, T_g = 105°C) or polystyrene (PS, T_g = 100°C). Like PIBA, Poly(isobornyl methacrylate) (PIBMA) is a novel transparent polymer resin, which can also be used as optical material. The general formula for PIBA is given in Figure 9. Since PIBMA and PIBA are widely used their thermal degradation behavior is an important aspect of polymer science [56].

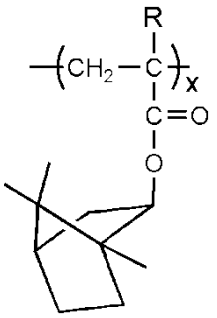

Figure 9. Poly(isobornyl acrylate) R=H, poly(isobornyl methacrylate) R=CH_3.

Although many studies have been carried out on thermal stability of methacrylate polymers containing various ester residues, the thermal degradation of methacrylate polymers containing the isobornyl moiety in the side chain has not been much studied. Due to its low vapor pressure and relatively high glass transition temperature of acrylic networks derived from it, isobornyl methacrylate is also used as reactive solvent of polyethylene (PE). With the aid of PIBMA, phase separation takes place in the course of polymerization generating a dispersion of PE domains in the acrylic matrix. This method is used to generate a multiphasic material with some improved properties (mechanical, thermal, optical, etc.), with respect to those of the pure components. In particular, these formulations are used to toughen the generated polymer network or to facilitate processing of the thermoplastic polymer. Since the resulting polymer includes PIBMA in the structure it is important to know thermal degradation mechanism and products of this polymer [57].

Since PIBMA is a secondary alkyl ester, its thermal decomposition is expected to proceed via both main and side chain scissions, of which the former leads to depolymerization to give a corresponding monomer and the latter includes an olefin elimination and other complicated degradations**.** Matsumoto and coworkers investigated the thermal degradation behavior of PIBMA in detail [58]. The decomposition behavior of the polymer was investigated by TGA in a nitrogen stream. The weight-loss curves of PIBMA showed two T_{max}'s at 314 and 436°C.This experiment was performed at 260 and 290°C for 1 h in vacuum, the volatile products trapped in a dry ice-methanol bath and was analyzed by NMR spectroscopy. The 'H-NMR spectra indicated that the decomposition at 260°C released camphene (I) as a

main product without a trace of corresponding olefin (II) as a β-elimination product (Scheme 1). Both camphene and IBMA were produced at 290°C and camphene production mechanism is shown in Scheme 2.

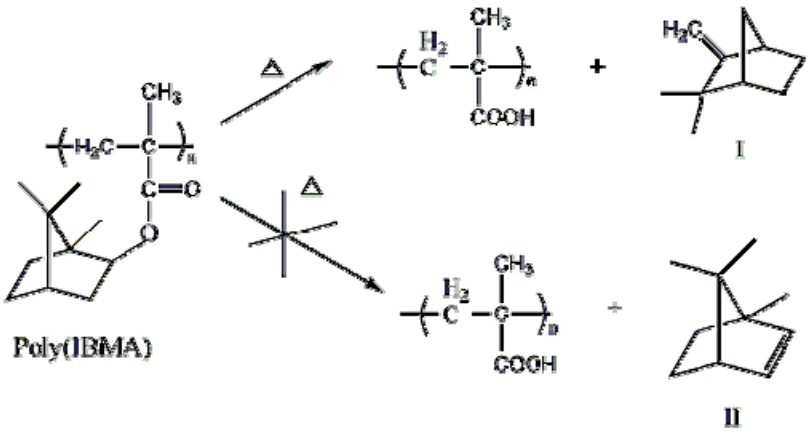

Scheme 1. Poly(isobornyl methacrylate) thermal degradation mechanism.

According to TGA curves, the weight loss at 400°C for PIBMA is close to the value calculated assuming the elimination of camphene and subsequent dehydration from the resulting poly (methacrylic acid) leading to the formation of poly (methacrylic anhydride).

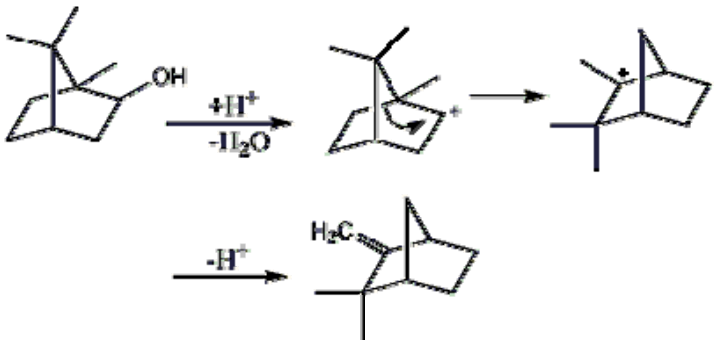

Scheme 2. Camphene formation reaction.

In another study, Doğan et al. investigated the kinetic of thermal degradation of PIBMA by TGA [59]. The apparent activation energies of thermal decomposition process were determined by multiple heating rate kinetics. Contrary to the results of Matsumoto and coworkers TGA curves showed that the thermal decomposition takes place mainly in one stage.

Jakubowski et al. synthesized well-defined statistical, gradient and block copolymers consisting of IBA and nBA via atom transfer radical polymerization (ATRP) [27]. Thermomechanical properties of synthesized materials were analyzed via DSC, dynamic mechanical analyses (DMA) and small-angle X-ray scattering (SAXS). While statistical copolymers showed a single Tg, block copolymers showed two Tgs and DSC thermogram for the gradient copolymer indicated a single, but very broad, glass transition. Presented results showed that only by changing arrangement of two different monomer units, one can obtain materials with significantly different properties. In a similar way, one can copolymerize other monomers and affect not only physical properties of final polymer materials but also their degradation rates and toxicity, both of which might be important, for example, in biomedical applications.

As explained above, although there is some estimations about the thermal degradation mechanisms of poly(isobornyl acrylate) and its kinetic parameters there is no study with Py-GC-MS or DP-MS about the thermal decomposition mechanism.

1.5 Aim of Work

Despite its advantages, the glass transition temperature of PMMA is about 100°C, which limits its application in the textile industry or in optical-electronic industry. As a result, fiber-optic applications of PMMA is limited to about 80°C, above which PMMA fiber becomes soft and loses its mechanical integrity. The other disadvantage of PMMA is its brittleness thus PMMA fibers cannot be used in textile industry for sensing purposes.

Therefore, to increase Tg of PMMA, it can be copolymerized with rigid or bulky monomers and with monomers that can form hydrogen bonds through the carbonyl group of methyl methacrylate.

For this purpose, monomers containing isobornyl, benzyl and butyl groups as side chain are chosen to copolymerize and to obtain fibers with PMMA. Due to the bulky side chains, the free rotation of the polymer will be restricted giving rise to the reduced chain flexibility and increase in the Tg of the resulting copolymers and fibers. Due to improved properties of these polymers their application area will also increase which makes the information about thermal degradation characteristics of PMMA and its corresponding copolymers and fibers also very important.

Most of the researches on thermal characterization are focused on TGA and DSC studies that can only give information on thermal stability, weight loss and kinetic parameters of thermal degradation. Few studies on thermal degradation products involved pyrolysis GC-MS, TGA-FTIR and TVA analyses. Yet, with the use of classic techniques secondary reactions during heating can not be eliminated and only stable degradation products can be detected. Thus, the data obtained can not be used to investigate the thermal degradation mechanism.

In this work, thermal degradation characteristics, thermal degradation products and mechanisms of

- methacrylate homopolymers: PMMA, PBMA, PIBMA, PBzMA
- acrylate homopolymers: PnBA, PtBA, PIBA,
- copolymers: P(MMA-co-nBA), P(MMA-co-IBA), P(MMA-co-BzMA), P(MMA-co-nBA-IBA), and P(MMA-nBA-co-IBA-co-Bz),
- copolymer fibers: P(MMA-co-BA)f, P(MMA-co-BzMA)f, and P(MMA-co-nBA-IBA)f

are analyzed via direct pyrolysis mass spectrometry.

The effects of

- substituents on the main and side chains,
- each component of the copolymer on thermal characteristics of the other and
- fiber formation

on thermal stability, degradation characteristics and thermal degradation mechanisms are investigated.

CHAPTER 2

EXPERIMENTAL

2.1 Materials

2.1.1 Homopolymers

Most of the homopolymers were prepared and characterized by Dr. Evren Aslan Gürel. The ^{1}H-NMR and FT-IR spectra are presented in Appendix. Methyl methacrylate (MMA, Aldrich), isobornyl acrylate (IBA, Aldrich), butyl acrylate (BA, Aldrich), and benzyl methacrylate (BzMA, Aldrich) were purified by passing through a basic alumina column and polymerized using azobis(isobutyronitrile) (AIBN), obtained from Aldrich, as the initiator. Poly(isobornyl methacrylate) PIBMA, poly(n-butyl methacrylate) PnBMAand poly(t-butyl acrylate) PtBA were received from Polymer Source and used as received. The number and weight average molecular weights and polydispersity indexes of the polymers determined by size exclusion chromatography (SEC) are summarized in Table 1.

Table 1: Molecular weights and polydispersity indexes of the homopolymers.

Name of the polymer	Mn	Mw	PDI
Poly(methyl methacrylate)	100625	318927	3.2
Poly(isobornyl methacrylate)	7000	9000	1.3
Poly(isobornyl acrylate)	73070	274863	3.8
Poly(n-butyl methacrylate)	1500	1700	1.2
Poly(n-butyl acrylate)	52101	120353	2.3
Poly(t-butyl acrylate)	13000	14500	1.1
Poly(benzyl methacrylate)	59089	468810	7.9

2.1.2 Copolymers

All the copolymers used were synthesized and characterized by Dr. Evren Aslan Gürel. In general, methyl methacrylate (MMA) was copolymerized with butyl acrylate (BA), benzyl methacrylate (BzMA) or isobornyl methacrylate (IBMA) in an aqueous suspension via free-radical polymerization using azobis(isobutyronitrile) (AIBN) and n-dodacene mercaptan as the initiator and chain transfer agents respectively, as shown in Scheme 3.

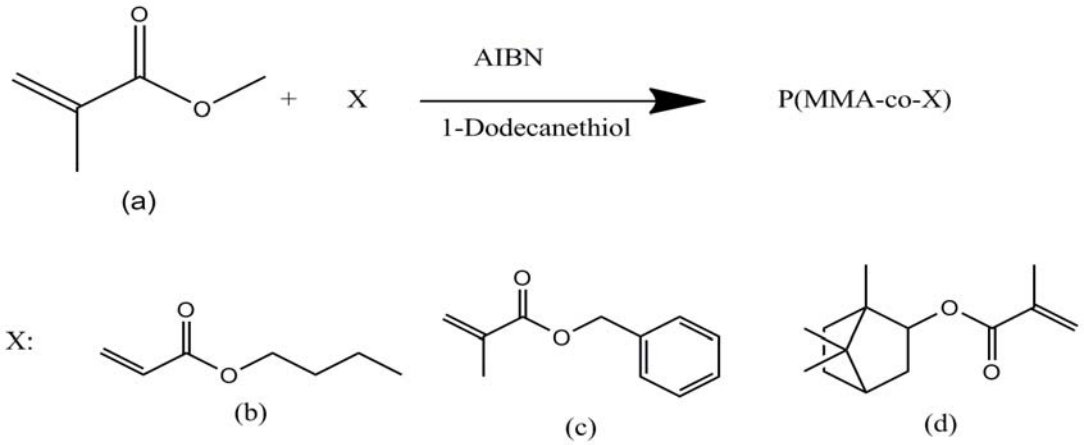

Scheme 3. Chemical structures of (a) MMA, (b) BA, (c) BzMA, (d) IBMA and co-polymerization reaction.

The same experimental conditions were used in the preparation of all the copolymers involving two, three or four different monomers. In summary, the AIBN initiator (0.16 g) and 1-dodecane thiol (0.2 mL) were dissolved in a solution containing the monomers (0.1 mol) and added to aqueous solution of polyvinyl alcohol (PVA) (1.2 g PVA in 184 mL water) in a three neck flask at 80°C by purging with nitrogen gas. The polymerization was carried out at 80°C for 6 hours by stirring at a rate of 800 rpm. The copolymer beads were isolated by filtration, washed with water and dried at 80°C in vacuum oven. After completion of the reaction, the polymer sample was dissolved in dichloromethane and precipitated in methanol and dried in high vacuum for 15 h.

The number, and weight average molecular weights and the polydispersity indexes of the copolymers were determined by gel permeation chromatography (GPC) (Viscotek GPC) using a UV detector (410 model refractive index). Samples were eluted with tetrahydrofuran through a linear ultrastryroge column at a flow rate of 1mL·min $^{-1}$. The molecular weights were determined relative to PMMA standard. The molecular weights and polydispersity indexes of the copolymers involving two monomers namely P(MMA-co-nBA), P(MMA-co-BzMA), P(MMA-co-IBA), those involving three monomers P(MMA-co-nBA-co-IBA) and those involving four monomers, P(MMA-co-nBA-co-IBA-co-BzMA) are given in Table 2.

Table 2: Molecular weights and polydispersity indexes of the copolymers.

Name of the copolymer	Composition (mol %)	Mn	Mw	Mw/Mn (PDI)
P(MMA-co-nBA)	87.5-12.5	105111	45565	4.3
P(MMA-co-IBA)	90-10	173489	53285	3.1
P(MMA-co-BzMA)	90-10	61101	34565	5.7
P(MMA-co-nBA-co-IBA)	90-5-5	39728	17460	4.4
P(MMA-co-nBA-co-IBA)	70-15-15	34586	16465	4.8
P(MMA-co-nBA-co-IBA-co-BzMA)	90-5-3-2	49039	16122	3.3

2.1.3 Fibers

The polymers were melt-spinned in a pilot melt spinning plant at Empa (Swiss Federal Laboratories for Materials Testing and Research) by Dr. Evren Aslan Gürel. The schematic diagram of the melt spinning process is shown in Figure 10. The polymers were molten using two single screw extruders. The fiber extrusion was done at 200^{o}C. The diameters of the extruder screws were 13 mm and 18 mm respectively, with a length-to-diameter (L/D) ratio of 25. Spin pumps enabled a constant mass flow of 0.5 to 40 cm^{3}·min^{-1}. A bi-component die consisted of a tube with 0.4 mm inner diameter and 0.7 mm outer diameter within a 1.2 mm capillary.

The evaporating monomers and oligomers were sucked in by an exhaust vent. The extruded fluid was spun into the 2.8 m drop shaft, which was equipped with a removable or extendable annealing tube at a maximum temperature of 350°C. The quenching chamber with a length of 1.4 m that can be adjusted had a maximum air flow of 520 $m^3 \cdot min^{-1}$. After cooling and wetting with a spin finish, the filaments were drawn by three heated godets. The maximum temperature of the godets was 160°C. Their speed can be varied between 100 to 1800 rpm. The draw ratios (given by the ratio of speeds of the godets) were typically chosen between 1.5 and 6. Finally a winder with a maximum speed of 2000 rpm was used to spool the filaments onto a bobbin. The molecular weight distribution and mole percentage of the corresponding fibers are given in Table 3.

Table 3: Molecular weights and mole percentages of fibers.

Fiber Composition	Mol %	Mn	Mw	Mw/Mn (PDI)
P(MMA-co-nBA)f	87-13	43710	88063	2.02
P(MMA-co-nBA-co-IBA)f	70-15-15	49886	111748	2.24
P(MMA-co-BzMA)f	87-13	37330	135611	3.63

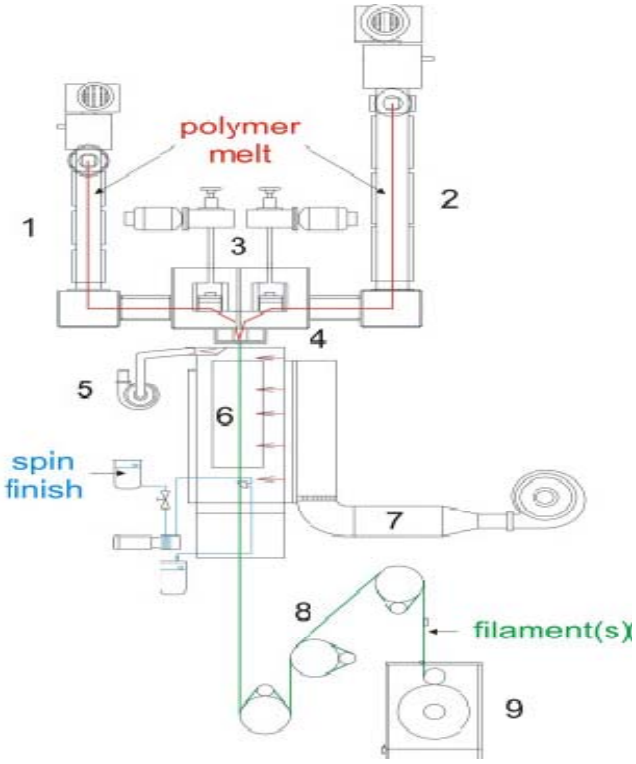

Figure 10. Schematic diagram of the existing bi-component melt spinning facility at Empa, Laboratory for Advanced Fibers.

2.2 Characterization

2.2.1 Fourier Transform Infrared (FTIR)

Attenuated Total Reflectance (ATR) Fourier Transform Infrared (FT-IR) spectra in the range of 400 to 4000 cm^{-1} were recorded with FT-IR spectrometer (Bio-Rad).

2.2.2 Differential Scanning Calorimetry (DSC)

Differential scanning calorimetry (DSC) analyses were carried out to determine T_g of the samples with Mettler Toledo DSC822. Differential calorimetry data were collected in the temperature of range 20 to 250°C at a heating rate of 10°C/min under nitrogen atmosphere.

2.2.3 Thermogravimetric Analyzer (TGA)

Thermal decompositions of the samples were studied by thermogravimetry analyzer (TGA). The analyses were conducted by Perkin Elmer STA 6000 simultaneous thermal analyzer at a heating rate 10°C·min^{-1} in the temperature range from 30 to 600°C.

2.2.4 Direct pyrolysis mass spectrometry (DP-MS)

Direct pyrolysis mass spectrometry (DP-MS) analyses were performed on a 5973 HP quadrupole mass spectrometry system coupled to a JHP SIS direct insertion probe pyrolysis system for thermal analyses. 70 eV EI mass spectra, at a rate of 2 scan·s^{-1}, were recorded. 0.01 mg samples in the flared glass sample vials were heated to 450°C at a rate of 10 °C·min^{-1}. The pyrolysis mass spectrometry analyses were repeated at least two times to ensure reproducibility.

Some of the pyrolysis experiments were repeated by using 25 eV ionization energy to investigate the effect of dissociative ionization on fragmentation pattern observed in the pyrolysis mass spectra. The elative intensities of high mass peaks increased, however in general reproducibility and signal to nose ratio were decreased. Thus, 70 eV EI mass spectra were used for analyses of thermal degradation behaviors.

For the analyses of pyrolysis mass spectra, the mass spectrum recorded at the TIC maximum was selected first. The next step was the identification of all intense peaks. The trends in the evolution profiles were used to group the products to determine whether the fragment was generated during pyrolysis or EI ionization. For each peak in a given group, assignments were made and tabulated considering the mass differences and possible dissociation processes, classical fragmentation pathways for organic compounds and taking into consideration the structure of the sample under investigation.

CHAPTER 3

RESULTS AND DISCUSSION

Thermal characterization of acrylate and methacrylate homopolymers and copolymers of PMMA with PBA, PBzMA and PIBA are investigated by direct pyrolysis mass spectrometry technique. Furthermore, the effect of fiber formation on thermal degradation characteristics is studied for P(MMA-co-BzMA), P(MMA-co-nBA) and P(MMA-co-BzMA-co-IBA) fibers. The effect of copolymerization and fiber formation on the degradation pathways and relative abundances of products are evaluated.

3.1 Homopolymers

3.1.1 Thermal Degradation of Poly(methyl methacrylate) PMMA

Thermal degradation of PMMA is studied in the literature in details [31-33]. It has been determined that thermal degradation of PMMA occurs by depolymerization mechanism yielding mainly the monomer. TGA curve of the PMMA is given in Figure 11. As can be seen the PMMA sample shows a two-step weight loss in the temperature range of 300–400°C due to polymer degradation.

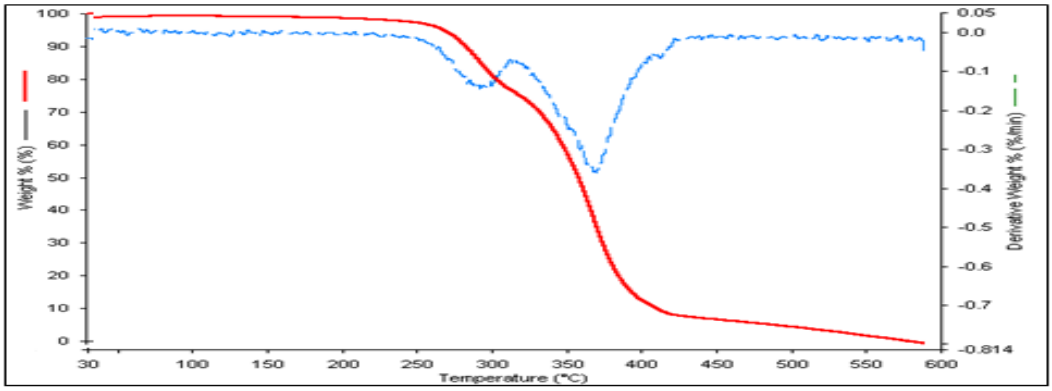

Figure 11. TGA curve of PMMA.

The total ion current (TIC) curve, variation of total ion yield as a function of temperature also shows two step thermal degradation, in consistent with TGA results (Figure 12). The mass spectra recorded at 325 and 420°C at the maximum of the peaks present in the TIC are also given in the figure.

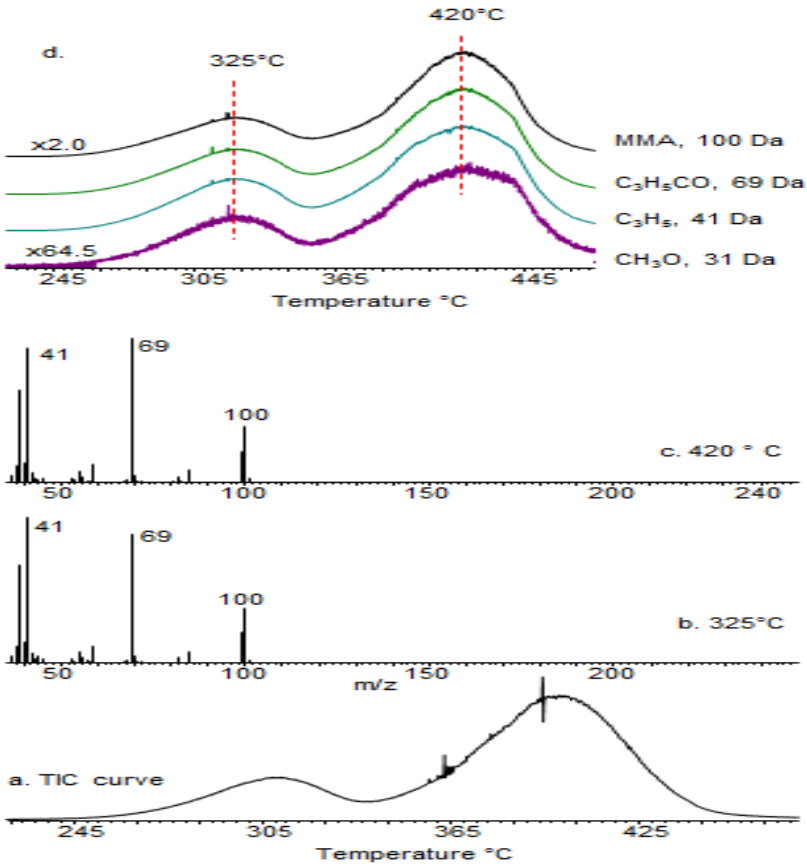

Figure 12. a. TIC curve, the pyrolysis mass spectra of PMMA at b. 325 and c. 420°C and d. single ion evolution profiles of some selected products.

The pyrolysis mass spectra of PMMA are expected to be similar to the mass spectrum of methyl methacrylate, as the main product of thermal degradation is the monomer. The mass spectrum of MMA monomer shows a moderate molecular ion peak at 100 Da, a base peak at 41 Da due to CH_2CCH_3 and an intense peak at 69 Da due to CH_2CCH_3CO fragments, generated by loss of $COOCH_3$ and OCH_3 respectively, as shown in Figure 13.

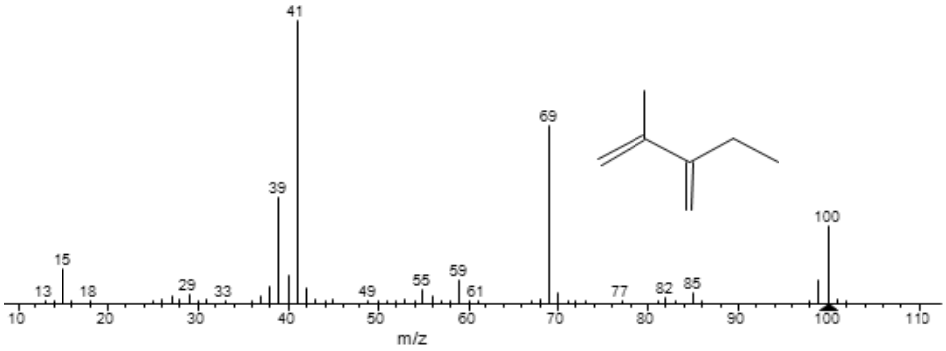

Figure 13. Mass spectrum of MMA.

The relative intensities (RI) and the assignments made for the intense and/or characteristic peaks present in the pyrolysis mass spectra of PMMA recorded at 325 and 420°C are collected in Table 4.

Table 4: The relative intensities and assignments made for the intense and/or characteristic peaks present in the pyrolysis mass spectra of PMMA recorded at 325 and 420°C.

m/z (Da)	Relative intensity		Assignments
	325°C	420°C	
18	29	10	H_2O
28	201	81	CO, C_2H_4
31	15	15	CH_3O
39	587	591	C_3H_3
41	1000	988	C_3H_5
44	18	14	CO_2
69	858	1000	C_3H_5CO
85	81	105	C_3H_5COO
86	4	5	C_3H_5COOH
99	204	263	M-H
100	385	513	M, monomer

For a better understanding, the single ion evolution profiles of some of the characteristic and/or intense products, namely CH_3O (39 Da), C_3H_5 (41 Da), C_3H_5CO (69 Da) and monomer, M (100 Da) recorded during the pyrolysis of PMMA are also given in Figure 13.

The pyrolysis mass spectra of PMMA recorded at around the peak maxima shows classical fragmentation pattern of MMA due to dissociative ionization, with a base peak at 69 Da associated with $CH_2C(CH_3)CO$ fragment in accordance with the depolymerization mechanism. The low temperature peak is assigned to thermal degradation of low molar mass oligomers, chains involving head-to-head linkages and loss of unsaturated end groups [31-33]. While the high temperature peak is attributed to a mixture of chain end and chain scission processes followed by depropagation step yielding mainly the monomer. Single ion evolution profiles included in Figure 13 clearly show identical trends indicating that all products are generated through the same decomposition pathways.

3.1.2 Thermal Degradation of Acrylates Involving Butoxy Groups

The mass spectra of the corresponding monomers of poly(n-butyl acrylate), poly(t-butyl acrylate) and poly(n-butyl methacrylate) are shown in Figure 14. For a polymer that degrades by a depolymerization mechanism the pyrolysis mass spectrum of the polymer resembles the mass spectrum of the corresponding monomer. As can be noted from the Figure 14, molecular ion peak is either absent or very weak in the mass spectrum of these molecules. The base peaks are due to the rupture of CO-OR bonds yielding CH_2CHCO (m/z = 55 Da) for the two acrylates. Fragment ions due to butoxy group, C_4H_9O (m/z=73 Da) are also abundant for these molecules. In case of methacrylate, CH_2CCH_3 (m/z = 41 Da) being a secondary carbocation is the base peak. The corresponding peak due to CH_2CH (m/z=27 Da) is also recorded in the mass spectra of the acrylates but is relatively weak. For, the methacrylate molecule, CH_2CCH_3CO (m/z = 69 Da) fragment ion due to cleavage of C-O bond and $CH_2CCH_3C(OH)_2$ fragment ion (m/z=87 Da) generated by double H-transfer reaction are also significantly abundant. For all the molecules, the peak due to C_4H_8 ion (m/z=56 Da) produced by McLafferty rearrangement reaction is pronounced but, the peak due to butyl is only intense for the t-butyl molecule.

The peak at 113 Da due to loss of CH_3 group is also recorded. Furthermore, peaks due to loss of ethyl from the butyl group at 29 Da are detected.

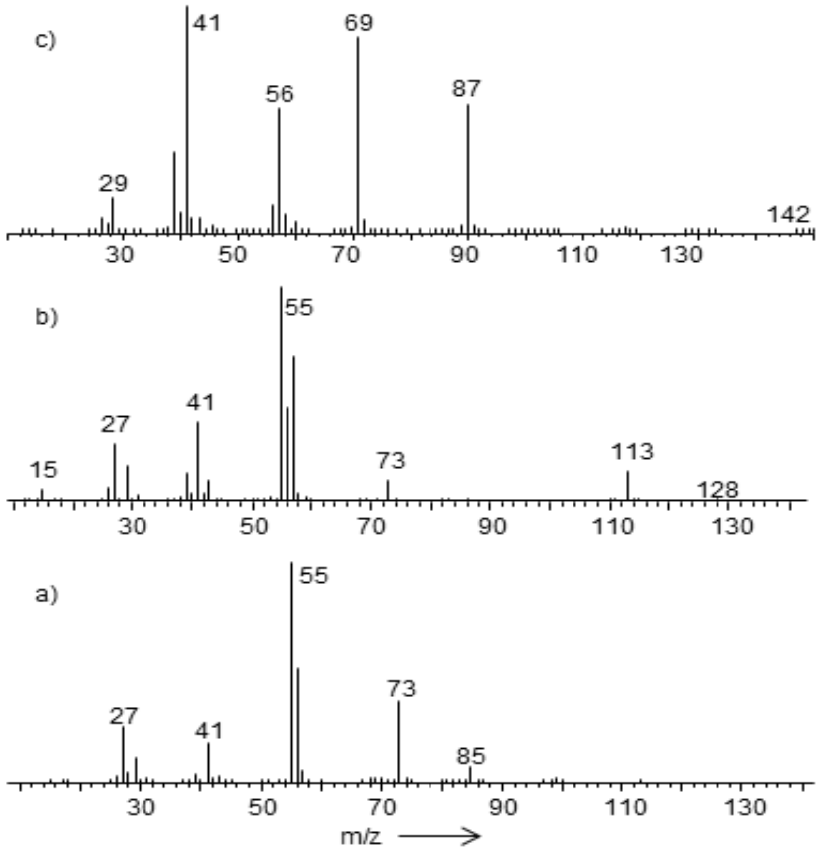

Figure 14. Mass spectra of monomers a) n-butyl acrylate, b) t-butyl acrylate and c) n-butyl methacrylate

In the light of the fragmentation patterns observed for the monomers, pyrolysis mass spectra of the corresponding polymers are analyzed.

3.1.2.1 Thermal Degradation of Poly(n-butyl methacrylate) PnBMA

When the TGA curve of the PnBMA is analyzed it is clear that most of the weight loss due to thermal degradation is observed at around 395°C. There is also some loss at around 425°C (Figure 15).

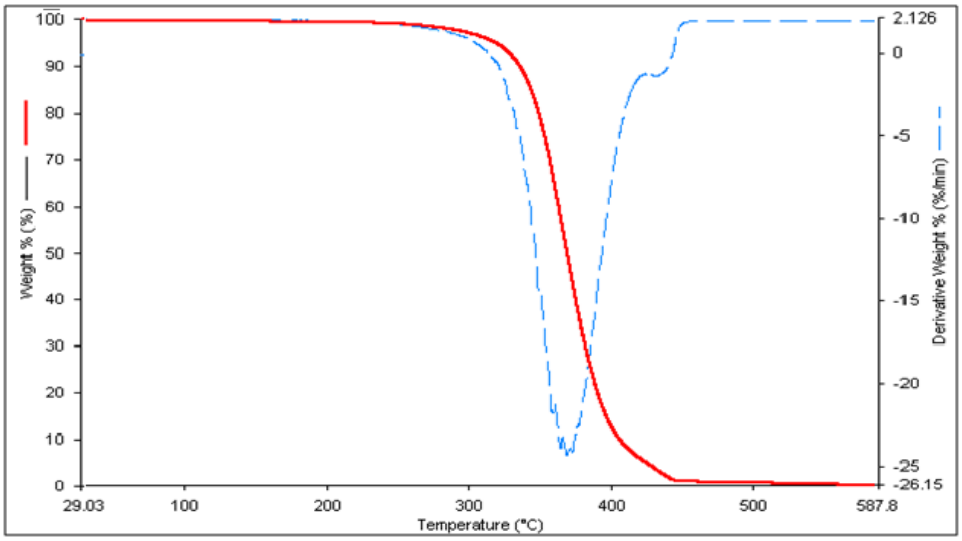

Figure 15. TGA curve of PnBMA.

Also, the TIC curve of PnBMA in Figure 16 shows a broad peak with a maximum at 395°C and a shoulder at 425°C in accordance with the TGA results. The mass spectrum recorded at the peak maximum is quite similar to that of the monomer, with intense peaks at 41, 56, 69, 87 and 113 Da indicating that depolymerization mechanism is the main thermal degradation pathway. This behavior can directly be associated with generation of a tertiary radical upon cleavage of the CH_3C-CH_2 bond.

The pyrolysis mass spectra of PnBMA recorded at around 425°C exhibits noticeable changes in the fragmentation pattern pointing out that at elevated temperatures, the degradation of the residual polymer followed different pathways other than depolymerization. In this region again CH_2CCH_3 is the most abundant fragment, however, significant decrease in the relative yields of other fragments diagnostic to monomer are observed. A careful study of the pyrolysis mass spectra revealed evolution of monomer, low mass oligomers, products involving unsaturation and H_2O, although not very pronounced, at around 412°C.

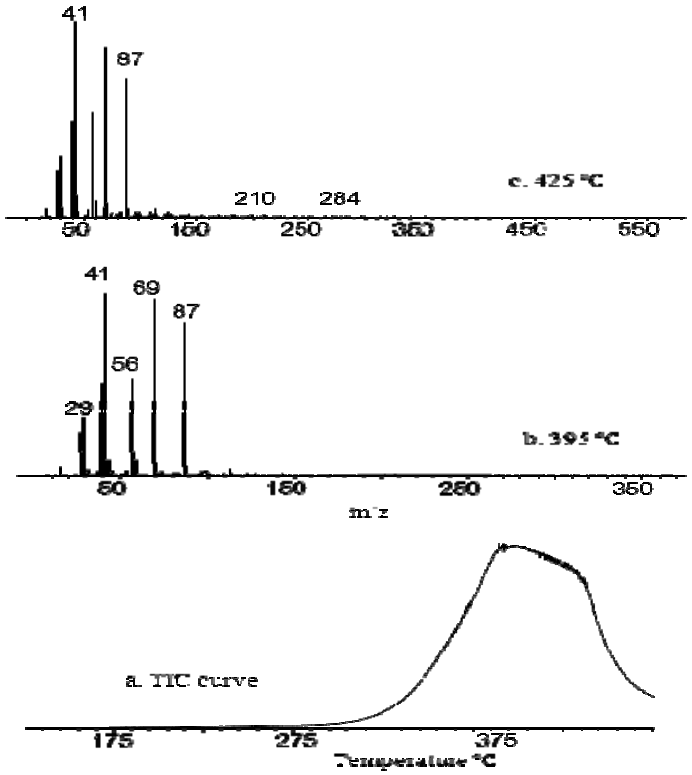

Figure 16. a. TIC curve and the pyrolysis mass of PnBMA at b. 395 and c. 425°C

The relative intensities and the assignments made for the characteristic and/or intense peaks present in the pyrolysis mass spectra recorded at 395 and 425°C are summarized in Table 5. Although the monomer and the oligomer, M_x, peaks recorded at 142, 284, 426, 568 Da for x=1 to 4 are significantly weak, the intensity of the peaks obtained after the degradation of depolymerization products by dissociative electron impact ionization are quite significant.

Table 5: The relative intensities and assignments made for the intense and/or characteristic peaks present in the pyrolysis mass spectrum of PnBMA at 395 and 425°C.

m/z (Da)	Relative Intensity		Assignments
	395°C	425°C	
18	1	8	H_2O
27	236	240	CH_2CH
29	307	226	C_2H_5
39	520	544	C_3H_3
41	1000	1000	CH_2CCH_3
44	17	113	CO_2
55	161	309	CH_2CHCO
56	510	654	$CH_2=CHCH_2CH_3$
57	127	186	C_4H_9
69	955	570	$CH_2=C(CH_3)CO$
73	16	14	C_4H_9O
87	838	324	$CH_2CCH_3C(OH)_2$
113	33	78	$M\text{-}CH_3$
123	8	135	$T\text{-}3COOC_4H_9$
136	2	71	$D\text{-}2HOC_4H_9$
137	1	196	$D\text{-}OC_4H_9\text{-}HOC_4H_9$
141	5	38	M-H
142	5	31	M, monomer
183	3	41	$D\text{-}COOC_4H_9$
228	-	13	MC_3H_5COOH
278	-	54	$T\text{-}2HOC_4H_9$
284	-	23	D, dimer
370	-	7	DC_3H_5COOH
426	-	5	T, trimer
568	-	4	Te, tetramer

When the side chains of the PnBMA polymer are cleaved at the carbonyl oxygen bond radicals $M_x\text{-}OC_4H_9$ where x=1 to 3, generating series of peaks at 69, 211, and 353 Da are obtained. The products at $M_x\text{-}COOC_4H_9$ (41, 183, 325 Da for x=1 to 3) are obtained by loss of side chains.

For a better understanding, the single ion evolution profiles of some of the characteristic and/or intense products, namely C_3H_5 (41 Da), C_4H_8 (56 Da), $C_3H_5C(OH)_2$ (87 Da), C_4H_9 (57 Da), H_2O (18 Da), CO_2 (44 Da), monomer, M (142 Da), MC_3H_5COOH (210 Da), and dimer, D (284 Da) recorded during the pyrolysis of PnBMA are given in Figure 17.

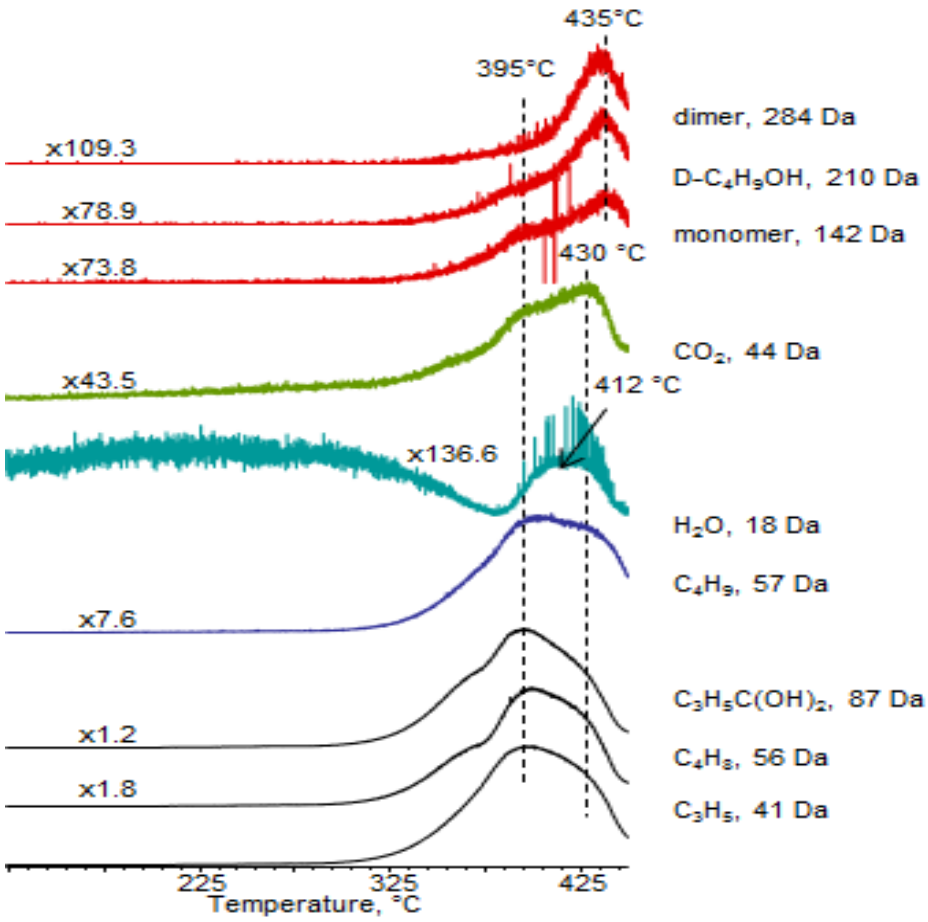

Figure 17. Single ion evolution profiles of some selected products detected during the pyrolysis of PnBMA.

Inspection of single ion evolution profiles of characteristic and/or intense products indicated that thermal degradation occurs above 320°C. Products associated with dissociative ionization of the monomer show identical evolution profiles with a maximum at 395°C. Whereas, the yield of monomer and oligomers are maximized

at around 430°C, indicating that thermal degradation by random chain scissions becomes more effective at high temperatures. Evolution of but-1-ene is detected over a broad temperature range. On the other hand, though quite low, detection of peaks due to H_2O at around 412°C and CO_2 may be associated with γ-H transfer reactions from the butyl groups (McLafferty rearrangement reactions) and elimination of butanol or H_2O generating anhydride units that may further eliminate CO_2 and CO yielding crosslinked and unsaturated units, as shown in Scheme 4. As a result of this reaction, the series of peaks obtained at 72, 200, 328, 456, 584 Da for R=H (for x=0 to 4) and 86, 228, 370, 512, 654 Da for R=CH_3 (for x=0 to 4) are obtained. However, taking into account the significantly low yields of these products, it may be concluded that for PnBMA, the major thermal degradation pathway is depolymerization and competing processes such as random chain scissions and H-transfer to carbonyl groups from the butyl groups have only negligible amount of contribution to product distribution.

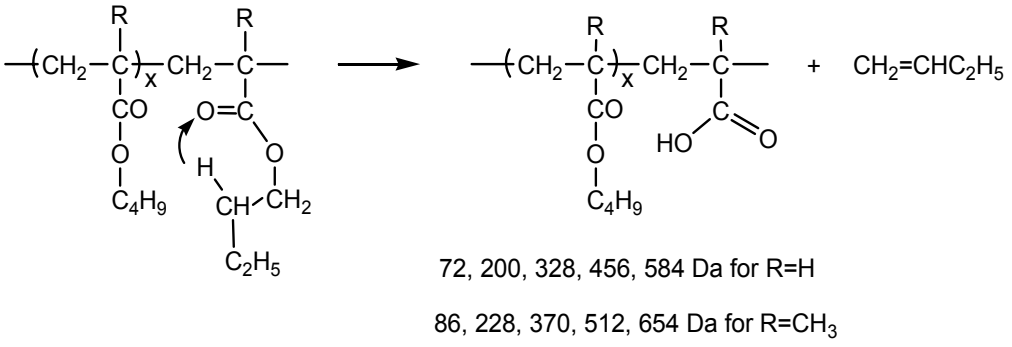

Scheme 4.a. γ-hydrogen transfer to the carbonyl group from the alkyl chain (McLafferty rearrangement reaction).

i.

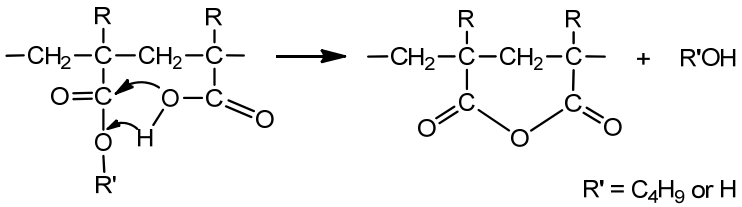

ii.

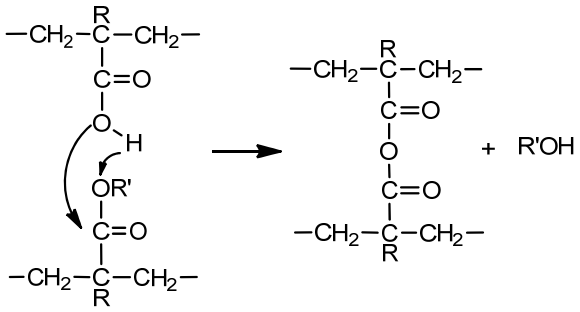

Scheme 4.b. Generation of anhydride units by **i.** intermolecular and **ii.** by intramolecular interactions.

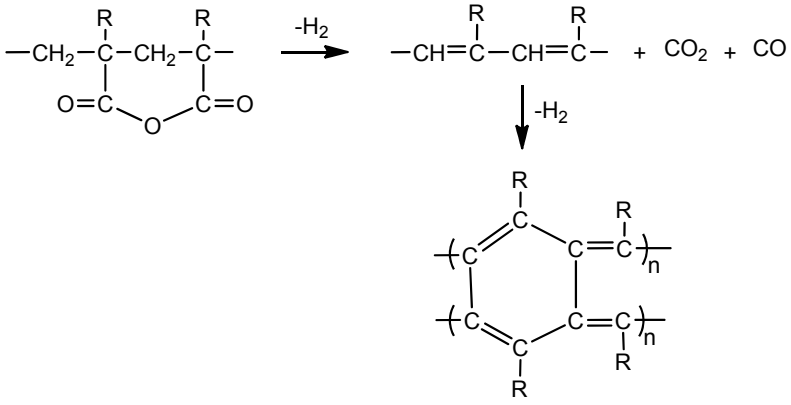

Scheme 4.c. Generation of crosslinked structure.

3.1.2.2 Thermal Degradation of Poly(n-butyl acrylate) PnBA

As can be seen from the TGA curve of the PnBA shown in Figure 18, the weight loss starts at around 300°C and most of the compound degrades at around 420°C. A shoulder at around 350°C is also recorded.

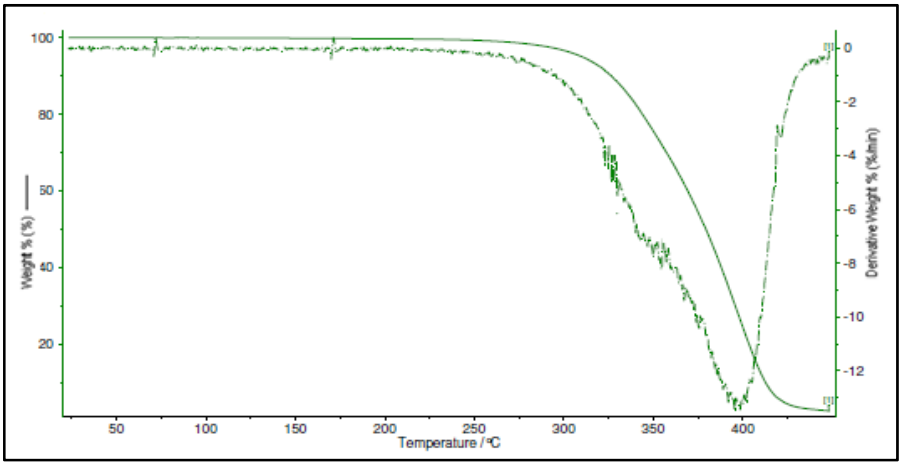

Figure 18. TGA curve of PnBA.

The total ion current (TIC) curve, recorded during the pyrolysis of PnBA given in Figure 19, shows two overlapping peaks, a weak one with maxima at around 280°C and an intense one with a maximum at 375°C and a shoulder at 420°C. The mass spectra recorded at the peak maxima are also shown in the figure. Although the fragmentation pattern observed in the pyrolysis mass spectra at 280 and 375°C are very similar to each other, it is almost totally different than that of the corresponding monomer. In both of the pyrolysis mass spectra, the most abundant peak is at 57 Da due to C_4H_9 fragment in accordance with the side group elimination. Other peaks with significant abundances are due to fragmentation of side chains of PnBA with m/z values 29, 41, 55 and 56 Da, due to successive losses of C_2H_5, C_3H_5, C_2H_3CO and CH_2=$CHCH_2CH_3$ groups during thermal degradation and/or dissociative ionization. As the monomer does not produce a stable molecular ion, the probability of detecting an intense monomer peak is quite low. However, if thermal degradation through depolymerization mechanism takes place the pyrolysis mass spectra should resemble to that of the monomer. Taking into account the dissimilarities in the mass

spectrum of the monomer and the pyrolysis mass spectra it can be concluded that depolymerization is not one of the major thermal degradation routes. Theoretically, since PnBA does not form a stable radical upon cleavage of CH_2-CH bonds, the yield of monomer is expected to be low compared to those of fragments generated by rupture of weaker C–O bonds present in the side chains. Thus, the experimental findings are in accordance with the theoretical expectations. The monomer and the oligomer, M_x, peaks are recorded at 128, 256, 384, 512, 640 Da for x=1 to 5, but are significantly weak, except the dimer peak, as expected. On the other hand, the intensity of the peak at 127 Da due to the loss of hydrogen from the monomer is quite significant.

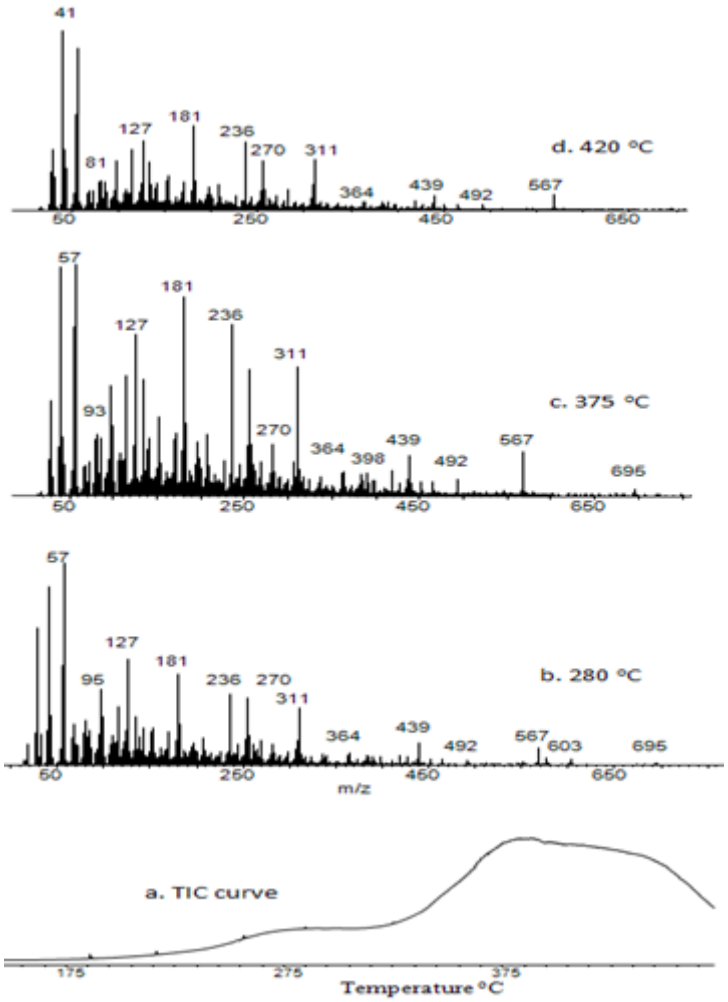

Figure 19. a. TIC curve, the pyrolysis mass of PnBA at b. 280, c. 375 and d. 420°C.

Other intense peaks recorded are at 181, 236 and 311 Da. Furthermore, high mass peaks at 390, 439, 492, 567 and 605 Da are also pronounced. The relative intensities and assignments made for the intense and/or characteristic peaks present in the pyrolysis mass spectra of PnBA recorded at 280 and 375°C are collected in Table 6.

Table 6: The relative intensities and assignments made for the intense and/or characteristic peaks present in the pyrolysis mass spectra of PnBA recorded at 280 and 375°C.

m/z (Da)	Relative intensity		Assignments
	280°C	375°C	
41	896	974	C_3H_5
44	128	122	CO_2
55	506	578	C_2H_3CO
56	486	698	$CH_2=CHCH_2CH_3$
57	1000	1000	C_4H_9
72	18	17	C_2H_3COOH
73	93	140	OC_4H_9
74	13	17	HOC_4H_9
86	184	256	$C_2H_3COOHCH_2$
91	66	71	C_7H_7
98	388	491	$C_2H_3COOC_2H_3$, C_4H_6COO
108	64	100	$C_2H_3COOC_3H_5$, T-$2C_4H_9OH$
127	542	722	M-H and/or DH-C_4H_9OH-C_4H_8
128	58	77	M, monomer
154	84	141	D-C_4H_9OH-CO
181	451	886	D-C_4H_9OH
182	143	267	DH-C_4H_9OH
183	221	313	D-OC_4H_9 or DH-C_4H_9OH
200	34	61	MC_2H_3COOH
208	141	276	T–$2C_4H_9OH$-CO
236	374	757	T–$2C_4H_9OH$
256	349	561	D, dimer
282	101	235	T–C_4H_9OH-CO
308	60	84	$(CH_2=CH)_3D – C_2H_5$

Table 6 (continued)

309	33	67	TeH $-2C_4H_9OH-C_4H_8$
311	275	583	TH-C_4H_9OH or T-C_4H_9O
328	6	10	T–C_4H_8
336	58	79	Te $-2C_4H_9OH$-CO
364	63	103	Te $-2C_4H_9OH$
384	56	90	T, trimer
400	4	11	Te–$2C_4H_8$
410	32	30	Te $-C_4H_9OH$-CO
438	23	45	Te $-C_4H_9OH$
439	128	178	Te-OC_4H_9 or the-C_4H_9OH
456	3	4	Te $-C_4H_8$
464	28	64	P–$2C_4H_9OH$-CO
492	29	70	P $-2C_4H_9OH$
512	5	13	Te, tetramer
538	10	18	TeH $-C_4H_9OH$-CO
567	102	193	P-OC_4H_9

As can be seen in Scheme 5, when the side chain of the PnBA polymer is cleaved form carbonyl oxygen bond, radicals M_x-OC_4H_9 where x=1 to 5, generating series of M_x peaks at 55, 183, 311, 439, 567 Da are obtained. Again as shown in Scheme 5, the peaks at 27, 155, 283, 411 and 539 Da can be attributed to elimination of the carbon monoxide after the loss of alkoxy group. Successive alkoxy and carbon monoxide losses generate series of products M_x-$COOC_4H_9$-OC_4H_9 (82, 210, 338, 466 and 594 Da for x=2 to 6), M_x- $2COOC_4H_9$(54, 182, 310, 438 and 566 Da for x=2 to 6), M_x-$2COOC_4H_9$-OC_4H_9 (109, 237, 365, 493 and 621 Da for x=3 to 7) and M_x-$3COOC_4H_9$ (81, 209, 337, 465, 593, 721 Da for x=3 to 7).

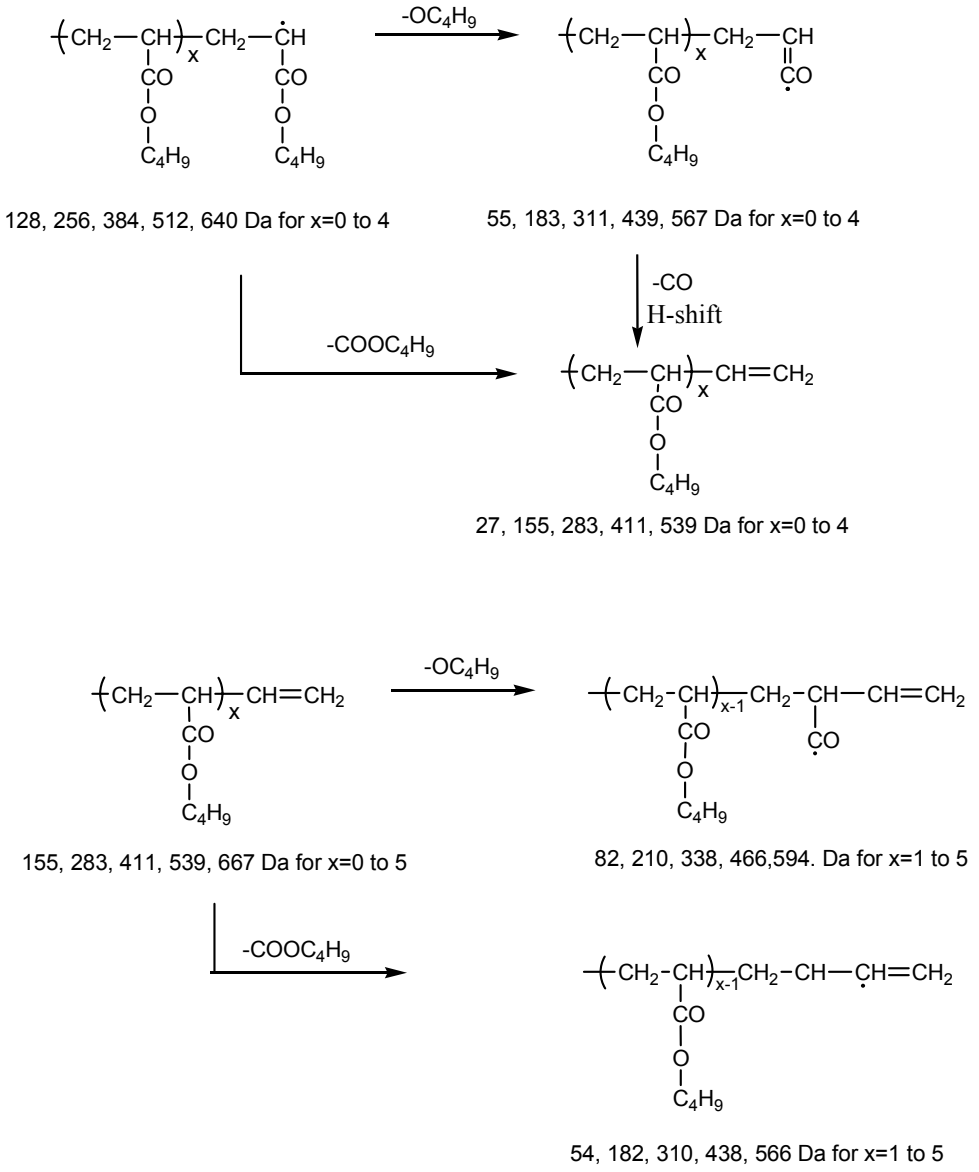

Scheme 5. Loss of alkoxy group from the side chain and subsequent carbon monoxide and unsaturated chain end production.

In general, the relative intensity of the peaks for a given series decreases as the number of repeating unit present in the product increases. Yet, some exceptions are noted. For example, the relative intensities of peaks due to M_x, M_xH, M_x-C_4H_9, M_xH-C_4H_9 and M_x-H-C_4H_9 for x=2 are significantly greater than the corresponding analogues for which x=1. Furthermore, the relative intensities of peaks due to M_x-H-$COOC_4H_9$, M_x-H-$2COOC_4H_9$, for x=3 and those of M_x-H-$2COOC_4H_9$-OC_4H_9 and M_x-

H-3COOC$_4$H$_9$ for x=4 are significantly higher than the rest of the peaks present in the same homologous series. It may be thought that in a given series of fragments low mass fragments should be more abundant. On the other hand, it may further be thought that as the probability of cleavages of one of the two, two of the three, three of the four, is greater than degradation of all side chains, some unexpected trends can be detected.

Some of the peaks recorded are due to different products generated by different decomposition pathways with the same m/z value such as M_x – HOC$_4$H$_9$ and M_x-H-OC$_4$H$_9$ for x=1 to n and M_x-2COOC$_4$H$_9$ and M_xH-2COOC$_4$H$_9$ for x=2 to n+1, and M_x – 2HOC$_4$H$_9$ and M_x-H-2OC$_4$H$_9$ for x=1 to n and M_x-2COOC$_4$H$_9$-OC$_4$H$_9$ and M_xH-2COOC$_4$H$_9$-HOC$_4$H$_9$ for x=2 to n+1.

Products $M_xC_2H_3COOH$ (72, 200, 328 and 456 Da or x=0 to 3) generated by γ-hydrogen transfer reactions from the butyl group are detected (Scheme 4) but are not very abundant. Since poly(n-butyl acrylate) also contains γ-hydrogens on the polymer backbone H-transfer to the carbonyl group from the polymer backbone in addition to the transfer of γ-hydrogen from the alkyl chain of the ester group is also possible(Scheme 6). Although the products are not very abundant, especially for high mass oligomers, the series of products, M_xH (129, 257, 385, 513 and 641 Da for x=0 to 6) and M_x-H (127, 255, 383, 511 and 639 Da for x=0 to 6) where M stands for the monomer may be generated.

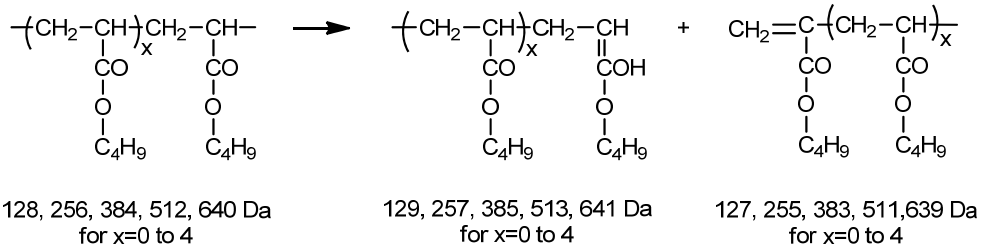

Scheme 6. McLafferty rearrangement, γ-Hydrogen transfer from the main chain to carbonyl groups. Generation of unsaturated chain ends.

When the process takes place at both ends, group of products M_xH_2 (130, 258, 386, 514 and 642 Da for x=1 to 6), M_x (128, 256, 384, 512 and 640 Da for x=1 to 6) and M_x-2H (126, 254, 383, 510 and 638 Da for x=1 to 6) can be produced.

The radicals generated can be stabilized by hydrogen abstraction reactions (Scheme 7). Consequently, series of peaks due to products M_xH (129, 257, 385, 513, 641….), M_x-H (127, 255, 383, 511, 639…), M_xH-OC_4H_9 (56, 184, 312, 440, 568…), M_x-H-OC_4H_9,($(C_2H_3)_2M_x$), (54, 182, 310, 438, 566…), M_xH-$COOC_4H_9$ (28, 156, 284, 412, 540…), M_x-H-$COOC_4H_9$ (26, 154, 282, 410, 538 Da for x=1 to 5), M_xH-$COOC_4H_9$-OC_4H_9 (83, 211, 339, 467 and 595 Da for x=2 to 6), M_x-H-$COOC_4H_9$-OC_4H_9 (81, 209, 337, 465 and 594 Da for x=2 to 6), M_xH-$2COOC_4H_9$ (55, 183, 311, 439, 567 and 695 Da for x=2 to 7), M_x-H-$2COOC_4H_9$ (53, 181, 309, 437 and 565 Da for x=2 to 6), M_xH-$3COOC_4H_9$ (82, 210, 338, 466, 594, 722 Da for x=3 to 8) and M_x-H-$3COOC_4H_9$ (80, 208, 336, 464, 592, 720 Da for x=3 to 8) can be generated.

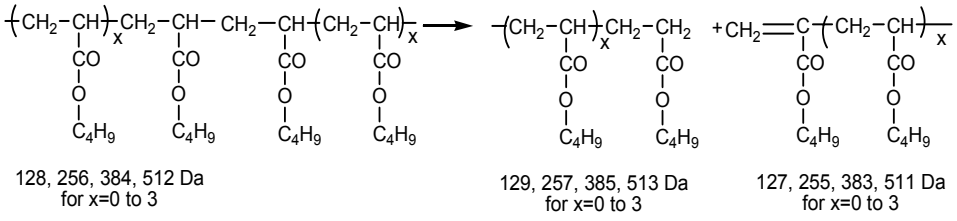

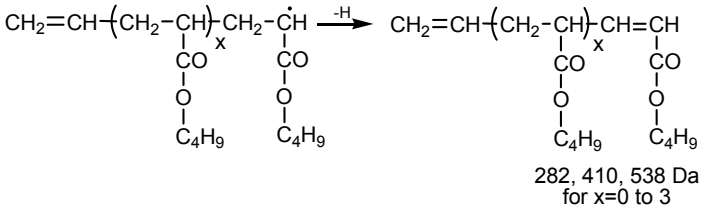

Scheme 7. Hydrogen abstraction reactions.

During the pyrolysis of PnBA, peaks due to all these products are detected. Yet, only M-H (127 Da) and dimer peaks are abundant. The significantly high yield of M-H may be associated with decomposition of several high mass products during both pyrolysis and dissociative ionization processes.

Therefore, the unexpectedly high intensity of the dimer peak may be presumably explained by the contribution of the products that can be stabilized by double bonds, with the same m/z value, generated by successive γ-hydrogen transfer reactions from the main chain to the carbonyl groups and/or hydrogen-abstraction reactions as shown in Scheme 8.

a.

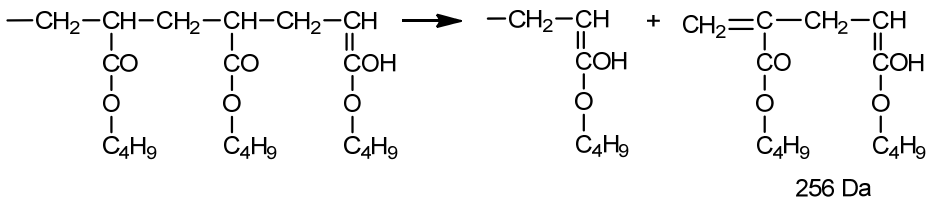

b.

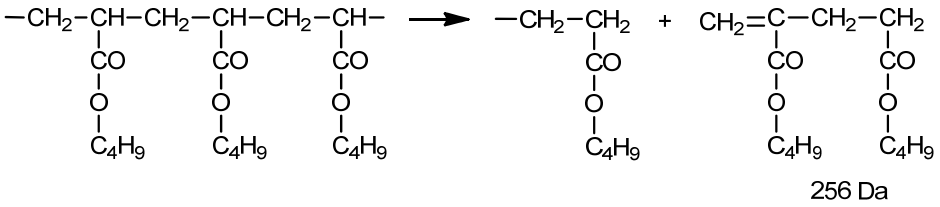

Scheme 8. Stabilization of dimer by; a. γ-hydrogen transfer reactions, b. hydrogen abstraction reactions.

Peaks that may directly be attributed to fragments generated by loss of OC_4H_9 from oligomers up to hexamer at 183, 311, 439, 567 and 695 Da are also unexpectedly prominent, considering the stability of OC_4H_9 and the radical chains produced. On the other hand, trans-esterification reactions between the OH groups generated (Scheme 6) and the ester group also led the same series of fragments as shown in Scheme 9, by elimination of C_4H_9OH and seems to be more appropriate. The loss of C_4H_8 from these products produces another series of fragments with m/z values 127, 255, 383, 511 and 639 Da. Note that these fragments have the same m/z values with M_x-H fragments (m/z= 127, 255, 383, 511 and 639 Da for x= 1 to 5).

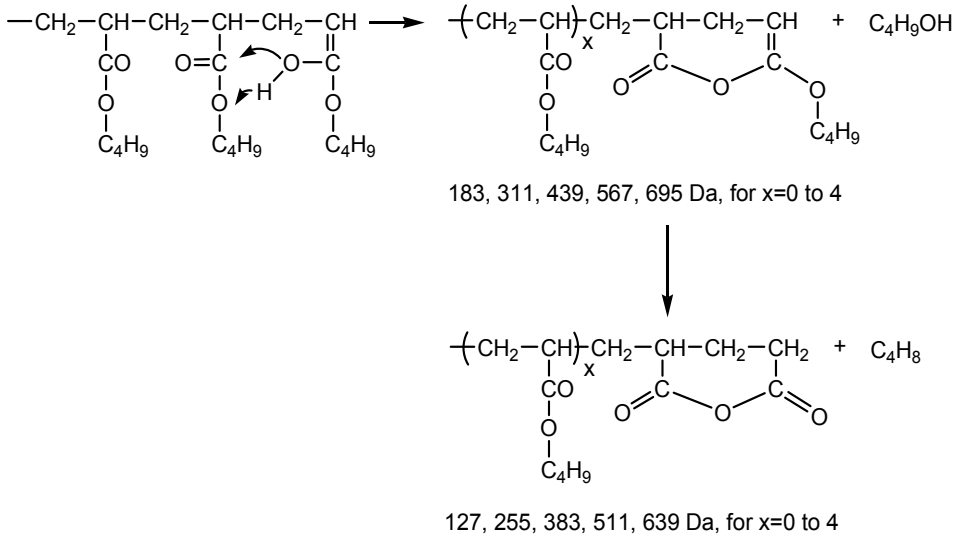

Scheme 9. Generation of anhydride units.

Peaks due to series of products with m/z values 181, 309, 437 and 565 Da having two different structures depending on the precursor fragment, may be generated by loss of butanol as shown in Scheme 10, are also recorded in the pyrolysis mass spectra. Among these, the peak at 181 Da is the most intense, indicating significantly high stability for the related product. The 181 Da products may involve four or six carbon atoms along the main chain depending on the mechanism of production. It is known that six-membered rings are thermodynamically most stable in systems with carbon-carbon bonds. Thus, the very high yield of this product may be regarded as a strong evidence for the generation of a six-membered cyclic structure as a consequence of cyclization of the product formed by γ-hydrogen transfer to carbonyl group from the butyl group as presented in Scheme 10.

a.

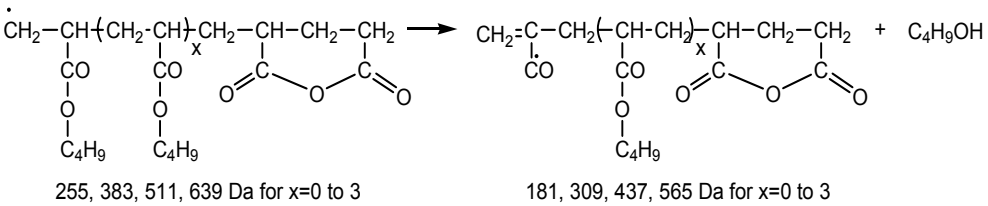

b.

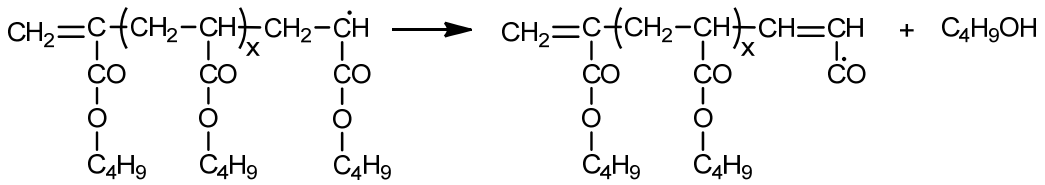

255, 383, 511, 639 Da, for x=0 to 3

181, 309, 437, 565 Da, for x=0 to 3

Scheme 10. Loss of butanol by hydrogen transfer reactions.

Peaks at 182, 310, 438 and 566 Da and 108, 236, 364 and 492 Da may be associated with series of products generated by loss of one or two C_4H_9OH molecules respectively from the polymer chains produced by random scissions of the main chain as shown in Scheme 11. Furthermore, the presence of peaks at 154, 282, 410, and 538 Da and 80, 208, 336, and 464 Da (for x=0 to 3) may be ascribed to fragments produced by subsequent loss of CO groups from these products.

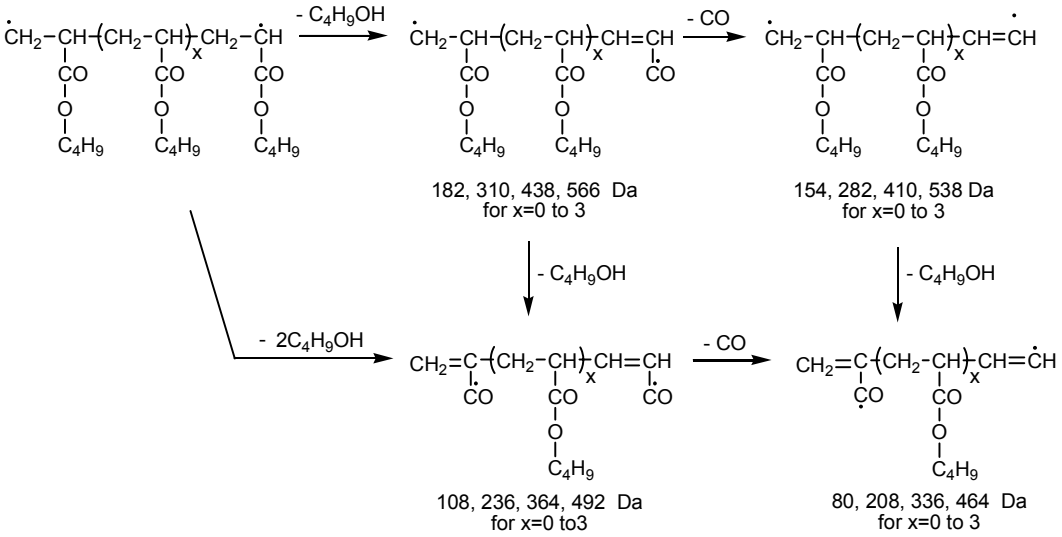

Scheme 11. Random scissions of the main chain.

The pyrolysis mass spectrometry results indicated that among the series of products that can be generated by the mechanisms given in Schemes 9-11, the ones involving six carbon atoms along the main chain (181, 208, 236, 282, 310, 311 Da) are the most abundant in the given series. The significantly high yield of these products may again be associated with cyclization of these fragments yielding six-membered rings that are thermodynamically stable.

In Figure 20, single ion evolution profiles of some selected thermal degradation products of PnBA, namely monomer, M (128 Da), dimer, D (256 Da) tetramer, Te (512 Da), products generated through the mechanisms given in Scheme 9, DH-C_4H_9OH (183 Da), TH-C_4H_9OH (311 Da), and PH-C_4H_9OH (567 Da), in Scheme 10, T-$2C_4H_9OH$-C_4H_8 (181 Da), and TeH_2-C_4H_9OH-C_4H_8 (309 Da), and in Scheme 11, T-C_4H_9OH-CO (282 Da), Te-C_4H_9OH-CO (410 Da), T-$2C_4H_9OH$ (236 Da), Te-$2C_4H_9OH$ (364 Da), T-CO-$2C_4H_9OH$ (208 Da), and Te-CO-C_4H_9OH (336 Da) are given.

The evolution profiles of almost all products showed a weak peak at around 270 ^oC. The low temperature decompositions may be associated with presence of low molecular weight chains and/or units involving head to head linkages as proposed for thermal degradation of poly(methyl methacrylate) in the literature [31-33]. In the light of above discussions it may be suggested that the group of products, reaching maximum yield at around 370°C, were predominantly generated by reactions involving γ-hydrogen transfer from the main chain to the carbonyl groups, followed by evolution of butanol by transesterification reactions. The negligible amount of products formed by γ-hydrogen transfer from the butyl groups and loss of C_4H_8 (Scheme 4) were mostly detected in the final stages of pyrolysis. As evolution of H_2O is not detected during the pyrolysis of PnBA, it may be concluded that segments of poly(acrylic acid) are not produced. Thus, the contribution of γ-hydrogen transfer reactions from the butyl groups to thermal degradation processes seems to be almost negligible.

Evolution of CO_2, C_4H_8 and products involving unsaturation such as C_3H_5 and C_7H_7 are considerably more significant at high temperatures revealing generation of unsaturated and crosslinked structures by loss of CO_2 from the anhydride units.

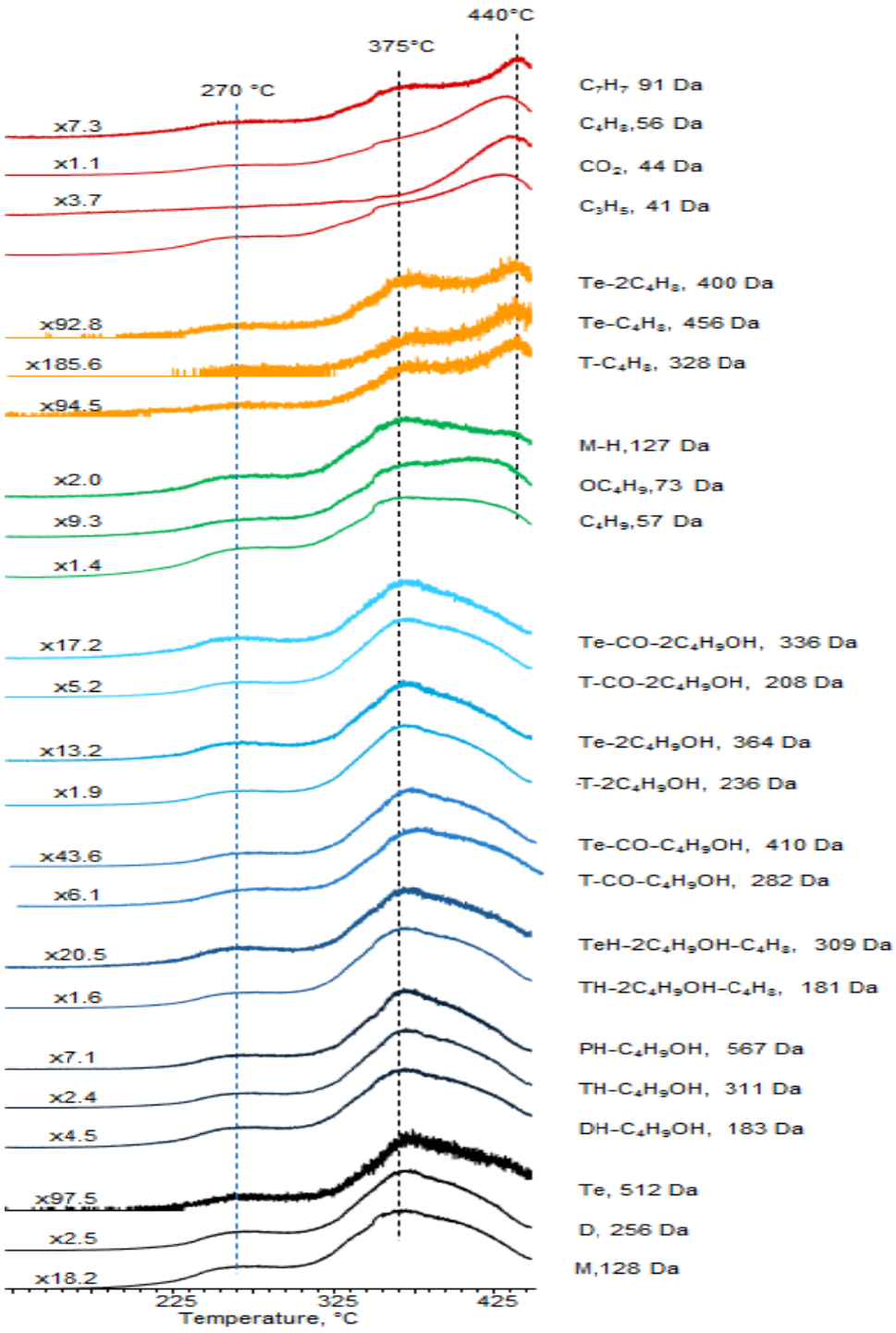

Figure 20. Single ion evolution profiles of some selected products detected during the pyrolysis of PnBA.

3.1.2.3 Thermal Degradation of Poly(t-butyl acrylate) PtBA

The TGA curve of PtBA shows a multi-step weight loss (Figure 21). The polymer starts to degrade at around 250°C and nearly half of the sample is lost at that temperature. There is also some weight loss at 266 and 440°C which contribute the remaining half of the polymer sample.

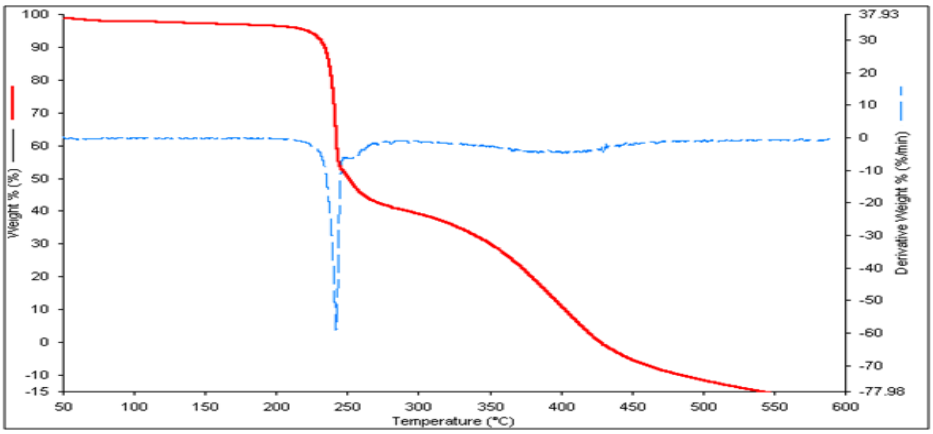

Figure 21. TGA curve of PtBA.

The total ion current curve of poly(t-butyl acrylate) is totally different than that of poly(n-butyl acrylate) (Figure 22). The TIC curve shows two distinct decomposition stages indicating a multi-step thermal degradation mechanism which is consistent with the TGA results of the sample. The mass spectra recorded at around 250°C show intense 56 Da peak that can readily be associated with C_4H_8. The evolution of butane can be attributed to McLafferty rearrangement reaction involving H-transfer from the t-butyl group (Scheme 4). Actually, for poly(n-butyl acrylate) the yield of butane is noticeably low. It may be thought that for poly(t-butyl acrylate) as there are nine available γ-hydrogen in the butyl group, the probability of McLafferty reaction increases. In addition, due to the symmetric structure and low polarity, $(CH_3)_2C=CH_2$ has higher stability than that of $C_2H_5CH=CH_2$. Thus, the elimination of C_4H_8 during the pyrolysis of PtBA becomes highly preferential not only because of the higher probability but also because of thermodynamics due to the stability of the products generated.

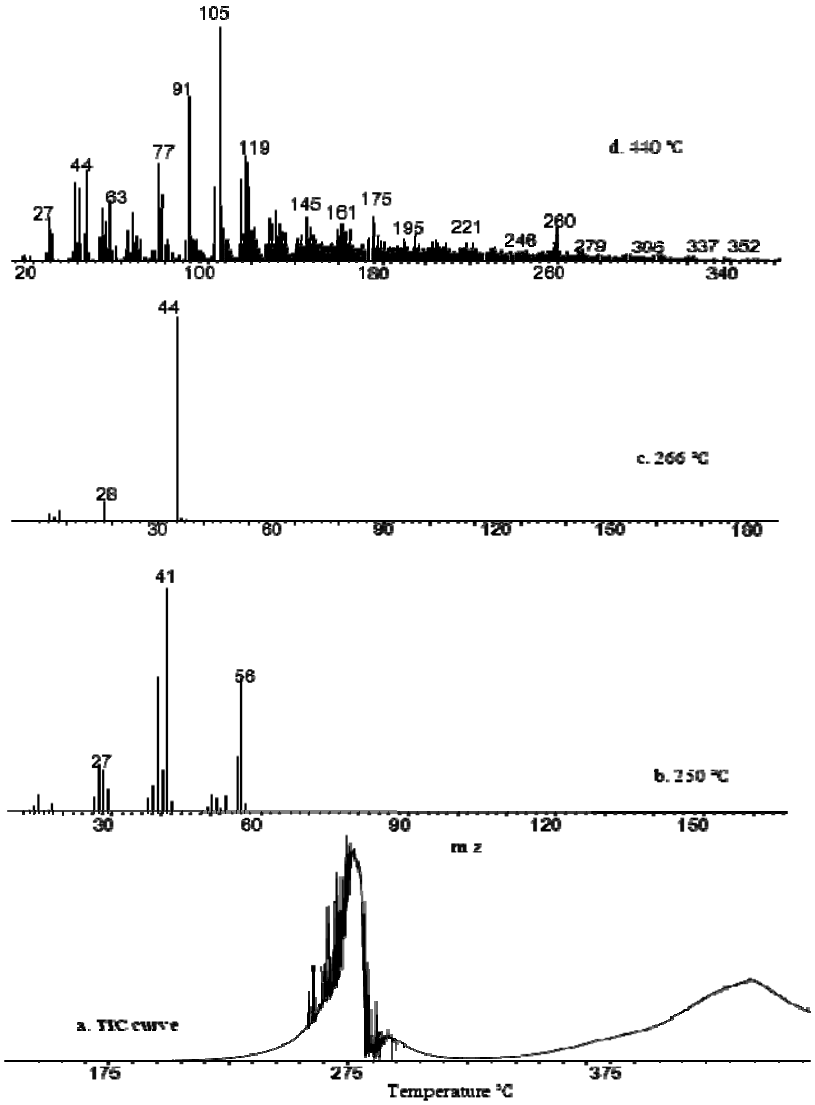

Figure 22. a. TIC curve, the pyrolysis mass of PtBA at b. 250 and c. 440°C.

The mass spectra recorded at around 440°C, of the third peak maximum in the TIC curve, are quite crowded and dominated with peaks that can be associated with unsaturated hydrocarbon fragments such as C_6H_5, (m/z=77 Da), C_7H_7, (m/z=91 Da) and C_8H_9, (m/z=105 Da). The relative intensities and the assignments made for the characteristic and/or intense peaks present in the pyrolysis mass spectra recorded at 250 and 440°C are summarized in Table 7.

Table 7: The relative intensities and assignments made for the intense and/or characteristic peaks present in the pyrolysis mass spectrum of PtBA at 250 and 440°C.

m/z (Da)	Relative Intensity		Assignments
	250°C	440°C	
18	44	22	H_2O
26	42	73	CH=CH
28	193	139	CO
39	605	364	C_3H_3
41	1000	324	C_3H_5
44	6	392	CO_2
52	21	112	$(CH=CH)_2$
55	256	277	C_4H_7
56	599	45	C_4H_8
77	1	423	C_6H_5
78	-	228	$(CH=CH)_3$
91	-	725	C_7H_7
105	-	1000	C_8H_9
117	-	448	C_9H_9
128	-	195	M, monomer
129	--	178	MH
130		67	$(CH=CH)_5$
145	-	201	$CH_2=CH(COOH)C_2H_4COOH$
176	-	167	$C_{10}H_8O_3$
200	-	44	MC_2H_3COOH
256	-	45	D, dimer
257	-	48	$MC_2H_3COOHC_4H_9$
260	-	149	$C_{20}H_{20}$
272	-	54	$C_{21}H_{20}$
328	-	18	DC_2H_3COOH
384	-	10	T, trimer
385	-	8	$DC_2H_3COOHC_4H_9$
456	-	8	TC_2H_3COOH
512	-	5	Te, tetramer

Since PtBA contains γ-hydrogen also on the main chain, McLafferty type rearrangement reaction that will occur on the main chain should also be considered.

As can be seen in Scheme 6 due to the McLafferty rearrangement reactions unsaturated chain ends may be produced. Consequently, the series of peaks due to products $M_xC_2H_3COOHC_4H_9$ (257, 385, 641 Da for x=1 to 4) may be obtained. In addition, anhydride units can be obtained by intra and/or intermolecular condensation reactions. Subsequent evolution of CO_2 and CO may produce unsaturated hydrocarbon linkages. Thermal degradation of these segments may generate series of peaks due to products $(CH=CH)_x$ (26, 52, 78, 104, 130 Da for x=1 to 5).

For a better understanding, single ion evolution profiles of some selected products, namely, C_4H_8 (56 Da), C_3H_5 (41 Da), H_2O (18 Da), CO_2 (44 Da), C_8H_9 and/or C_6H_5O (105 Da), $C_{13}H_{20}$ and/or $C_{10}H_8O_3$ (176 Da), $C_{20}H_{20}$ (260 Da), and $C_{21}H_{20}$ (272 Da), are given in Figure 23.

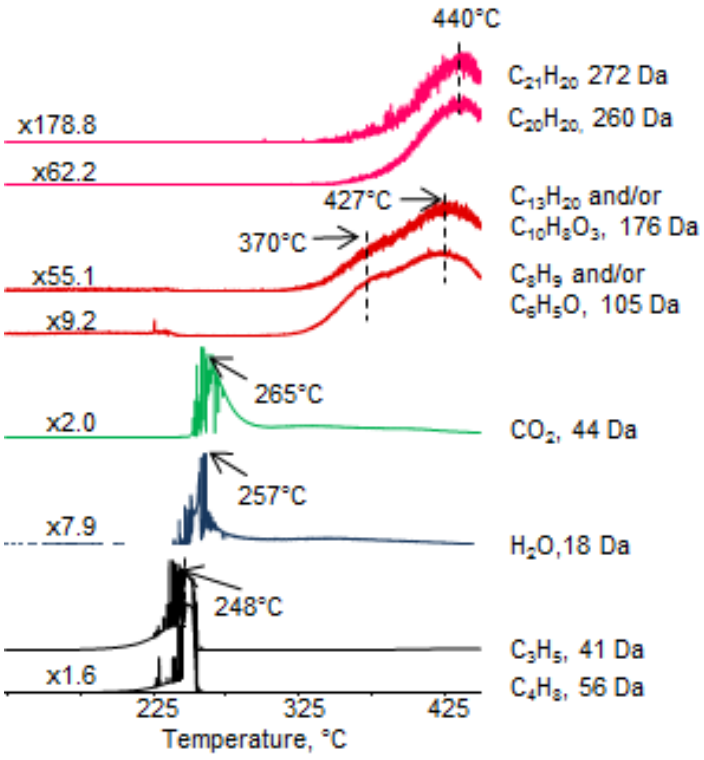

Figure 23. Single ion evolution profiles of some selected products detected during the pyrolysis of PtBA.

The trends in the evolution profiles clearly show that $CH_2C(CH_3)_2$ elimination takes place at around 250°C. Considering the similarities in the evolution profiles of the products with m/z values 39 and 41 Da with that of the $CH_2C(CH_3)_2$, it can be concluded that these fragments are generated during dissociative ionization of $CH_2C(CH_3)_2$. The loss of H_2O and CO_2 takes place at slightly higher temperatures, at around 265°C (Figure 23). These processes occur in a relatively narrow temperature range. On the other hand, the unsaturated polymer backbone degrades over a broad temperature range above 300°C. Maximum yield for the fragments involving unsaturation are detected at 425°C. Thus, experimental data clearly proves the proposed mechanism to be the major thermal degradation pathway. On the other hand, at elevated temperatures weak peaks due to monomer and oligomers and due to products generated by decomposition of side chains are detected. Their yields are maximized at around 450°C. Fragments involving acrylic acid units show identical evolution profiles with these products (Figure 23). Compared to poly(n-butyl acrylate), the relative yields of butene, water and carbon dioxide are about five-folds higher, whereas those of the products generated by random cleavages are significantly lower when generated during the pyrolysis of poly(tertiary butyl acrylate).

Taking into consideration the trends observed in single ion pyrograms it can be concluded that thermal degradation of poly(t-butyl acrylate) occurs in a multi-step mechanism involving;

- McLafferty rearrangement reactions, loss of $(CH_3)_2C=CH_2$
- Intra and/or intermolecular condensation reactions, elimination of H_2O and generation of anhydride units
- Evolution of CO_2 and CO yielding unsaturated hydrocarbon linkages
- Degradation of unsaturated hydrocarbon chains generated

3.1.3 Thermal Degradation of Poly (isobornyl acrylate) PIBA

The TGA curve of PIBA given in Figure 24 is a direct evidence for a complex, multi-step thermal degradation process. Although the largest portion of the weight loss is observed at around 300°C there is also some degradation at around 440°C.

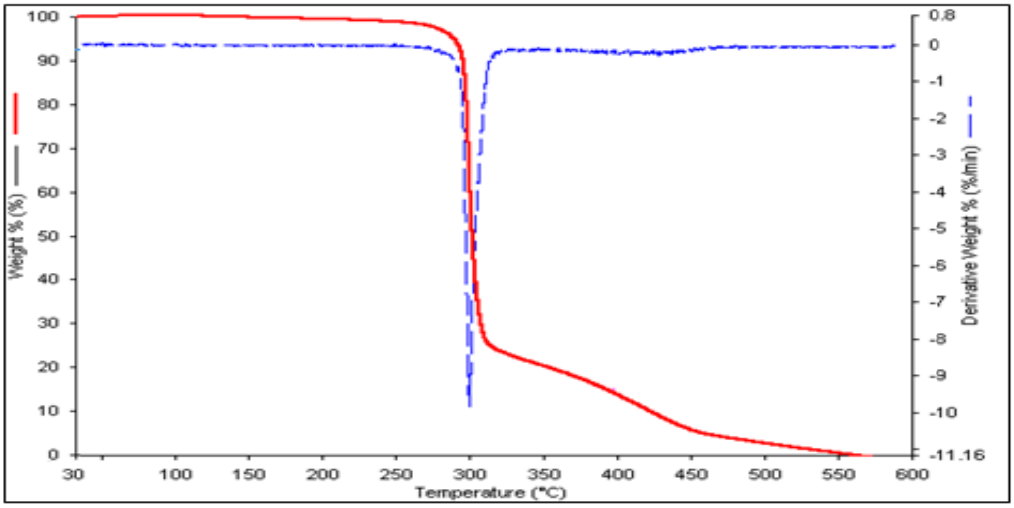

Figure 24. TGA curve of PIBA.

For a better interpretation of pyrolysis mass spectra of poly(isobornyl acrylate), PIBA the mass spectrum of isobornyl acrylate is studied (Figure 25). In the mass spectrum of the monomer the molecular ion peak at 208 Da is significantly weak and the base peak is at 55 Da due to CH_2CHCO fragment generated by the cleavage of CO-O bond. Peaks due to fragmentation of isobornylene (136, 121, 108, and 93 Da) are of moderate intensity. Peak due to the fragment generated by loss of $C(CH_3)_2$ from isobornyl is also abundant.

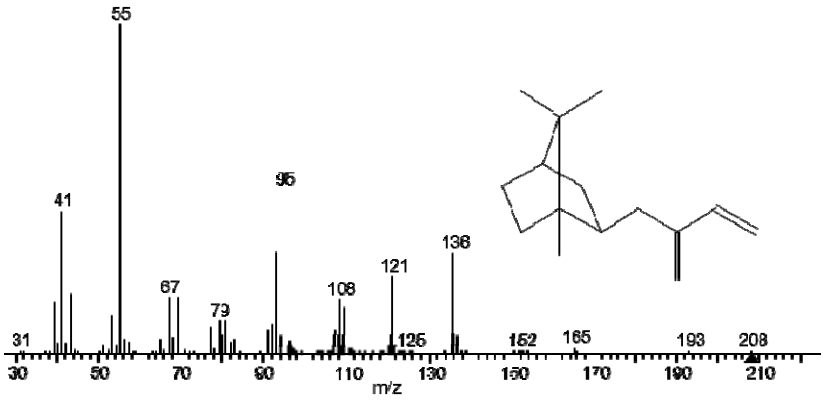

Figure 25. Mass spectrum of isobornyl acrylate.

The total ion current (TIC) curve, recorded during the pyrolysis of PIBA is given in Figure 26. Two overlapping intense peaks with maxima at 320 and 330°C and a broad and a weaker peak with a maximum at 440°C are present in the TIC curve. Presence of more than one peak in the TIC curve is a direct evidence for a complex, multi-step thermal degradation process.

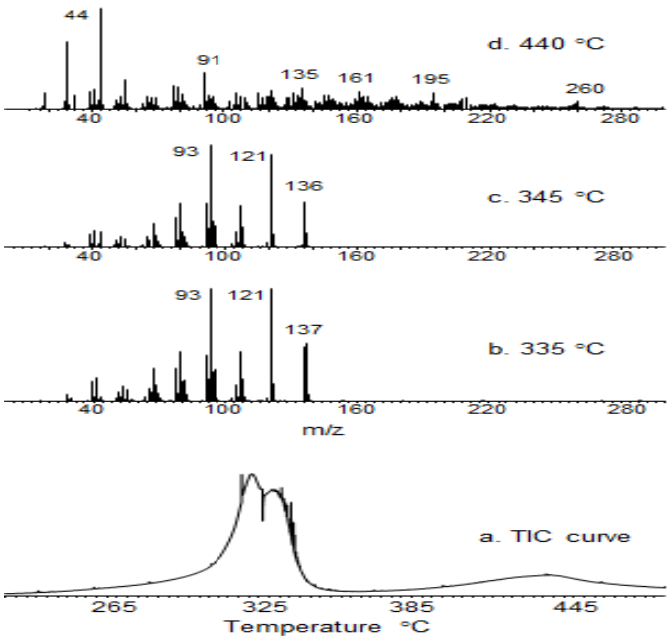

Figure 26. a. TIC curve and the pyrolysis mass of PIBA at b. 335, c. 345 and d. 440°C.

The mass spectra recorded at the peak maxima are also shown in Figure 26. The fragmentation patterns observed in the pyrolysis mass spectra at 320 and 330°C are almost identical and show classical fragmentation pattern of isobornylene (136 Da) (Figure 27). The most abundant peaks are at 121 and 93 Da due to successive losses of CH_3 and CH_2CH_2 groups. The base peak in the mass spectra recorded at around 440°C is at 44 Da that can be readily attributed to evolution of CO_2.

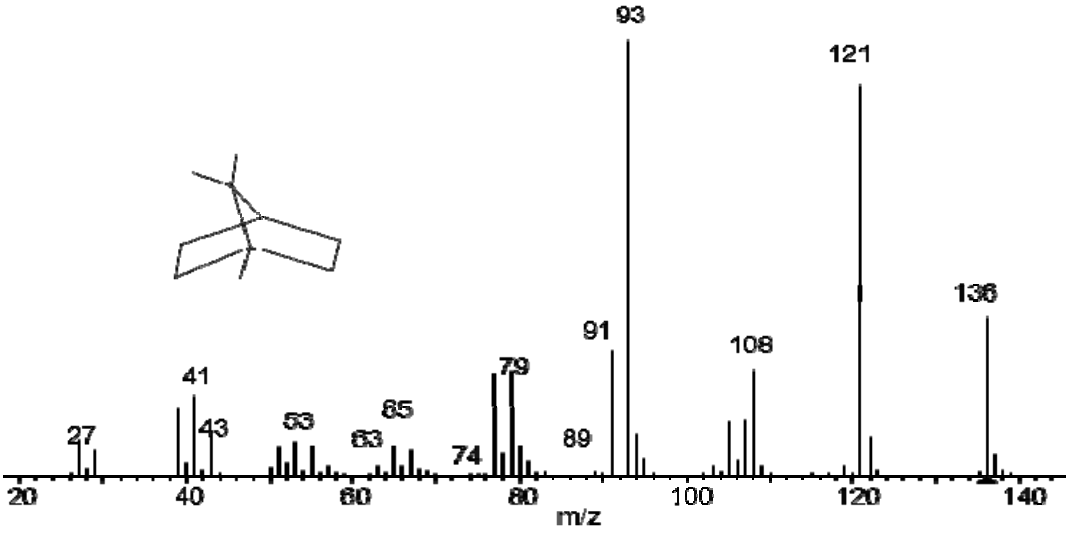

Figure 27. Mass spectrum of isobornylene

The relative intensities and the assignments made for the characteristic and/or intense peaks present in the pyrolysis mass spectra recorded at 335 and 440°C are summarized in Table 8.

Table 8: The relative intensities and assignments made for the intense and/or characteristic peaks present in the pyrolysis mass spectrum of PIBA at 335 and 440°C.

m/z (Da)	Relative intensity		Assignments
	335°C	440°C	
18	3	4	H_2O
27	69	44	CH_2CH
41	203	164	C_3H_5
44	7	27	CO_2
54	20	18	C_4H_6
71	5	3	CH_2CHCO_2
77	296	283	C_6H_5
81	132	94	C_6H_9
82	54	45	$CH_2C(CH_3)C_3H_5$
91	418	419	C_7H_7

Table 8 (continued)

93	996	992	C_7H_9, C_9H_{13}-C_2H_4
121	1000	1000	C_9H_{13}, $C_{10}H_{16}$- CH_3
126	1	1	$CH_2CHCO_2C_3H_4CH_3$
136	499	507	$C_{10}H_{16}$, M-C_2H_3COOH
137	278	114	$C_{10}H_{17}$
195	-	1	$C_{15}H_{15}$
208	1	1	M, monomer
260	-	1	$C_{21}H_8$
279	1	1	MCH_2CHCO_2
334	1	1	$MCH_2CHCO_2C_3H_4CH_3$
416	1	1	D, dimer
487	1	1	DCH_2CHCO_2
542	1	1	$DCH_2CHCO_2C_3H_4CH_3$
624	1	1	T, trimer

For a better understanding, single ion evolution profiles of some selected products, namely, C_6H_9 (81 Da), $C_{10}H_{17}$ (137 Da), D (416 Da), C_7H_7 (91 Da), C_7H_9 (93 Da), C_9H_{13} (121 Da), $C_{10}H_{16}$ (136 Da), C_2H_3 (27 Da), H_2O (18 Da), CO_2 (44 Da), dimer, $C_{15}H_{15}$ (195 Da) and $C_{21}H_8$ (260 Da) are given in Figure 28.

The product peaks start to appear in the pyrolysis mass spectra recorded just above 250°C are maximized at around 330°C and almost totally disappear at around 340°C. In this temperature range isobornyl is the most abundant product. Loss of isobornyl, $C_{10}H_{17}$ (137 Da) may be due to the cleavage of O-isobornyl bond during thermal degradation and/or dissociative ionization of the monomer and low mass oligomers (Scheme 12.a). Isobornyl, $C_{10}H_{17}$ (137 Da) and its degradation products such as C_6H_9 (81 Da) and CH_2CHCO_2 (71 Da) reach maximum yield at 330°C, whereas, the monomer, M (208 Da), dimer, D (416 Da) and trimmer (624 Da) are detected at slightly higher temperatures, showing maximum at around 335°C. The maximum in the evolution profiles of CH_2CH (27 Da), C_3H_5 (41 Da) and C_4H_6 (54 Da), generated by decomposition of the segments formed upon loss of isobornyl side chains, are even at slightly higher temperatures, at around 340°C.

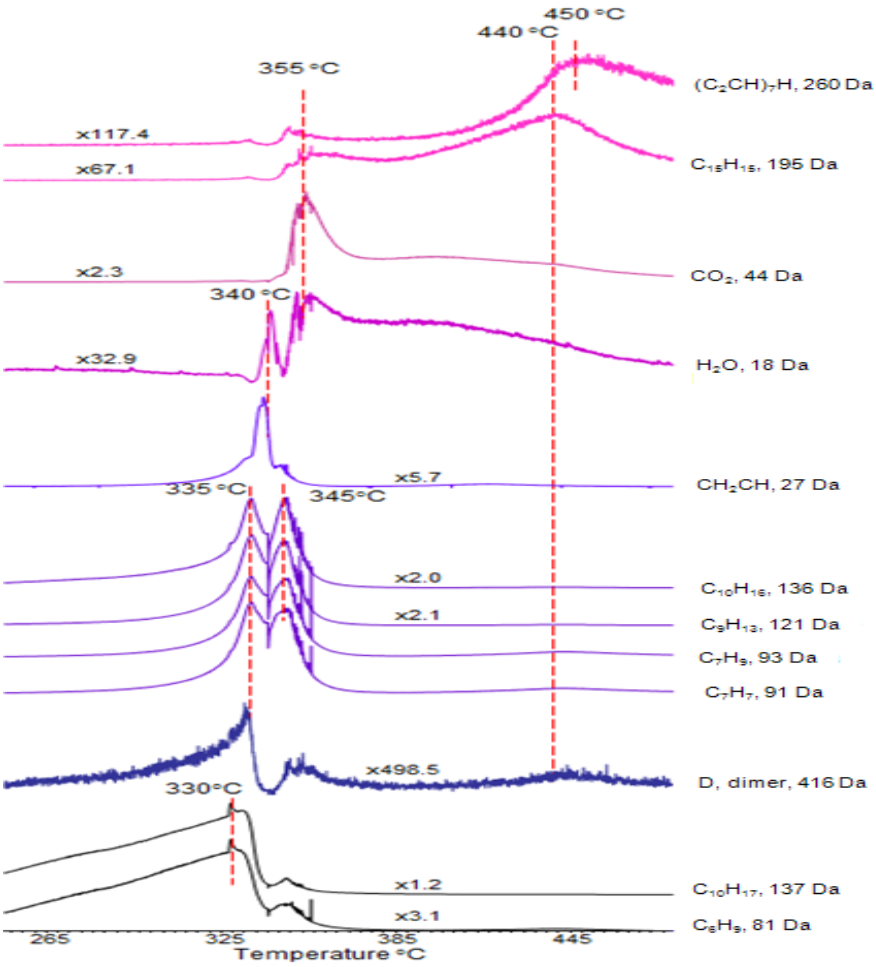

Figure 28. Single ion evolution profiles of some selected products detected during the pyrolysis of PIBA.

Products indicating decomposition of the isobornyl ring, such as $CH_2C(CH_3)C_3H_5$ and $MCH_2CHCO_2C_3H_4CH_3$ with m/z values 82, 126 and 334 Da respectively as shown in Scheme 12.b also show a maximum at 335°C in their evolution profiles. However, the yields of monomer, low mass oligomers and products indicating decomposition of isobornyl ring are significantly low. Thus, it may be concluded that thermal degradation of PIBA is started by loss of side chains and unzipping reactions yielding mainly monomer and low mass oligomers or decomposition of isobornyl ring were almost trivial (Scheme 12.a).

a.

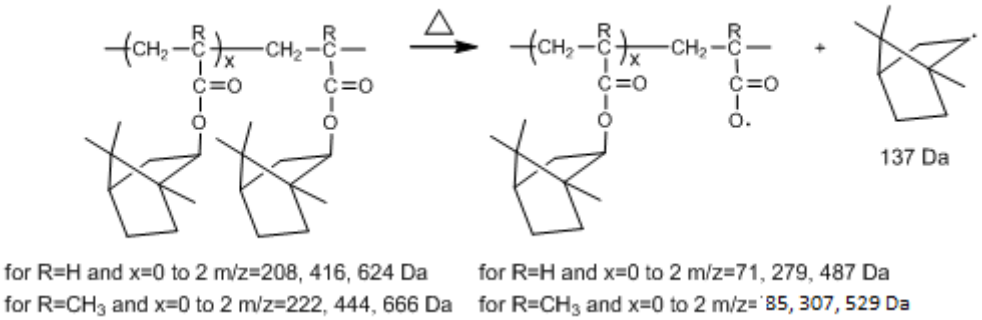

for R=H and x=0 to 2 m/z=208, 416, 624 Da
for R=CH_3 and x=0 to 2 m/z=222, 444, 666 Da

for R=H and x=0 to 2 m/z=71, 279, 487 Da
for R=CH_3 and x=0 to 2 m/z=85, 307, 529 Da

b.

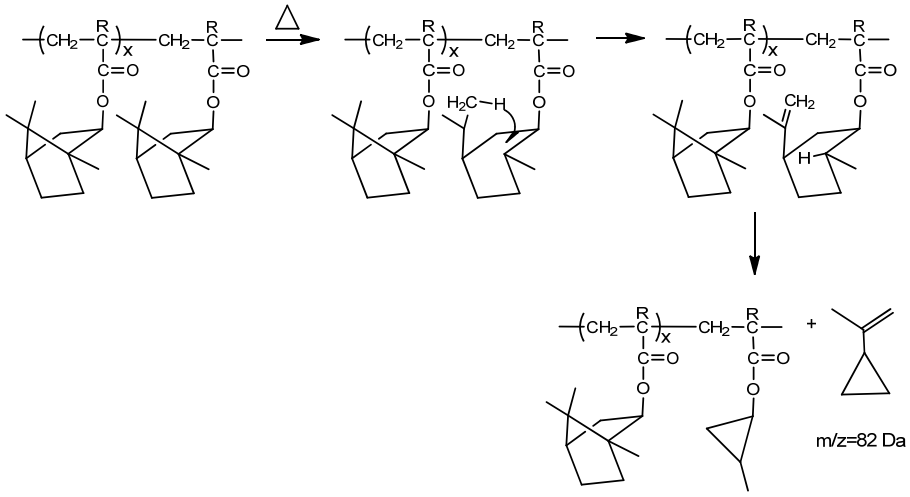

for R=H and x=0 to 2 m/z=126, 334, 542 Da
for R=CH_3 and x=0 to 2 m/z=140, 362, 584 Da

Scheme 12. Thermal degradation of PIBA; a. Degradation via loss of side chains, b. Decomposition of isobornyl rings.

The group of intense product ions, C_9H_{13} (121 Da), C_7H_7 (91 Da) and C_6H_5 (77 Da) showing two sharp overlapping peaks with maxima at 335 and 345°C can readily be attributed to dissociative electron impact ionization products of isobornylene (136 Da) that can be generated by a McLafferty type rearrangement reactions as shown in Scheme 13. Upon further heating, the polyacrylic acid formed can eliminate H_2O

to generate anhydride units (Scheme 4.b). These anhydride groups, impeding thermal decomposition of the main chain, can promote further side reactions leading to the formation of char by loss of CO_2 and CO as shown in Scheme 4.c.

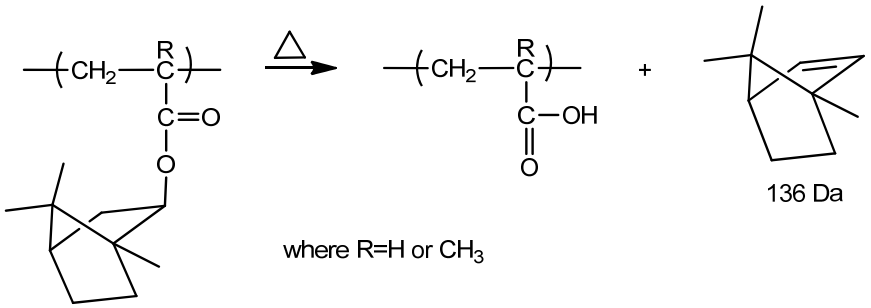

Scheme 13. Generation of poly(acrylic acid) and isobornylene.

Evolution of H_2O and CO_2 are detected just above 330°C. The maxima in the evolution profiles are at 340 and 355°C for H_2O and CO_2 respectively supporting the proposed thermal degradation mechanism yielding a crosslinked structure. Products involving hydrogen deficiency are recorded at relatively high temperatures confirming the generation of an unsaturated/crosslinked structure (Figure 28).

γ-H's on a carbon atom along the main chain may also be involved in the process of protonation of CO groups. Such a process can be observed for both PIBA and polyacrylic acid generated and will generate unsaturated chain ends as shown in Scheme 14. These chains may interact to from crosslinked structures. Detection of H_2O evolution also at high temperatures supports this proposal. The products associated with degradation of units involving unsaturation and/or crosslinking are maximized over a broad temperature range. Generation of such linkages through various reaction pathways may be the possible cause.

a.

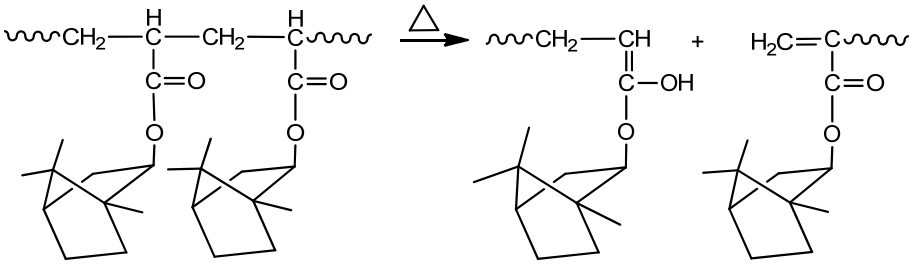

b.

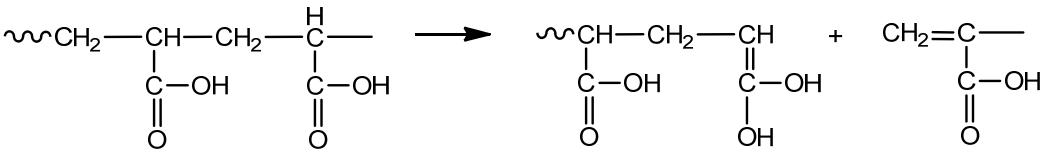

Scheme 14. Generation of unsaturated chain ends via degradation of a. PIBA, b. poly(acrylic acid).

Yet, in order to investigate the importance of γ-H transfer from a C atom along the main chain DP-MS analysis were also carried out using poly(isobornyl methacrylate) PIBMA, for which there is no available γ-H on a C atom along the main chain.

3.1.4 Thermal Degradation of Poly(isobornyl methacrylate) PIBMA

The TGA curve of PIBMA given in Figure 29 is a direct evidence for a complex, multi-step thermal degradation process. The weight loss starts at around 220°C and the largest portion of the polymer degrades at around 340°C. The remaining portion of the sample weight which is less than the half degrades at around 440°C.

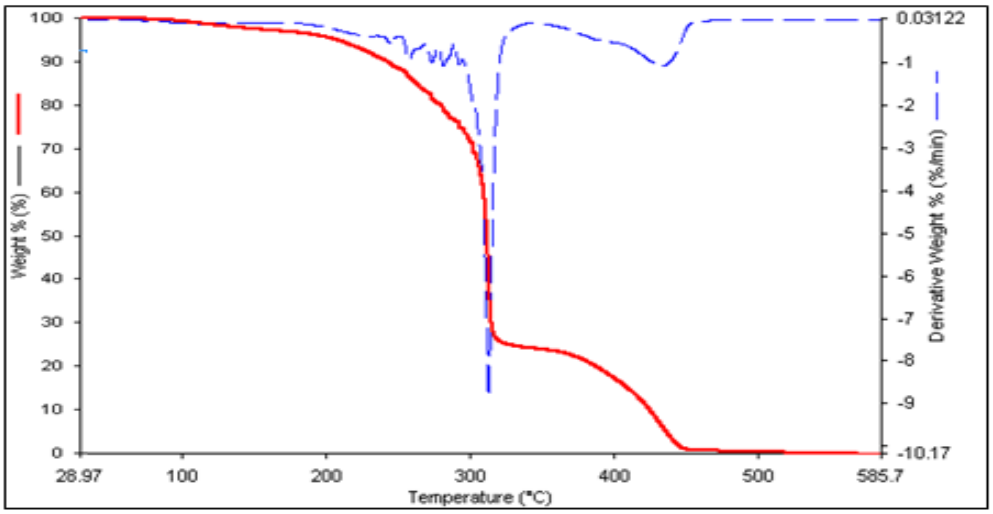

Figure 29. TGA curve of PIBMA.

The TIC curve recorded during the pyrolysis of PIBMA is quite similar to that of PIBA, showing an intense peak at around 345°C and a broad peak at around 440°C (Figure 30) in consistent with the TGA results. However, since there is γ-H on the isobornyl ring thermal degradation processes involving generation of poly(methacrylic acid) should also be incorporated for PIBMA thermal degradation process.

At low temperatures, at around 225°C, detection of monomer peak at 222 Da and diagnostic fragment peaks indicate presence of unreacted monomer. Above 300°C degradation products of the polymer appeared in the pyrolysis mass spectra. Unlike PIBA, the yield of isobornyl radical due to rupture of O-isobornyl bond is quite low. On the other hand, the mass spectra recorded at around 345 and 355°C are almost similar to the ones during the pyrolysis of PIBA recorded at around 345°C. Furthermore, the spectra recorded at elevated temperatures are quite crowded again as in case of PIBA.

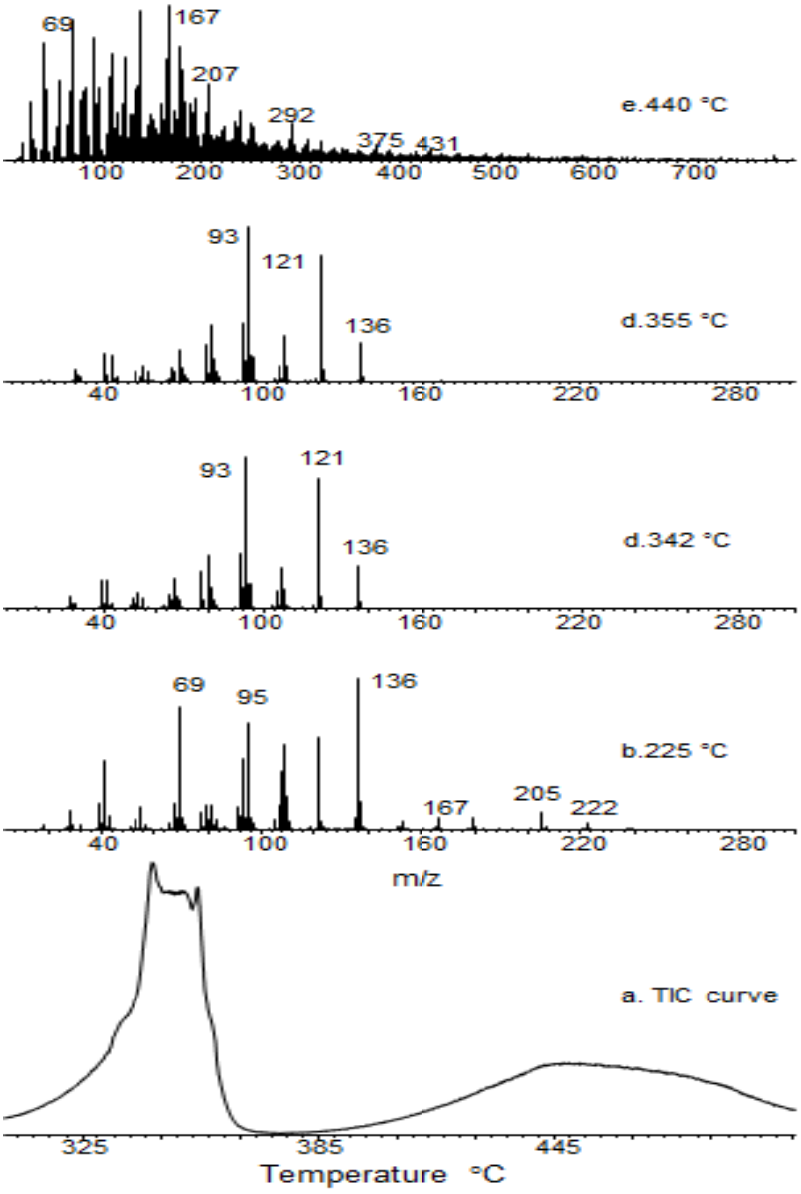

Figure 30. a. TIC curve and the pyrolysis mass of PIBMA at b. 225, c. 342, d.355 and e. 440°C.

The relative intensities and the assignments made for the characteristic and/or intense peaks present in the pyrolysis mass spectra recorded at 342 and 444°C are summarized in Table 9.

Table 9: The relative intensities and assignments made for the intense and/or characteristic peaks present in the pyrolysis mass spectrum of PIBMA at 342 and 440°C.

m/z (Da)	Relative Intensity		Assignments
	342°C	440°C	
18	21	127	H_2O
27	168	120	CH_2CH
41	291	683	$CH_3C=CH_2$
44	5	472	CO_2
55	82	414	$CH_2=CHCO$
82	26	288	$CH_2C(CH_3)C_3H_5$
91	348	797	C_7H_7
93	1000	367	C_7H_9
121	709	555	C_9H_{13}
136	222	430	$C_{10}H_{16}$
137	31	974	$C_{10}H_{17}$
207	1	531	$C_{16}H_{15}$
222	-	233	M, monomer
292	-	220	$(C_2CCH_3)_5C_3H$
444	-	39	D, dimer
666	-	10	T, trimer

In Figure 31 single ion evolution profiles of some characteristic products namely $C_{10}H_{17}$ (137 Da), D (444 Da), C_7H_7 (91 Da), C_7H_9 (93 Da), C_9H_{13} (121 Da), $C_{10}H_{16}$ (136 Da), C_3H_5 (41 Da), H_2O (18 Da), CO_2 (44 Da), $C_{16}H_{15}$ (207 Da) and $C_{23}H_{16}$ (292 Da) are given. Contrary to what is observed for PIBA, the yield of isobornylene is significantly higher than that of isobornyl. The ratio of the yields of isobornyl radical to that of isobornylene is decreased almost ten-folds. In addition, weak peaks indicating decomposition of isobornyl ring almost totally disappeared in the pyrolysis mass spectra of PIBMA. The yields of monomer and low mass oligomers are relatively more intense than what is detected for PIBA, but still not very abundant. Presence of intense isobornylene and related peaks (136, 121, 93 and 91 Da) maximizing at around 340°C, and peaks due to decomposition of the main chain, such as CH_2CCH_3 (41 Da), $CH_2C(CH_3)CH_2$ (55 Da), $CH_2C(CH_3)_2$ (82 Da) maximizing at slightly higher temperatures at around 350°C reveals that the thermal

degradation of PIBMA starts by loss of isobornylene generated by McLafferty type γ-H transfer reaction from the isobornyl ring yielding poly(methacrylic acid) chains (Scheme 14.b).

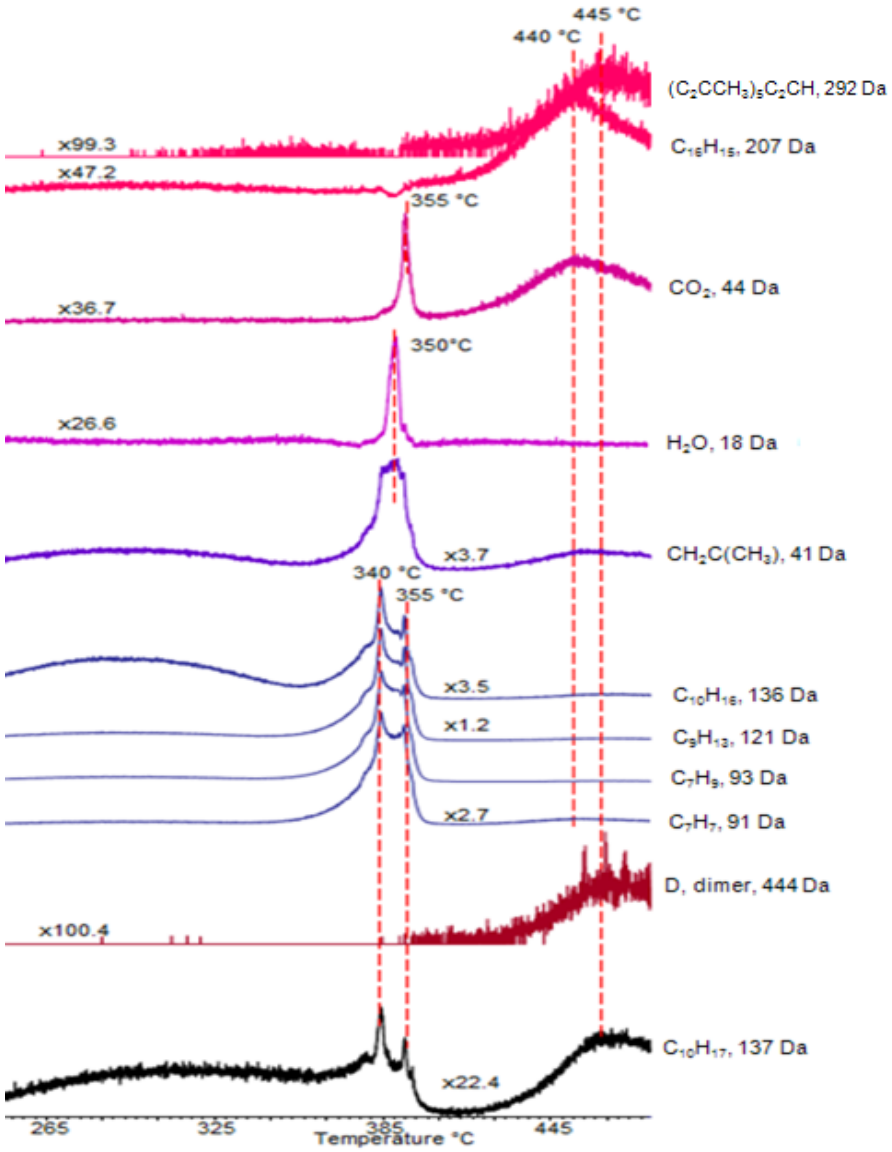

Figure 31. Single ion evolution profiles of some selected products detected during the pyrolysis of PIBMA.

Again, the evolutions of H_2O and CO_2 are detected at around 350 and 355°C respectively. However, although evolution of H_2O is recorded only in a very narrow temperature region, loss of CO_2 is also detected at elevated temperatures yielding a

broad high temperature peak with a maximum at 440°C in the single ion pyrogram. Furthermore, contrary to what is observed for PIBA, the relative yield of CO_2 is decreased significantly almost about 16-folds although the relative yield of H_2O is almost comparable to the corresponding value for PIBA. Consequently, it may be concluded that the extent of crosslinked structure is limited for PIBMA.

It may further be thought that the loss of side chains by cleavage of O - isobornyl bond became effective only when a γ-H on the carbon atom along the main chain takes place as in case of PIBA. In any case, the results clearly suggests that for both PIBA and PIBMA polymer samples, γ-H transfer from the isobornyl ring to the carbonyl group is predominantly effective in various thermal decomposition pathways.

3.1.5 Thermal Degradation of Poly(benzyl methacrylate) PBzMA

As can be seen from the TGA curve of PBzMA shown in Figure 32, thermal degradation of PBzMA is a two step thermal degradation process. The weight loss of the sample starts at around 280°C and the entire polymer is degraded at around 380°C. The largest portion of the polymer loss is obtained between 330 and 400°C.

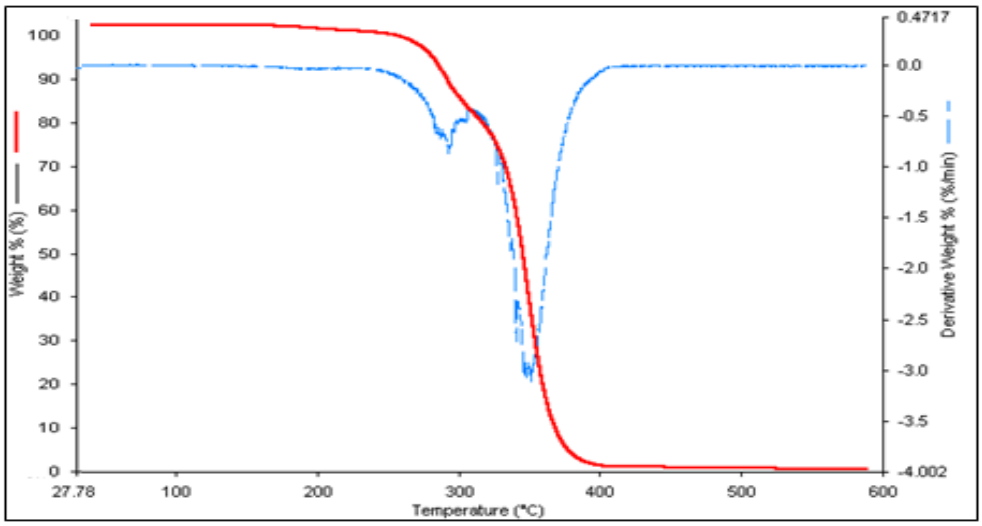

Figure 32. TGA curve of PBzMA.

Like PMMA, thermal degradation of PBzMA occurs by depolymerization reaction yielding the monomer. Thus for a better understanding of the pyrolysis mass spectral data related to PBzMA mass spectrum of benzyl methacrylate is also studied (Figure 33).

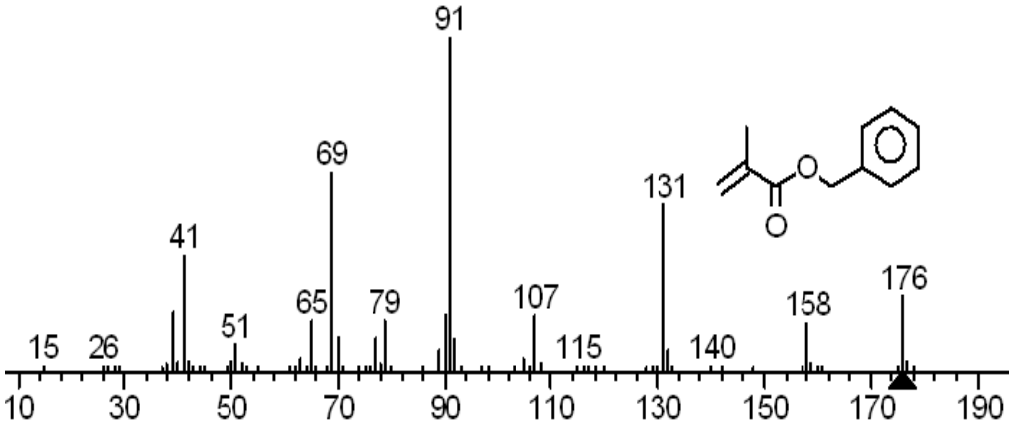

Figure 33. Mass spectrum of benzyl methacrylate.

The molecular ion peak at 176 Da is quite significant. The base peak is at 91 Da due to tropylium, C_7H_7, ion. Peaks at 158 and 131 Da can be associated with products generated by loss of H_2O and COOH by complex rearrangement reactions. Intense peaks at 107, 77, 51, 41 and 39 Da due to $C_6H_5CH_2O$, C_6H_5, C_4H_3, C_3H_5 and C_3H_3 are produced by dissociation of side groups and phenyl ring. Whereas those at 69 and 41 Da are due to CH_2CCH_3CO and CH_2CCH_3fragments respectively.

The total ion current (TIC) curve of PBzMA shows two peaks maximizing at 330 and 415°C (Figure 34). The pyrolysis mass spectra are quite similar to that of the monomer. The molecular ion peak at 176 Da is present together with other diagnostic peaks at 158, 131, 69 and 41 Da. Again, the peaks present in the pyrolysis mass spectra at 39, 51, 65, 77 and 91 Da are attributed to decomposition of $C_6H_5CH_2$ group by dissociative ionization inside the mass spectrometer.

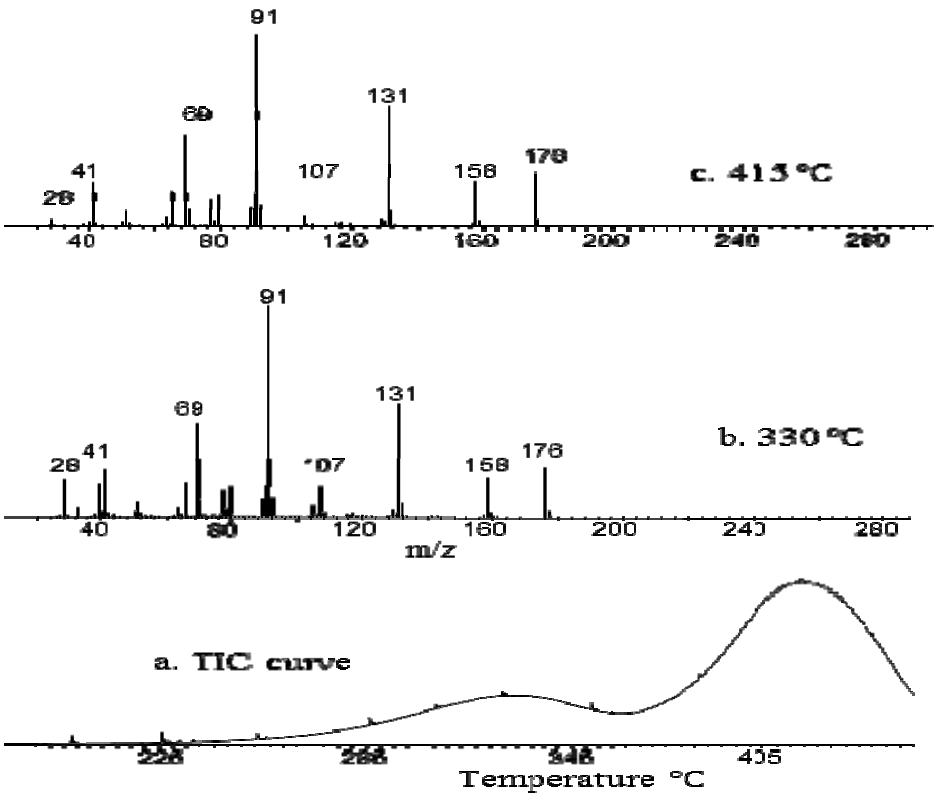

Figure 34. Single ion evolution profiles of some selected products detected during the pyrolysis of PBzMA.

The relative intensities and assignments made for the intense and/or characteristic peaks present in the pyrolysis mass spectra of PBzMA recorded at 330 and 415°C are collected in Table 10. At both temperatures, although the monomer peak at 176 Da is significantly intense the oligomer, M_x, peaks at 352, 528 and 704 Da for x=2 to 4 are totally absent.

Table 10: The relative intensities and assignments made for the intense and/or characteristic peaks present in the pyrolysis mass spectrum of PBzMA at 330 and 415°C.

m/z (Da)	Relative Intensity		Assignments
	330°C	415°C	
28	302	41	C_2H_4, CO
39	152	156	C_3H_3
41	223	231	$CH_3C=CH_2$
51	72	80	C_4H_3
65	161	182	C_5H_5
69	453	478	C_3H_5CO
77	123	144	C_6H_5
79	140	166	C_6H_7
85	5	3	C_3H_5COO
86	3	4	C_3H_5COOH
91	1000	1000	C_7H_7
107	143	175	$C_6H_5CH_2OH$
131	543	628	M-COOH
158	180	236	M-H_2O
176	224	279	M, monomer

In Figure 35 single ion evolution profiles of C_3H_3 (39 Da), $CH_3C=CH_2$ (41 Da), C_4H_3 (51 Da), C_3H_5CO (69 Da), C_6H_7 (79 Da), C_7H_7 (91 Da), M-COOH (131 Da), M-H_2O (158 Da) and monomer (176 Da) are given as representative examples. As can be seen from the single ion evolution profiles (Figure 35) all the low mass products show the same trends with that of the monomer indicating generation through the dissociative ionization processes inside the mass spectrometer, pointing out that thermal degradation occurs via depolymerization mechanism, yielding monomer. The low temperature peak with maximum of 330°C is attributed to thermal degradation of low mass PBzMA chains, and units involving head-to-head linkages as in case of PMMA and PIBMA.

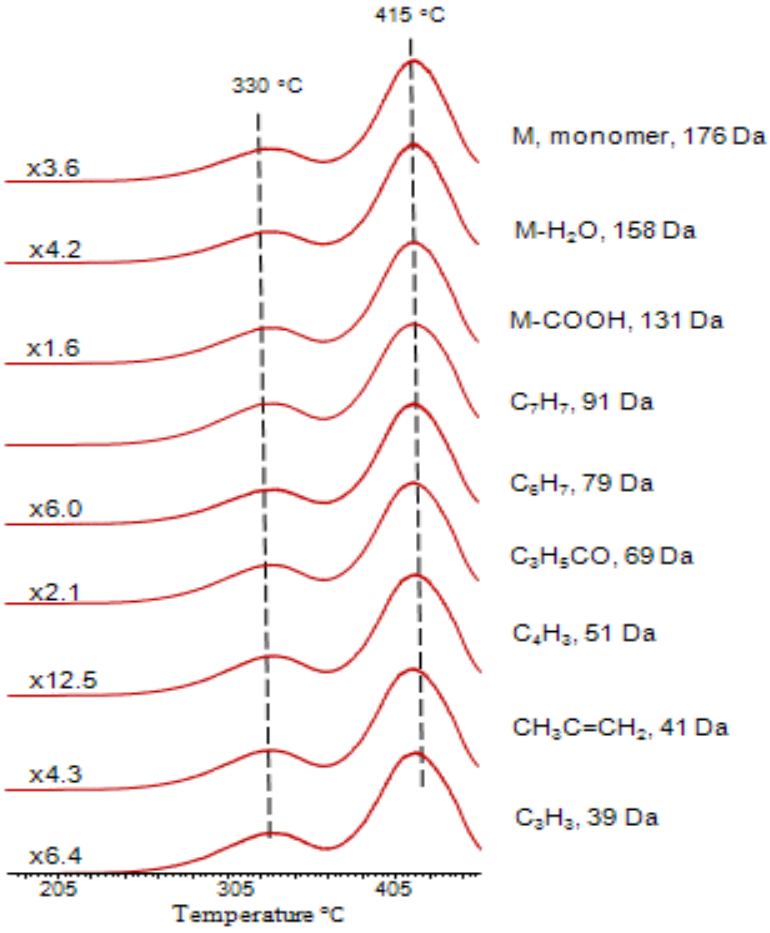

Figure 35. Single ion evolution profiles of some selected products detected during the pyrolysis of PBzMA.

3.2 Copolymers

3.2.1 Poly(methyl methacrylate-co-nbutyl acrylate) P(MMA-co-nBA)

TGA curve of P(MMA-co-nBA) polymer shows that the weight loss of the sample starts at around 300°C and most of the sample is lost at around 420°C (Figure 36). It is clear that the degradation is a two step process.

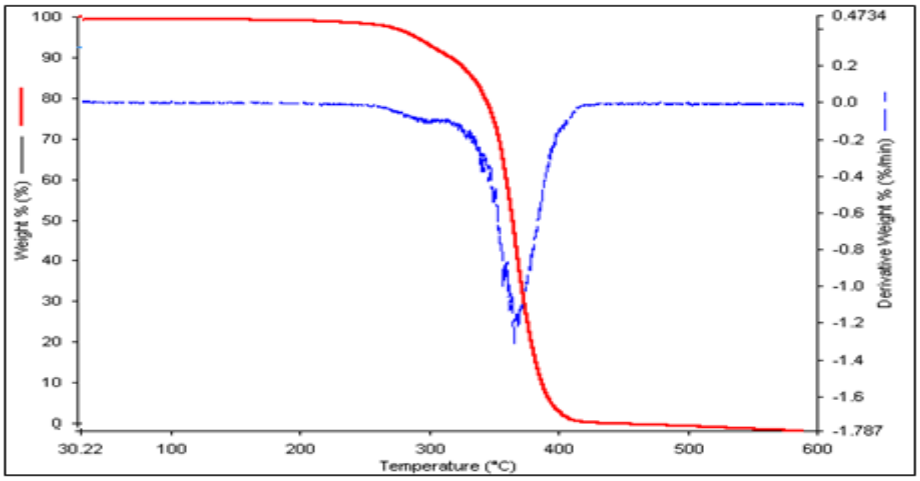

Figure 36. TGA curve of P(MMA-co-nBA).

The TIC curve recorded during the pyrolysis of P(MMA-co-nBA) is quite consistent with TGA. It shows two broad peaks maximizing at around 325 and 420°C (Figure 37). The mass spectra recorded at the peak maxima are also shown in Figure 37. Both spectra are dominated mainly by PMMA based peaks.

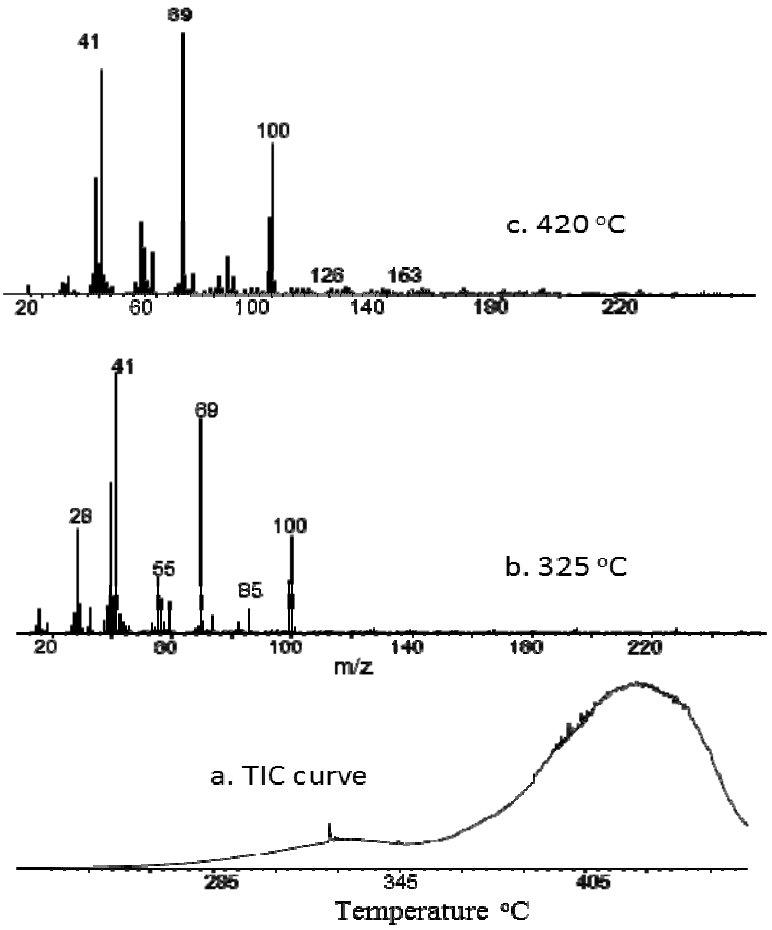

Figure 37. a. TIC curve and the pyrolysis mass of P(MMA-co-nBA) at b. 325 and c. 420°C.

Diagnostic peaks of MMA, monomer, are noticeably intense indicating that the main thermal degradation pathway for PMMA chains is depolymerization as in case of the homopolymer. Their evolution profiles again show two peaks with maxima at 325 and 420°C, identical to those detected for the corresponding homopolymer. The relative intensities and assignments made for the intense and/or characteristic peaks present in the pyrolysis mass spectra of P(MMA-co-nBA) recorded at 325 and 420°C are collected in Table 11.

Table 11: The relative intensities and assignments made for the intense and/or characteristic peaks present in the pyrolysis mass spectrum of P(MMA-co-nBA) at 325 and 420°C.

m/z (Da)	Relative Intensity		Assignments
	325°C	420°C	
31	19	16	CH_3O
39	589	434	C_3H_3
41	1000	838	C_3H_5
44	28	19	CO_2
45	27	29	COOH
55	225	270	C_2H_3CO
56	119	169	$CH_2=CHCH_2CH_3$
57	39	47	C_4H_9
69	824	1000	$CH_2C(CH_3)CO$
70	48	72	C_3H_5CHO
72	10	14	C_2H_3COOH
73	67	77	OC_4H_9
74	5	6	HOC_4H_9
81	11	22	$(CH_2=CH)_3$
85	92	139	CH_2CCH_3COO and/or $CH_2CCOOCH_3$
86	8	15	$C_2H_3COOHCH_2$ and/or CH_2CCH_3COOH
91	8	15	C_7H_7
100	372	559	M_{MMA}, monomer
101	25	49	$C_3H_5COHOCH_3$
108	3	10	D-$2C_4H_9OH$
126	12	29	$C_4H_6C_2O_3$
127	19	26	M_{BA}-H
128	6	13	M_{BA}, monomer
151	3	11	$C_2H_2CO_2COC_4H_5$
181	8	14	D-H-C_4H_9OH
182	3	6	D-C_4H_9OH
183	3	4	DH-C_4H_9OH
189	1	10	$(C_4H_5CH_3)_2C_4H_5$
208	2	7	T-$2C_4H_9OH$-CO
211	1	5	$C_3H_5CO_2COC_4H_5CO_2H$
228	17	16	mix dimer

Table 11 (continued)

236	1	4	T-2C_4H_9OH
249	1	5	$(C_4H_3CH_3)_3C_4H_3$
256	5	5	D, dimer
282	3	4	T-CO-C_4H_9OH
309	-	2	TeH-2C_4H_9OH-C_4H_8
311	1	1	TH-C_4H_9OH
328	-	1	DC_2H_3COOH
336	-	1	Te-CO-2C_4H_9OH
364	-	1	Te-2C_4H_9OH
400	-	1	Te-2C_4H_8
410	-	1	Te-CO-C_4H_9OH
439	-	1	Te-OC_4H_9
456	-	1	Te-C_4H_8
512	-	1	Te, tetramer

In Figure 38 single ion evolution profiles of diagnostic products of PMMA namely $CH_3C=CH_2$ (41 Da), C_3H_5CO (69 Da), and MMA (100 Da), those of PBA such as C_2H_3CO (55 Da), C_4H_9O (73 Da), COOH (45 Da), C_4H_8 (56 Da), $CH_2CHCOOH$ (72 Da), TH-2C_4H_9OH-C_4H_8 (181 Da), T-CO-2C_4H_9OH (208 Da), T-2C_4H_9OH (236 Da), TH-C_4H_9OH (311 Da), CO_2 (44 Da), $C_4H_6C_2O_3$ (126 Da), and as new products, mixed dimer (228 Da), C_3H_5CHO (70 Da), $C_3H_5COHOCH_3$ (101 Da), CH_3O (31 Da), $CH_2C(CH_3)COOH$ (86 Da), C_7H_7 (91 Da), BA (128 Da), $C_2H_2CO_2COC_4H_5$ (151 Da), $(C_4H_5CH_3)_2C_4H_5$ (189 Da), $(C_4H_3CH_3)_3C_4H_3$ (249 Da) and $C_3H_5CO_2COC_4H_5CO_2H$ (211 Da) are given as representative examples.

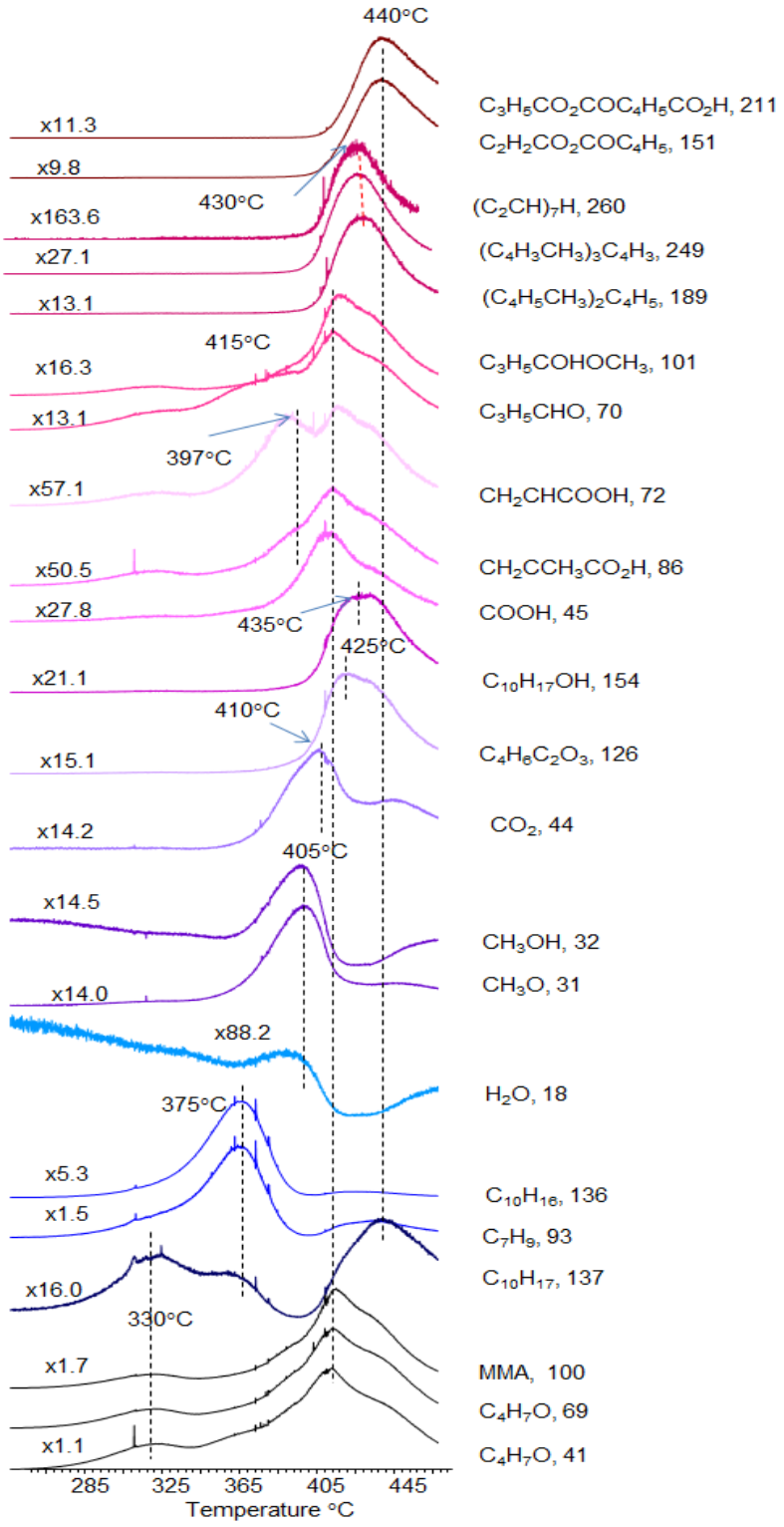

Figure 38. Single ion evolution profiles of some selected products recorded during pyrolysis of (PMMA-co-nPBA).

As can be noted from the single ion evolution profiles, the trends observed in PMMA based products detected during the pyrolysis of the copolymer are identical to those recorded from the homopolymer. Two peaks with a maximum at 325 and 420°C are present in the single ion evolution profiles of PMMA based products as in case of the homopolymer. On the other hand, significant changes are present in the single ion evolution profiles of PnBA based products (Figure 38).

Firstly, the yield of products characteristic to PnBA are low as expected due to the composition of the copolymer. Furthermore, it is clear that all BA chains are stabilized to some extent. The weak peak observed in the evolution profiles of thermal degradation products of PnBA homopolymer at around 270°C is totally absent in the evolution profiles of PnBA based products of the copolymer.

Presence of randomly distributed BA units along the PMMA chains randomly, should increase the yield of BA monomer, as the PMMA degradation proceeds through depolymerization. The molecular ion peak is absent in the mass spectrum of BA (Figure 14.a), however, the products obtained at 55 and 73 Da due to the dissociative ionization of the butyl acrylate monomer show identical evolution profiles maximizing at 415°C supporting evolution of BA during the depolymerization process. In addition, a new peak that can be directly attributed to a mix dimer is observed at 228 Da. The yield of this product is maximized at around 408°C. It also shows a second but weaker peak at 325°C in its evolution profile.

Contrary to what is observed for PBA, the single ion evolution profiles of products $CH_2CHCOOH$ (72 Da), COOH (45 Da) and C_4H_8 (56 Da) generated by McLafferty type rearrangement reactions involving γ-H transfer from the butyl groups to CO groups of PBA (Scheme 4.a) show a single peak, with a maximum at 420°C. The evolution of high mass fragments involving acrylic acid units such as $M_xCH_2CHCOOH$ where x=2 to 5 are only detected at elevated temperatures, at around 440°C. The decrease in the yield of $CH_2CHCOOH$ (72 Da), C_4H_8 (56 Da) is about 1.7 and 5.1 folds respectively, but, the yield of COOH (45 Da) is about same. It is clear that the decrease in the yield of products that may be associated with loss of C_4H_8 and generation of acrylic acid is less than the expected considering the composition of the copolymer. It is clear that the decrease in the yield of C_4H_8 is less than the expected considering the composition of the copolymer.

It may be thought that the H-transfer reactions to CO groups from the butyl groups become preferential when the H-transfer reactions from the main chain become less likely. For the PBA homopolymer, the yield of the monomer is quite low, whereas those of M-H (127 Da), M_x-OC_4H_9 or MH-HOC_4H_9 (183, 311, 439, 567 Da for x=2 to 5) that may be generated through reaction pathways given in Scheme 9 and the products involving six or more carbon atoms along the main chain and generated through the reaction pathways given in Schemes 10 and 11, such as TH-$2C_4H_9OH$-C_4H_8 (181 Da) and TeH-C_4H_9OH-C_4H_8 (309 Da),T-C_4H_9OH-CO (282 Da), T-$2C_4H_9OH$ (236 Da), TH -$2C_4H_9OH$-CO (208 Da) are significantly intense. Contrary to what is observed for the homopolymer, the yield of all products involving more than one monomer unit are reduced significantly, more than ten-folds during the pyrolysis of the copolymer. On the other hand the decrease in the yield of BA, the monomer is only 3.6 folds. In addition only 1.3 and 5.1 folds decreases are recorded in the relative yields of OC_4H_9 (73 Da) and C_4H_8 (56 Da) respectively. The decrease in the yield of the segments involving more than one repeating unit may directly be attributed to the composition of the copolymer. It may be thought that the random copolymer involving only 12.5 % BA does not involve sufficiently long BA segments that degrade into segments involving more than one monomer unit. As a consequence, degradation by rearrangement reactions involving γ-H transfer from the main chain as shown in Schemes 9 and 10 cannot be preferential. The presence of methyl group on the main chain of the polymer backbone due to the longer methyl methacrylate segments hinders the hydrogen transfer reactions from the main chain to the carbonyl groups. This explains the reductions in the yields of products such as those at 127, 181, and 309 Da fragments (Schemes 9 and 10).

High mass products such as Te (512 Da), Te-CO-C_4H_9OH (410 Da), Te-$2C_4H_8$ (400 Da), Te-$2C_4H_9OH$ (364 Da), Te-CO-$2C_4H_9OH$ (336 Da) and Te-$2C_4H_9OH$-C_4H_9 (309 Da), show a single peak with a maximum at around 440 °C in their evolution profiles. Actually, their yields are lower than the expected considering the composition of the copolymer; i.e. the decrease in the yield of tetramer of BA is more than 44-folds compared to what is recorded for PBA. It may be thought that high mass products are only generated at high temperatures due to the decomposition of segments involving crosslinking.

As in case of PBA homopolymer, evolution of H_2O is not observed but the production of CO_2, fragments that can be associated with anhydride units such as $C_4H_6C_2O_3$ (126 Da) reaching maximum yield at around 434°C and unsaturated products like C_7H_7 maximizing at 437°C can be regarded as a direct evidence for anhydride decomposition and subsequent crosslinking of the polymer. The decrease in the generation of CO_2 and C_7H_7, being 14 and 8-folds respectively, compared to the corresponding homopolymer, reveals the decrease in the extent of crosslinking.

It may be thought that H_2O evolved during the anhydride formation process may react with MMA units generating methacrylic acid (86 Da) and methanol and/or it may react with BA units yielding acrylic acid and butanol as shown in Scheme 15.

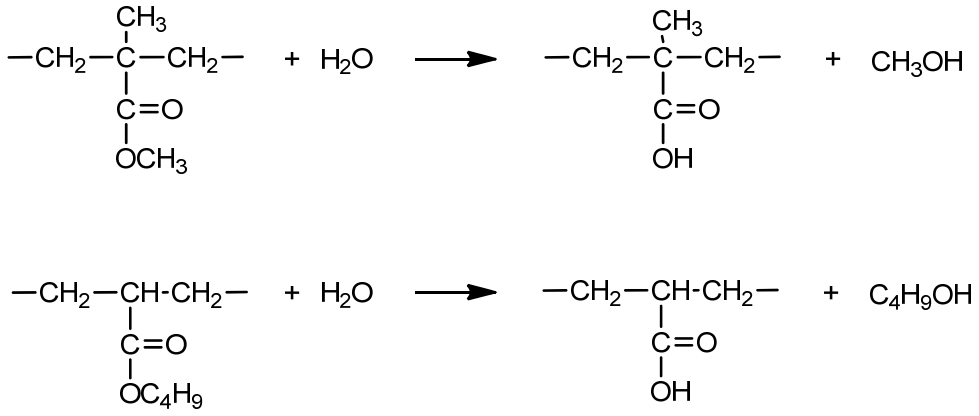

Scheme 15. Reaction between H_2O-MMA and H_2O-nBA.

Since, the yield of products obtained as a result of rearrangement reactions involving γ-H transfer to the carbonyl from the alkyl chain of PBA is very low, it can be concluded that the generation of segments with acidic side chains should also be limited. As, there is negligible amount of acrylic acid units generated by loss of but-1-ene from PBA chains, the transesterification reaction between the MMA and acrylic acid as shown in Scheme 16 should not be very likely. Absence of 32 Da peak, due to evolution of CH_3OH as a result of transesterification reaction, may be regarded as a direct evidence for this proposal. However, CH_3O (31 Da) fragment that can directly be attributed to cleavage of CH_3O-CO bond of MMA, shows a very

slightly different evolution profile compared to those of MMA (100 Da), CH_2CCH_3CO (69 Da) and CH_2CCH_3 (41 Da) with a maximum at 425°C, pointing out presence of a different source for its generation.

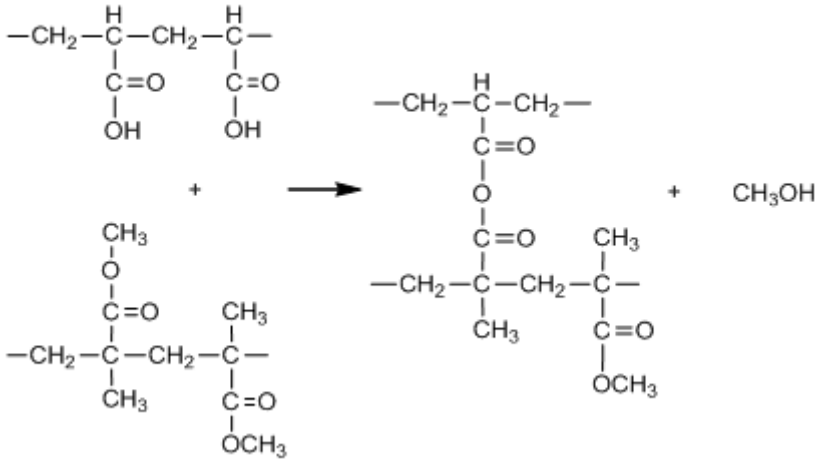

Scheme 16. Trans-esterification reaction between acrylic acid and methyl methacrylate units.

As a consequence of transesterification reactions between MMA and acrylic acid units, generation of new fragments can be expected. On the basis of DP-MS findings, the peaks at 211 and 151 Da may be assigned to $CH_2C(CH_3)CO_2COCHCH_2C(CO_2H)CH_2$ and $CH_2CCO_2COCHCH_2CCH_2$ respectively. The evolution profiles of these products show a maximum at 445°C.

Presumably, the series of peaks at 325, 257, 189, and 121 Da may be assigned to $(C_4H_5CH_3)_{x-1}C_4H_5$ for x=5 to 2 and those at 315, 249, 183 and 117 Da may be attributed to $(C_4H_3CH_3)_{x-1}C_4H_3$ for x=5 to 2. These products reach maximum yield at around 437°C. Single ion evolution profiles of $(C_4H_5CH_3)_2C_4H_5$ (189 Da), $(C_4H_3CH_3)_3C_4H_3$ (249 Da), $CH_2CCO_2COCHCH_2CCH_2$ (151 Da) and $CH_2C(CH_3)CO_2COCHCH_2C(CO_2H)CH_2$ (211 Da) are given in Figure 38 as representative examples.

Degradation of the segments generated by the mechanism given in Scheme 16 should yield $CH_2CHCOOCH_3$ (86 Da) and OCH_3 (31 Da). Under the experimental

conditions it is not possible to estimate which mechanism is more fundamental. However, the similarities in the evolution profiles of 86 and 31 Da products and lack of CH_3OH support existence of transesterification reaction also between CH_3OH and acrylic acid units as shown in Scheme 17. Thermal degradation of this units will also yield methacrylate $CH_2CHCOOCH_3$ (86 Da).

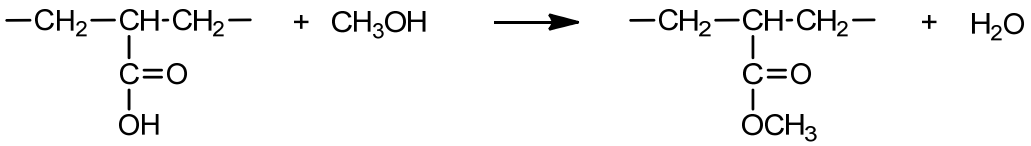

Scheme 17. Transesterification reaction between acrylic acid units and methanol.

Another possible degradation process involves the γ-H transfer to the carbonyl group of MMA from the adjacent BA units. This process if occurs will also produce 86 Da peak due to $CH_2C(CH_3)COOH$ and/or $CH_2CCOHOCH_3$ (Scheme 18). In addition new products such as $CH_2C(CH_3)CHOHOCH_3$ (102 Da), $CH_2C(CH_3)COHOCH_3$ (101 Da) and $CH_2C(CH_3)CHO$ (70 Da) should be generated. Among these products the single ion evolution profiles of the most abundant ones due to $CH_2C(CH_3)CHO$ (70 Da) and $CH_2C(CH_3)COHOCH_3$ (101 Da) are given in Figure 38 as representative examples.

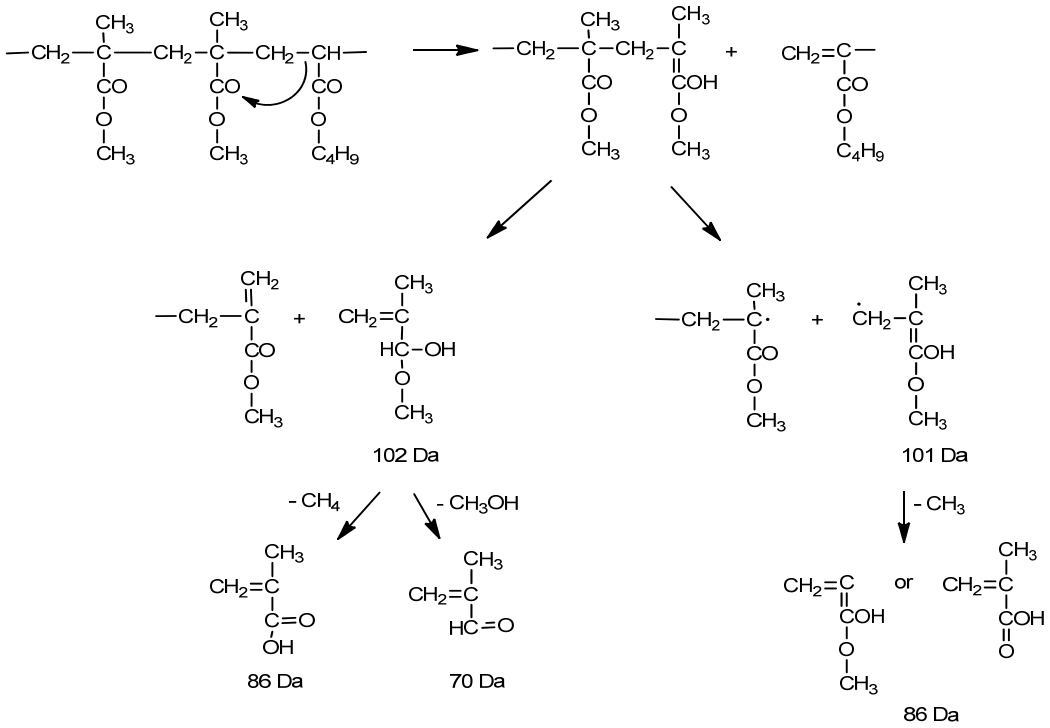

Scheme 18. Reaction between BA and MMA units due to H-transfer reactions.

To conclude, it can be said that although the presence of butyl acrylate does not affect the thermal stability of PMMA chains in a considerable manner, the butyl acrylate chains are stabilized to some extend by the presence of methyl methacrylate chains. While the degradation of PBA chains in the homopolymer starts at around 270°C and maximum product yield is observed at 375°C, in the copolymer low temperature shoulder is observed at 325°C and maximum yields of PBA based products are detected in the temperature range 416 to 420°C. As a consequence of the composition of the copolymer, long PBA chains do not exist. Thus, significant decrease in the relative yields of high mass fragments is detected. Furthermore, H-transfer reactions from the butyl group to the CO group become preferential compared to H-transfer reactions from the main chain which results in increase in the relative yield of acrylic acid units compared to PBA. Anhydride formation followed by evolution of CO_2 generates unsaturated and/or crosslinked units. Strong evidences for trans-esterification reactions between H_2O and MMA and BA yielding methacrylic and acrylic acid segments and reactions between CH_3OH and acrylic acid yielding methacrylate segments are detected. Although not

abundant, products indicating reactions between MMA and BA units are also observed.

3.2.2 Poly(methyl methacrylate-co- isobornyl acrylate) P(MMA-co-IBA)

TGA curve recorded during the degradation of P(MMA-co-IBA) polymer shows that the degradation of copolymer is a multi step process (Figure 39). The first portion of the weight loss is observed at around 320°C and then at around 375°C there is a larger amount of weight loss observed. The third and the fourth points of temperatures where the remaining portion of the sample is lost are at around 410 and 440°C.

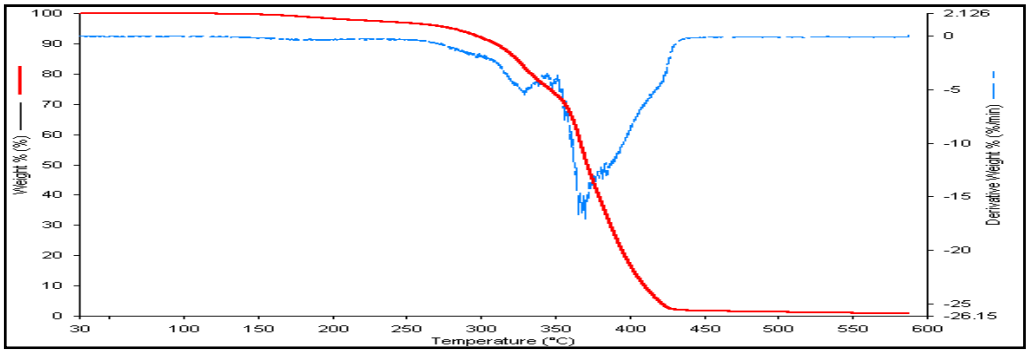

Figure 39. TGA curve of P(MMA-co-IBA).

The results of the pyrolysis mass spectrometry analyses are quite consistent with that of the thermogravimetry analysis. The TIC curve recorded during the pyrolysis of P(MMA-co-IBA) shows two broad peaks with a low temperature tail (Figure 40). The mass spectra recorded at around 320 and 375°C are dominated with characteristic peaks of both components. On the other hand, the mass spectrum recorded at the maximum of the high temperature peak; at 407°C shows mainly PMMA based peaks. In addition, new peaks that are not present in the pyrolysis mass spectra of PMMA and PIBA are detected at temperatures above 400°C. The relative intensities (RI) and assignments made for the intense and/or characteristic peaks present in the pyrolysis mass spectra of PMMA-co-PIBA recorded at 375 and 407°C are collected in Table 12.

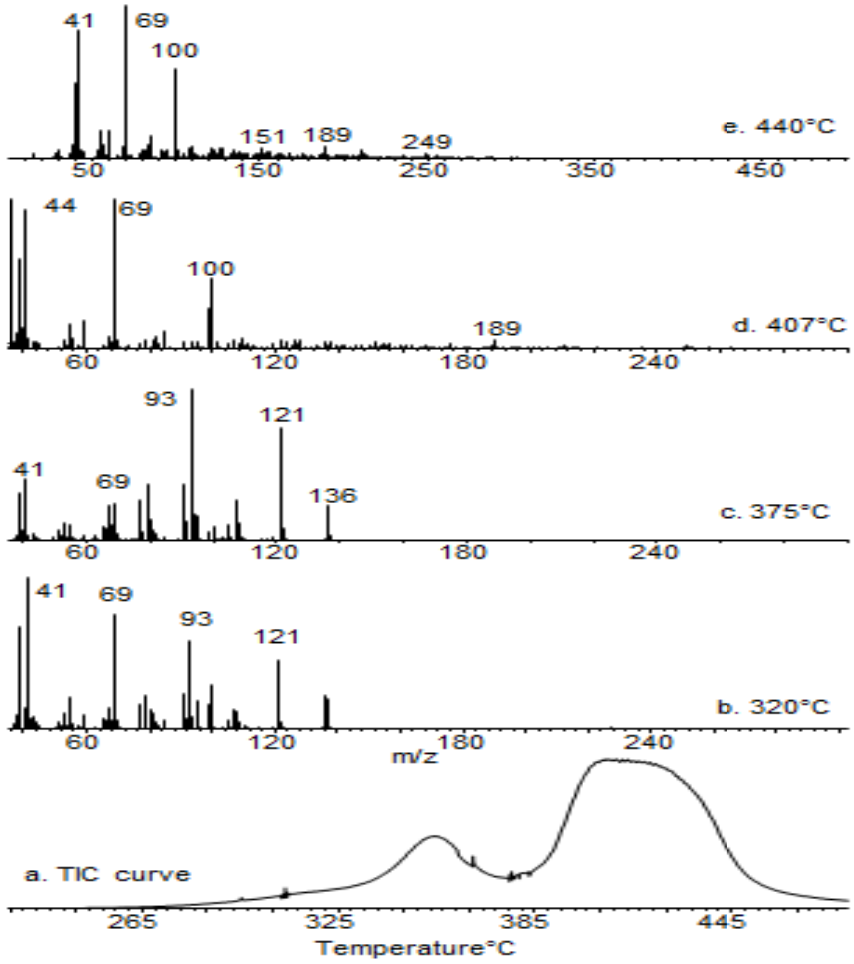

Figure 40. a. TIC curve and the pyrolysis mass of P(MMA-co-IBA) at b. 320, c. 375 and d. 407°C

Table 12: The relative intensities and assignments made for the intense and/or characteristic peaks present in the pyrolysis mass spectrum of P(MMA-co-IBA) at 375 and 407°C.

m/z (Da)	Relative Intensity		Assignments
	375°C	407°C	
18	10	1	H_2O
31	28	20	CH_3O
32	46	12	CH_3OH
41	562	841	$CH_3C{=}CH_2$
44	24	45	CO_2
45	12	33	COOH
69	372	1000	C_3H_5CO
70	52	74	C_3H_5CHO
81	74	65	C_6H_9
86	4	15	$CH_2CCH_3CO_2H$
91	345	58	C_7H_7
93	1000	54	C_7H_9
100	156	588	MMA, monomer
101	10	65	$CH_2CCH_3COHOCH_3$
117	5	15	$(C_4H_3CH_3)C_4H_3$
121	772	73	C_9H_{13}, TBA - $CH_2CHCOOH$ - CH_3
126	3	76	$C_4H_6C_2O_3$
132	-	6	$(C_4H_3CH_3)_2$
136	249	37	$C_{10}H_{16}$, IBA-$CH_2CHCOOH$
137	41	57	$C_{10}H_{17}$
151	1	78	$CH_2CCO_2COCHCH_2CCH_2$
154	1	54	$C_{10}H_{17}OH$
183	1	14	$(C_4H_3CH_3)_2C_4H_3$
189	1	87	$(C_4H_5CH_3)_2C_4H_5$
198	-	11	$(C_4H_3CH_3)_3$
204	-	13	$(C_4H_5CH_3)_3$
211	-	61	$CH_2C(CH_3)CO_2COCHCH_2C(CO_2H)CH_2$
249	-	41	$(C_4H_3CH_3)_3C_4H_3$
260	-	6	$(C_2CH)_7H$

Inspection of single ion evolution profiles of diagnostics products of the components of the copolymer P(MMA-co-IBA) indicates significant differences compared to the corresponding homopolymers (Figure 41). Diagnostic peaks of MMA are noticeably intense indicating that the main thermal degradation pathway for PMMA chains is depolymerization as in case of the homopolymer. Their evolution profiles again show two peaks with maxima at 330 and 415°C, almost identical to those detected for the corresponding homopolymer. However weak shoulders at around 375 and 445°C are present.

On the other hand, more significant differences are detected in the evolution profiles of the thermal degradation products of PIBA. Firstly, the evolution profiles are broader. Three peaks, the first two being overlapped, with maxima at 330, 375 and 440°C are present in the evolution profile of isobornyl (137 Da) radical. Isobornylene evolution is mainly detected at around 375°C. Yet, weak shoulders/peaks are also detected at around 330 and 440°C. Contrary to the results of PIBA, during the pyrolysis of the copolymer, the ratio of relative yields of isobornylene to isobornyl increased from 0.6 to 3.0 indicating that generation of isobornylene is enhanced. Single ion evolution profile of acrylic acid generated upon loss of isobornylene shows two overlapping peaks with maxima at 397 and 415°C.

In contrast, a decrease in the yield of H_2O is detected. The broad peak in its evolution profile is associated with desorption of H_2O from the surfaces of the probe under the vacuum conditions of the DP-MS system. The small peak on the H_2O background has a maximum at 405°C. The fragment with m/ z value 126 Da reaching maximum yield above 410°C may be associated with $C_4H_5C_2O_3$ having anhydride structure. A detailed analysis of the pyrolysis mass spectra indicates evolution of CH_3OH (32 Da) following the isobornylene generation. The trends in the single ion evolution profiles of CH_3O (31 Da) due to cleavage of CH_3O-CO bond of MMA and those of the products with m/z values 31 and 32 Da generated during the pyrolysis of the copolymer clearly supports generation of methanol (32 Da), producing CH_3O (31 Da) during the ionization process. In the light of present findings, a transesterification reaction between the MMA and acrylic acid units generated by loss of isobornylene from PIBA chains can be proposed as shown in Scheme 16.

Evolution of CO_2 is detected in a broad temperature region pointing out degradation of anhydride units. The yield of CO_2 is maximized at around 410°C but is continued until the end of the pyrolysis process. Products involving unsaturation observed in the final stages of thermal degradation, as in case of PIBA, are again detected. As an example the evolution profile of product with m/z 260 Da tentatively $(C_2CH)_7H$ is given in Figure 41.

In addition, as a consequence of transesterification reactions between MMA and acrylic acid units, generation of new fragments can be expected as in case of poly(MMA-co-BA). On the basis of DP-MS findings, the peaks at 211 and 151 Da may again be assigned to $CH_2C(CH_3)CO_2COCHCH_2C(CO_2H)CH_2$ and $CH_2CCO_2COCHCH_2CCH_2$ respectively. Presumably, the series of peaks at 340, 272, 204 and 136 Da may be assigned to $(C_4H_5CH_3)_x$ while those at 324, 255, 189 and 121 Da to $(C_4H_5CH_3)_{x-1}C_4H_5$ for x=5 to 2. Similarly peaks at 330, 264, 198 and 132 Da may be associated with $(C_4H_3CH_3)_x$ and 315, 249, 183 and 117 Da may be attributed to $(C_4H_3CH_3)_{x-1}C_4H_3$ for x=5 to 2.

Thus, it can be concluded that generation of anhydride units impeding depolymerization reactions, generates H_2O and CH_3OH and promotes further side reactions leading to the formation of crosslinked structure by loss of CO_2.

Actually the low yield of H_2O may be due to possible transesterification reactions between H_2O and MMA and IBA. When MMA units are involved this reactions should generate methacrylic acid (86 Da) in addition to methanol (Scheme 15). Evolution profile of methacrylic acid follows almost identical trends with that of COOH, indicating that anhydride formation for methacrylic acid does not take place. When IBA units are involved in trans-esterification reactions with H_2O, acrylic acid and isobornyl alcohol should be generated. The high temperature peak in the evolution profile of acrylic acid with a maximum at 415°C may be attributed to acrylic acid units generated by reactions of IBA with H_2O. Evolution of isobornyl alcohol is also recorded at elevated temperatures supporting the existence of these transesterification reactions.

Another possible degradation process involves the γ-H transfer to the carbonyl group of MMA from the adjacent IBA units as in case of poly(MMA-co-BA) given in Scheme 18. Again, as discussed for poly(MMA-co-BA), this process, if occurs, will also produce 86 Da peak due to $CH_2C(CH_3)COOH$ and/or $CH_2CCOHOCH_3$, $CH_2C(CH_3)CHOHOCH_3$ (102 Da), $CH_2C(CH_3)COHOCH_3$ (101 Da) and $CH_2C(CH_3)CHO$ (70 Da). Among these products the single ion evolution profiles of the most abundant ones due to $CH_2C(CH_3)CHO$ (70 Da) and $CH_2C(CH_3)COHOCH_3$ (101 Da) are given in Figure 41 as representative examples.

In Figure 41 single ion evolution profiles of PMMA based products C_3H_5 (41 Da), C_3H_5CO (69 Da), monomer, MMA (100 Da), and PIBA based products such as $C_{10}H_{17}$ (137 Da), C_7H_9 (93 Da), $C_{10}H_{16}$ (136 Da), H_2O (18 Da), CH_3O (31 Da), CH_3OH (32 Da), CO_2 (44 Da), $C_4H_6C_2O_3$ (126 Da), $C_{10}H_{17}OH$ (154 Da), CO_2H (45 Da), CH_2CCH_3COOH (86 Da), $CH_2CHCOOH$ (72 Da), $CH_2C(CH_3)CHO$ (70 Da), $CH_2C(CH_3)COHOCH_3$ (101 Da), $(C_4H_5CH_3)_2C_4H_5$ (189 Da), $(C_4H_3CH_3)_3C_4H_3$ (249 Da), $(C_2CH)_7H$ (260 Da), $C_2H_2CO_2COC_4H_5$ (151 Da) and $C_3H_5CO_2COC_4H_5CO_2H$ (211 Da) are given as representative examples.

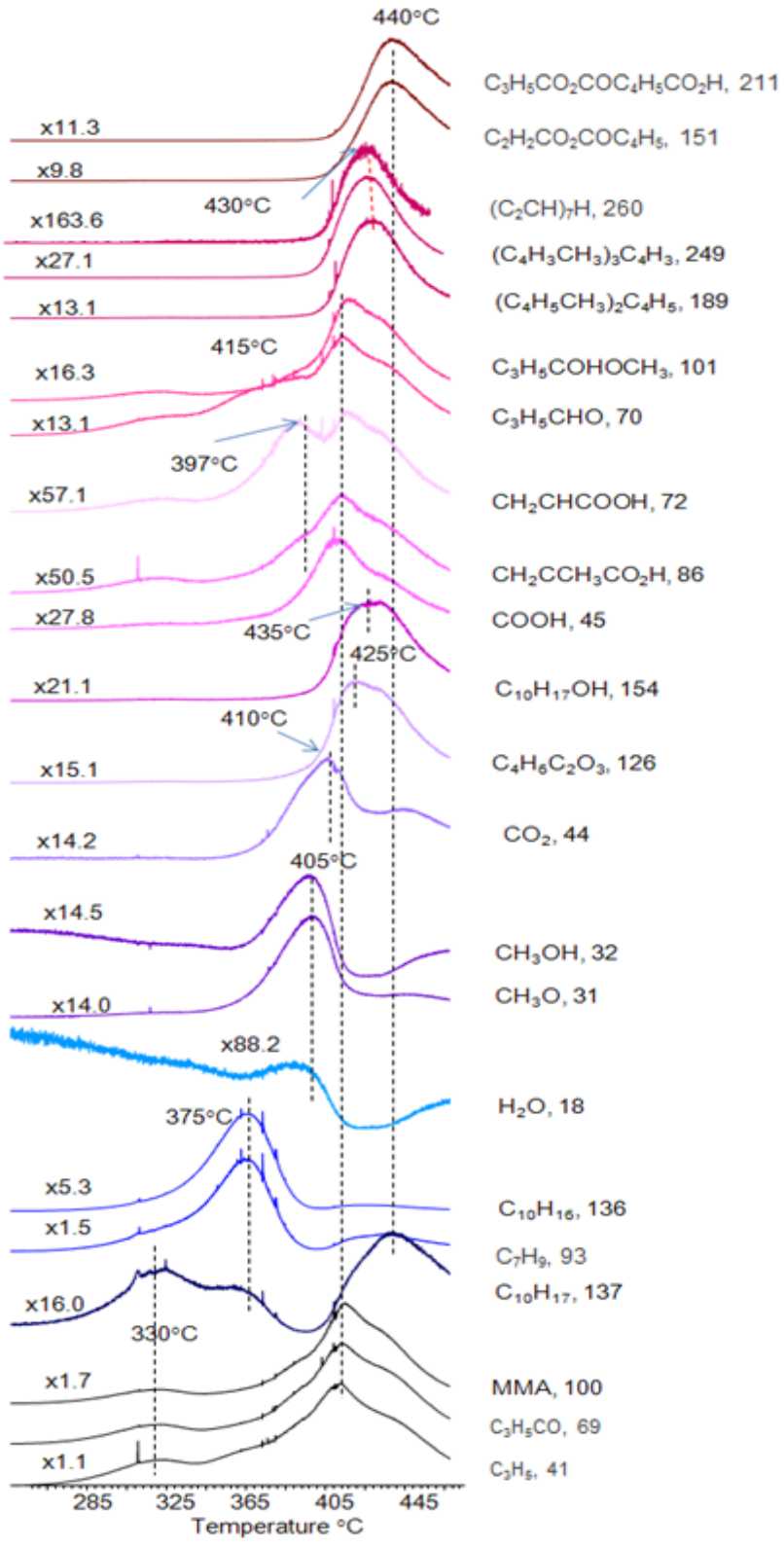

Figure 41. Single ion evolution profiles of some selected products recorded during pyrolysis of P(MMA-co-IBA).

Thus, it can be concluded that PMMA chains of the copolymer involving 12.5 % IBA units, degrades mainly by depolymerization as in case of pure PMMA, yet, H-transfer from the isobornyl group to CO of IBA and from the back bone of PIBA to CO of MMA units generate acrylic acid and methacrylic acid to a certain extent. Anhydride formation by elimination of H_2O, and generation of crosslinked and/or unsaturated linkages by loss of CO_2 and CO are detected. Strong evidences for trans-esterification reaction between MMA and acrylic acid and H_2O and those between IBA and H_2O are detected.

Compared to P(MMA-co-nBA), the relative yields of acrylic acid and products due to transesterification reactions are noticeably higher for P(MMA-co-IBA). The degradation via H-transfer from the isobornyl group to CO group is the main thermal degradation pathway for the homopolymer PIBA, whereas H-transfer butyl group to CO group is only one of the competing degradation processes for the homopolymer PBA. Thus, the generation of acrylic acid during the decomposition of P(MMA-co-IBA) is more likely. Acrylic acid generation takes place more readily at lower temperatures for PIBA and its copolymer with MMA, at around 335 and 375°C respectively. Whereas for PBA and its copolymer with MMA, its generation takes place above 375 and 410°C respectively, very close to the temperature region where PMMA chains start to degrade. Thus, transesterification reactions of acrylic acid and H_2O with MMA seem to be more likely for the copolymer involving IBA. The increase in the relative yields of related products during the pyrolysis of poly(MMA-co-IBA) confirms this proposal.

3.2.3 Poly(methyl methacrylate-co-benzyl methacrylate) P(MMA-co-BzMA)

The TGA curve of P(MMA-co-BzMA) given in Figure 42 shows that the thermal degradation of the sample starts at around 250°C. It is a two-step thermal degradation process. The first portion of the weight loss occurs at around 300°C and the remaining portion of the polymer degrades at around 360°C.

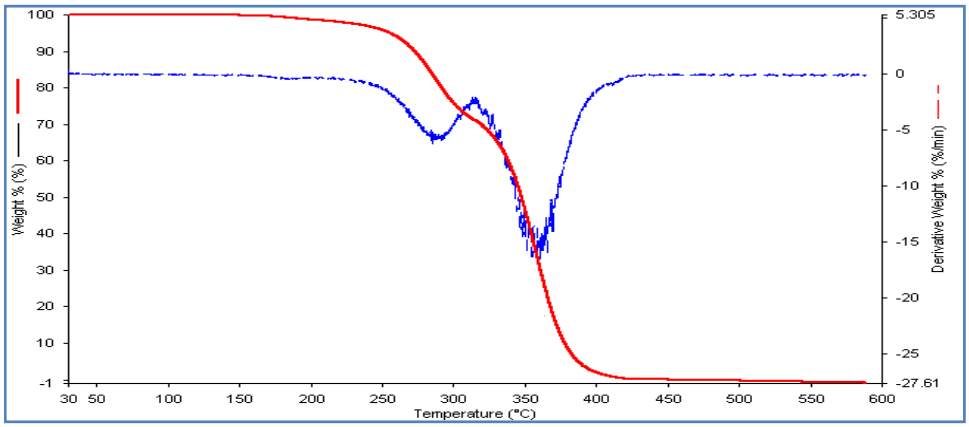

Figure 42. TGA curve of P(MMA-co-BzMA).

The TIC curve recorded during the pyrolysis of P(MMA-co-BzMA) shows two broad peaks maximizing at 320 and 400°C (Figure 43) with TGA data. The mass spectra recorded at both maxima are dominated with characteristic peaks of both components. Diagnostic peaks of both MMA and BzMA are noticeably intense indicating that the main thermal degradation pathway is depolymerization as in case of the homopolymers.

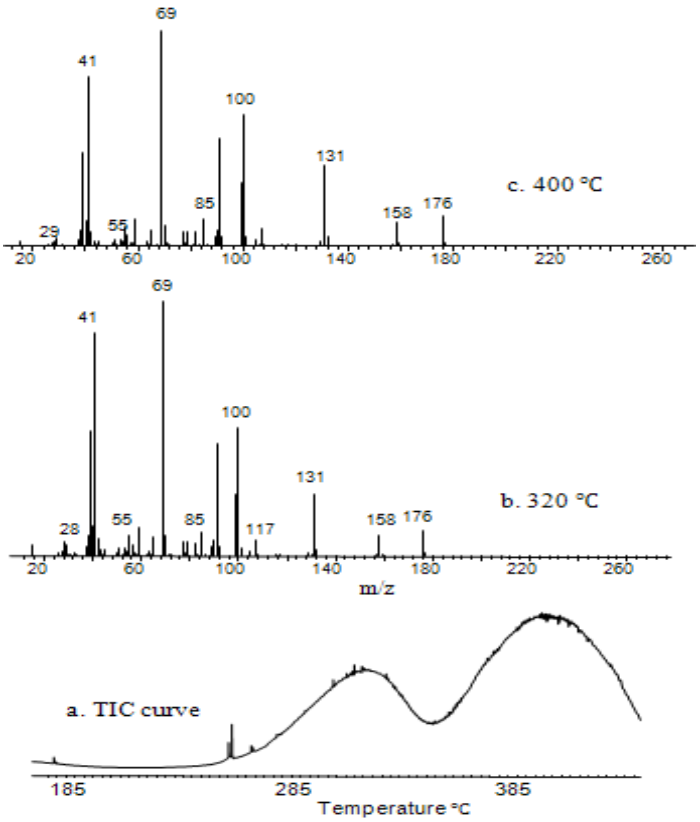

Figure 43. a. TIC curve and the pyrolysis mass of P(MMA-co-BzMA) at b. 320 and c. 400°C.

The relative intensities and assignments made for the intense and/or characteristic peaks present in the pyrolysis mass spectra of P(MMA-co-BzMA) recorded at 320 and 400°C are collected in Table 13. At both temperature maxima 39 and 41 Da peaks due to C_3H_3 and $CH_3C{=}CH_2$ fragments respectively are the most intense. The monomer and tropylium ion's peak at 176 and 91 Da respectively are quite significant as in case of homopolymer, poly(benzyl methacrylate). The products with m/z values 51, 65, 77, 79, 91 Da generated by dissociation of side groups and phenyl ring show similar evolution profiles with those of benzyl methacrylate homopolymer. Products with m/z values 158 and 131 Da which are associated with products generated by loss of H_2O and COOH by complex rearrangement reactions are also very abundant. A new product that can readily be assigned to mix dimer (276 Da) is detected. Its evolution profile shows two peaks with maxima at 320 and 413 °C.

Table 13: The relative intensities and assignments made for the intense and/or characteristic peaks present in the pyrolysis mass spectrum of P(MMA-co-BzMA) at 320 and 400°C.

m/z (Da)	Relative Intensity		Assignments
	320°C	400°C	
28	377	182	C_2H_4
39	636	635	C_3H_3
40	140	136	C_3H_4
41	1000	1000	$CH_3C=CH_2$
44	31	22	CO_2
51	36	35	C_4H_3
65	63	68	C_5H_5
69	902	946	C_3H_5CO
77	52	54	C_6H_5
79	48	53	C_6H_7
85	69	78	$CH_2C(CH_3)COO$
86	4	6	$CH_2C(CH_3)COOH$
91	350	373	C_7H_7
100	342	377	M_{MMA}, monomer
107	42	47	$C_6H_5CH_2O$
131	164	171	M_{BzMA}-COOH
158	52	55	M_{BzMA}-H_2O
176	64	65	M_{BzMA}, monomer
276	1	1	mix dimer

In Figure 44 single ion evolution profiles of diagnostic products of PMMA chain namely C_3H_5 (41 Da), C_3H_5CO (69 Da), monomer, MMA (100 Da) and those of PBzMA chains CO_2 (44 Da), C_6H_5 (77 Da), C_7H_7 (91 Da), M-COOH (131 Da), M-H_2O (158 Da), monomer, BzMA (176 Da) and as new product, mix dimer (276 Da) are given as representative examples.

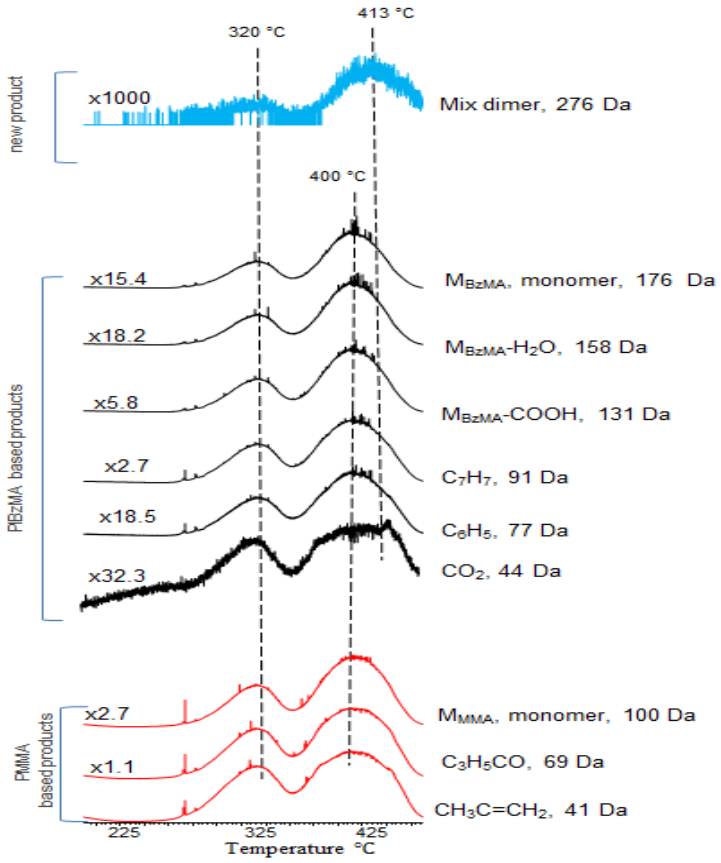

Figure 44. Single ion evolution profiles of some selected products detected during the pyrolysis of P(MMA-co-BzMA).

As can be seen from the single ion evolution profiles, the products of both PMMA and PBzMA show the same degradation trends. All products show two peaks in their evolution profiles with maxima at 320 and 400°C which are very close to corresponding values detected for the homopolymers.

The yield of CO_2 generated during the pyrolysis of the copolymer is almost same compared to PMMA and PBzMA homopolymers. Its evolution profile has two broad peaks with maximums at 320 and 400°C. Therefore, it can be concluded that the extent of crosslinked structure is not affected due to the copolymerization. Also, the lack of 32 Da peak due to methanol evolution that should be obtained as a result of methanol evolution is not observed during ionization of the copolymer which shows that there is no transesterification reaction in the degradation process. There is also γ-H transfer to the carbonyl of MMA from the benzyl ring, which produces

$CH_2C(CH_3)COOH$ (86 Da). The relative yield of 86 Da peak is increased about 2.5-folds compared to corresponding value for PMMA and PBzMA homopolymer. This product is also maximized at 400 and 320°C.

To conclude, it is clear that the copolymerization of methyl methacrylate with benzyl methacrylate polymer does not make a drastic change in their thermal degradation behavior of both components.

3.2.4 Poly(methyl methacrylate-co-nbutyl acrylate-co-ısobornyl acrylate) P(MMA-co-nBA-co-IBA)

The thermal degradation of two different composition of the poly(methyl methacrylate-co-nbutyl acrylate-co-ısobornyl acrylate) copolymer is studied. The first sample includes 90% MMA - 5% nBA -5% IBA and the second sample is composed of 70% MMA-15% nBA-15% IBA by weight.

a. P(MMA-co-nBA-co-IBA) (90% - 5% - 5%)

TGA curve of the P(MMA-co-nBA-co-IBA) is given in Figure 45. The copolymer sample shows a two-step weight loss in the temperature range of 280–400°C due to polymer degradation. Although the highest portion of the weight loss is observed at around 400°C there is also some amount of weight loss at around 300°C.

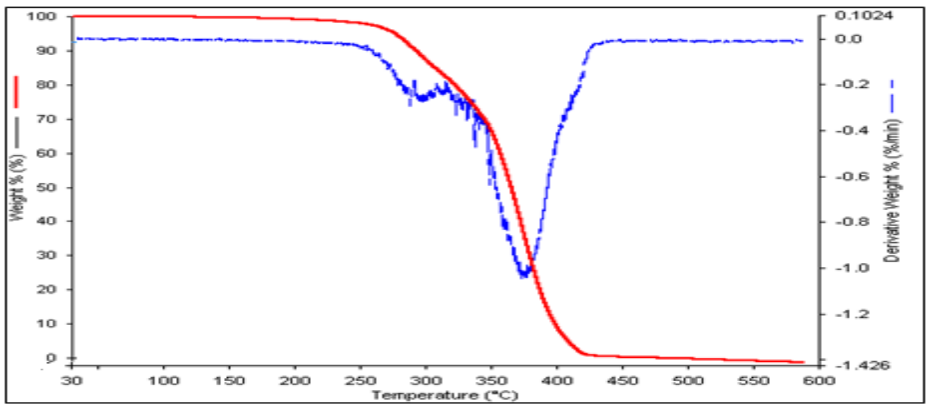

Figure 45. TGA curve of P(MMA-co-nBA-co-IBA).

Consistent with TGA results, the TIC curve recorded during the pyrolysis of P(MMA-co-IBA-co-nBA) shows two broad peaks with a low temperature tail (Figure 46). The mass spectra recorded at around 332°C are dominated mainly with characteristic peaks of PMMA but also showed peaks due to thermal degradation of PIBA and PBA. On the other hand, the mass spectrum recorded at the maximum of the high temperature peak, at around 440°C shows mainly PMMA based peaks and some high mass peaks due to fragments that has been associated with reactions between MMA and acrylic acid generated by H-transfer reactions from the side groups, to carbonyl groups of IBA and BA respectively. In general, the yields of diagnostic products of both PIBA and PBA are quite low in accordance with the composition of the copolymer.

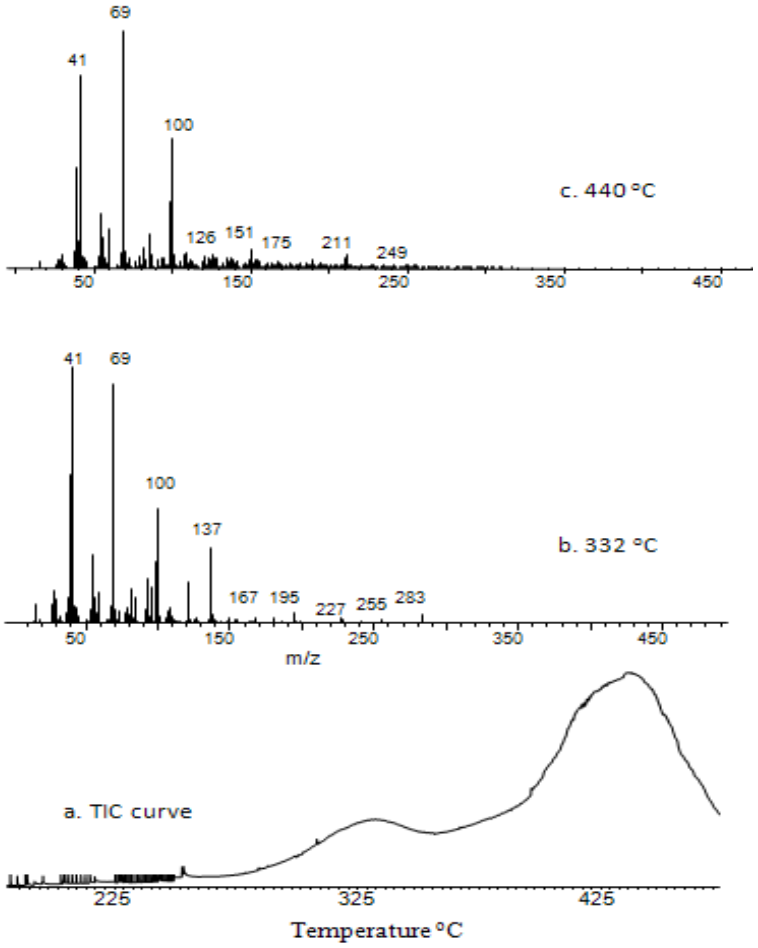

Figure 46. a. TIC curve and the pyrolysis mass of P(MMA-co-IBA-co-nBA) at b. 332 and c. 440°C.

The relative intensities and assignments made for the intense and/or characteristic peaks present in the pyrolysis mass spectra of P(MMA-co-IBA-co-nBA) at 332 and 440°C are collected in Table 14. As can be seen from the table, while at low temperature maximum 41 Da peak is the most intense fragment, those at high temperature is 69 Da.

Table 14: The relative intensities and assignments made for the intense and/or characteristic peaks present in the pyrolysis mass spectrum of P(MMA-co-IBA-co-nBA) at 332 and 440°C.

m/z (Da)	Relative Intensity		Assignments
	332°C	440°C	
18	16	2	H_2O
31	18	20	CH_3O
32	31	12	CH_3OH
39	580	423	C_3H_3
41	1000	798	C_3H_5
44	20	42	CO_2
45	27	31	COOH
55	263	230	C_2H_3CO
56	106	131	$CH_2=CHCH_2CH_3$
57	42	41	C_4H_9
69	923	1000	$CH_2C(CH_3)CO$
70	60	71	C_3H_5COH
72	11	16	C_2H_3COOH
73	49	46	OC_4H_9
74	4	6	HOC_4H_9
86	9	17	$C_2H_3COOHCH_2$ and/or CH_2CCH_3COOH
91	56	41	C_7H_7
93	168	47	C_7H_9
100	454	543	M_{MMA}, monomer
101	32	58	$CH_2C(CH_3)COHOCH_3$
126	14	62	$C_4H_6C_2O_3$
127	24	42	M_{BA}-H
128	8	43	M_{BA}, monomer
136	149	30	$C_{10}H_{16}$
137	296	49	$C_{10}H_{17}$

Table 14 (continued)

151	4	80	$C_2H_2CO_2COC_4H_5$
154	8	38	$C_{10}H_{17}OH$
181	21	22	$C_4H_5M_{BA}$
189	3	36	$(C_4H_5CH_3)_2C_4H_5$
208	4	13	$C_4H_5D_{BA}$–$COOC_4H_9$
211	1	60	$C_3H_5CO_2COC_4H_5CO_2H$
228	17	13	mix dimer M_{MA}-M_{BA}
236	2	10	$C_4H_5D_{BA}$ –OC_4H_9
249	3	18	$(C_4H_3CH_3)_2C_4H_3$
311	2	4	$T_{BA}H$-C_4H_9OH

In Figure 47.a single ion evolution profiles of some characteristic fragments of PMMA namely C_3H_5 (41 Da), C_3H_5CO (69 Da), monomer, MMA (100 Da), and those of PIBA namely $C_{10}H_{17}$ (137 Da), C_7H_9 (93 Da), $C_{10}H_{16}$ (136 Da), H_2O (18 Da), CH_3O (31 Da), CH_3OH (32 Da), CO_2 (44 Da) and as new products $C_{10}H_{17}OH$ (154 Da), $(C_4H_5CH_3)_2C_4H_5$ (189 Da), $(C_2H_7)_7H$ (260 Da), $C_4H_2OCO_2COC_4H_5$ (151 Da), $C_3H_5CO_2COC_4H_5CO_2H$ (211 Da) are given as representative examples.

In Figure 47.b single ion evolution profiles of some characteristic fragments of PMMA namely C_3H_5CO (69 Da) and those of PBA namely C_2H_3CO (55 Da), OC_4H_9 (73 Da), C_4H_8 (56 Da), C_4H_9 (57 Da), HOC_4H_9 (74 Da), CO_2H (45 Da), $CH_2CHCOOH$ (72 Da), $C_4H_5M_{BA}$ (181 Da), T_{BA}-CO-$2C_4H_9OH$ (208 Da), TH-C_4H_9OH (311 Da), CO_2 (44 Da) , $C_4H_6C_2O_3$ (126 Da) and as new products mixed dimer (228 Da), $CH_2C(CH_3)CHO$ (70 Da), $CH_2C(CH_3)COHOCH_3$ (101 Da), CH_3O (31 Da), CH_2CCH_3COOH (86 Da), M_{BA} (128 Da), $(C_4H_5CH_3)_2C_4H_5$ (189 Da), $C_2H_2CO_2COC_4H_5$ (151 Da) are given as representative examples.

In general, the relative yields of PIBA and PBA based products are decreased compared to the corresponding homopolymers and the copolymers with MMA, namely P(MMA-co-IBA) and P(MMA-co-nBA) as expected due to the decrease in IBA and BA percentages from 12.5 to 5. Inspection of single ion evolution profiles of diagnostics products of MMA indicates that again the main thermal degradation pathway for PMMA chains is depolymerization as in case of the homopolymer and

the copolymers involving two components. The evolution profiles of PMMA based products again show two peaks with maxima at 330 and 432°C, indicating an increase in thermal stability as the yield of MMA is maximized at 420°C during the thermal degradation of PMMA, and P(MMA-co-nBA) and at 415°C during the thermal degradation of P(MMA-co-IBA). Isobornylene evolution is mainly detected at around 395°C, again at slightly higher temperature regions. Unlike what is observed for P(MMA-co-IBA), evolution of CH_3OH is also recorded at around 395°C. The ratio of relative yields of isobornylene to isobornyl is 0.8, slightly higher than the corresponding value for the homopolymer but significantly lower than the value for the copolymer P(MMA-co-IBA) indicating that generation of isobornylene is diminished in the presence of BA units.

Similarly, the yield of PBA based products, especially those involving more than one repeating unit, are decreased. As in case of the copolymers involving MMA and IBA or BA, acrylic acid formation is detected. No significant change is observed in its yield. Actually, the yield of acrylic acid generated during the thermal degradation of copolymers P(MMA-co-IBA) and P(MMA-co-nBA) involving 12.5 % IBA or nBA are almost identical. As a consequence, no significant change in the yield of acrylic acid generated during the pyrolysis of P(MMA-co-IBA-co-nBA) involving 5 % IBA and 5 % BA is noted. However, most probably due to the increase of thermal stability of both IBA and BA segments, evolution of acrylic acid is only detected at elevated temperatures, in the region where PMMA chains starts to decompose.

For this sample, evolution of H_2O is detected as in case of P(MMA-co-IBA). Condensation of acrylic acid segments yielding anhydride units is diminished noticeably as expected compared to PIBA and PBA. The decrease in the amount of evolved H_2O may be regarded as the reason for the decrease in the yields of butanol, isobornyl alcohol and methacrylic acid that are generated by transesterification reactions with BA, IBA and MMA respectively. Actually generation of anhydride units and thus H_2O are more efficient for PIBA. Thus, it may be thought that the chain length of the segments involving repeating anhydride units significantly decreased when % IBA is decreased in P(MMA-co-nBA-co-IBA). It may further be thought that as thermal stability of IBA chains is increased, generation of acrylic acid and in turn anhydride units also shifts to higher temperatures decreasing the probability of transesterification reactions in the temperature region where PMMA chains start to decompose.

The increase in the yield of methacrylic acid is only about 1.2 folds with respect to P(MMA-co-nBA). Yet, compared to P(MMA-co-IBA) more than 4-folds decrease in its intensity is recorded supporting the above discussions.

Contrary to expectations, the yield of products due to transesterification reactions between MMA and acrylic acid are increased significantly compared to P(MMA-co-nBA) and slightly with respect to P(MMA-co-IBA). One possible reason may be the decrease in the extent of competing reactions between MMA and H_2O and MMA and butyl and isobornyl alcohols.

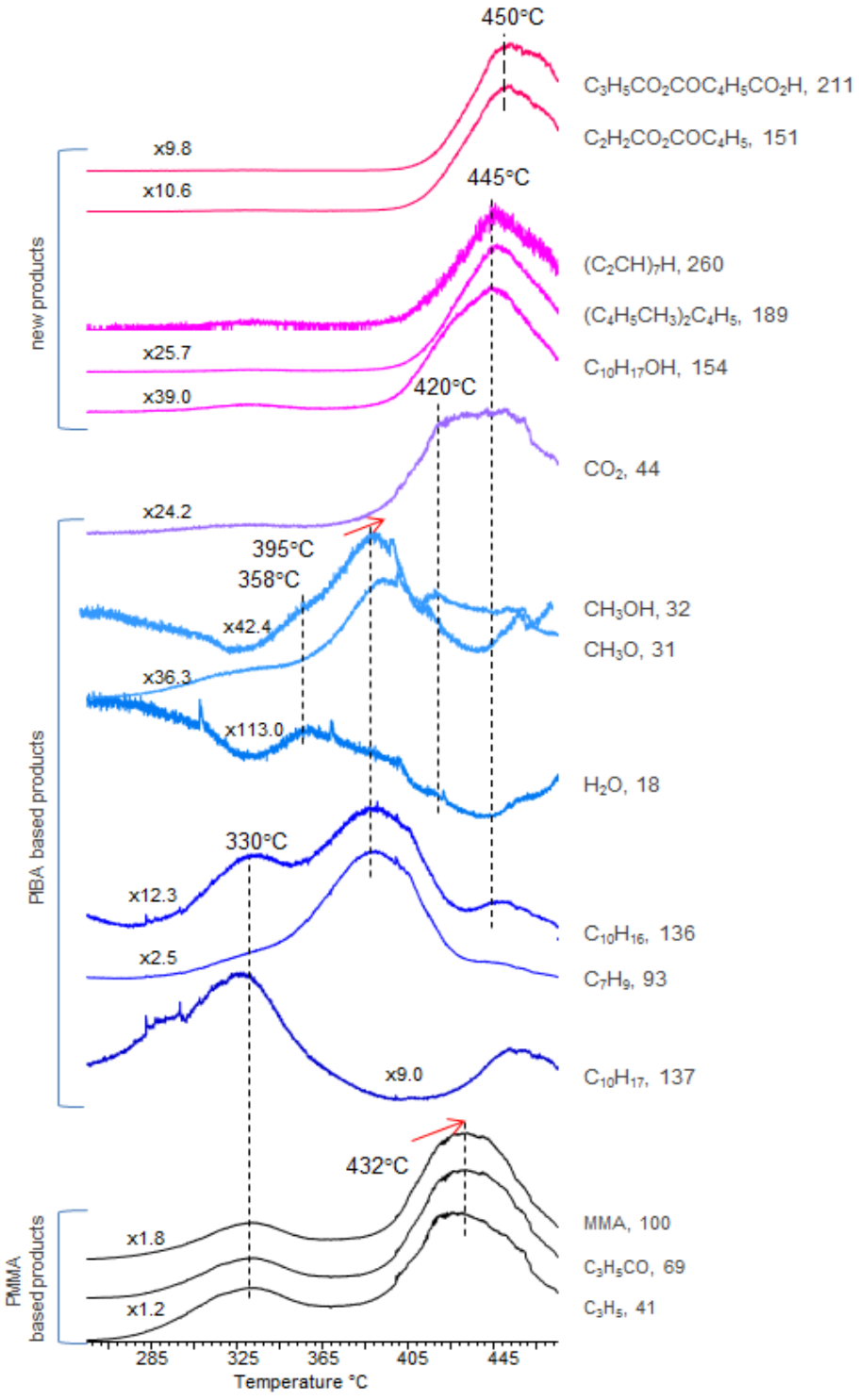

Figure 47.a. Single ion evolution profiles of some selected PIBA and PMMA based products recorded during pyrolysis of P(MMA-co-IBA-co-nBA).

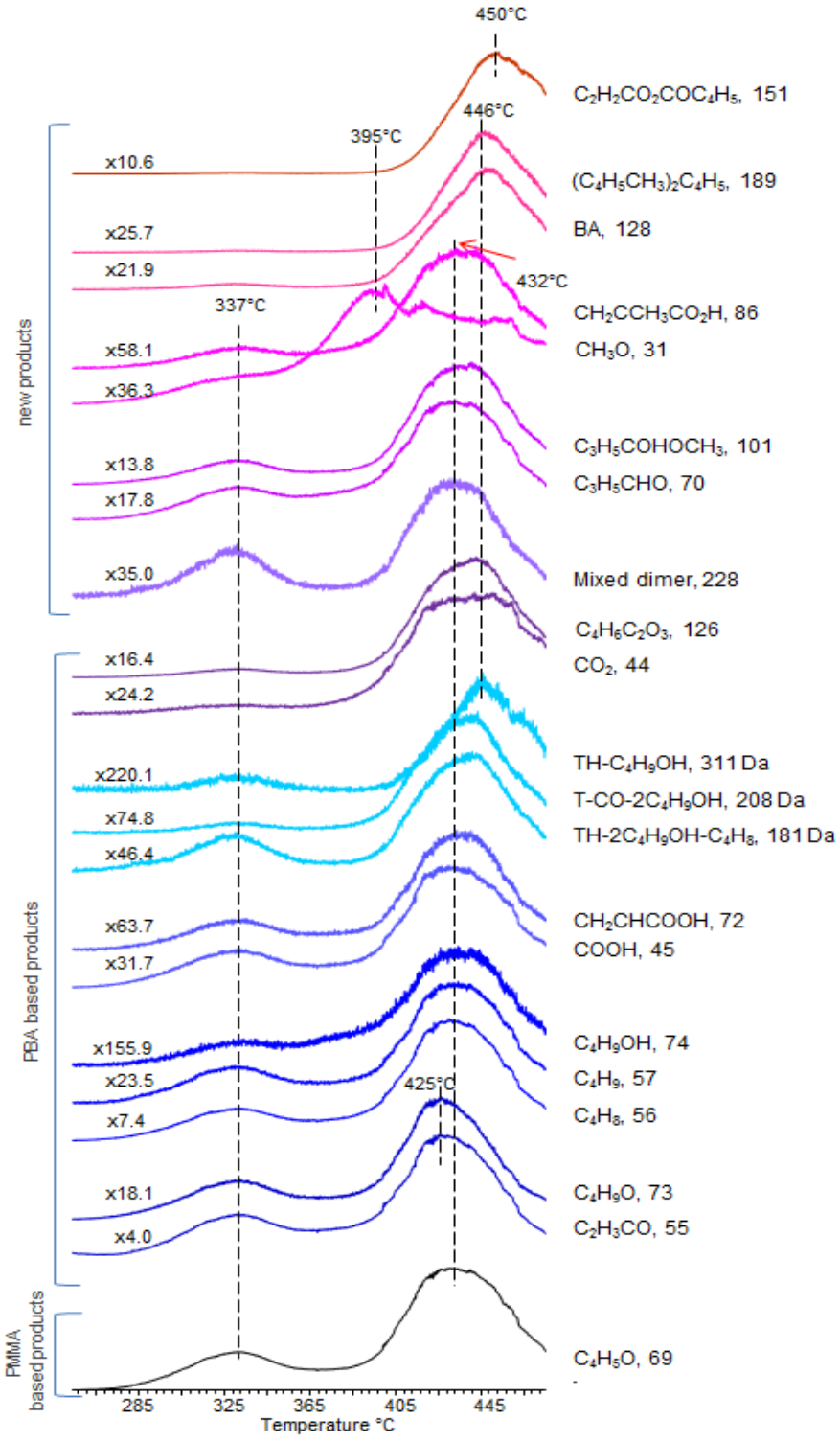

Figure 47.b. Single ion evolution profiles of some selected PBA and PMMA based products recorded during pyrolysis of P(MMA-co-IBA-co-nBA).

The DP-MS findings indicate that thermal decomposition of IBA and BA shifts to high temperature ranges when both of them are present as a component in the copolymer involving 90 % MMA, compared to the corresponding homopolymers and copolymers involving only 10.0 % IBA or 12.5 % BA. Among these polymers PIBA is the least stable one. Its degradation starts mainly by loss of side chains, generating acrylic acid units above 300°C. During the thermal decomposition the copolymer P(MMA-co-IBA) involving 12.5 % IBA, the loss of side chains shifts to high temperature ranges, while thermal stability of PMMA decreases slightly. In case of P(MMA-co-BA) thermal stability of BA chains also increases but its presence does not affect the thermal stability of PMMA chains. This behavior may be due to the higher thermal stability of PBA homopolymer that mainly decomposes by reactions involving H-transfer reactions from the main chain. As the percentage of IBA decreases from 12.5 to 5 %, the temperature range at around which the elimination of side chains occurs increases even more. The increase in the thermal stability of these segments may be associated with the decrease in the probability of degradation routes involving H-transfer reactions from the main chain as the percentage of IBA decreases. On the other hand, although thermal stability of PMMA decreases slightly in the presence of 12.5 % IBA, when the percentage of IBA decreases to 5 % an increase in the thermal stability of PMMA chains is also noted and increase in thermal stability of IBA segments. The increase in thermal stability of PMMA chains when the percentage of IBA decreases from 12.5 to 5 % may be attributed to presence of unsaturated and crosslinked units. In addition, the evolution of BA based products are also shifted to higher temperatures compared to P(MMA-co-nBA), most probably due to the increase in thermal stability of PMMA chains.

b. P(MMA-co-nBA-co-IBA) (70% - 15% - 15%)

TGA curve of the P(MMA-co-nBA-co-IBA) involving 15 % nBA and 15 % IBA separately, is given in Figure 48. The copolymer sample shows a two-step weight loss due to polymer degradation. In the derivative weight loss curve the first portion of the weight is loss is recorded at around 330°C and the second at around 400°C.

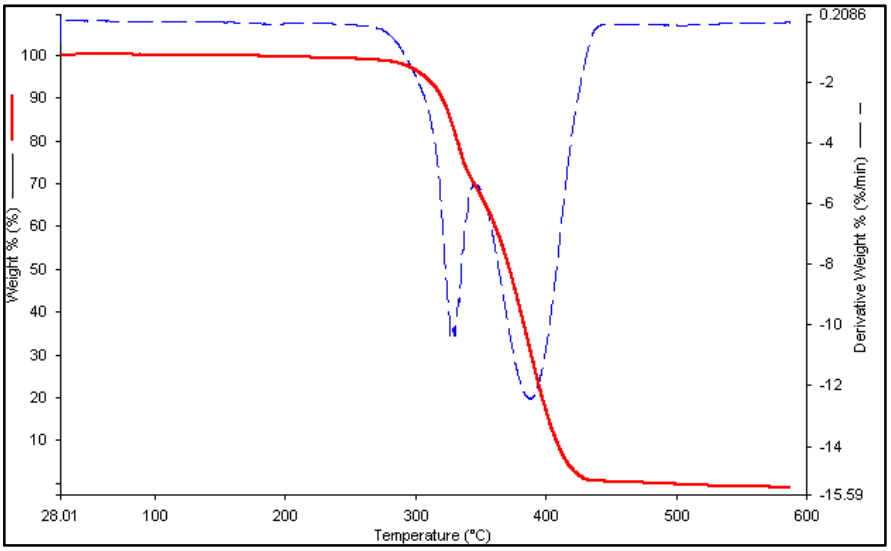

Figure 48. TGA curve of P(MMA-co-nBA-co-IBA)**.**

Also, the TIC curve recorded during the pyrolysis of P(MMA-co-nBA-co-IBA) shows two broad peaks with a high temperature shoulder (Figure 49). The mass spectra recorded at 358, 403 and 427°C are also given in the figure.

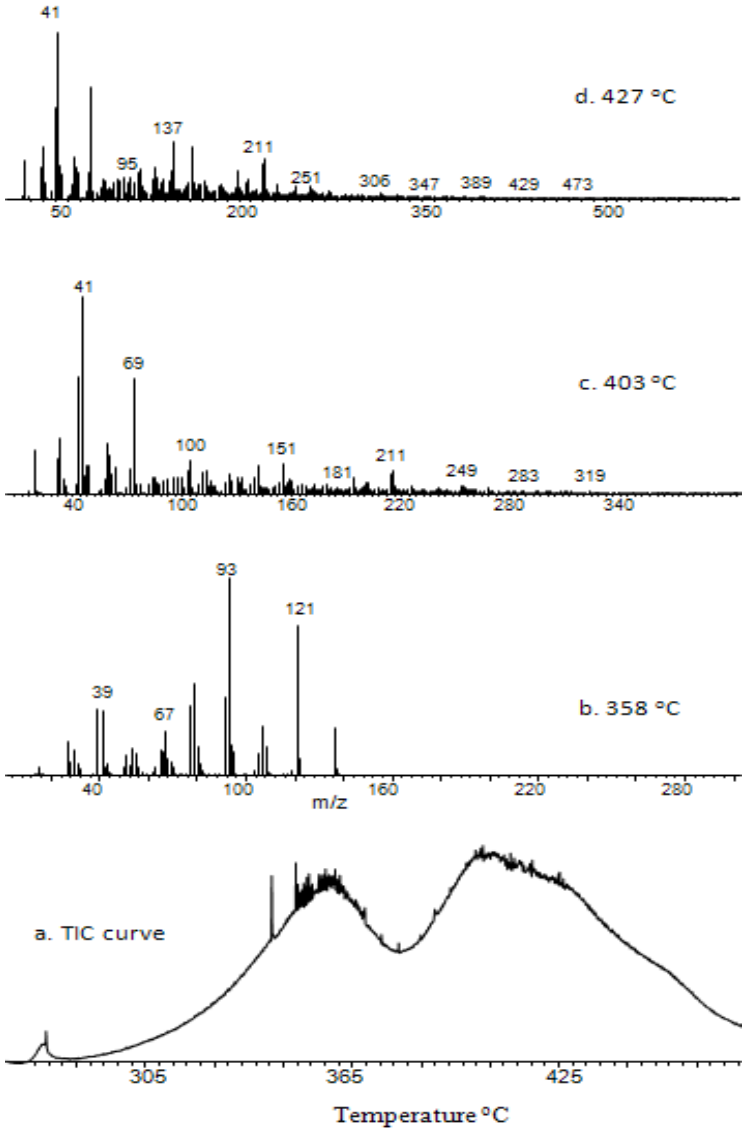

Figure 49. a. TIC curve and the pyrolysis mass of P(MMA-co-nBA-co-IBA) at b. 358 and c. 403, d. 427°C.

The mass spectrum recorded at around 360°C is almost identical to the pyrolysis mass spectra of PIBA recorded at around 335°C indicating an increase in the thermal stability of PIBMA chains (Figure 49). As the temperature increases, the peaks due to degradation of BA and MMA chains start to appear in the pyrolysis mass spectra. However, the most intense peak is at 93 Da due to lose of C_2H_4 and CH_3 groups from the isobornylene. Only for this copolymer, the base peak is due to the dissociation of IBA units during pyrolysis and/or dissociative ionization and is not

diagnostic to PMMA that is the main component of the copolymer film. Actually, this fragment is the base peak in the mass spectrum of isobornyl acrylate, and in the pyrolysis mass spectra of PIBA (See Figures 11 and 12).

The relative intensities and assignments made for the intense and/or characteristic peaks present in the pyrolysis mass spectra of P(MMA-co-nBA-co-IBA) at 358 and 403°C are collected in Table 15.

Table 15: The relative intensities and assignments made for the intense and/or characteristic peaks present in the pyrolysis mass spectrum of P(MMA-co-nBA-co-IBA) at 358 and 403°C.

m/z (Da)	Relative Intensity		Assignments
	358°C	403°C	
18	2	8	H_2O
31	57	80	CH_3O
32	29	36	CH_3OH
39	363	597	C_3H_3
41	351	1000	C_3H_5
44	17	139	CO_2
45	7	41	COOH
55	135	255	C_2H_3CO
56	47	190	$CH_2=CHCH_2CH_3$
57	14	93	C_4H_9
69	58	603	$CH_2C(CH_3)CO$
70	38	46	C_3H_5COH
72	-	-	C_2H_3COOH
73	5	46	OC_4H_9
74	6	9	HOC_4H_9
86	4	-	$C_2H_3COOHCH_2$ and/or CH_2CCH_3COOH
91	389	77	C_7H_7
93	1000	87	C_7H_9
100	9	175	M_{MMA}, monomer
101	-	35	$CH_2C(CH_3)COHOCH_3$
126	2	87	$C_4H_6C_2O_3$
127	-	57	M_{BA}-H

Table 15 (continued)

128	1	79	M_{BA}, monomer
136	218	-	$C_{10}H_{16}$
137	28	138	$C_{10}H_{17}$
151	1	149	$C_4H_2OCO_2COC_4H_5$
154	1	73	$C_{10}H_{17}OH$
181	1	33	C_4H_5MBA
189	1	84	$(C_4H_5CH_3)_2C_4H_5$
208	-	20	$C_4H_5D_{BA}–COOC_4H_9$
211	-	107	$C_3H_5CO_2COC_4H_5CO_2H$
228	1	23	mix dimer MMA-BA
236	-	34	$C_4H_5D_{BA}$ $–OC_4H_9$
249	-	44	$(C_4H_3CH_3)_3C_4H_3$
260	-	10	$(C_2CH)_7H$
311	-	9	TH-C_4H_9OH

The single ion evolution profiles of diagnostic products reveal that the thermal stability of the PMMA chains is decreased in the presence of 15 % IBA and BA. For the copolymer containing only 10 % IBA a slight decrease in thermal stability of PMMA chains is also observed. However, the decrease is now more pronounced. Loss of fragments diagnostic to BA and IBA are also shifted to lower temperature ranges compared to the copolymer involving 5% IBA and BA.

In case of P(MMA-co-nBA-co-IBA) involving only 5 % IBA, the increase in the thermal stability of PIBA based products are associated with the decrease in the chain lengths of IBA segments and the decrease in the probability of degradation routes involving H-transfer reactions from the main chain as the percentage of IBA decreases. Thus, the decrease in thermal stability of PIBA units may be regarded as an evidence for the increases in the chain lengths of IBA units and the probability of H-transfer reactions from the main chain. Among all the three components present in the copolymer, the homopolymer of IBA is the least stable. Thus, the decrease in thermal stability can be associated with the decrease in thermal stability of IBA segments most probably involving more IBA repeating units as the percentage of IBA in the copolymer increases.

In Figure 50.a single ion evolution profiles of some characteristic fragments of PMMA namely C_3H_5 (41 Da), C_3H_5CO (69 Da), monomer, MMA (100 Da), and those of PIBA namely $C_{10}H_{17}$ (137 Da), C_7H_9 (93 Da), $C_{10}H_{16}$ (136 Da), H_2O (18 Da), $C_4H_6C_2O_3$ (126 Da), CO_2 (44 Da), and as new products CH_3O (31 Da), CH_3OH (32 Da), COOH (45 Da), CH_2CCH_3COOH (86 Da), $C_{10}H_{17}OH$ (154 Da), $CH_2C(CH_3)CHO$ (70 Da), $(C_4H_5CH_3)_2C_4H_5$ (189 Da), $(C_4H_3CH_3)_3C_4H_3$ (249 Da), $(C_2H)_7H$ (260 Da), $C_2H_2CO_2COC_4H_5$ (151 Da), $C_3H_5CO_2COC_4H_5CO_2H$ (211 Da) are given as representative examples.

In Figure 50.b single ion evolution profiles of some characteristic fragments of PMMA namely C_3H_5CO (69 Da) and those of PBA namely C_2H_3CO (55 Da), OC_4H_9 (73 Da), C_4H_8 (56 Da), C_4H_9 (57 Da), HOC_4H_9 (74 Da), CO_2H (45 Da), $C_4H_5M_{BA}$ (181 Da), T-CO-$2C_4H_9OH$ (208 Da), TH-C_4H_9OH (311 Da), CO_2 (44 Da) , $C_4H_6C_2O_3$ (126 Da) and as new products mixed dimer (228 Da), $CH_2C(CH_3)CHO$ (70 Da), $CH_2C(CH_3)COHOCH_3$ (101 Da), CH_3O (31 Da), CH_2CCH_3COOH (86 Da), M_{BA} (128 Da), $(C_4H_5CH_3)_2C_4H_5$ (189 Da), $C_2H_2CO_2COC_4H_5$ (151 Da) are given as representative examples.

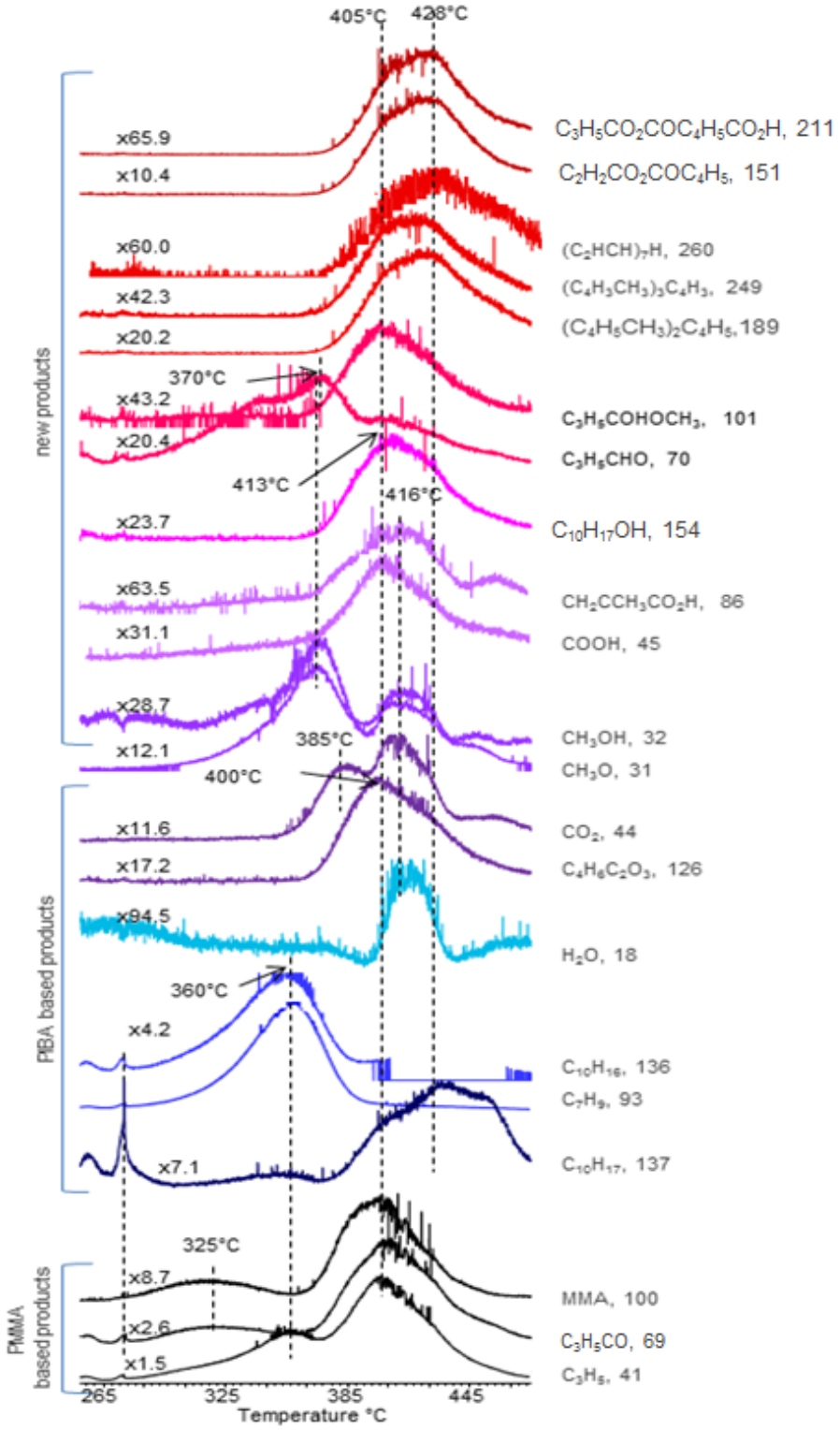

Figure 50.a. Single ion evolution profiles of some selected PBA and PMMA based products recorded during pyrolysis of P(MMA-co-nBA-co-IBA).

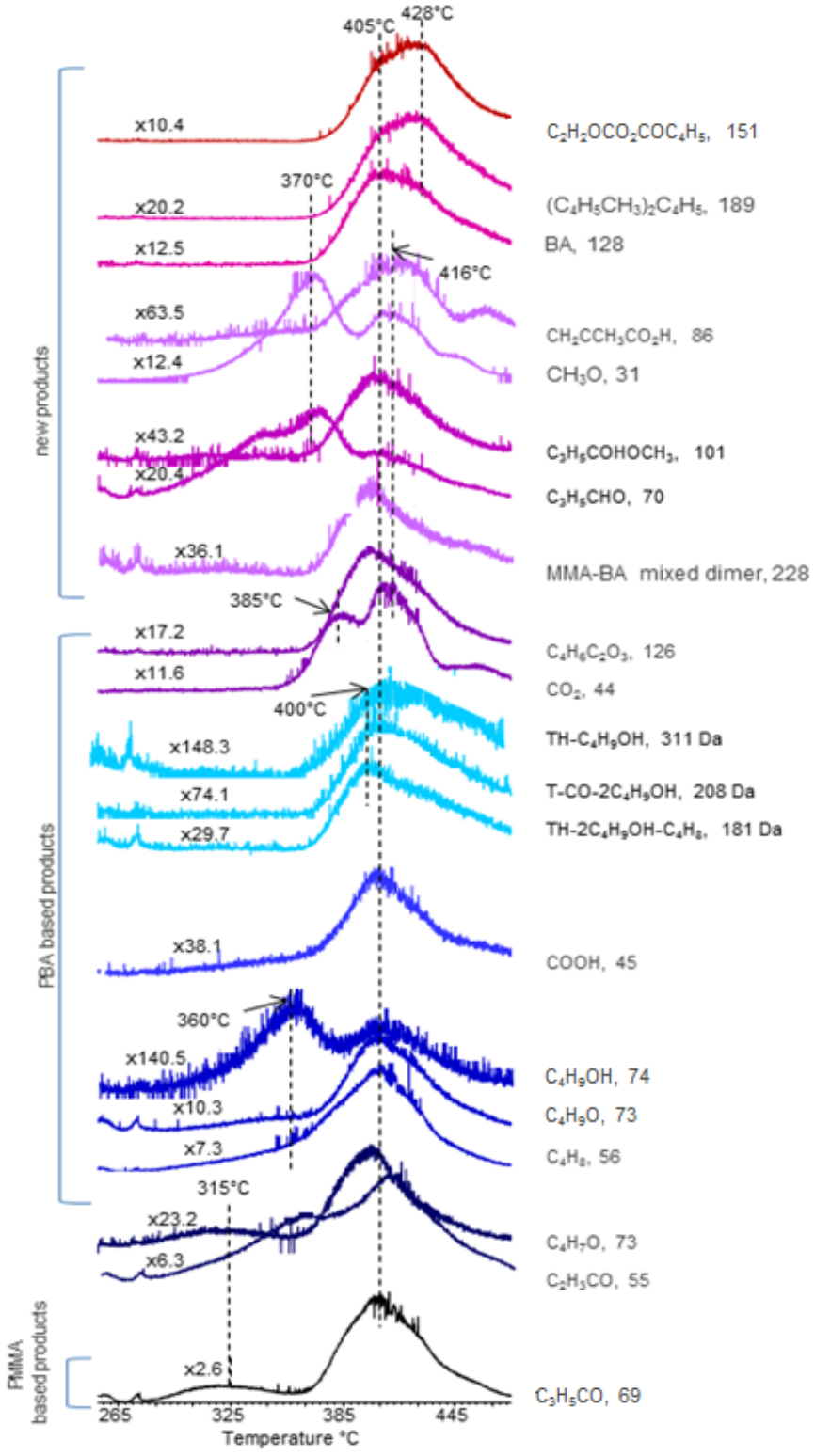

Figure 50.b. Single ion evolution profiles of some selected PBA and PMMA based products recorded during pyrolysis of P(MMA-co-nBA-co-IBA).

The trends observed in the single ion evolution profiles of PMMA based products recorded during the pyrolysis of the copolymer containing 15 % nBA and IBA are almost identical to those observed during the pyrolysis of all copolymers. The low temperature peak in the evolution profile of C_3H_5 (41 Da) can directly be related to contribution of the fragment generated during the pyrolysis or dissociative ionization of IBA with the same m/z value.

PBA based products are also maximized at around 405°C, at slightly higher temperature than the PMMA based products. On the other hand, IBA based products show a maximum at around 360°C, at higher temperatures than that is detected for PIBA, but at lower temperatures than that are recorded for P(MMA-co-IBA) and P(MMA-co-BA-co-IBA) containing 5 % IBA.

In general, besides the decrease in thermal stability, noticeable changes are detected in product distributions. The relative yields of products associated with thermal degradation of PBA chains are increased compared to P(MMA-co-nBA) and P(MMA-co-nBA-co-IBA) containing 5 % BA. A slight increase in the generation of butanol is also noted. On the other hand, the relative yield of butene is decreased with respect to P(MMA-co-BA) and is constant compared to that is detected for P(MMA-co-BA-co-IBA) containing only 5 % BA and IBA. This behavior may be associated with the increase in the probability of H-transfer reactions from the main chain, competing with H-transfer reactions from the side chains, as in case of homopolymer PnBA.

The relative yield of isobornylene is increased by 1.3 and 2.9-folds compared to P(MMA-co-IBA) and P(MMA-co-BA-co-IBA) containing % 5 nBA respectively. The ratio of the relative yields of isobornylene to isobornyl is 1.7, noticeably higher than the value for the copolymer P(MMA-co-BA-co-IBA) indicating that generation of isobornylene is enhanced as the percentage of IBA is increased from 5 to 15 %, however, it is still lower than the value for the P(MMA-co-IBA). The generation of isobornylene actually indicates formation of acrylic acid. However, only negligible amount of acrylic acid is evolved. Furthermore, the yield of anhydride units is almost constant. These fragments are detected at relatively low temperatures and are reached to maximum yield at around 385°C. Their evolutions are continued over a broad temperature range. However, 1.2 and 2.1- folds of increases in the yield of CO_2 compared to P(MMA-co-IBA) and P(MMA-co-BA-co-IBA) containing % 5 nBA

respectively are detected. Thus, it may be thought that almost all acrylic acid produced is reacted and generated anhydride linkages that eliminate CO and CO_2 and produce unsaturated units. Almost 5-folds increase in the yield of the product with m/z 260 Da tentatively $(C_2CH)_7H$ supports this proposal.

Compared to P(MMA-co-BA-co-IBA) containing % 5 BA, not only the relative yield of isobornylene but also that of isobornyl alcohol is increased indicating existence of trans-esterification reactions between IBA and H_2O. Almost 2-folds decrease in the relative yields of methanol, and methacrylic acid due to trans-esterification reactions between H_2O and MMA, compared to P(MMA-co-IBA) may be associated with the decrease in the MMA composition from 90 % to 70 %, although IBA % increased from 10 to 15 %. On the other hand, compared to P(MMA-co-BA-co-IBA) the relative yield of CH_3OH is increased about 1.5 folds, when the IBA composition is increased from 5 to 15%. Another point that should be noticed is the evolution of CH_3OH and CO_2 in two distinct regions. The maxima in the evolution profiles of CH_3OH are at 370 and 416°C and at 385 and 416°C in the evolution profile of CO_2. This behavior may be attributed to generation of methanol through different mechanisms. The low temperature evolution may be associated with reactions of acrylic acid generated at relatively low temperatures upon loss of isobornylene and MMA, while the high temperature evolutions may be related to transesterification reactions H_2O with MMA yielding again CH_3OH. Actually, eliminations of isobornyl and butyl alcohols are also detected above 400°C, at around 413 and 405°C this temperature range.

Furthermore, although slight, decrease in the relative yields of fragments such as 101 and 70 Da associated with reactions given in Scheme 18 and increase in the relative yields of fragments such as 189, 249 Da fragments generated through reactions given in Scheme 16 are noted. This behavior may be associated with the decrease in composition of MMA in the copolymer from 90 to 70 %.

Thus, it can be concluded that when the IBA percentage increases thermal stability of the copolymer decreases. Degradation starting with H-transfer reactions from the isobornyl group to carbonyl group proceeds through several trans-esterification reactions generating methanol, isobornyl and butyl alcohols.

3.2.5 Poly(methyl methacrylate-co-nbutylacrylate-co-ısobornyl acrylate) P(MMA-co-nBA-co-IBA-co-BzMA)

The TGA curve of P(MMA-co-nBA-co-IBA-co-BzMA) given in Figure 51 shows that; the thermal degradation of the sample is a two step mechanism. The largest portion of the weight loss occurs between 300 and 400°C. However, different than P(MMA-co-IBA-co-nBA) copolymer, there is also a very small amount of weight loss observed at around 175°C.

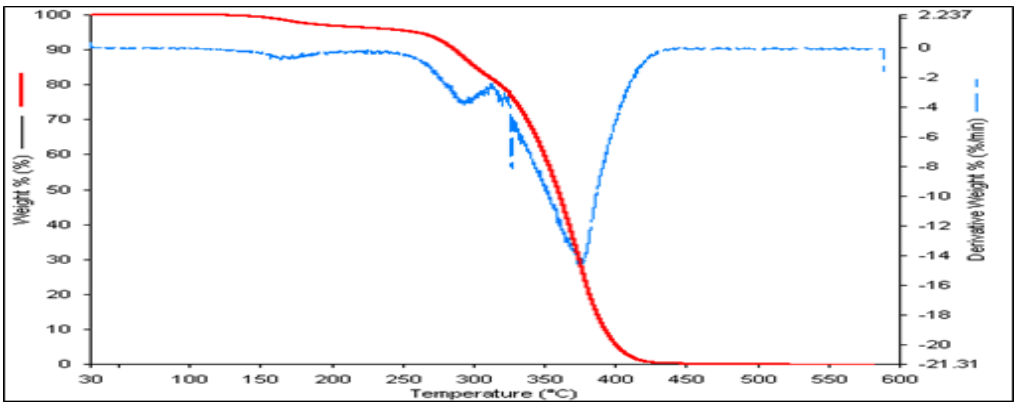

Figure 51. TGA curve of P(MMA-co-nBA-co-IBA-co-BzMA)**.**

The TIC curve recorded during the pyrolysis of P(MMA-co-nBA-co-IBA-co-BzMA) shows two broad peaks maximizing at 338 and 440°C with a low temperature tail (Figure 52). The results are very similar to those obtained with TGA.

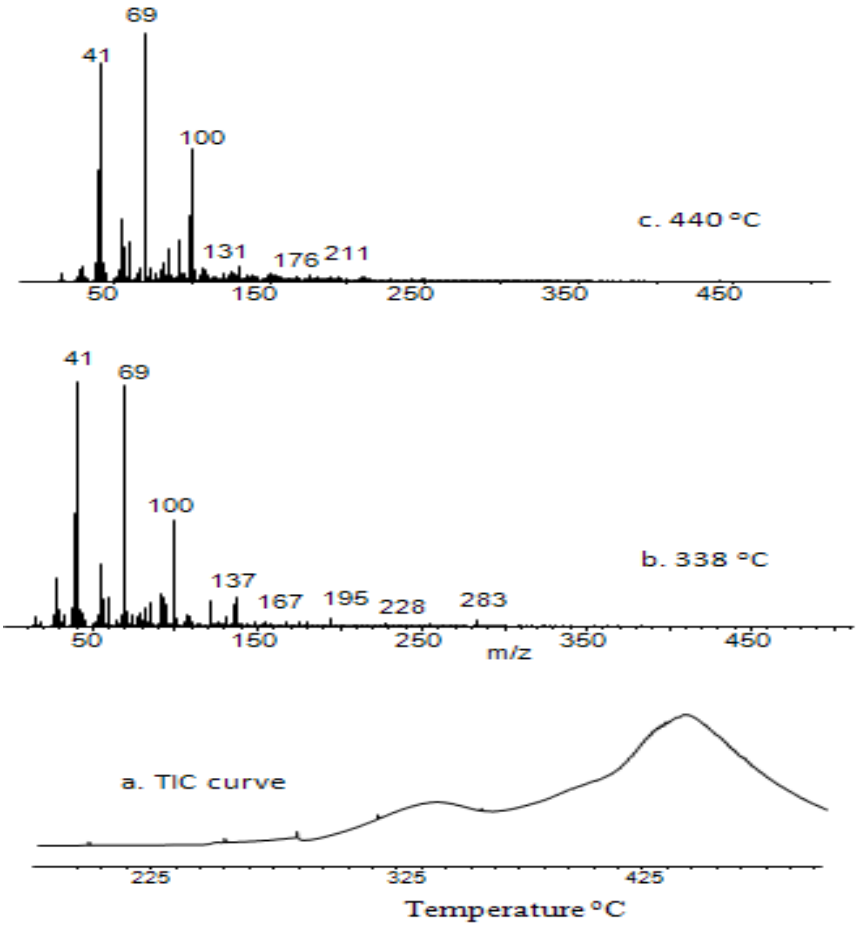

Figure 52. a. TIC curve and the pyrolysis mass of P(MMA-co-IBA-co-BA-co-BzMA) at b. 338 and c. 440°C.

Since PMMA constitutes the highest percentage of the copolymer sample, the mass spectra recorded at both maxima are dominated with characteristic peaks of PMMA. Although they are not very intense, there are also peaks due to thermal degradation of PnBA, PIBA and PBzMA. The relative intensities and assignments made for the intense and/or characteristic peaks present in the pyrolysis mass spectra of P(MMA-co-nBA-co-IBA-co-BzMA) recorded at 338 and 440°C are collected in Table 16. At the temperature maxima 41 and 69 Da peaks due to C_3H_5 and $CH_2C(CH_3)CO$ fragments respectively are the most intense ones.

Table 16: The relative intensities and assignments made for the intense and/or characteristic peaks present in the pyrolysis mass spectrum of P(MMA-co-IBA-co-nBA-co-BzMA) at 338 and 440°C.

m/z (Da)	Relative Intensity		Assignments
	338°C	440°C	
18	15	2	H_2O
31	14	19	CH_3O
32	49	14	CH_3OH
39	459	446	C_3H_3
41	1000	875	C_3H_5
44	21	32	CO_2
45	26	30	COOH
55	248	250	C_2H_3COOH
56	107	135	$CH_2=CHCH_2CH_3$
57	38	42	C_4H_9
65	25	30	C_5H_5
69	975	1000	$CH_2C(CH_3)CO$
70	64	75	C_3H_5COH
72	11	14	C_2H_3CO
73	50	57	OC_4H_9
74	4	7	HOC_4H_9
77	38	34	C_6H_5
86	8	15	$C_2H_3COOHCH_2$ and/or CH_2CCH_3COOH
91	130	163	C_7H_7
93	114	35	C_7H_9
100	432	527	M_{MMA}, monomer
101	30	48	$CH_2C(CH_3)COHOCH_3$
126	12	42	$C_4H_6C_2O_3$
127	22	34	M_{BA}-H
128	9	28	M_{BA}
131	42	64	M_{BzMA}-COOH
136	85	18	$C_{10}H_{16}$
137	113	22	$C_{10}H_{17}$
151	4	33	$C_4H_2OCO_2COC_4H_5$
154	7	24	$C_{10}H_{17}OH$
158	14	23	M_{BzMA}-H_2O
176	17	29	M_{BzMA}, monomer

Table 16 (continued)

181	15	17	$C_4H_5M_{BA}$
189	3	20	$(C_4H_5CH_3)_2C_4H_5$
208	3	10	$C_4H_5D_{BA}$–$COOC_4H_9$
211	2	20	$C_3H_5CO_2COC_4H_5CO_2H$
228	15	11	mix dimer
236	1	6	$C_4H_5D_{BA}$ –OC_4H_9
249	2	9	$(C_4H_3CH_3)_2C_4H_3$
311	1	3	$T_{BA}H$-C_4H_9OH

When the single ion evolution profiles of the copolymer are analyzed it is clear that the diagnostic peaks of PMMA based products are slightly stabilized compared to P(MMA-co-BA-co-IBA) copolymer. The low temperature peaks of PMMA based products are shifted from 330 to 338°C and the high temperature peaks are shifted from 432 to 440°C (Figure 53.a). Inspection of single ion evolution profiles of diagnostics products of MMA indicates that again the main thermal degradation pathway for PMMA chains is depolymerization.

The PBzMA based peaks are also stabilized. When compared to P(MMA-co-BzMA) sample, the low temperature maximum is shift from 320 to 338°C and those of the high temperature is shift from 400 to 440°C. Since BzMA percentage is 10 % for the P(MMA-co-BzMA) and it is decreased to 2 % for P(MMA-co-IBA-co-nBA-co-BzMA) sample, the yield of BzMA based products are decreased as expected. However there is a 3-fold increase in the yield of mixed dimer product observed at 276 Da. As can be seen from Figure 50.a. the evolution profiles of 65 and 91 Da peaks due to C_5H_5 and C_7H_7 fragments respectively have shoulders at around 397°C which can be attributed to the decomposition of PBzMA part of the copolymer sample and the stronger maximum at around 440°C is due to PnBA degradation.

In Figure 53.a single ion evolution profiles of some characteristic fragments of PMMA namely C_3H_5 (41 Da), C_3H_5CO (69 Da), monomer, MMA (100 Da) and those of PBzMA namely C_5H_5 (65 Da), C_7H_7 (91 Da), BzMA-COOH (131 Da), BzMA-H_2O (158 Da), BzMA (176 Da) and mixed dimer (276 Da) are given as representative examples.

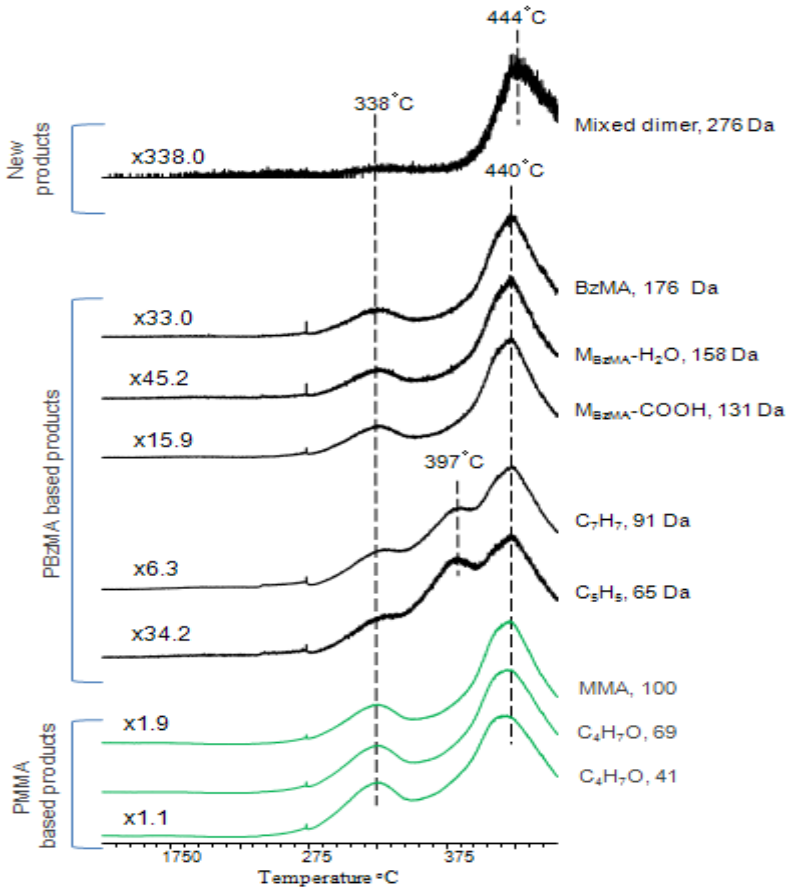

Figure 53.a. Single ion evolution profiles of some selected PBzMA and PMMA based products recorded during pyrolysis of P(MMA-co-IBA-co-nBA-co-BzMA).

In Figure 53.b single ion evolution profiles of some characteristic fragments of PMMA namely C_3H_5CO (69 Da), and those of PnBA namely C_5H_5 (65 Da), OC_4H_9 (73 Da), C_4H_8 (56 Da), C_4H_9 (57 Da), C_4H_7OH (74 Da), CO_2H (45 Da), $CH_2CHCOOH$ (72 Da), $C_4H_5M_{BA}$ (181 Da), T-CO-$2C_4H_9OH$ (208 Da), TH-C_4H_9OH (311 Da), CO_2 (44 Da), $C_4H_6C_2O_3$ (126 Da) and as new products mixed dimer (228 Da), $CH_2C(CH_3)CHO$ (70 Da), $CH_2C(CH_3)COHOCH_3$ (101 Da), CH_3O (31 Da), CH_2CCH_3COOH (86 Da), M_{BA} (128 Da), $(C_4H_5CH_3)_2C_4H_5$ (189 Da), $C_4H_2OCO_2COC_4H_5$ (151 Da) are given as representative examples. The diagnostic peaks of PnBA based products are stabilized about 8°C compared to copolymer involving three components.

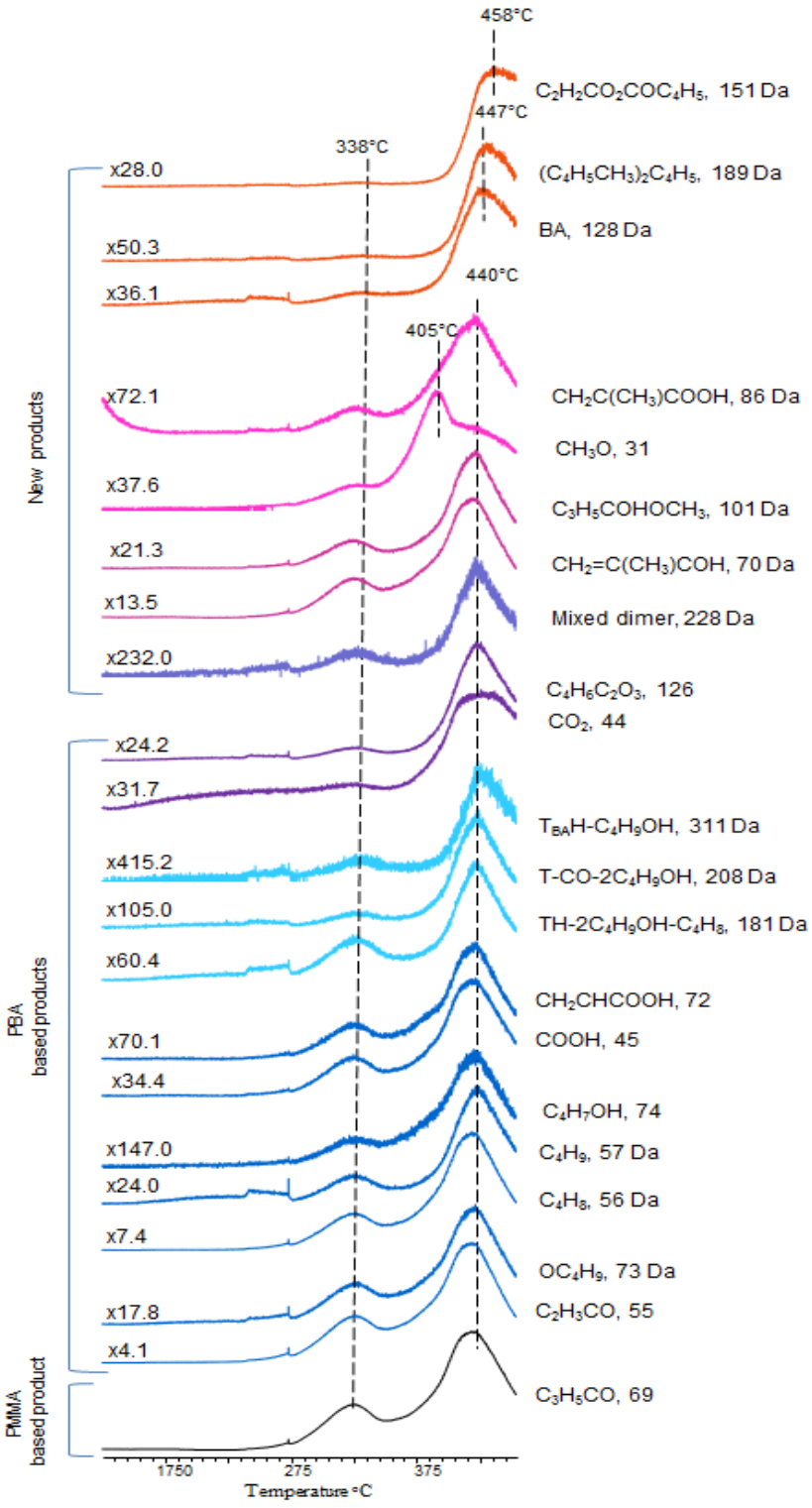

Figure 53.b. Single ion evolution profiles of some selected PBA and PMMA based products recorded during pyrolysis of P(MMA-co-IBA-co-nBA-co-BzMA).

Both for P(MMA-co-IBA-co-BA) and P(MMA-co-IBA-co-nBA-co-BzMA) samples the percentage of PBA is 5 %. Therefore, it is expected to have almost the same yield for BA based products. Although the yield of the products with m/z values 31, 55, 56, 57, 73 and 74 Da due to CH_3O, C_2H_3CO, C_4H_8, C_4H_9, C_4H_7O, C_4H_7OH, are about the same with those recorded during the pyrolysis of P(MMA-co-IBA-co-BA) copolymer. The yields of the rest of the products shown in Figure 53.b are decreased to some extend.

In Figure 53.c single ion evolution profiles of some characteristic fragments of PMMA namely C_3H_5CO (69 Da), and those of PIBA namely $C_{10}H_{17}$ (137 Da), C_7H_9 (93 Da), $C_{10}H_{16}$ (136 Da), H_2O (18 Da), CH_3O (31 Da), CH_3OH (32 Da), CO_2 (44 Da) and as new products $C_{10}H_{17}OH$ (154 Da), $(C_4H_5CH_3)_2C_4H_5$ (189 Da), $(C_2CH)_7H$ (260 Da), $C_4H_2OCO_2COC_4H_5$ (151 Da), $C_3H_5CO_2COC_4H_5CO_2H$ (211 Da) are given as representative examples. As can be noted from Figure 53.c the trends observed in the single ion evolution profiles of the products diagnostic to PIBA are very similar to those recorded for the copolymer involving three components. Since the percentage of PIBA is decreased from 5 % to 3 % the yield of products are also decreased. Also, the isobornylene evolution is mainly detected at around 405°C, again at slightly higher temperature regions. The evolution of CH_3OH is also recorded at around 405°C. The ratio of relative yields of isobornylene to isobornyl is 1.0, slightly higher than the corresponding value for the copolymer involving three components. In addition, although the evolution of acrylic acid is mostly detected in the region of PMMA chain decomposition, at around 440°C, there is also some amount of generation at lower temperature region, at around 338°C.

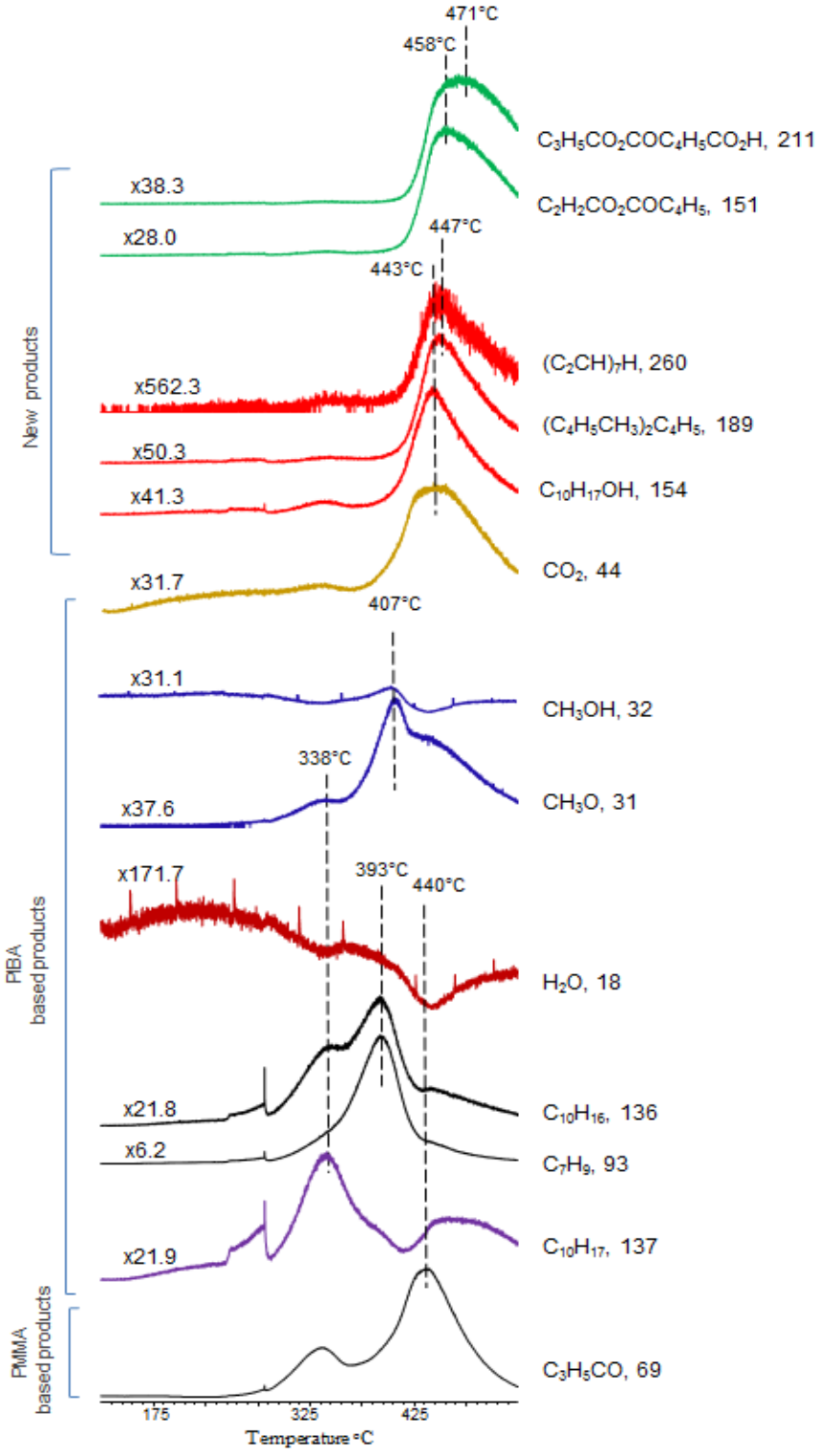

Figure 53.c. Single ion evolution profiles of some selected PIBA and PMMA based products recorded during pyrolysis of P(MMA-co-IBA-co-nBA-co-BzMA).

To conclude, the thermal decomposition of IBA is not affected by the addition of BzMA units as a third component in the copolymer sample. However, the thermal decomposition of PBA and PMMA shifts to a slightly higher temperature region. The BzMA units are the most seriously affected by copolymerization of the sample with PMMA, PBA and PIBA. Although it is used 2 % in the copolymer sample the maximum of the high temperature peak is shifted about 40°C to higher temperature region.

3.3 Fibers

3.3.1 P(MMA-co-nBA) Fiber

TGA curve of P(MMA-co-nBA) fiber shows that the weight loss of the sample starts at around 325 °C and almost all of the sample is lost at around 420 °C (Figure 54). Since the TGA results of first, second and end part of the fiber are almost identical, only the second part of the fiber TGA curve is given in Figure 54. Contrary to TGA results obtained for the corresponding copolymer the derivative weight loss curve of the fiber seems to be a one step process.

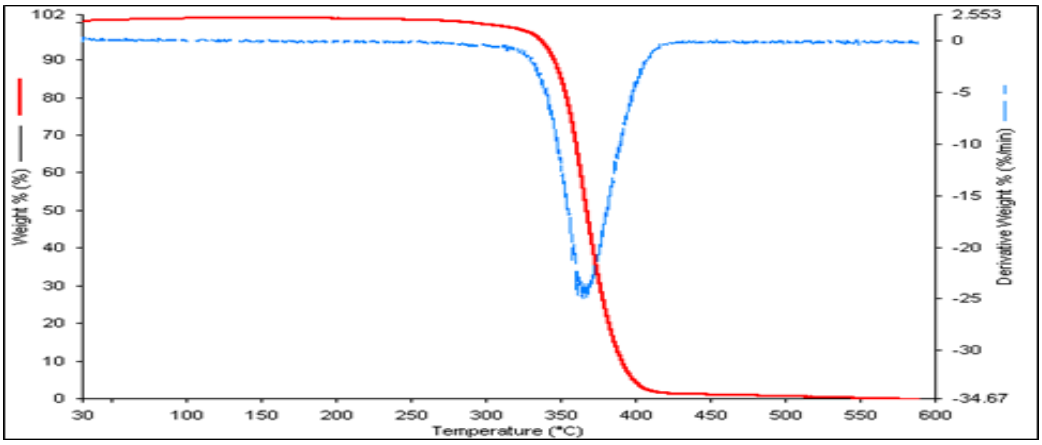

Figure 54. TGA curve of the second part of the P(MMA-co-nBA) fiber.

TIC curves recorded during the pyrolysis of first, second and third part of the P(MMA-co-nBA) fiber are given in Figure 55. The mass spectra recorded at the peak maxima are also shown in the figure. For all parts of the fiber samples there are two intense overlapping peaks at high temperature region and a weak peak at around 323°C. The temperatures of the peak maxima for different parts of the fiber samples are not identical. In the TIC curves of the first, second and third part of the fibers, the low and high temperature maxima are 392-433, 392-440 and 396-425°C respectively.

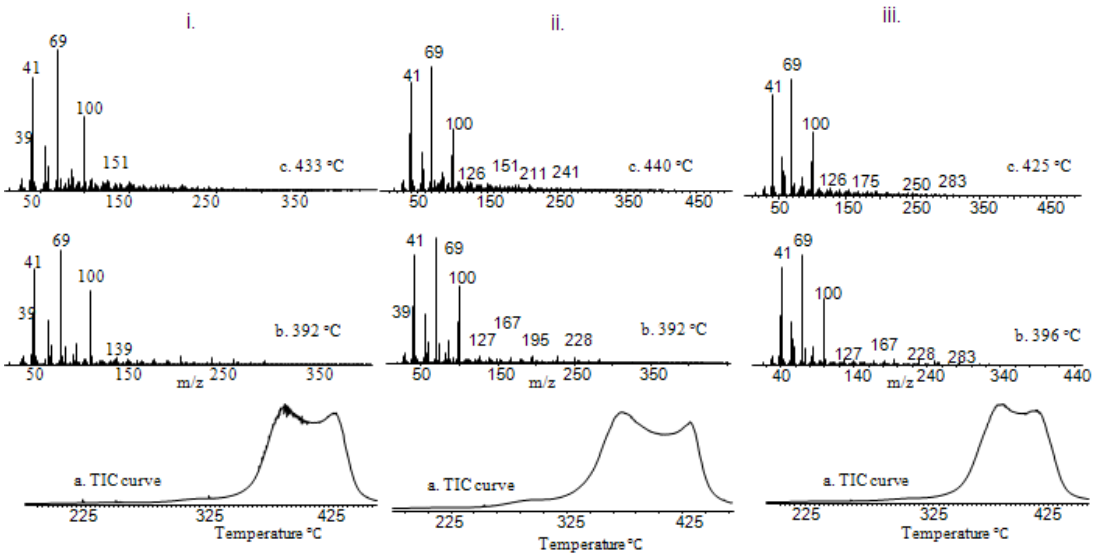

Figure 55. a. TIC curve and the pyrolysis mass of P(MMA-co-nBA) fiber i. the first part at b. 392 and c. 433°C, ii. the second part at 392 and 440°C and iii. the third part at b. 396 and c. 425°C.

Diagnostic peaks of MMA, are noticeably intense indicating that the main thermal degradation pathway for MMA chains is depolymerization as in case of PMMA and P(MMA-co-nBA) copolymer. Their evolution profiles show a weak peak with maximum at around 323°C and a stronger one with a maximum at around 388°C. Compared to the corresponding copolymer it is clear that the stability of PMMA related products are decreased to some extent. The relative intensities and assignments made for the intense and/or characteristic peaks present in the pyrolysis mass spectra of first, second and third part of the fiber at their peak maxima are collected in Table 17. For all parts of the fiber samples, 69 Da peak, due to C_3H_5CO fragment, is the base peak at both peak maxima.

Table 17: The relative intensities and assignments made for the pyrolysis mass spectra of first, second and third parts of the P(MMA-co-nBA) fiber, the intense and/or characteristic peaks present at their peak maxima.

m/z (Da)	Relative Intensities						Assignments
	First Part		Second Part		Third Part		
	392°C	433°C	392°C	440°C	396°C	425°C	
18	1	1	1	2	1	2	H_2O
31	16	22	17	24	16	19	CH_3O
32	18	26	9	19	9	12	CH_3OH
39	442	402	463	375	452	426	C_3H_3
41	856	807	870	767	867	835	$CH_3C{=}CH_2$
44	19	39	19	49	17	30	CO_2
45	33	32	34	29	32	31	COOH
55	398	321	390	237	388	336	C_2H_3CO
56	241	199	244	181	232	212	$CH_2{=}CHCH_2CH_3$
57	78	70	81	67	78	73	C_4H_9
69	1000	1000	1000	1000	1000	1000	C_3H_5CO
70	81	77	81	74	76	76	C_3H_5COH
73	158	88	154	50	149	107	OC_4H_9
74	10	10	10	10	10	10	HOC_4H_9
85	179	157	183	140	174	161	$CH_2C(CH_3)COO$
86	22	25	22	27	22	24	$CH_2C(CH_3)COOH$
91	16	45	16	60	17	34	C_7H_7
93	39	63	43	67	43	56	C_7H_9
99	345	303	344	267	328	303	M_{MMA}-H
100	633	542	630	485	607	554	M_{MMA}, monomer
101	66	65	66	65	63	61	$CH_2C(CH_3)COHOCH_3$
126	43	75	45	86	45	65	$C_4H_6C_2O_3$
127	54	65	56	67	56	60	M_{BA}-H
128	17	53	18	79	19	38	M_{BA}
136	8	29	8	48	10	21	$C_{10}H_{16}$
137	13	47	13	103	16	32	$C_{10}H_{17}$
151	9	62	10	135	11	34	$C_2H_2CO_2COC_4H_5$
154	19	48	20	62	22	39	$C_{10}H_{17}OH$

Table 17 (continued)

181	34	39	36	40	38	39	$C_4H_5M_{BA}$
189	6	41	6	68	9	26	$(C_4H_5CH_3)_2C_4H_5$
208	13	22	15	23	15	21	$C_4H_5D_{BA}$–$COOC_4H_9$
211	5	43	5	127	6	20	$C_3H_5CO_2COC_4H_5CO_2H$
228	51	30	54	28	50	33	mixed dimer
236	15	16	16	26	18	14	C_4H_5D –OC_4H_9
249	6	24	7	38	8	17	$(C_4H_3CH_3)_2C_4H_3$
311	8	8	9	12	9	7	TH-C_4H_9OH

In Figure 56 single ion evolution profiles of diagnostic products of PMMA namely $CH_3C=CH_2$ (41 Da), C_3H_5CO (69 Da), and MMA (100 Da), those of PBA such as C_2H_3CO (55 Da), C_4H_9O (73 Da), C_4H_8 (56 Da), C_4H_9 (57 Da), C_4H_7OH (74 Da), COOH (45 Da), TH-$2C_4H_9OH$-C_4H_8 (181 Da), T-CO-$2C_4H_9OH$ (208 Da), TH-C_4H_9OH (311 Da), CO_2 (44 Da), $C_4H_6C_2O_3$ (126 Da), and as new products, mixed dimer (228 Da), C_3H_5CHO (70 Da), $C_3H_5COHOCH_3$ (101 Da), CH_3O (31 Da), $CH_2C(CH_3)COOH$ (86 Da), BA (128 Da), $(C_4H_5CH_3)_2C_4H_5$ (189 Da), $(C_4H_3CH_3)_3C_4H_3$ (249 Da), $C_2H_2CO_2COC_4H_5$ (151 Da) and $C_3H_5CO_2COC_4H_5CO_2H$ (211 Da) are given as representative examples.

As can be noted from the single ion evolution profiles, the trends observed in PnBA based products detected during the pyrolysis of the copolymer are totally different than those recorded from the copolymer. Two overlapping peaks with maxima at 388 and 415°C are present in the single ion evolution profiles of PnBA based products. Upon fiber formation, the low temperature peaks in the evolution profiles of PnBA based products at around 325°C are disappeared and in addition, the maxima of PnBA based products are shifted to 388°C, to slightly lower temperatures than the corresponding values for P(MMA-co-nBA).

Another point that should be discussed is the increase in the relative yields of most of the products associated with thermal degradation of PBA chains upon fiber formation. At the same time increases in the relative yields of products associated with reactions of BA segments with MMA units are observed.

Thus, it may be concluded that the extent of reactions among BA and MMA chains are enhanced upon fiber formation. Since after fiber formation the polymer chains become more aligned and closely packed so the interaction between the molecules are also increased.

The single ion evolution profiles of products, COOH (45 Da) and C_4H_8 (56 Da) generated by McLafferty type rearrangement reactions involving γ-H transfer from the butyl groups to CO groups of PBA show two overlapping peaks, with maximum at 388°C and a shoulder at around 442°C. Compared to the corresponding copolymer, the increase in the yield of C_4H_8 (56 Da) and COOH (45 Da) is about 1.4 and 1.1-folds respectively. In addition, the yield of the products due to $CH_2CHCOOCH_3$ (86 Da) and OCH_3 (31 Da) fragments, obtained as a result of degradation of the segments generated by the trans-esterification reaction between acrylic acid and methyl methacrylate units are 1.4 and 1.1-fold increased compared to those of the copolymer.

C_4H_7OH and CO_2 show maxima at 388 and at 446°C in their evolution profiles respectively. For the P(MMA-co-nBA) copolymer sample the corresponding values are 370 and 385°C respectively. This behavior may be associated with higher thermal stability of the fiber compared to the copolymer.

The maxima of the products with m/z values 181, 208, 311 Da due to TH-$2C_4H_9OH$-C_4H_8, T-CO-$2C_4H_9OH$ and TH-C_4H_9OH fragments are shifted about 26°C to lower temperature ranges. In addition, the relative yields of these fragments are increased 2.7, 2.3 and 8.0-folds compared to those of the copolymer.

As in case of copolymer, evolution of H_2O is not observed but the production of CO_2 and the fragments that can be associated with anhydride units such as $C_4H_6C_2O_3$ (126 Da) are observed. The single ion evolution profile of 126 Da fragment shows two peaks with maxima at around 399 and 422°C, while those of the copolymer sample shows a single broad peak with a maximum at around 434°C. The yield of the 126 Da fragment is increased about 1.4-fold compared to those of the copolymer which can be attributed to the increase in the anhydride production upon fiber formation.

The relative yields of the $CH_2C(CH_3)CO_2COCHCH_2C(CO_2H)CH_2$ (211 Da) and $CH_2CCO_2COCHCH_2CCH_2$ (151 Da) fragments generated as a consequence of transesterification reactions between MMA and acrylic acid units are increased about 6.7 and 4.1-folds respectively . The evolution profiles of these products show the same maxima with those of the copolymer.

Also the maxima observed at around 442°C in the single ion evolution profiles of $(C_4H_5CH_3)_2C_4H_5$ (189 Da), $(C_4H_3CH_3)_3C_4H_3$ (249 Da) fragments are very close to the corresponding values of the copolymer. The yield of these fragments is also increase about 3-folds.

The yield of the products obtained due to $CH_2C(CH_3)CHO$ (70 Da) and $CH_2C(CH_3)COHOCH_3$ (101 Da) fragments are about same with those of the copolymer. Therefore, it can be said that, the γ-H transfer to the carbonyl groups of MMA from the adjacent BA units is not affected by fiber formation.

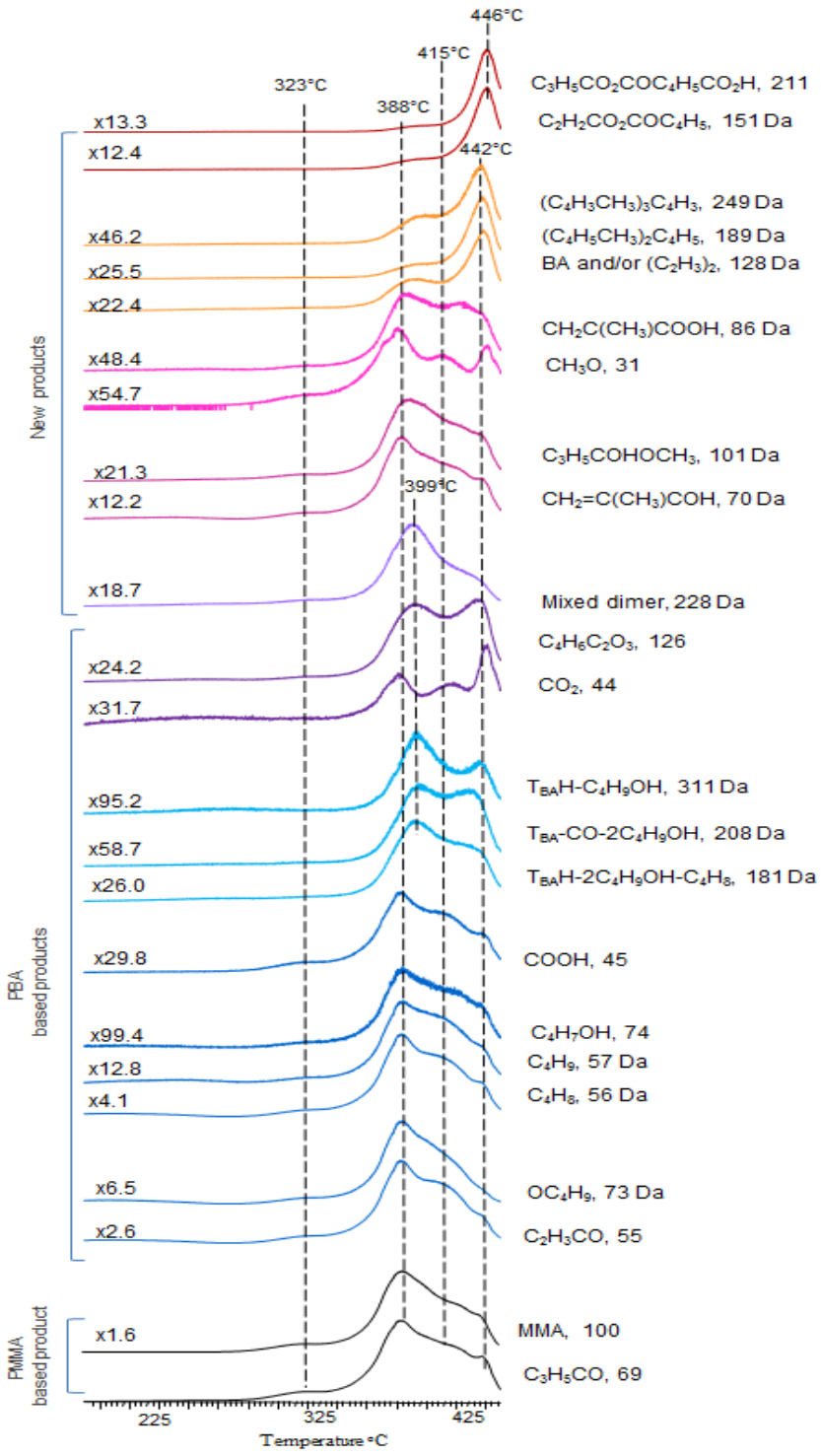

Figure 56. Single ion evolution profiles of some selected products recorded during pyrolysis of the second part of the P(MMA-co-nBA) fiber.

To conclude, the increase in the relative yields of PBA based products generated during the pyrolysis of the fiber is about 1.5-1.7 folds with respect to the copolymer. On the other hand the increase in relative yields of products generated by the reactions between acrylic acid and MMA units such as 211 and 151 is greater than 4-folds. Furthermore, about 3-folds increase in the fragments such as 189 and 249 produced by lose of CO_2 and CO from these units are detected. Thus, as a consequence, the yield MMA that can be evolved by depolymerization decreases as the extent of reactions with BA units increases. Which in turn leads to an increase in relative yields of BA based products also. Consequently, it can be concluded that the intermolecular interactions increases upon fiber formation and this may be a cause for the decrease in the thermal stability.

3.3.2 P(MMA-co-BzMA) fiber

The TGA curve results of first, second and end part of the P(MMA-co-BzMA) fibers are almost identical so only second part of the fiber TGA curve is given in Figure 57. However, compared to the corresponding copolymer, the weight loss at 250°C is absent for all fiber parts, which show a one step weight loss with maximum at around 400°C.

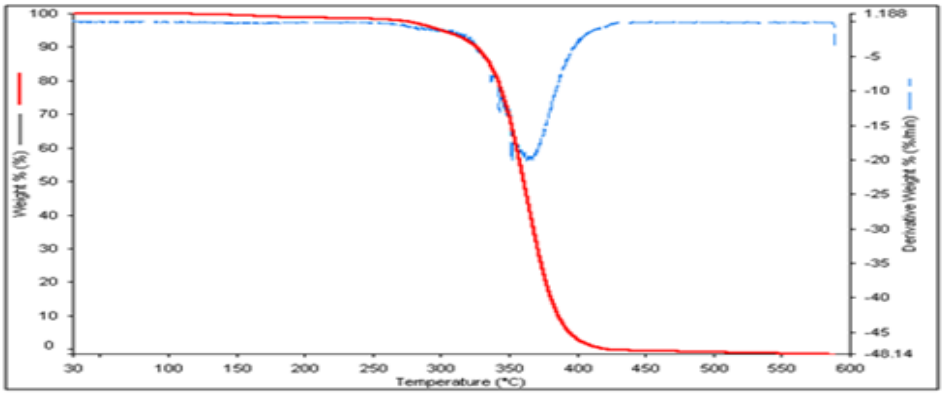

Figure 57. TGA curve of the second part of the P(MMA-co-BzMA) fiber.

TIC curves recorded for three different parts of the fiber samples are given in Figure 58.a, b and c. As can be seen from the figures, all of the fiber parts show almost the same thermal degradation behavior. They show a sharp peak at around 403°C and a very broad one at around 322°C (Figure 58.a, b and c). The decrease in the low temperature peak of all the evolution profiles can be attributed to the decrease in the low molecular weight chains and/or units involving head to head linkages in the fiber samples. The mass spectra recorded at both maxima are dominated with characteristic peaks of both components. Diagnostic peaks of both MMA and BzMA are noticeably intense indicating that the main thermal degradation pathway is depolymerization as in case of the copolymers.

The relative intensities and assignments made for the intense and/or characteristic peaks present in the pyrolysis mass spectra of first, second and end part of the P(MMA-co-BzMA) fibers recorded at 322 and 403°C are collected in Table 18. As can be noted from the table the relative yields of the products are also very close to each other. At both temperature maxima, 69 Da peak due to C_3H_5COfragment is the most intense one. The monomer and tropylium ion's peak at 176 and 91 Da respectively are more intense then the corresponding copolymer. The products with m/z values 51, 65, 77, 79, 91 Da generated by dissociation of side groups and phenyl ring show the similar evolution profiles with those of the corresponding copolymer. The relative yield of peaks at 158 and 131 Da which are associated with products generated by loss of H_2O and COOH by complex rearrangement reactions are also increased by 2.4 and 2.2-folds compared to those recorded during the pyrolysis of the copolymer. However, the relative yield of mixed dimer (276) Da is decreased about 1.9-folds upon fiber formation.

In Figures 58.a, b and c single ion evolution profiles of some diagnostic products of PMMA namely C_3H_5CO (69 Da), MMA (100 Da) and those of PBzMA namely CO_2 (44 Da), monomer, C_6H_5 (77 Da), C_7H_7 (91 Da), M-COOH (131 Da), M-H_2O (158 Da), monomer, BzMA (176 Da) and as new product, mix dimer (276 Da) are given as representative examples.

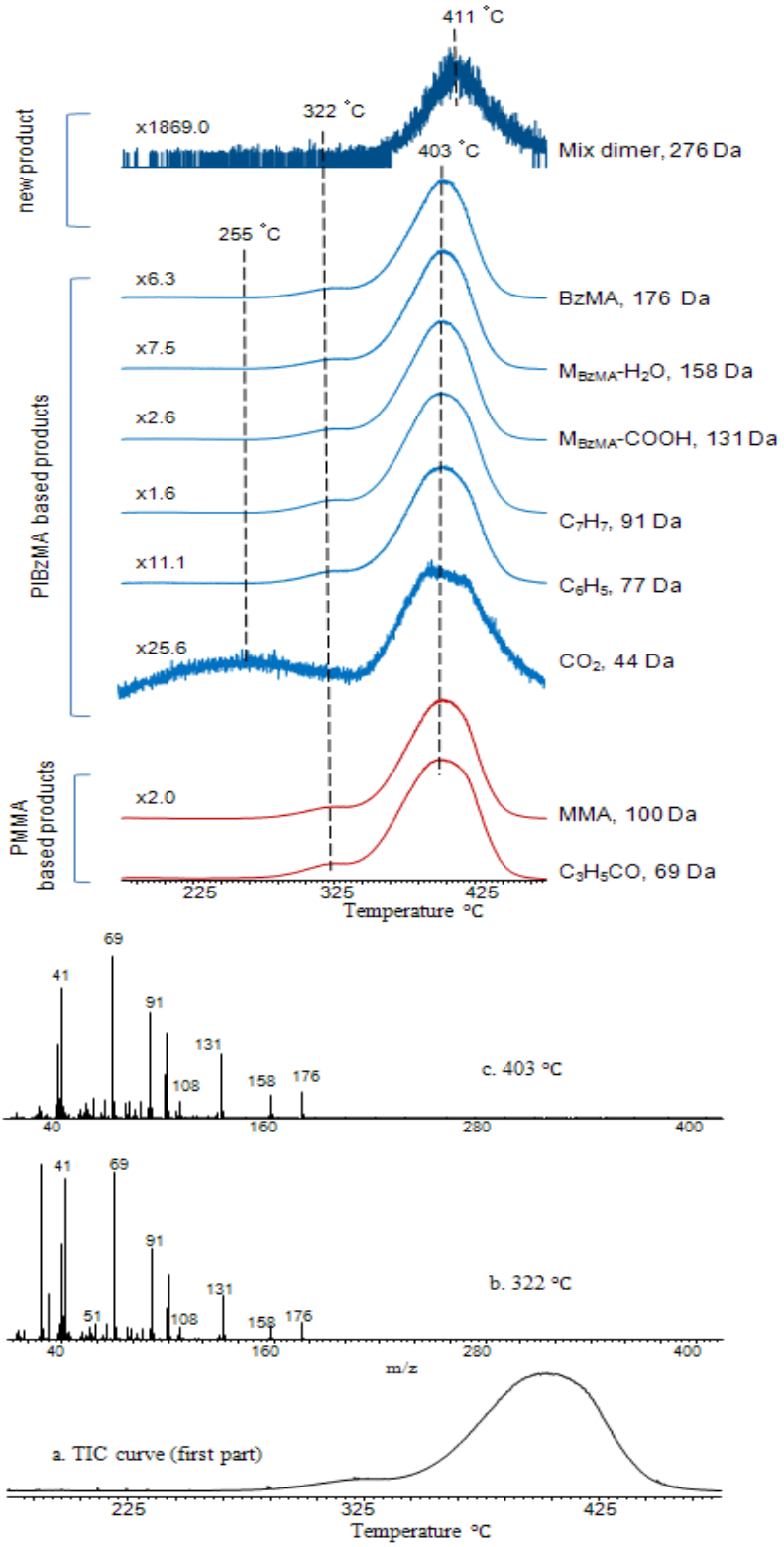

Figure 58.a TIC curve and single ion evolution profiles of some selected products recorded during pyrolysis of the first part of the P(MMA-co-BzMA) fiber.

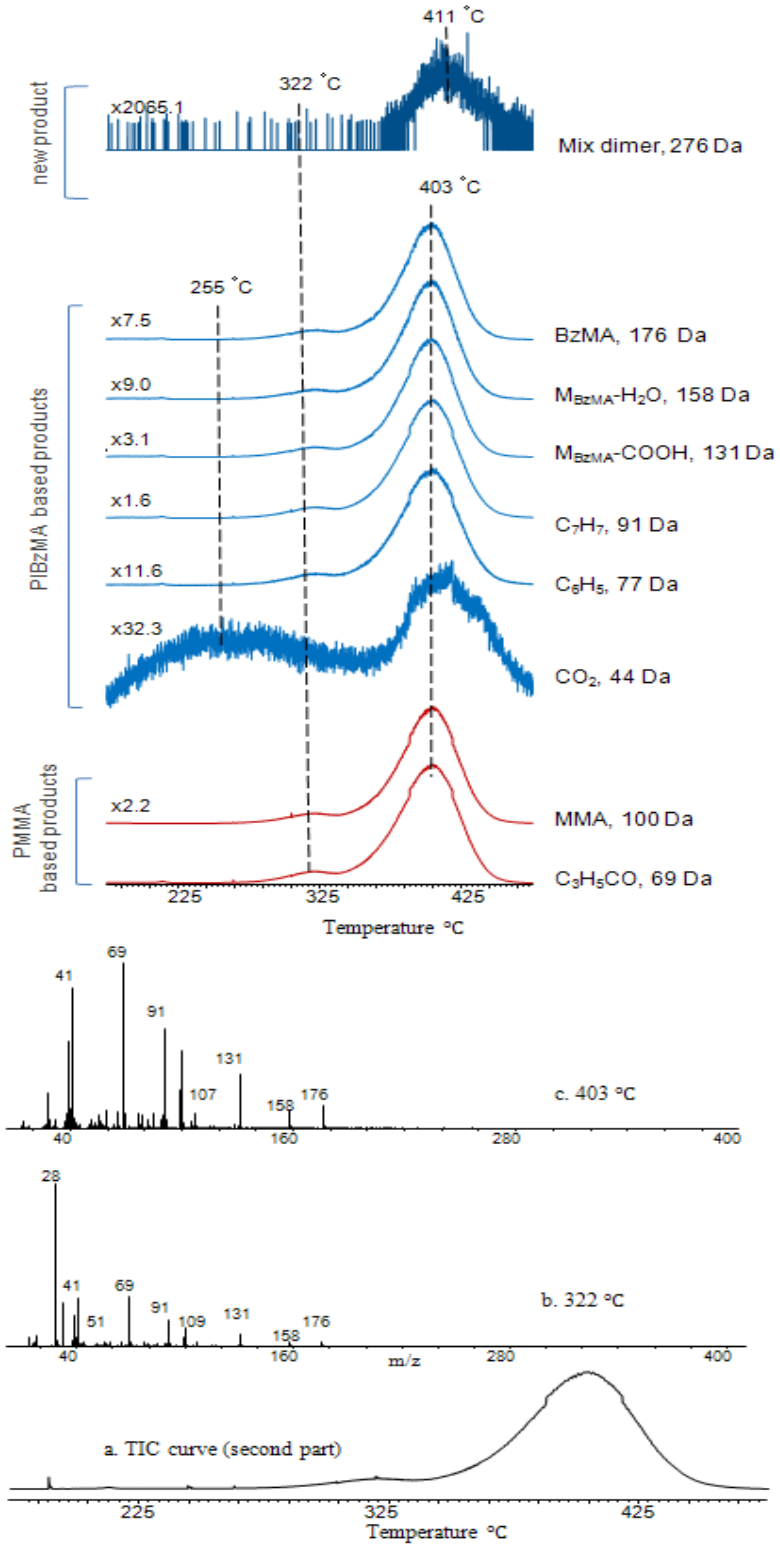

Figure 58.b TIC curve and single ion evolution profiles of some selected products recorded during pyrolysis of the second part of P(MMA-co-BzMA) fiber.

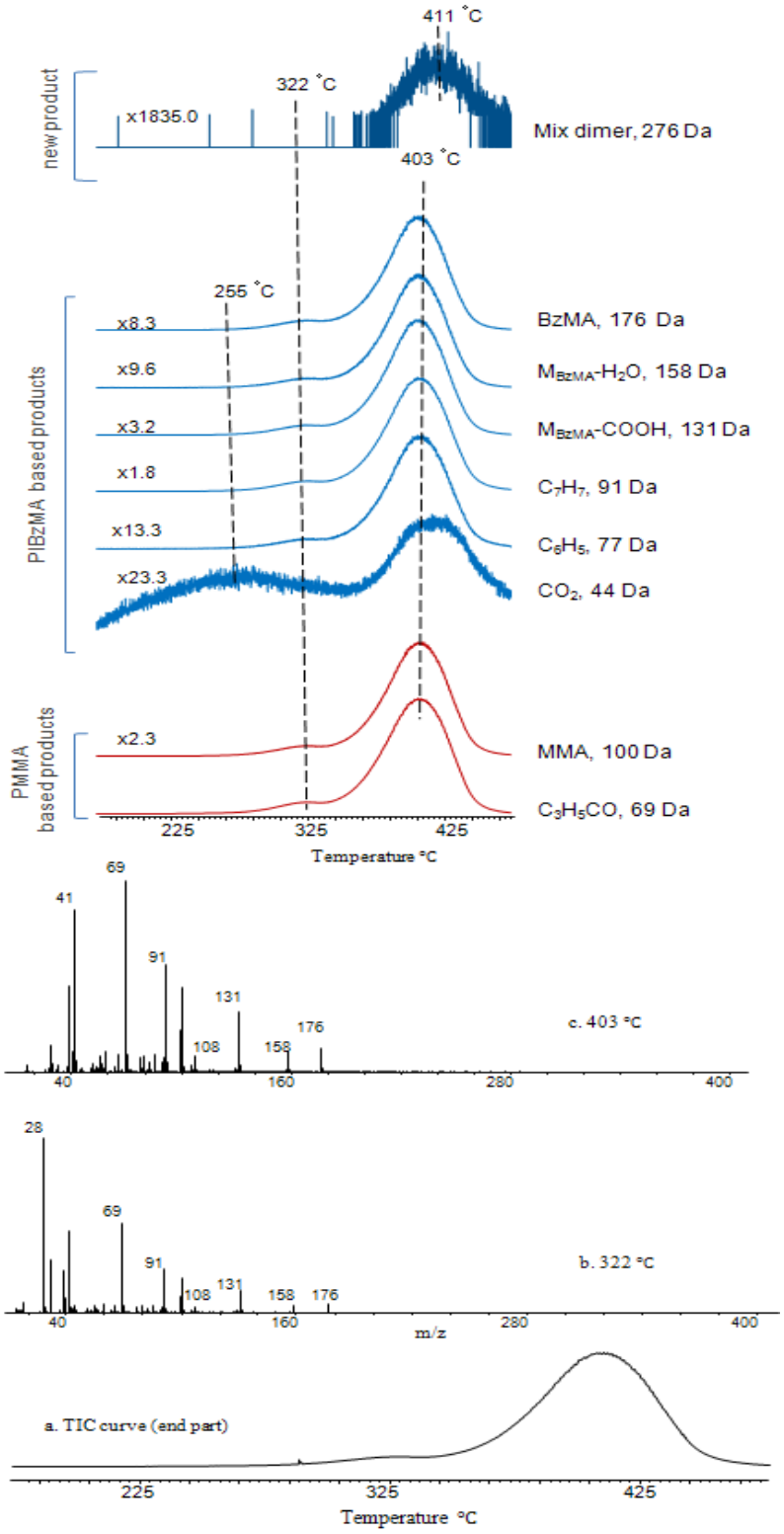

Figure 58.c TIC curve and single ion evolution profiles of some selected products recorded during pyrolysis of the end part of P(MMA-co-BzMA) fiber.

Table 18: The relative intensities and assignments made for the pyrolysis mass spectra of first, second and third parts of P(MMA-co-BzMA) fiber, the intense and/or characteristic peaks present at 322 and 403°C.

m/z (Da)	Relative Intensities						Assignments
	First Part		Second Part		Third Part		
	322°C	403°C	322°C	403°C	322°C	403°C	
39	593	440	640	526	472	446	C_3H_3
40	157	113	207	122	161	109	C_3H_4
41	984	788	931	854	922	838	$CH_3C{=}CH_2$
44	56	14	109	16	90	14	CO_2
51	49	48	53	49	42	42	C_4H_3
65	94	105	95	98	77	88	C_5H_5
69	1000	1000	1000	1000	1000	1000	C_3H_5CO
77	79	90	84	86	63	75	C_6H_5
79	77	95	77	84	75	79	C_6H_7
85	79	103	77	89	77	89	$CH_2C(CH_3)COO$
86	9	9	11	7	10	8	$CH_2C(CH_3)COOH$
91	545	634	511	607	491	557	C_7H_7
99	187	256	186	229	190	216	M_{MMA}-H
100	375	509	364	465	385	441	M_{MMA}, monomer
107	74	104	70	88	71	85	$C_6H_5CH_2O$
131	273	385	245	324	263	311	M-COOH
158	84	134	81	111	88	104	M_{BzMA}-H_2O
176	106	158	102	134	102	121	M_{BzMA}, monomer
276	-	1	-	-	-	-	mix dimer

The yield of CO_2 generated during the pyrolysis of the fiber is also increased about 1.3-folds compared to copolymer. Its evolution profile has two broad peaks with maxima at 255 and 400°C.

To conclude, it is clear that; samples taken from different parts of the fibers do not show different thermal degradation behavior. In addition, there is not much difference between the results obtained with copolymer samples and fibers, except the decrease in the low temperature peak of all the evolution profiles.

3.3.3 P(MMA-co-nBA-co-IBA) fiber

The TGA curve of P(MMA-co-nBA-co-IBA) fiber given in Figure 59 indicates that the thermal degradation of the sample is a two-step process. The first, second and third part of the fiber samples yield the similar TGA curves. Therefore, only the TGA curve of the end part of the fiber is given in the figure. The first portion of the weight loss occurs at around 330°C and the largest portion of sample is lost at around 400°C.

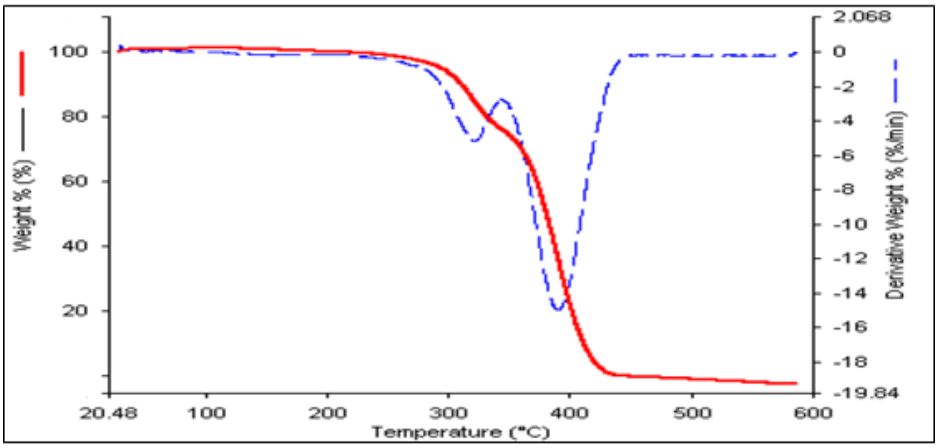

Figure 59. TGA curve of the third part of the P(MMA-co-nBA-co-IBA) fiber.

The mass spectrum recorded at around 370°C is almost identical to the pyrolysis mass spectra of PIBA recorded at around 335°C indicating an increase in the thermal stability of PIBMA chains (Figure 60).

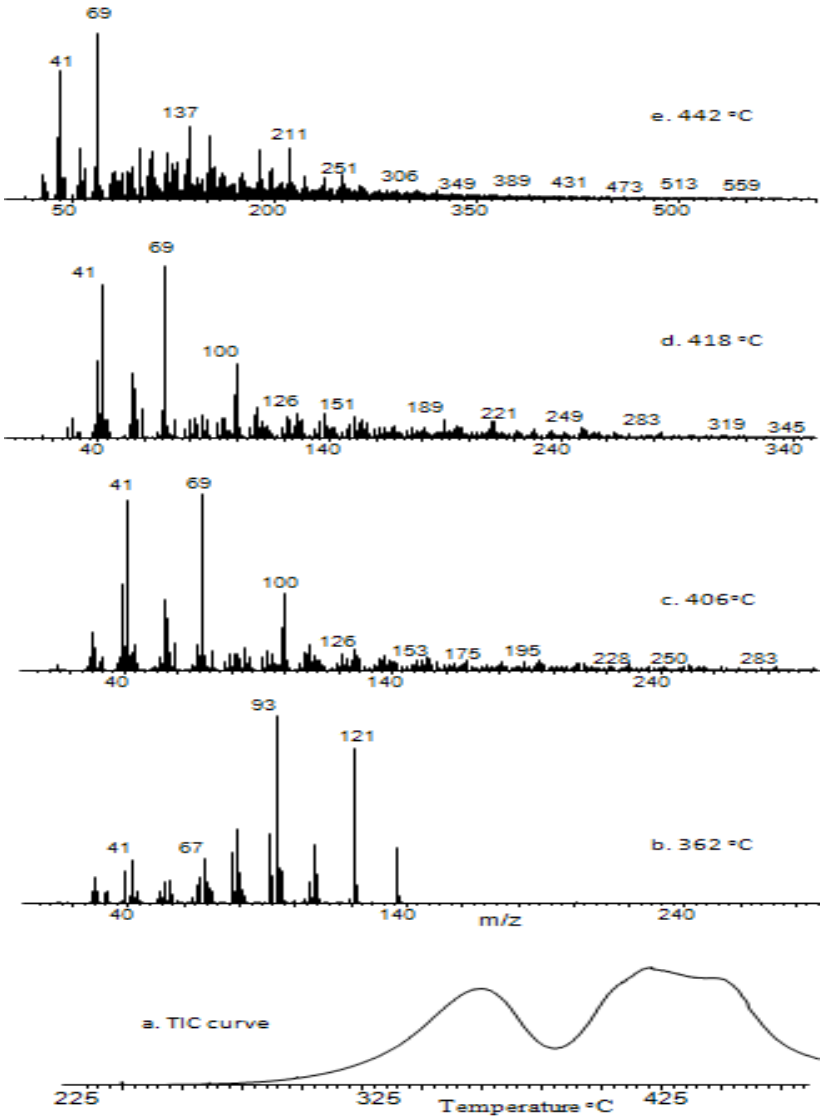

Figure 60. a. TIC curve and the pyrolysis mass spectrum of third part of P(MMA-co-nBA-co-IBA) fiber at b. 362, c. 406, d. 418 and e. 442°C.

As in case of the corresponding copolymer the base peak is at 93 Da due to lose of C_2H_4 and CH_3 groups from the isobornylene. The characteristic and/or intense peaks in the pyrolysis mass spectra of P(MMA-co-nBA-co-IBA) fiber are given in Table 19.

Table 19: The relative intensities and assignments made for the pyrolysis mass spectra of first, second and third parts of P(MMA-co-nBA-co-IBA) fiber, the intense and/or characteristic peaks present at 362 and 418°C.

m/z (Da)	Relative Intensities						Assignments
	First Part		Second Part		Third Part		
	362°C	418°C	362°C	418°C	362°C	418°C	
31	49	44	66	60	52	35	CH_3O
32	33	26	75	53	37	20	CH_3OH
39	191	460	258	599	181	437	C_3H_3
41	231	933	307	1000	229	835	$CH_3C{=}CH_2$
44	11	128	28	147	13	108	CO_2
45	4	40	6	44	4	37	COOH
55	104	393	122	344	115	380	C_2H_3CO
56	42	297	51	269	48	293	C_4H_8
57	14	115	17	127	15	111	C_4H_9
69	73	1000	84	965	79	1000	C_3H_5CO
70	51	80	59	75	61	81	C_3H_5COH
72	1	31	1	14	1	17	$CH_2CHCOOH$
74	5	13	6	13	5	13	HOC_4H_9
85	4	133	4	106	4	143	$CH_2C(CH_3)COO$
86	3	44	4	39	4	48	$CH_2C(CH_3)COOH$
93	1000	123	1000	130	1000	129	C_7H_9
99	7	226	9	193	7	248	M_{MMA}-H
100	12	386	14	297	14	458	M_{MMA}, monomer
101	2	63	2	59	2	72	$C_3H_5COHOCH_3$
126	2	137	2	127	2	150	$C_4H_8C_2O_3$
136	273	83	217	88	335	87	$C_{10}H_{16}$
137	35	164	30	203	43	153	$C_{10}H_{17}$
151	1	151	2	197	1	137	$C_4H_2OCO_2COC_4H_5$
154	1	107	1	106	1	115	$C_{10}H_{17}OH$
189	1	128	1	132	1	124	$(C_4H_5CH_3)_2C_4H_5$
208	-	34	-	23	-	40	T-CO-2C_4H_9OH-T_{BA}
211	-	115	1	121	-	100	$C_3H_5CO_2COC_4H_5CO_2$
228	1	5	1	25	1	58	MMA-BA mix dimer
249	-	67	-	53	-	70	$(C_4H_3CH_3)_3C_4H_3$
276	-	15	-	11	-	16	MMA-IBA mix dimer

In Figure 61.a single ion evolution profiles of some characteristic fragments of PMMA namely C_3H_5 (41 Da), C_3H_5CO (69 Da), monomer, MMA (100 Da) and those of PIBA namely $C_{10}H_{17}$ (137 Da), C_7H_9 (93 Da), $C_{10}H_{16}$ (136 Da), $CH_2CHCOOH$ (72 Da), H_2O (18 Da), $C_4H_6C_2O_3$ (126 Da), CO_2 (44 Da) and as new products CH_3O (31 Da), CH_3OH (32 Da), COOH (45 Da), $CH_2CCH_3CO_2H$ (86 Da), $C_{10}H_{17}OH$ (154 Da), C_3H_5CHO (70 Da), $C_3H_5COHOCH_3$ (101 Da), $(C_4H_5CH_3)_2C_4H_5$ (189 Da), $(C_4H_3CH_3)_3C_4H_3$ (249 Da), $C_2H_2CO_2COC_4H_5$ (151 Da) and $C_3H_5CO_2COC_4H_5CO_2H$ (211 Da) are given as representative examples.

In Figure 61.b single ion evolution profiles of some characteristic fragments of PMMA namely C_3H_5CO (69 Da), and those of PnBA namely C_2H_3CO (55 Da), C_4H_9O (73 Da), C_4H_8 (56 Da), C_4H_9 (57 Da), C_4H_7OH (74 Da), CO_2H (45 Da), $CH_2CHCOOH$ (72 Da), TH-$2C_4H_9OH$-C_4H_8 (181 Da), T-CO-$2C_4H_9OH$ (208 Da), TH-C_4H_9OH (311 Da), CO_2 (44 Da), $C_4H_6C_2O_3$ (126 Da) and as new products MMA-BA mixed dimer (228 Da), $CH_2C(CH_3)CHO$ (70 Da), $CH_2C(CH_3)COHOCH_3$ (101 Da), CH_3O (31 Da), CH_2CCH_3COOH (86 Da), M_{BA} (128 Da), $(C_4H_5CH_3)_2C_4H_5$ (189 Da), $C_2H_2CO_2COC_4H_5$ (151 Da) are given as representative examples.

In general, upon fiber formation, the single ion evolution profiles of almost all characteristic products of P(MMA-co-nBA-co-IBA) are sharpened and shifted to higher temperatures (Figure 61.a-b). The trends observed in the single ion evolution profiles of PMMA based products recorded during the pyrolysis of the fiber show small changes compared to those observed during the pyrolysis of all copolymers under investigation. Upon fiber formation, the low temperature peaks in the evolution profiles of PMMA based products at around 325°C are again disappeared as in case of P(MMA-co-nBA).

The peak maxima in the single ion pyrograms of PMMA based products are at 415°C as in case of P(MMA-co-IBA), and are about 10°C higher than the corresponding copolymer. Fragments due to the pyrolysis of IBA segments are maximized at around 365°C, indicating also a slight increase in thermal stability with fiber formation.

On the other hand, PBA based products are also maximized at around 420°C, at slightly higher temperature than the corresponding copolymer during the pyrolysis of the fiber. Another point that should be noticed is the slight increase in the relative yields of products associated with thermal degradation of PBA chains upon fiber formation. As at the same time increases in relative yields of products associated with reactions of BA segments with MMA units are observed it mat be concluded that the extent of reactions among BA and MMA chains are enhanced upon fiber formation.

CH_3OH and CO_2 show maxima at 382 and 394°C respectively, in their evolution profiles. The corresponding values are at 370 and 385°C respectively, for the corresponding copolymer. The second, high temperature peak in the evolution profiles of CH_3OH is disappeared. On the other hand, the high temperature peak in the evolution profile of CO_2 is shifted to 443°C from 416°C. This behavior may be associated with higher thermal stability of the fiber compared to the copolymer. Similarly, the evolution of isobornyl alcohol is maximized at around 420°C, slightly higher temperatures than the corresponding copolymer. In addition, the evolution of butanol is also shifted about 15°C to high temperature ranges. Thus, it can be concluded that upon fiber formation the thermal degradation shifts slightly higher temperatures.

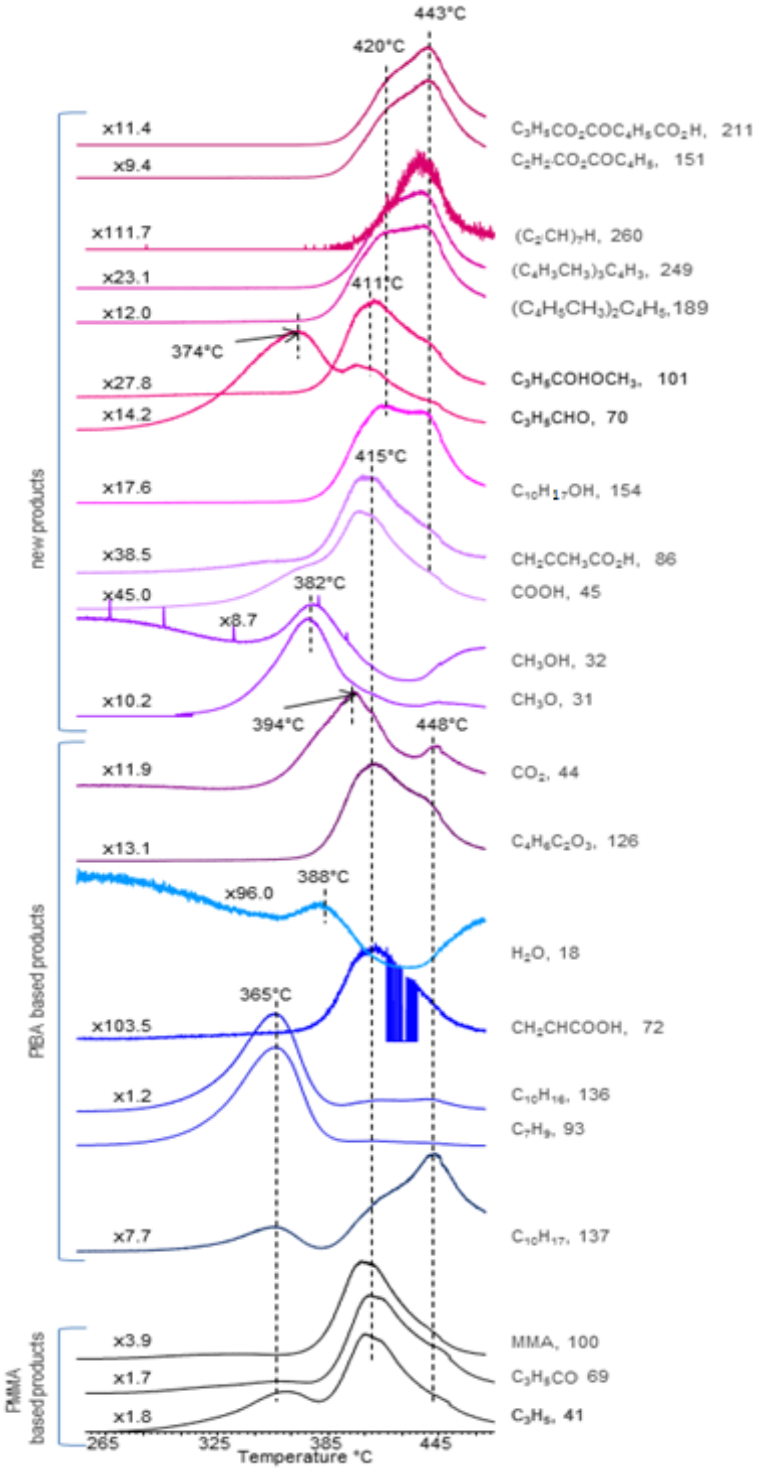

Figure 61.a. Single ion evolution profiles of some selected PIBA and PMMA based products recorded during pyrolysis of P(MMA-co-nBA-co-IBA) fiber.

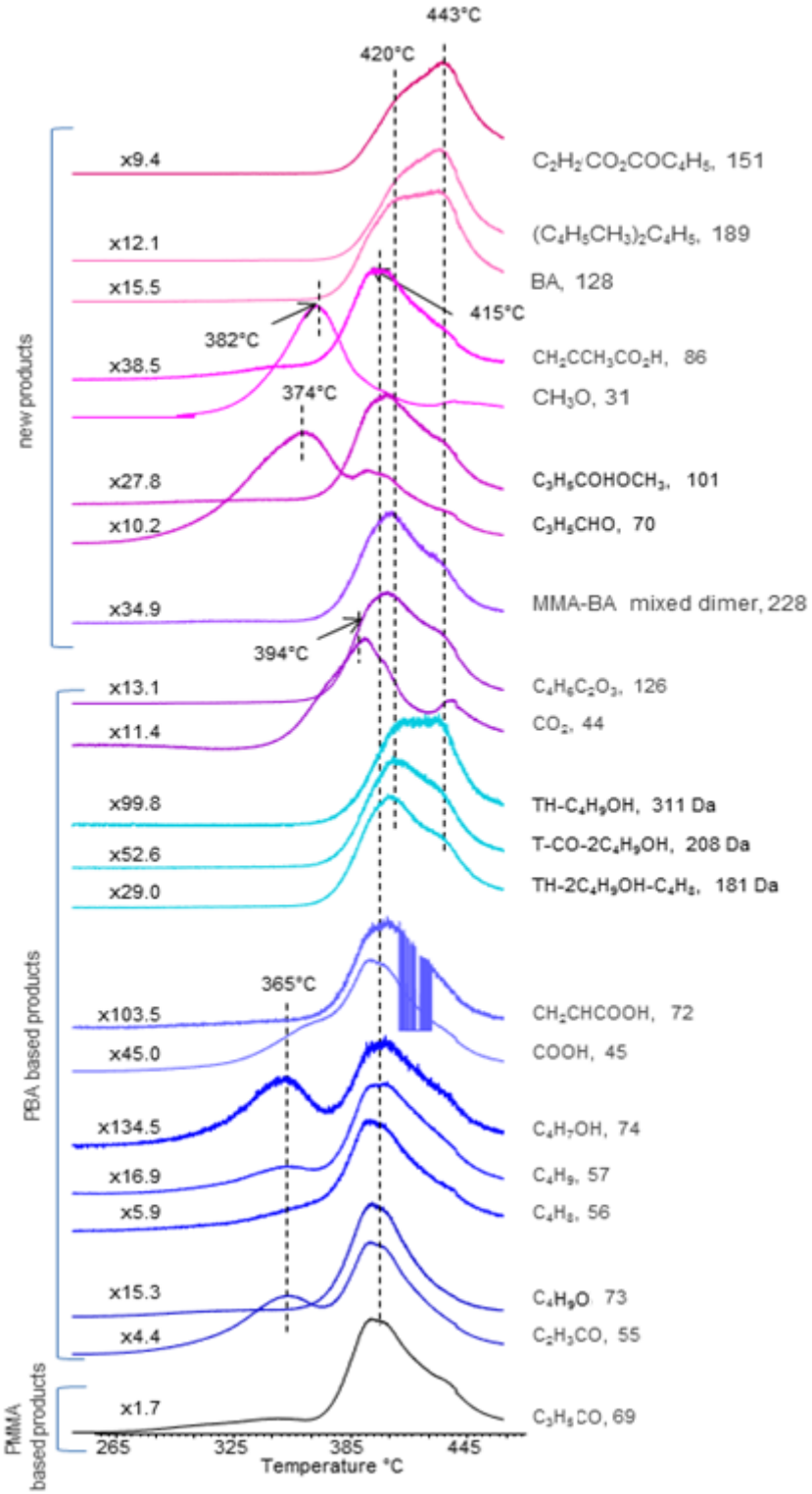

Figure 61.b. Single ion evolution profiles of some selected PBA and PMMA based products recorded during pyrolysis of P(MMA-co-nBA-co-IBA) fiber.

The relative yields of CO_2 and butyl alcohol are almost identical to the corresponding values of the copolymer, while slight increases in the relative yields of anhydride units, butene and isobornyl alcohol are detected.

On the other hand, generation of isobornylene is increased drastically, about more than 3 folds. About 1.7-folds increase in the relative yield of methyl acrylate-methacrylic acid (86 Da) is observed. Furthermore, although still very low, acrylic acid evolution is also recorded.

In summary, it is clear that the evolution of CO_2 is enhanced as the IBA composition increases and fiber formation does not affect its yield noticeably. Similarly, the change in the yield of isobornyl alcohol seems to depend mainly only on the percentage of IBA present in the copolymer. On the other hand, the H-transfer reactions from the isobornyl side chain to the carbonyl group are enhanced upon fiber formation. As the generation of CH_3OH that is only efficient in the presence of IBA, is significantly enhanced during the pyrolysis of the fiber, it can be concluded that the trans-esterification reactions between the acrylic acid units and MMA (Scheme 16) are enhanced during the pyrolysis of the fiber. The increases, though less pronounced, in the yields of 86 Da's fragment due to methyl acrylate and/or methacrylic acid and anhydride units support this proposal.

CHAPTER 4

CONCLUSIONS

In this work, thermal degradation characteristics, thermal degradation products and mechanisms of;

- methacrylate homopolymers; poly(methyl methacrylate) PMMA, poly(butyl methacrylate) PBMA, poly(isobornyl methacrylate) PIBMA and poly(benzyl methacrylate) PBzMA,

- acrylate homopolymers: poly(n-butyl acrylate) PnBA, poly(t-butyl acrylate) PtBA, poly(isobornyl acrylate) PIBA,

- copolymers: poly(methyl methacrylate-co-n butyl acrylate) P(MMA-co-nBA), poly(methyl methacrylate-co-isobornyl acrylate) P(MMA-co-IBA), poly(methyl methacrylate-co-benzyl methacrylate) P(MMA-co-BzMA), poly(methyl methacrylate-co-n butyl acrylate-co-isobornyl acrylate) P(MMA-co-nBA-co-IBA), and poly(methyl methacrylate-co-n butyl acrylate-co-isobornyl acrylate-co-benzyl methacrylate) P(MMA-co-nBA-co-IBA-co-BzMA) and

- copolymer fibers: poly(methyl methacrylate-co-n butyl acrylate) P(MMA-co-nBA)f, poly(methyl methacrylate-co-benzyl methacrylate) P(MMA-co-BzMA)f, and poly(methyl methacrylate-co-n butyl acrylate-co-isobornyl acrylate) P(MMA-co-nBA-co-IBA)f,

are analyzed via direct pyrolysis mass spectrometry.

The effects of substituents on the main and side chains, each component of the copolymer on thermal characteristics of the other and fiber formation on thermal stability, degradation characteristics and thermal degradation mechanisms are investigated.

- In general, depolymerization mechanism yielding mainly the monomer is the main thermal decomposition route for methacrylate polymers. On the other hand, thermal degradation of acrylate polymers starts by H-transfer reactions from the main chain to the carbonyl groups. However, when the alkoxy group involves γ-H, then, H-transfer reactions from the alkoxy group to the CO group also takes place and usually thermal degradation proceeds through competing reactions leading to a complex thermal degradation mechanism;

  - PnBMA degrades mainly via depolymerization associated with generation of a tertiary radical upon cleavage of the $CH_3C\text{-}CH_2$ bond.

  - PnBA degradation proceeds through simultaneous and subsequent processes, γ-hydrogen transfer from the main chain to carbonyl group, transesterification reactions causing loss of butanol, and generation of six-membered products stabilized by cyclization reactions being among the major decomposition routes.

  - PtBA thermal degradation starts by elimination of C_4H_8 by γ-hydrogen transfer reactions from the t-butyl groups to the carbonyl groups producing poly(acrylic acid) chains that forms anhydride linkages by condensation reactions and unsaturated units by subsequent loss of CO_2 and CO that decompose at elevated temperatures.

  - PIBA degrades via complex degradation mechanism and γ-H transfer from the isobornyl ring to the carbonyl group. Evolution of isoborylene yields polyacrylic acid that eliminates water by inter and intra molecular interactions and forms anhydride units capable of crosslinking by lose of CO_2 and CO.

- PIBMA also shows similar characteristics with PIBA, indicating that presence of methyl substituent does not affect thermal degradation behavior as it does in case of PMMA.

- Like PMMA, thermal degradation of PBzMA occurs by depolymerization reaction yielding mainly the monomer.

- In general, during the thermal degradation of copolymers of MMA intermolecular interactions between the components become effective.

  - For poly(methyl methacrylate-co-n butyl acrylate), P(MMA-co-BA) sample, although the presence of butyl acrylate does not affect the thermal stability of PMMA chains in a considerable manner, the butyl acrylate chains are stabilized to some extend by the presence of methyl methacrylate chains. Furthermore, H-transfer reactions from the butyl group to the CO group become preferential compared to H-transfer reactions from the main chain. Anhydride formation followed by evolution of CO_2 generates unsaturated and/or crosslinked units. Strong evidences for trans-esterification reactions between H_2O and MMA and BA yielding methacrylic and acrylic acid segments and reactions between CH_3OH and acrylic acid yielding methacrylate segments are also detected.

  - For, poly(methyl methacrylate-co-isobornyl acrylate), P(MMA-co-IBA), thermal degradation mechanism is again affected by intermolecular interactions between PIBA and PMMA. Based on evolution of methanol, a transesterification reaction between the MMA and acrylic acid units generated by loss of isobornylene from PIBA chains is proposed. The relative yields of acrylic acid and products due to transesterification reactions are noticeably higher than those of the poly(MMA-co-BA) sample, indicating that transesterification reactions of acrylic acid and H_2O with MMA seem to be more likely for the copolymer involving IBA, as confirmed by the increase in relative yields of related products during the pyrolysis of poly(MMA-co-IBA).

- Thermal degradation characteristics of poly(methyl methacrylate-co-benzyl methacrylate), P(MMA-co-BzMA), copolymer does not show a drastic changes compared to those of the corresponding homopolymers.

    - The DP-MS findings for the poly(methyl methacrylate-co-n butyl acrylate-co-isobornyl acrylate) P(MMA-co-nBA-co-IBA) involving 5 % nBA and 5 % IBA separately, indicate that thermal decomposition of IBA and BA shifts to high temperature ranges when both of them are present as a component in the copolymer involving 90 % MMA, compared to the corresponding homopolymers and copolymers involving only 10.0 % IBA or 12.5 % BA. As the percentage of IBA decreases from 12.5 to 5 %, the temperature ranges at around which the elimination of side chains occur increases. The increase in the thermal stability of these segments may be associated with the higher thermal stability of PMMA chains and the decrease in the probability of degradation routes involving H-transfer reactions from the main chain as the percentage of IBA decreases. On the other hand, the increase in thermal stability of PMMA chains when the percentage of IBA decreases from 10 to 5 % may be attributed to presence of unsaturated and crosslinked units generated by elimination of CO_2 and CO from the anhydride units formed by condensation of the acrylic acid units.

- In general, for the poly(methyl methacrylate-co-n butyl acrylate-co-isobornyl acrylate) P(MMA-co-nBA-co-IBA) involving 15 % nBA and 15 % IBA separately, besides the decrease in thermal stability, noticeable changes are detected in product distributions. Compared to P(MMA-co-BA) and P(MMA-co-BA-co-IBA) containing only 5 % BA and IBA, increase in the probability of H-transfer reactions from the main chain, competing with H-transfer reactions from the side chains, as in case of homopolymer PnBA is detected.

  The generation of isobornylene is enhanced as the percentage of IBA is increased from 5 to 15 %. however, it is still lower than the value for the P(MMA-co-IBA). The results indicate that almost all acrylic acid produced

is reacted and generated anhydride linkages that eliminate CO and CO_2 and produce unsaturated units. Thus, it can be concluded that when the IBA percentage increases thermal stability of the copolymer decreases, degradation starting with H-transfer reactions from the isobornyl group to carbonyl group proceeds through several trans-esterification reactions generating methanol, isobornyl and butyl alcohols.

- In general, upon fiber formation; samples taken from different parts of the fibers do not show different thermal degradation behavior. However, changes in the thermal degradation characteristics are detected upon fiber formation.

  - In general, significant increase in the relative yields of products generated by the reactions between acrylic acid and MMA units pointing out enhancement of the intermolecular interactions upon fiber formation is detected. These interactions may be the reason of the decrease in the thermal stability.

  - For poly(methyl methacrylate-co-n butyl acrylate-co-isobornyl acrylate) P(MMA-co-nBA-co-IBA) fiber; the H-transfer reactions from the isobornyl side chain to the carbonyl group and the reactions with acrylic acid and MMA changes are enhanced at relatively low temperatures, decreasing the thermal stability of MMA chains. On the other hand, the reactions among PBA and MMA units are diminished during the pyrolysis of the fiber most probably due to the decrease in thermal stability of MMA chains.

REFERENCES

1) Drews, M. J., Barker, R. H., Hatcher, J. D., Fiber-Forming Polymers, Applied Polymer Science, 1985; 285, 441-467.

2) D'Alelio, G. F., Fundamental Principles of Polymerization, John Wiley & Sons, New York, 1952; 27-28.

3) Ahluwalia, V. K., Mishra, A., Polymer Science Textbook, Ane books India, 2008; 139-140.

4) Oswald, T. A., Understanding Polymer Processing, Hanser publications, Germany, 2011; 137-138.

5) Walczak, Z. K., Prosses of Fiber Formation, Elsevier Ltd., New York, 2002; 135.

6) Salem, D. R., Structure Formation in Polymeric Fibers, Hanser Publishers, Munich, 2001; 397-398.

7) Hacaloğlu, J., Direct insertion probe mass spectrometry (DIP-MS) of polymer, Advances in Polymer Science, 2011; 248, 69-103.

8) Chatloff, R. P., Sircar, A.K., Thermal Analysis of Polymer, Encyclopedia of Polymer Science and Technology, John Wiley & Sons, 2005.

9) Fares, M. M., Hacaloğlu, J., Suzer, S., Characterization of degradation products of polyethylene oxide by pyrolysis mass spectrometry, European Polymer Journal, 1994; 30, 845-850.

10) Gupta, M. C. Viswanath, S. G., Role of Metal Oxides in the Thermal Degradation of Poly(vinyl chloride), American Chemical Society, Ind. Eng. Chem. Res., 1998; 37 (7), 2707–2712.

11) Reich, L., Lee, H.T., Levi, D., Kinetic Parameters in Polymer Degradation by Dynamic Thermogravimetric Analysis, Journal of Applied Polymer Science, 1965; 9, 351-358.

12) Schild, H. G., Application of TGA/ FTIR to the Thermal Degradation Mechanism of Tetrafluoroethylene-Propylene Copolymers, Journal of Polymer Science: Part A: Polymer Chemistry, John Wiley &Sons, Inc., 1993; 31, 1629-1632.

13) Raemaekers, K.G.H., Bart, J.C.J., Applications of simultaneous thermogravimetry-mass spectrometry in polymer analysis, ThermochimicaActa, 1997; 295, 1-58.

14) McNeill, I. C., Thermal Volatilization Analysis: A New Method for the Characterization of Polymers and the Study of Polymer Degradation, Journal of Polyme Science, 1966; 4 (1), 2479-2485.

15) Guo, X., Huang B., Dyakonov T., Chen Y., Padron L., Thayne V. T., Kun J., HodkiewczJ.,Stevenson W. T. K, Thermal Volatilization Analysis: A Versatile Platform for Spectroscopic Investigations of Polymer Degradation Processes, Applied Spectroscopy, 1999; 53(11), 1403-1410.

16) Menczel, J. D., Judovits, L., Prime, R. B.,Bair, E. H., Reading, M. and Swier, S., Thermal Analysis of Polymers, John Wiley & Sons, Inc., 2009;7-9.

17) Pielichowski, K., Njuguana J., Thermal Degradation of Polymeric Materials, Rapra Technology Ltd., 2005; 19.

18) Irwin, W. J., Dekker, M., Analytical Pyrolysis: A Comprehensive Guide, New York, 1982.

19) Hacaloğlu, J., Yalçın T., Mass Spectrometry in Polymers Research, Applied Mass Spectroscopy Handbook, editted by Mike Lee, John Wiley & Sons, Inc., Chap 46, 2012; 1119-1142.

20) Hacaloğlu, J., Pyrolysis Mass Spectrometry for Molecular Ionization Methods, The Encyclopedia of Mass Spectrometry: Ionization methods, Eddited by Michael L. Gross& Richard M. Caprioli. Elsevier Science Ltd, 2007; 6, 925-938.

21) Zhang, S., Shin, Y. S., Mayer, R., Basile, F., On-probe pyrolysis desorption electrospray ionization (DESI) mass spectrometry for the analysis of non-volatile pyrolysis products , Journal of Analytical and Applied Pyrolysis, 2007; 80, 353.

22) Whitson, S. E., Erdodi, G., Kennedy, J. P., Lattimer, R. P., Direct probe-atmospheric pressure chemical ionization mass spectrometry of cross-linked copolymers and copolymer blends, Analytical Chemistry, 2008; 80, 7778.

23) "polyacrylate" Encyclopædia Britannica. Encyclopædia Britannica Online Academic Edition. Encyclopædia Britannica Inc., 2012. Web. 01 Aug. 2012. <http://www.britannica.com/EBchecked/topic/1551195/polyacrylate>.

24) Czech, Z., Pełech, R., Thermal degradation of poly(alkyl methacrylates), Jornal of Thermal Analaysis and Calorimetry, 2010; 101, 309–313.

25) Mahalik,J. P., Madras, G., Effect of the Alkyl Group Substituents on the Thermal and Enzymatic Degradation of Poly(*n*-alkyl acrylates), Ind. Eng. Chem. Res., 2005; 44(12).

26) Soeriyadi, A. H., Bennet, F., Whittaker, M. R., Barker, P.J.,Kowollik, C. B.,Davis, T. P., Degradation of Poly(Butyl Methacrylate) Model Compounds Studied via High-Resolution Electrospray Ionization Mass Spectrometry, Jornal of Polymer Science: Part A: Polymer Chemistry, 2011; 49, 848–861.

27) Jakubowski, W., Juhari, A., Best,A., Koynov, K., Pakula, T., Matyjaszewski, K., Comparison of thermomechanical properties of statistical, gradient and block copolymers of isobornyl acrylate and n-butyl acrylate with various acrylate homopolymers, Science Direct, 2008; 49, 1567-1578.

28) Kurt, A., Kaya, E., Synthesis, Characterization and Thermal Degradation Kinetics of the Copolymer Poly(4-methoxybenzyl methacrylate-co-isobornyl methacrylate), Journal of Applied Polymer Science, 2010; 115, 2359–2367.

29) Konaganti, V. K.,Madras, G., Photocatalytic and Thermal Degradation of Poly(methyl methacrylate), Poly(butylacrylate) and Their Copolymers, Ind. Eng. Chem. Res, 2009; 48, 1712–1718.

30) Vinu, R., Madras, G., Photocatalytic degradation of methyl methacrylate copolymers, Polymer Degradation and Stability, 2008; 93, 1440–1449.

31) Grassie, N., Recent work on the thermal degradation of acrylate and methacrylate homopolymers and copolymers, Department of Chemistry, University of Glasgow, Glasgow W2, Scotland.

32) Grassie, N., Torrance, B. J. D., Thermal Degradation of Copolymers of Methyl Methacrylate and Methyl Acrylate. Products and General Characteristics of the Reaction, Journal of Polymer Science, 1968; 6(1), 3303-3314.

33) Grassie, N., Torrance, B. J. D., Thermal Degradation of Copolymers of Methyl Methacrylate and Methyl Acrylate. Chain Scission and the Mechanism of the Reaction, Journal of Polymer Science, 1968; 6(1), 3315-3326.

34) Manring, L.E., Thermal degradation of poly(methly methacrylate). 4. Random side group scission, Macromolecules, 1991; 24, 3304–3309

35) Holland, B.J., Hay J.N., The kinetics and mechanisms of the thermal degradation of poly(methyl methacrylate) studied by thermal analysis-Fourier transform infrared spectroscopy, Polymer 2001; 42, 4825–4835.

36) Lehrle, L., Place, E.J., Degradation mechanism of poly(methyl acrylate)s I. An assessment of the participation of random chain scissions. PolymDegrad Stab 1997; 56, 215.

37) Lehrle, L., Place, E.J., Degradation mechanism of poly- (methyl acrylate)s II. The contribution of depropagation with intramolecular transfer. PolymDegrad Stab 1997; 56, 221.

38) Lehrle, L., Place, E.J., Degradation mechanism of poly(methyl acrylate)s III. An assessment of the participation of secondary reactions from the dependence of pyrolysis yields on sample thickness. PolymDegrad Stab. 1997; 57, 247.

39) Bertini, F., Audisio, G., Zuev, V., Investigation on the thermal degradation of poly-n-alkyl acrylates and poly-n-alkyl methacrylates (C1–C12). PolymDegradStab., 2005; 89, 233-239.

40) Manring, L. E., Thermal Degradation of Poly(methyl methacrylate). 4. Random Side-Group Scission, Macromolecules, 1991; *24,* 3304-3309.

41) Czech, Z., Pelech, R., Zych, K., Swiderska, J., Thermal degradation of copolymers based on selected alkyl methacrylates J Therm Anal Calorim. 2012; 109, 573-576.

42) Czech, Z., Pelech, R., Thermal degradation of butyl acrylate-methyl acrylate-acrylic acid-copolymers. J Therm Anal Calorim., 2009; 96, 583-586.

43) Murphya, R. E., Schureb, M. R., Foley, J. P., Quantitative analysis of poly(methyl methacrylate–butyl acrylate) copolymer composition by liquid chromatography–particle beam mass spectrometry, Journal of Chromatography, 1998; 824, 181–194.

44) Konaganti, V.K., Madras, G., Photooxidative and pyrolytic degradation of methyl methacrylate-alkyl acrylate copolymers, Polymer Degradation and Stability, 2009; 94, 1325–1335.

45) Leskovac, M., Fles, V. K. R., Hace, D., Thermal Stability of Poly(Methyl Methacrylate-co-Butyl Acrylate) and Poly(Styrene-co-Butyl Acrylate) Polymers, Poymer Engineering and Science, 1999; 39(3), 600-608.

46) Haken, J. K., Tan, L., Thermal Degradation of Isomeric Poly(propyl Acrylate)s and Poly(butyl Acrylate)s Using Pyrolysis Gas Chromatography-Mass Spectrometry,Journal of Polymer Science: Part A: Polymer Chemistry, 1987; 25, 1451-1456.

47) Lazzari, M., Chiantore, O., Thermal-ageing of paraloid acrylic protective polymers. Polymer 2000; 41, 6447-6455.

48) Soeriyadi, A.H.,Trouillet, V.,Bennet, F., Bruns, M.I.,Whittaker, M.R.,Boyer, C.,Barker, P.J.,Davis, T.P., Barner-Kowollik, C., A Detailed Surface Analytical Study of Degradation Processes in Methacrylic Polymers. J Polym Sci Part A: Polym Chem, 2012; 50, 1801–1811.

49) Chiantore, O., Trossarelli, L., Lazzari, M., Photooxidative degradation of acrylic and methacrylic polymers. Polymer, 2000; 41, 1657-1668.

50) Chiantore, O., Lazzari, M., Photo-oxidative stability of paraloid acrylic protective polymers. Polymer, 2001; 42, 17-27.

51) Goikoetxea, M., Barandiaran, M.J., Asua J., Mechanisms of n-Butanol Formation in Butyl Acrylate Latexes, Journal of Polymer Science: Part A: Polymer Chemistry, 2007; 45, 5838–5846.

52) Daraboina, N., Madras, G., Thermal and Photocatalytic Degradation of Poly(methyl methacrylate), Poly(butyl methacrylate), and Their Copolymers, *Ind. Eng. Chem. Res.,* 2008;*47,* 6828–6834.

53) Arribas, C., Masegosa, R. M., Salom, C., Arevalo, E., Prolongo, S. G., Prolongo, M. G., Epoxy/poly (benzyl methacrylate) blends: miscibility, phase seperation on curing and morphology, Journal of Thermal Analysis and Calorimetry, 2006; 86(3), 693–698.

54) Tsai, Y., Wang, W., Polybenzyl Methacrylate Brush Used in the Top-Down/ Bottom-Up Approach for Nanopatterning Technology, Journal of Applied Polymer Science, 2006; 101, 1953–1957.

55) Ishikawa, M., Noguchi, T., Niwa, J., Controlled release of theophylline from plasma-irradiated double-compressed tablet composed of a wall material containing polybenzylmethacrylate, Chemical & Pharmaceutical Bulletin, 1995; 43(12), 2215-2220.

56) Dervax, B., Camp, W., Renterghem, L., Duprez, F. E., Synthesis of Poly(isobornyl acrylate) Containing Copolymers by Atom Transfer Radical Polymerization, Wiley Inter Science, 2007.

57) Schnell, M., Borrajo, J., Williams, R. J. J., Wolf, B.A., Isobornyl Methacrylate as a Reactive Solvent of Polyethylene, Macromolecular Materials Engineering, 2004; 289, 642–647.

58) Matsumoto, A., Mızuta, K., Otsu, T., Synthesis and Thermal Properties of Poly (cycloalkyl methacrylate)s Bearing Bridged- and Fused-Ring Structures, Journal of Polymer Science, 1993; 31, 2531-2539.

59) Doğan, F., Kaya, İ., Yürekli, M., Kinetic of thermal degradation of poly(isobornyl methacrylate), Catalysis Letters, 2007; 114, 1–2.

60) Ferriol, M., Gentilhomme, A., Cochez, M., Oget, N., Mieloszynski, J. L., Thermal degradation of poly(methyl methacrylate) (PMMA): modelling of DTG and TG curves, *Polym. Deg. Stab.,* 2003; *79(2),* 271.

61) Hu, Y. H., Chen, C. Y., The effect of end groups on the thermal degradation of poly(methyl methacrylate), Polym. Deg. Stab., 2003; 82, 81-88.

APPENDIX A

SPECTRAL DATA

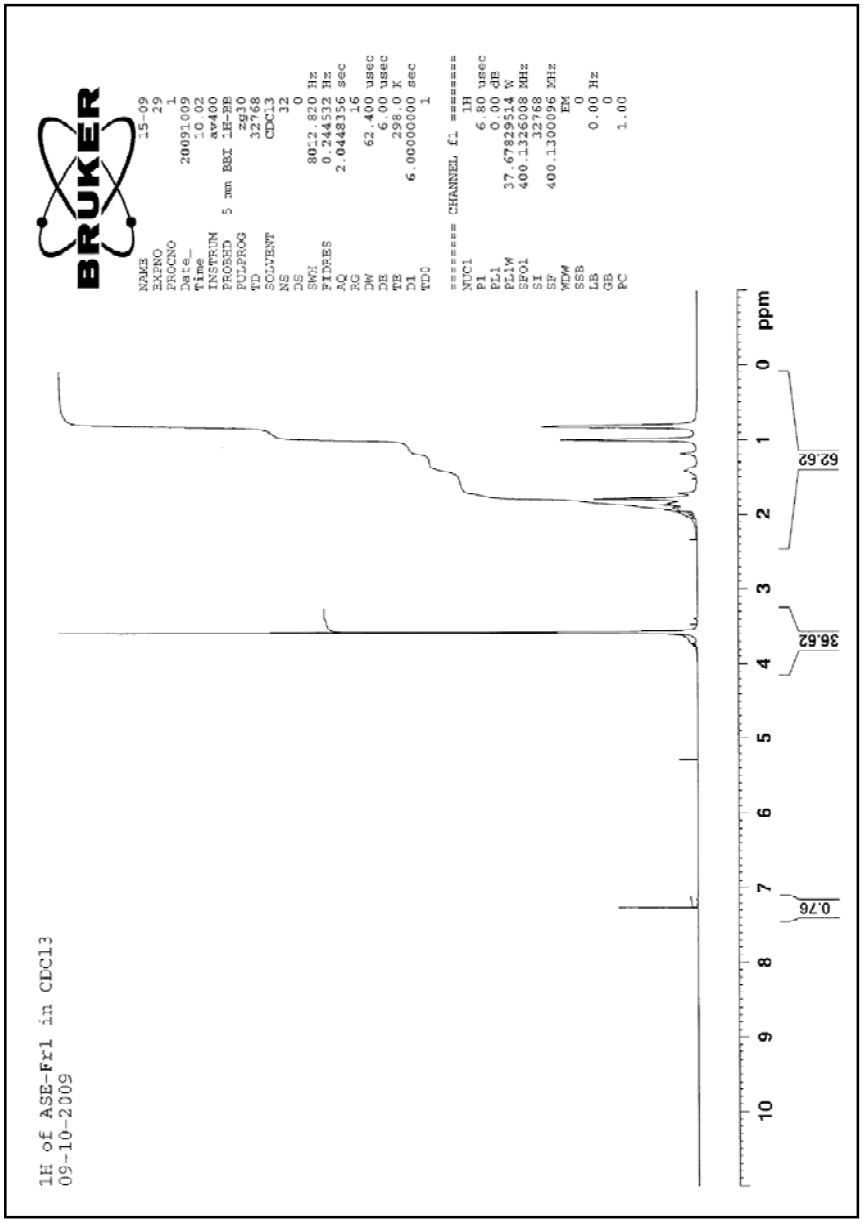

Figure 62. ^{1}H-NMR spectrum of poly(methyl methacrylate)

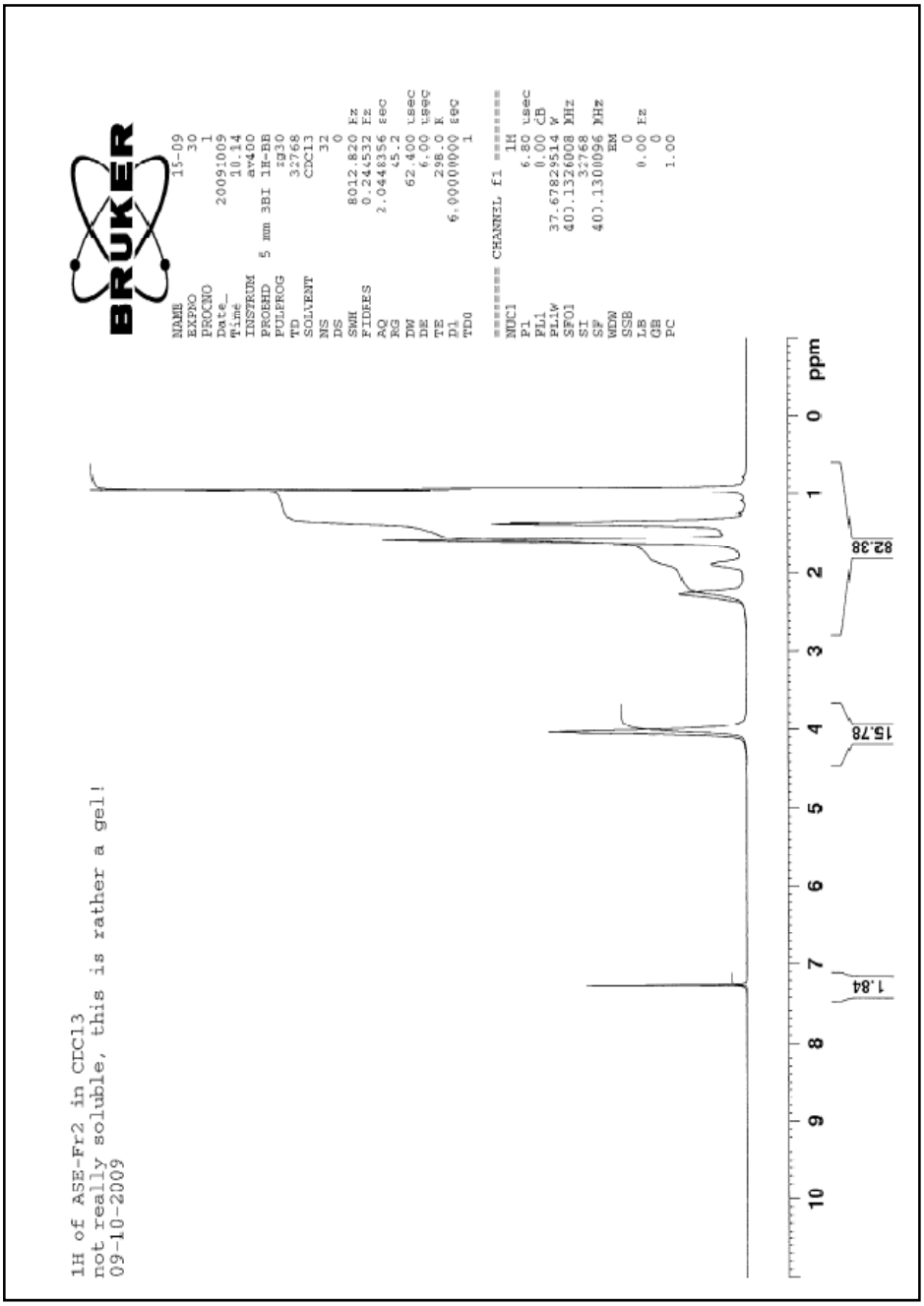

Figure 63. ^{1}H-NMR spectrum of poly(n-butyl acrylate)

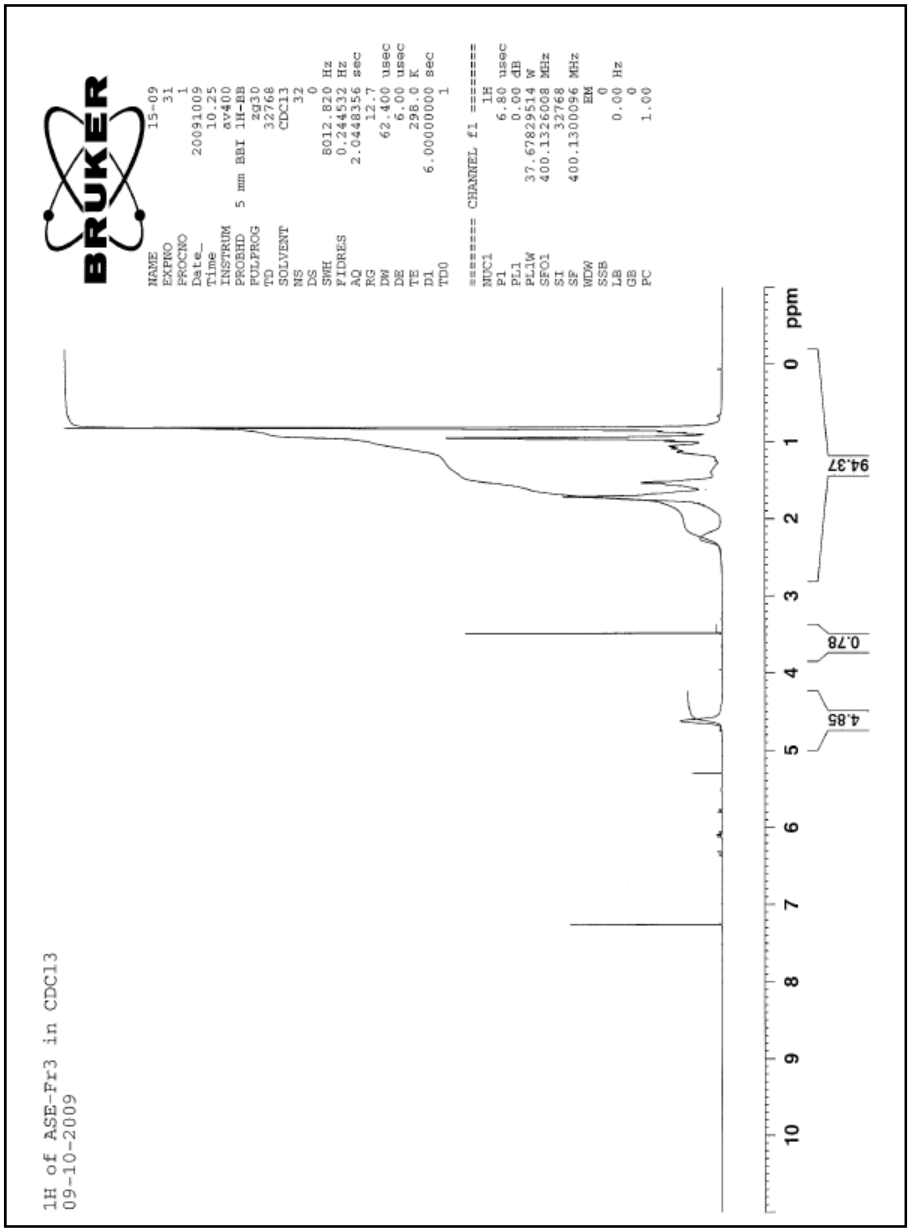

Figure 64. ^{1}H-NMR spectrum of poly(isobornyl acrylate)

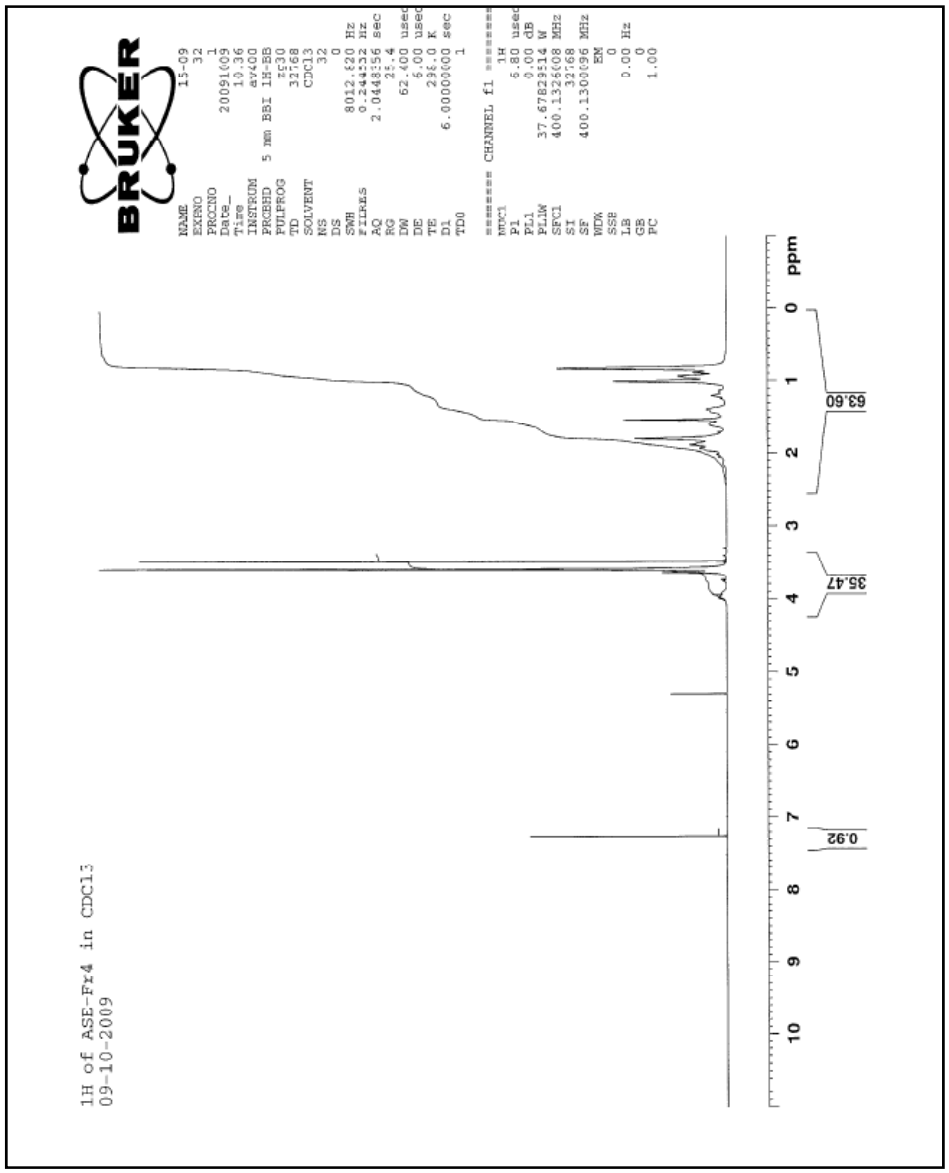

Figure 65. ^{1}H-NMR spectrum of P(methyl methacrylate-co-n butyl acrylate)

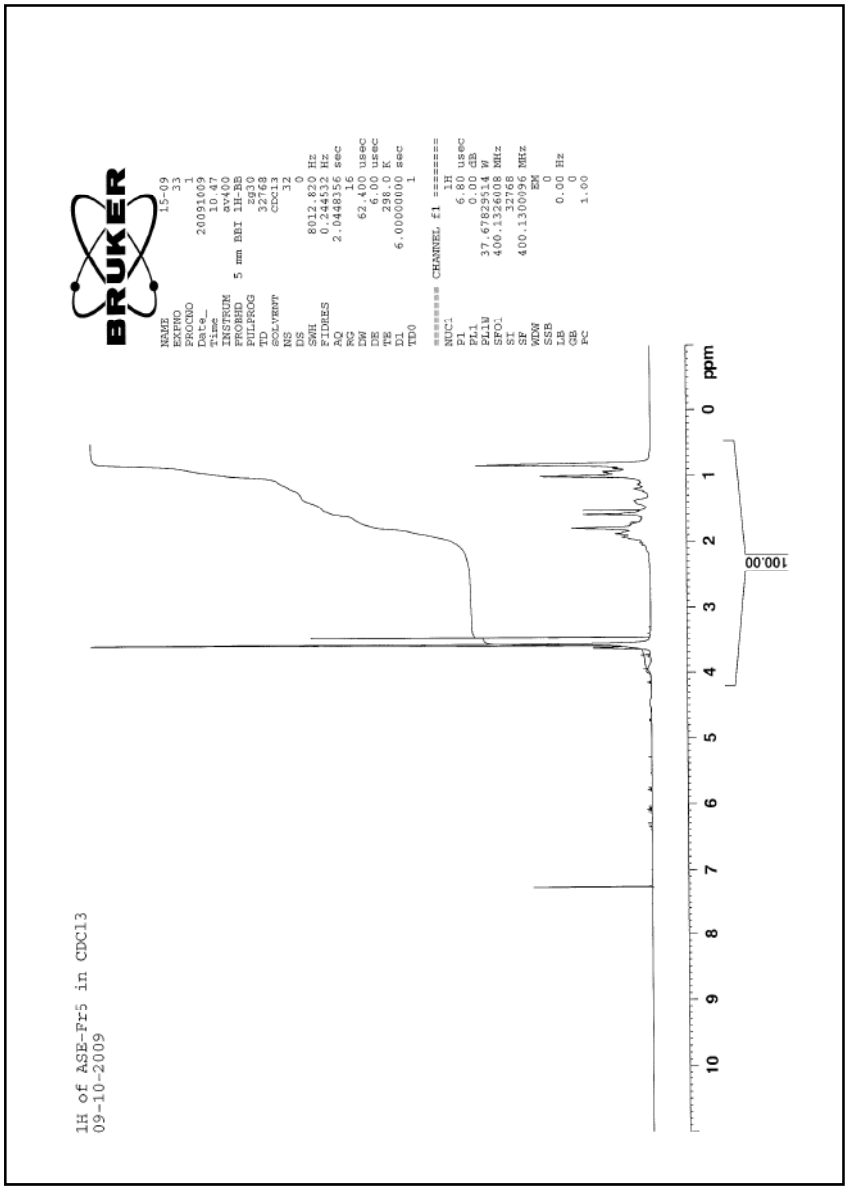

Figure 66. [1]H-NMR spectrum of P(methyl methacrylate-nbutyl acrylate-isobornyl acrylate)

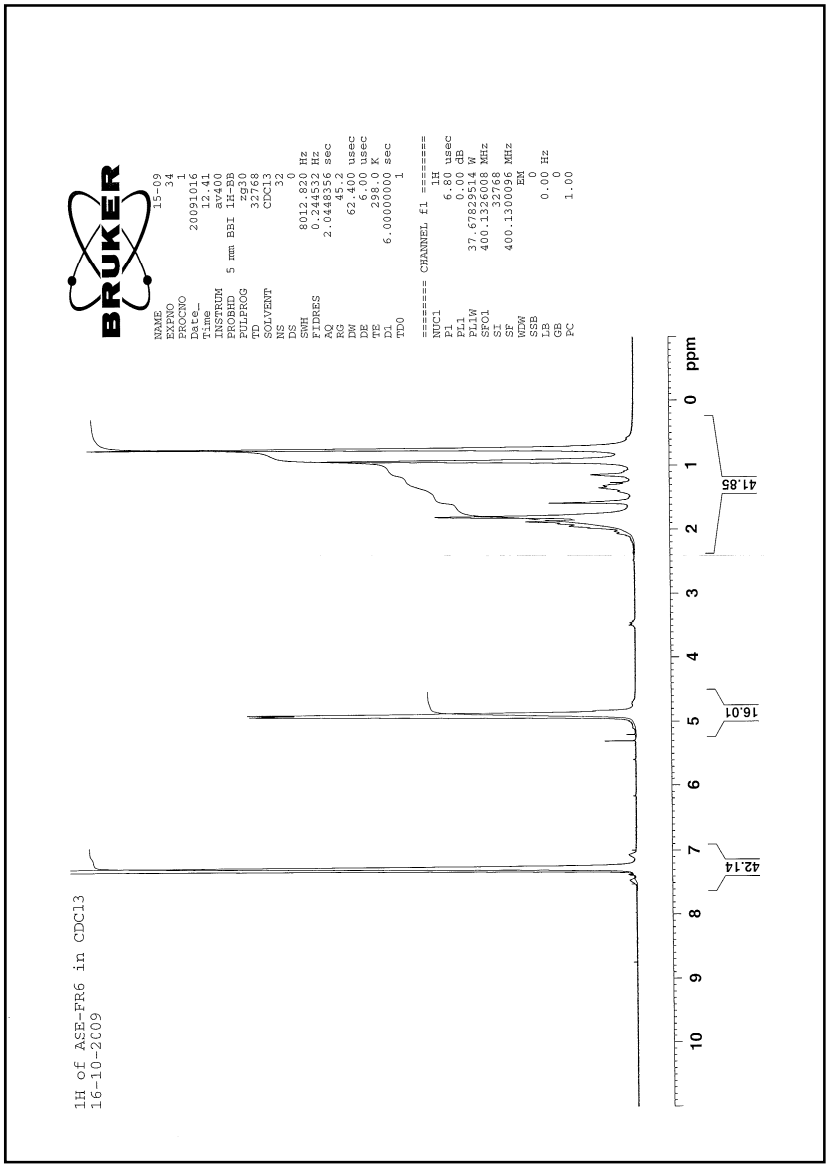

Figure 67. ^{1}H-NMR spectrum of P(benzyl methacrylate)

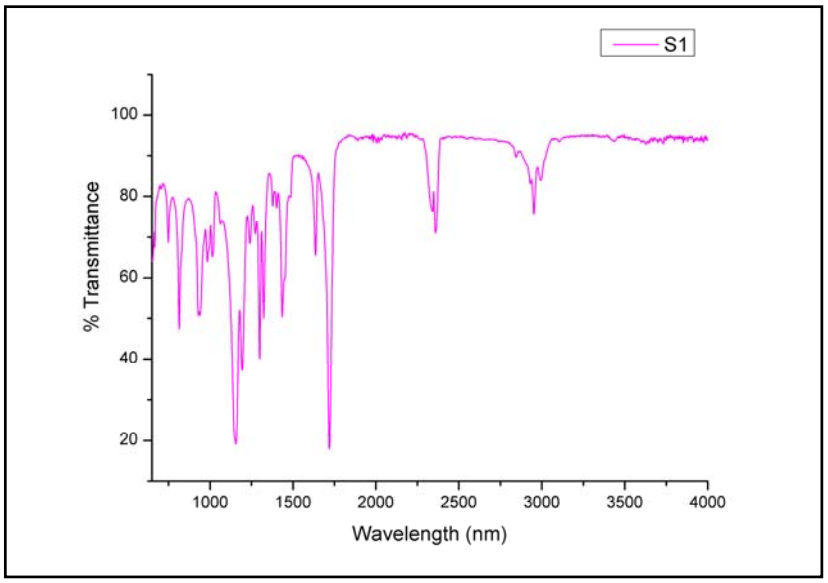

Figure 68. FT-IR Spectrum of PMMA

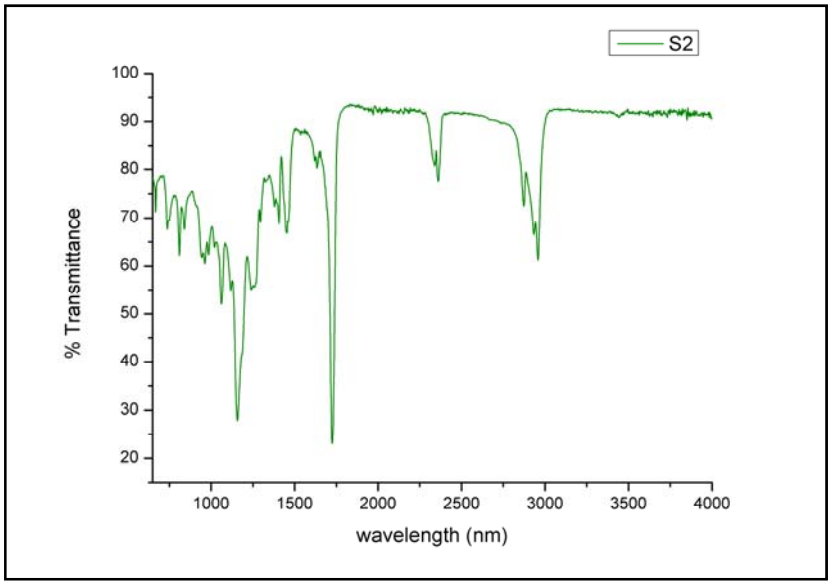

Figure 69. FT-IR Spectrum of PnBA

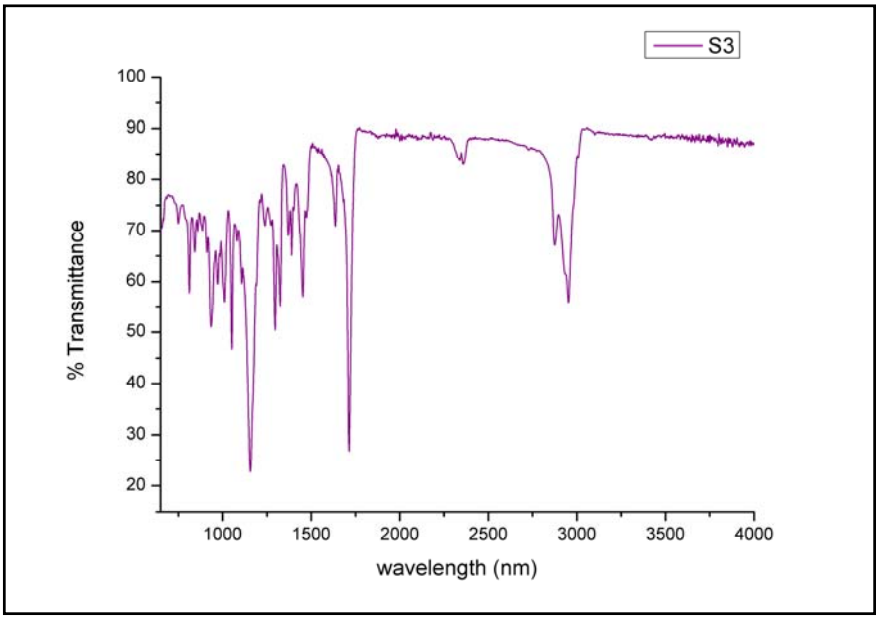

Figure 70. FT-IR Spectrum of PIBA

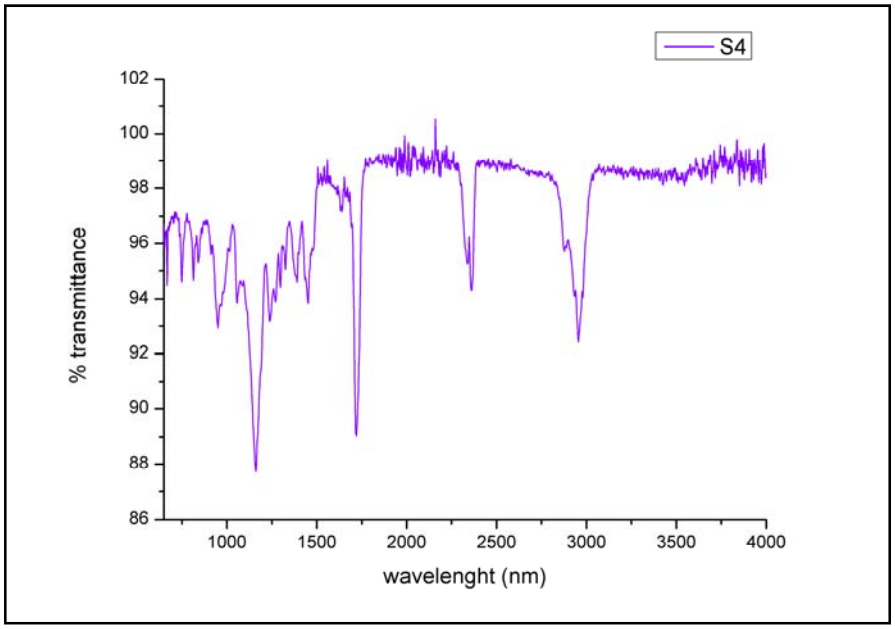

Figure 71. FT-IR Spectrum of P(MMA-co-nBA)

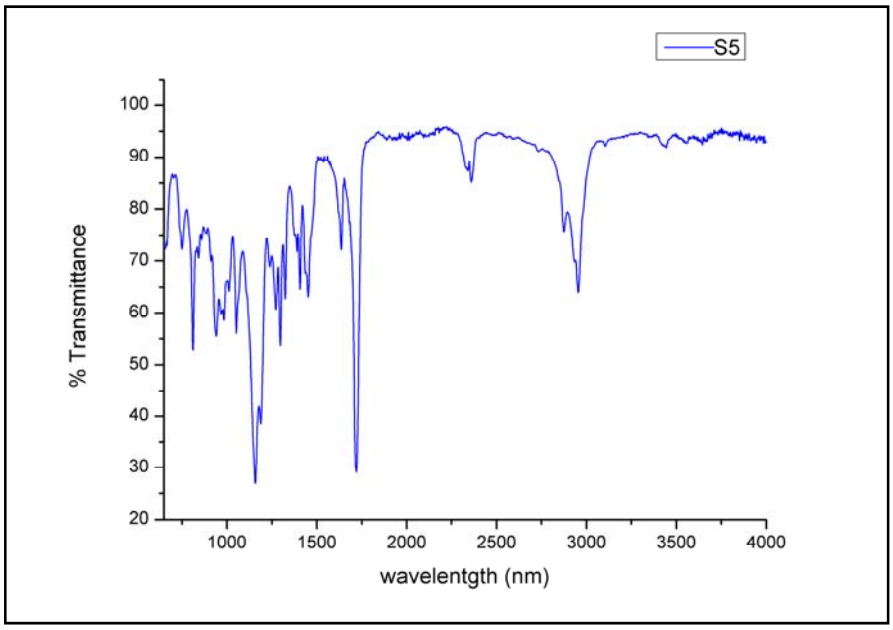

Figure 72. FT-IR Spectrum of P(MMA-co-nBA-co-IBA)

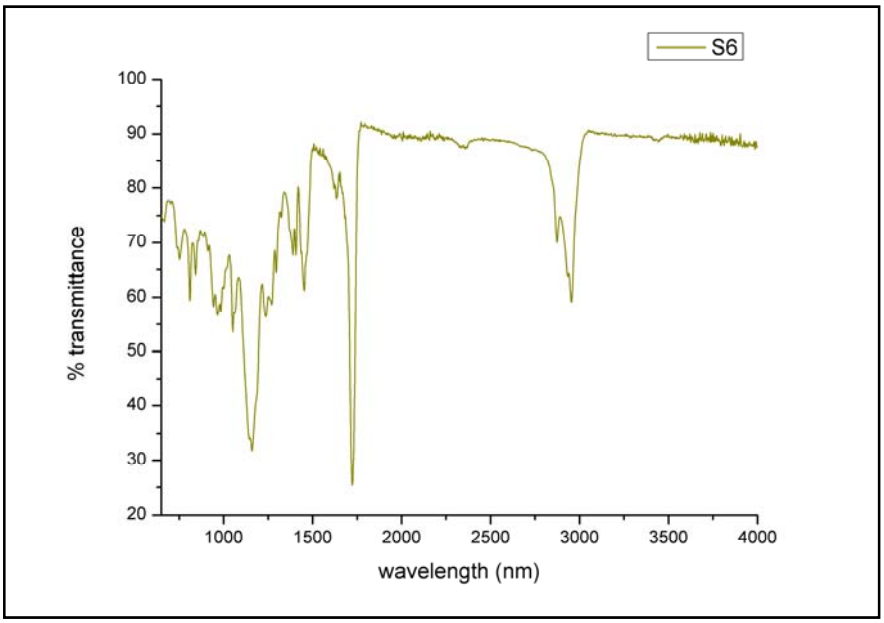

Figure 73. FT-IR Spectrum of PBzMA

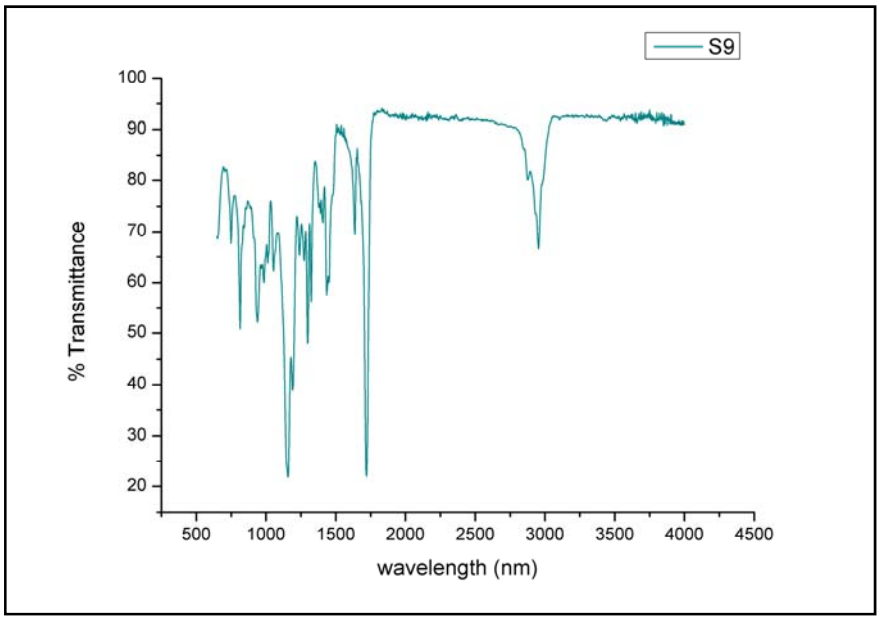

Figure 74. FT-IR Spectrum of P(MMA-co-BzMA)

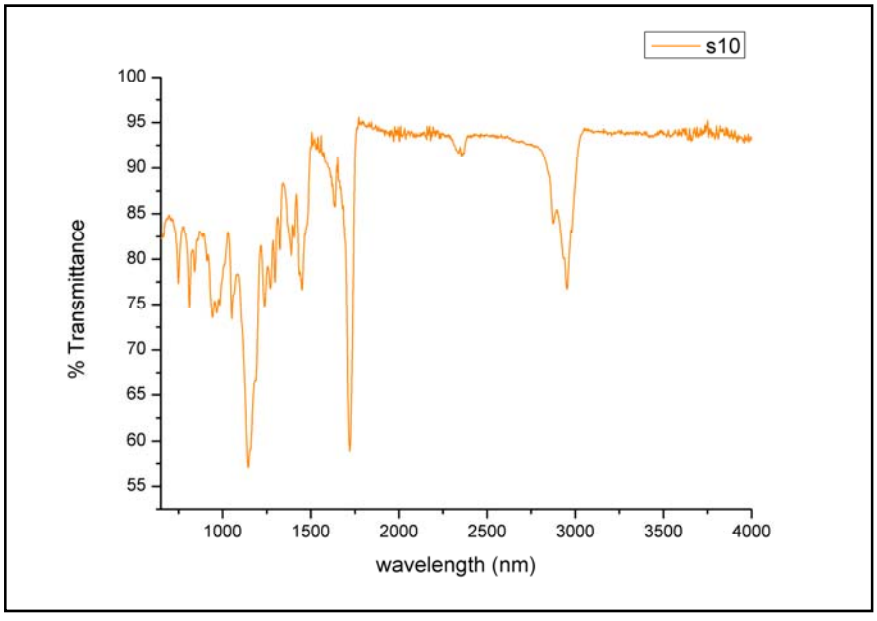

Figure 75. FT-IR Spectrum of P(MMA-co-nBA-co-IBA-co-BzMA).

CURRICULUM VITAE

PERSONAL INFORMATION

Name-Surname: Suriye Özlem Gündoğdu

Date of Birth: 19.02.1983

Place of Birth: Kırcaali/ Bulgaria

Nationality: Turkish

Marital Status: Married

e-mail: suozlem@yahoo.com

EDUCATION

Degree	Institution	Year
M.Sc.	METU, Chemistry Dept.	2006-2008
B.Sc.	METU, Chemistry Dept.	2001-2006
High School	Bursa Girl's High School	1997-2001

WORK EXPERIENCE

Place	Position	Year
İLKO R&D Center	R&D Specialist	2012-present
METU, Chemistry Dept.	Research Assistant	2006-2012

FOREIGN LANGUAGE

English, Bulgarian

COMPUTER SKILLS

Excel, Word, Power Point, ChemDraw, Paint, MastRe-C, Photoshop, Science Finder, Origin and Internet.

METU HIGH HONOUR LIST

2006- 2007 (Spring)

2005- 2006 (Spring)

2005- 2006 (Fall)

PUBLICATIONS

1. Ozlem, S., Hacaloğlu, J., Thermal Degradation of poly(n-butyl methacrylate), poly(n-butyl acrylate) and poly(t-butyl acrylate) J Anal. Appl. Pyrol. 2012. submitted.

2. Ozlem, S., Gürel, E.A., Rossi, M. R., Hacaloğlu, J., Thermal Degradation of Poly(isobornyl acrylate) and Its Copolymer with Poly(methyl methacrylate)via Pyrolysis Mass Spectrometry. J Anal. Appl. Pyrol. 2012.http://dx.doi.org/10.1016/j.jaap.2012.10.024

3. Ozlem, S., Iskin, B., Yilmaz, G., Kukut, M., Hacaloğlu, J., Yağcı, Y., Synthesis and pyrolysis of ABC type miktoarm star copolymers with polystyrene, poly(lactic acid) and poly(ethylene glycol) arms, European Polymer Journal, 2012; 48, 1755-1767.

4. Ozlem, S., Akkaya, E. U., Thinking Outside the Silicon Box: Molecular AND Logic as an Additional Layer of Selectivity in Singlet Oxygen Generation for Photodynamic Therapy, JACS, 2009; 131, 48-49. (featured in C & EN News, Science and Technology Concentrates, January 19, 2009)

Articles in preparation

1. Gundogdu-Ozlem, S., Gürel, E.A., Hacaloğlu, J., Thermal Degradation of poly(methyl methacrylate-co-n-butyl acrylate-co- isobornyl acrylate) copolymers.

2. Gundogdu-Ozlem, S., Gürel, E.A, Hacaloğlu, J., Thermal Degradation of poly(methyl methacrylate-co-benzyl methacrylate) copolymer and copolymer fiber.

3. Gundogdu-Ozlem, S., Gürel, E.A., Hacaloğlu, J., Thermal Degradation of copolymers of methyl methacrylate fibers.